

**The role of the flagellum
attachment zone
in *Leishmania*
mexicana flagellar pocket
architecture**

Clare Halliday

This thesis is submitted in partial fulfilment of
the requirements of the award for the degree
of Doctor of Philosophy

Awarded by Oxford Brookes University

Submission date: October 2021

Declaration

I declare that no material contained in this thesis has been used in any other submission for an academic award.

I confirm that all the research and findings presented in this thesis are my own work unless otherwise indicated through the use of a clear referencing system.

Abstract

Leishmania spp are flagellate protozoan parasites, with a digenetic life cycle, alternating between a mammalian host and insect vector. Within both the host and vector *Leishmania* adopts different morphologies and cell types, which are adapted to that ecological niche. One of the key architectural features in the determination of cell morphology is the flagellar pocket, which is the sole site of endo/exocytosis. It was shown that a large cytoskeletal structure, the flagellum attachment zone (FAZ), which connects the flagellum to the cell body, was an important contributor to the maintenance of the flagellar pocket architecture and its function. However, a poor understanding of FAZ molecular organisation and the specific roles of its constituent proteins remains.

Here, 28 FAZ proteins were discovered by the endogenous tagging of the orthologs of *T. brucei* FAZ proteins identified through TrypTag. These proteins were categorised into five classes based on their localisation patterns. The classes sit within the three structural domains, the flagellum, intracellular and cell body of the FAZ structure. A deletion screen of these proteins revealed functional groups responsible for flagellum attachment and cell morphogenesis, with the specific function of these proteins connected to their exact location within the FAZ. Analyses of the flagellum domain proteins FAZ27 and FAZ34 revealed their importance for flagellum attachment. Moreover, the cell body domain CC2D was shown to be required for flagellum attachment and anterior cell tip morphogenesis and was dependent on FAZ2 for assembly. Importantly, the analysis of these proteins defined the assembly hierarchy of the three FAZ structural domains, with the cell body domain required for the assembly of the intracellular and flagellum domains and FAZ2 of the cell body domain being a key foundational protein. Together these results have provided crucial insights into the molecular organisation and function of the FAZ in *Leishmania*.

Acknowledgements

I would like to start by thanking my supervisor, Dr Jack Sunter, for his support and patience throughout this PhD. I really valued his scientific knowledge and advice through lab experiments, manuscript and the writing of this thesis.

I also would like to thank Professor Keith Gull and members of Sunter, Vaughan and Wheeler labs for useful discussions. It was a pleasure to share this journey with my fellow PhD researchers, Laura Smithson, Shahaan Shafiq, Manu Ahmed and Lauren Wilburn.

A special thanks goes to my parents for believing in me and giving me lots of support since day one, my late grandparents for their belief in education, my friends who are still on the side-lines cheering me on and Matthew, for his encouragement and producing decent gin and tonics particularly during the thesis writing phase.

And lastly, thanks to the Nigel Groome Scholarship for funding this PhD project.

Table of Contents

Declarations	3
Abstract	5
Acknowledgements	6
Table of Contents	7
List of Figures and Tables	13
Abbreviations	18
1 Introduction	20
1.1 <i>Leishmania</i> and leishmaniasis	21
1.1.1 <i>Leishmania</i> life cycle.....	21
1.2 The flagellar pocket is critical for the determination of cell morphology in trypanosomatids	22
1.3 Flagellar pocket structure in <i>T. brucei</i> and <i>L. mexicana</i>	25
1.3.1 <i>T. brucei</i>	25
1.3.2 <i>L. mexicana</i>	27
1.4 Flagellar pocket shape is critical for its function	29
1.5 FAZ is important for cell and flagellar pocket morphogenesis ..	29
1.6 The FAZ is intimately associated with flagellar pocket duplication and segregation	36
1.7 Flagellar pocket is important for pathogenicity	39
1.7.1 Endocytosis, Sorting and recycling	39
1.7.2 Nutrient Uptake	40
1.7.3 Exocytosis	40
1.7.4 The flagellar pocket is important for flagellum assembly	41
1.7.5 Secretion of molecules in the host.....	41
1.8 Aims	44
2 Materials and Methods	45
2.1 Bioinformatics	46
2.1.1 Identifying FAZ proteins in <i>Trypanosoma brucei</i> using TrypTag ..	46

2.1.2	Identifying protein ortholog in <i>Leishmania mexicana</i>	46
2.1.3	Proteome analysis	46
2.2	Molecular Biology	46
2.2.1	Generation of FAZ and flagellar pocket markers tagging constructs	46
2.2.2	Generation of FAZ deletion constructs	48
2.2.3	The confirmation of null mutant cell lines	49
2.2.4	Generation of FAZ addback plasmids	49
2.3	<i>Leishmania mexicana</i> cell culture	53
2.3.1	Maintenance of cells	53
2.3.2	Generation of tagging, null mutant and addback cell lines	53
2.3.3	Growth Curves	53
2.4	Light Microscopy	54
2.4.1	Imaging the tagging, null mutant and addback cell lines	54
2.4.2	Measurement of cell cycle position numbers and abnormalities	55
2.4.3	Measurement of flagellum length and cell body length/width ...	55
2.4.4	Confirmation of flagellum loss by vortex	56
2.4.5	Motility assay	56
2.5	Methodology for Transmission Electron Microscopy	56
2.5.1	Fixing cells and single osmium preparation	56
2.5.2	2.5.2 Thin sectioning and imaging	57
2.6	Approach to data collection and analysis	57
3	Discovery of 28 FAZ proteins with 5 different FAZ localisation classes in <i>L. mexicana</i>	59
3.1	Preface	60
3.2	58 orthologs of <i>T. brucei</i> FAZ proteins were identified in <i>L. mexicana</i>	61
3.3	FAZ2 and FLA1BP were chosen as FAZ protein markers for resolution and clarity in localisation screen	70
3.4	Localisation screen identified 29 FAZ proteins categorised into five localisation classes	71

3.5	<i>T. brucei</i> FAZ protein localisation and domain pattern correlated with <i>L. mexicana</i> orthologs	84
3.6	26 <i>L. mexicana</i> orthologs did not localise to the FAZ	87
3.7	All five FAZ localisation classes begin to assemble a new FAZ structure during flagellum biogenesis	90
3.8	Discussion	93
3.8.1	Five FAZ localisation classes were identified in <i>L. mexicana</i>	93
3.8.2	FAZ classes in <i>L. mexicana</i> correlate with specific groups in <i>T. brucei</i>	95
3.8.3	20 <i>T. brucei</i> FAZ proteins are specific to trypomastigote and epimastigote morphology	96
4	Analysis of 23 FAZ proteins from 5 FAZ localisation classes revealed functional groups responsible for flagellum attachment and cell morphogenesis	98
4.1	Preface	99
4.2	A pipeline was established for the functional analysis of FAZ null mutants	100
4.3	Class I	102
4.3.1	Loose flagella and short flagellum cells were present in FAZ27, FAZ34 and FLA1BP null mutants	102
4.3.2	Cell cycle was only marginally altered in class I null mutants	105
4.3.3	Flagellar streamers are prevalent throughout the cell cycle of cAMP binding protein null mutant	105
4.3.4	FAZ assembly was affected in Class I null mutants	107
4.3.5	FAZ27, FAZ34 and FLA1BP null mutants had shorter cell bodies .	109
4.4	Class II	111
4.4.1	Loose flagella, short flagellum cells and flagellum to flagellum connections were observed in Class II null mutants	111
4.4.2	Deletion of FAZ5, FAZ2 and CC2D resulted in cell cycle changes .	114
4.4.3	FLA1BP localisation was affected in Class II null mutants	115

4.4.4	Cell body length was reduced in FAZ5, CC2D and FAZ2 null mutants	117
4.5	Class III	119
4.5.1	FAZ3 null mutant phenotype was similar to parental	120
4.6	Class IV	122
4.6.1	Cell cycle was only marginally affected in Class IV null mutants .	123
4.6.2	FLA1BP::mCh localisation was not affected in Class IV null mutants	124
4.6.3	Flagellum and cell body size was not affected in Class IV null mutants but FAZ10 had 'zip-like' flagella morphology	126
4.7	Class V	128
4.7.1	Class V null mutants have no cell cycle or morphological defects	128
4.8	Discussion	132
4.8.1	Each FAZ localisation class represents a functional group with specific roles	132
4.8.2	Class I is associated with flagellum attachment and cell morphology	132
4.8.3	Class II is associated with flagellum attachment, cell morphology and anterior cell tip morphogenesis	133
4.8.4	Class III could be important for correct FAZ assembly	135
4.8.5	FAZ10 has a role in cytokinesis	135
4.8.6	Class V proteins likely located further away from the attachment region	136
5	Class I proteins FAZ27 and FAZ34 are important for flagellum attachment and flagellar pocket morphology	138
5.1	Preface	139
5.2	Phenotype of FAZ27 and FAZ34 null mutants changes over time	140
5.3	The likelihood of flagellum loss correlated with increasing flagellum length	147

5.4	The re-introduction of FAZ27 and FAZ34 genes confirmed flagellum loss was directly related to FAZ27 and FAZ34 deletion	152
5.5	Both EF1 and EF2 domains of FAZ34 were required for maintaining flagellum attachment	155
5.6	The deletion of flagellum domain proteins FAZ27 and FAZ34 disrupted FAZ organisation	158
5.7	Disruption of FAZ organisation reduces attachment and alters flagellar pocket size and shape	163
5.8	Change in FAZ organisation and attachment affected cell motility	166
5.9	Discussion	169
5.9.1	FAZ has a key role in flagellum attachment	169
5.9.2	FAZ organisational structure is important for flagellar pocket shape	170
5.9.3	FAZ attachment and flagellar pocket shape is important for directional movement	172
5.9.4	FAZ27 and FAZ34 function is similar to FLA1BP and FAZ5	172
6	Class II protein CC2D is required for flagellum attachment and anterior cell tip morphogenesis	174
6.1	Preface	175
6.2	Phenotype of CC2D null mutant changes over time	176
6.3	Flagellum in CC2D null mutant was hard to detach by shear force, but the likelihood increased with length	182
6.4	Add-back of CC2D gene confirms CC2D null mutant phenotype was directly related to CC2D deletion	184
6.5	The deletion of CC2D disrupts FAZ organisation	186
6.6	FAZ2 necessary for assembly of CC2D into <i>L. mexicana</i> FAZ	190
6.7	CC2D deletion reduced flagellar pocket size	192
6.8	Change in FAZ organisation and attachment affected cell motility	194

6.9	Discussion	195
6.9.1	CC2D has a key role in anterior cell tip morphogenesis	195
6.9.2	FAZ2 is the start of FAZ assembly hierarchy	198
6.9.3	CC2D has a role in flagellum attachment	200
6.9.4	CC2D and cell body domain proteins play a smaller role in cell morphogenesis	201
6.9.5	CC2D is important for motility	201
7	Conclusions and Outlook	202
7.1	Towards a greater understanding of FAZ function in <i>Leishmania</i>	203
7.1.1	Identification of FAZ proteins in <i>L. mexicana</i>	203
7.1.2	Identification of FAZ functional groups in <i>L. mexicana</i>	204
7.1.3	Specific functions of FAZ27, FAZ34 and CC2D	204
7.2	Limitations and future perspectives	205
7.3	Concluding remarks	206
8	References	207
9	Appendix	218
A	Primers for tagging FAZ orthologs in <i>L.mexicana</i>	219
B	Non-FAZ localisations in <i>L. mexicana</i>	225
C	Primers for FAZ deletion in <i>L. mexicana</i>	231
D	Deletion confirmation primers	233
E	Publications related to this thesis	235

List of Figures and Tables

1. Introduction		
Figure 1.1	Morphology across trypanosomatids	24
Figure 1.2	There are similarities and differences in <i>T. brucei</i> and <i>L. mexicana</i> flagellar pocket structure	28
Figure 1.3	There are three main FAZ domains in trypanosomes	31
Table 1.1	FAZ proteins identified in <i>T. brucei</i>	32
Figure 1.4	FAZ proteins in <i>L. mexicana</i> are split into classes based on localisation pattern	35
Figure 1.5	Flagellar pocket duplication in <i>T. brucei</i> and <i>L. mexicana</i>	38
Figure 1.6	Endocytosis and exocytosis pathways in <i>Trypanosomatids</i>	43
2. Materials and Methods		
Table 2.1	Primers used for the generation of addback plasmids	51
Table 2.2	Addback plasmids generated	51
Figure 2.1	Generation of addback constructs	52
Table 2.3	Selection drugs	53
Figure 2.2	Measurements in ImageJ	55
Table 2.4	Approach to data collection	58
3. Discovery of 28 FAZ proteins with 5 different FAZ localisation classes in <i>L. mexicana</i>		
Figure 3.1	FAZ proteins in <i>T. brucei</i> were classified based on their localisation patterns	62
Table 3.1	FAZ proteins in <i>T. brucei</i> with orthologs in <i>L. mexicana</i> identified	63
Figure 3.2	FAZ protein conservation analysis across species	69
Figure 3.3	FAZ2 and FLA1BP were selected as FAZ markers	70
Figure 3.4	<i>Leishmania</i> FAZ proteins with Class 1; FAZ on flagellum side localisation	72
Figure 3.5	<i>Leishmania</i> FAZ proteins with Class 2; FAZ on cell body side localisation	74

Figure 3.6	<i>Leishmania</i> FAZ protein with Class 3; FAZ ring/horseshoe at collar region localisation	76
Figure 3.7	<i>Leishmania</i> FAZ proteins with Class 4; FAZ ring/horseshoe at exit point localisation	77
Figure 3.8	<i>Leishmania</i> FAZ proteins with Class 5; FAZ ring/horseshoe at exit point localisation	80
Figure 3.9	<i>Leishmania</i> FAZ proteins with Class 6; Complex FAZ localisations	82
Table 3.2	Comparison of FAZ localisations in <i>L. mexicana</i> and <i>T. brucei</i>	86
Table 3.3	Proteins with non-FAZ localisations	88
Figure 3.10	Non FAZ localisation examples	89
Figure 3.11	New FAZ begins to form by the time new flagellum emerges out of the flagellar pocket	92
Figure 3.12	Two flagella were seen in the pre-existing flagellar pocket before segregation in <i>L. mexicana</i>	93
Figure 3.13	Five FAZ classes were defined by their localisation pattern in <i>L. mexicana</i>	94

4. Analysis of 23 FAZ proteins from 5 FAZ localisation classes revealed functional groups responsible for flagellum attachment and cell morphogenesis

Table 4.1	23 FAZ proteins taken forward for functional analysis screening in <i>L. mexicana</i>	101
Figure 4.1	Diagnostic PCR confirmed gene deletion for Class I null mutants	103
Figure 4.2	Deletion of FAZ27, FAZ34 and FLA1BP resulted in cells with short flagellum and loose flagella	104
Figure 4.3	Deletion of Class I FAZ proteins did not affect the cell cycle	106
Figure 4.4	FAZ2 and FLA1BP localisation was affected in Class I null mutants	108
Figure 4.5	Cell body length was reduced in FAZ27, FAZ34 and FLA1BP null mutants	110

Figure 4.6	Diagnostic PCR confirmed gene deletion for Class II null mutants	112
Figure 4.7	CC2D null mutant has loose flagella and short flagellum cells like FAZ5 and F-F connections like FAZ2	113
Figure 4.8	Cell cycle was affected in Class II null mutants	115
Figure 4.9	FLA1BP::mCh localisation was affected in Class II null mutants ..	116
Figure 4.10	Cell body length was reduced in FAZ5, CC2D and FAZ2 null mutants	118
Figure 4.11	Diagnostic PCR confirmed gene deletion for Class III FAZ3 null mutant	119
Figure 4.12	Deletion of class III, FAZ3 has no effect on cell cycle and morphology	121
Figure 4.13	Diagnostic PCR confirmed gene deletion for Class IV null mutants	122
Figure 4.14	Little change in the cell cycle of Class IV null mutants	124
Figure 4.15	FLA1BP::mCh localisation was not affected in Class IV null mutants	125
Figure 4.16	FAZ10 null mutant has flagellar morphology defects	126
Figure 4.17	Diagnostic PCR confirmed Class V FAZ gene deletions	129
Figure 4.18	Cell cycle and FLA1BP::mCh localisation was not affected in Class V null mutants	130
Figure 4.19	Flagella and cell body lengths were not affected in Class V null mutants	131
Figure 4.20	Potential roles of the different FAZ domains within the FAZ structure in <i>L. mexicana</i>	137

5. Class I proteins FAZ27 and FAZ34 are important for flagellum attachment and flagellar pocket morphology

Figure 5.1	FAZ27 and FAZ34 null mutants were successfully re-generated .	141
Figure 5.2	Phenotype of FAZ27 & FAZ34 null mutant cells changed over time	144

Figure 5.3	Cell body length in FAZ27 & FAZ34 null mutants reduced over time	146
Figure 5.4	Mechanical stress from vortexing caused flagellum loss	148
Figure 5.5	Likelihood of flagellum loss increased with increasing flagellum length	150
Figure 5.6	Kinetoplast attachment correlated with flagellum length in FAZ34 null mutant	151
Figure 5.7	FAZ27 and FAZ34 null mutant phenotype was the consequence of protein loss	154
Figure 5.8	EF-1 and EF-2 domains are both important for FAZ34 function ..	157
Figure 5.9	Localisations of six proteins representing different FAZ domains in the parental cell line	160
Figure 5.10	Deletion of FAZ27 affected the localisation of flagellum, intermembrane, and cell body FAZ domain proteins	161
Figure 5.11	Deletion of FAZ34 affected the localisation of flagellum, intermembrane, and cell body FAZ domain proteins	162
Figure 5.12	FAZ27 and FAZ34 loss disrupted flagellar pocket shape and organisation	164
Figure 5.13	Flagellar pocket size and attachment was reduced in FAZ27 and FAZ34 null mutants	166
Figure 5.14	FAZ27 loss reduced swimming speed and progressive movement	167
Figure 5.15	FAZ34 loss reduced swimming speed and progressive movement	168
Figure 5.16	FAZ molecular structure is disrupted in FAZ27 and FAZ27 null mutants	171

6. Class II protein CC2D is required for flagellum attachment and anterior cell tip morphogenesis

Figure 6.1	CC2D null mutant was successfully re-generated	177
Figure 6.2	Change in CC2D null mutant phenotype occurs over time	179

Figure 6.3	No morphological changes were detected in CC2D null mutant over time	181
Figure 6.4	Loose flagella are longer than the attached flagella in CC2D null mutant	183
Figure 6.5	CC2D null mutant phenotype was the consequence of CC2D deletion	185
Figure 6.6	Localisations of six proteins represents different domains in the parental cell line	188
Figure 6.7	Deletion of CC2D affected the localisation of flagellum, intermembrane, and cell body FAZ domain proteins	189
Figure 6.8	FAZ2 is required for CC2D assembly	191
Figure 6.9	CC2D loss disrupted flagellar pocket shape	193
Figure 6.10	CC2D loss reduced swimming speed and progressive movement	194
Figure 6.11	F-F connections in CC2D null mutant is predicted to be similar to FAZ2 null mutant	197
Figure 6.12	FAZ2 is head of FAZ assembly hierarchy	199

Abbreviations

1F	One flagellum
2F	Two flagella
1F1N1K	One flagellum, one nucleus, one kinetoplast
2F1N1K	Two flagella, one nucleus, one kinetoplast
2F2N1K	Two flagella, two nuclei, one kinetoplast
2F2N2K	Two flagella, two nuclei, two kinetoplasts
A	Anterior
aa	Amino acids
BB	Basal body
BSF	Bloodstream form
BLAST	Basic local alignment search tool
bp	Base pairs
cAMP	Cyclic adenosine monophosphate
Cas9	CRISPR-associated gene 9
CRISPR	Clustered regularly interspaced short palindromic repeats
DAPI	4, 6-diamidino-2-phenylindole
DMSO	Dimethyl sulfoxide
dTNPs	Deoxyribonucleotide triphosphates
ddH₂O	Double distilled water
FAZ	Flagellum attachment zone
FCS	Fetal calf serum
F-F	Flagellum-to-flagellum
gDNA	Genome DNA
GFP	Green fluorescent protein
HiFi	High fidelity
K	Kinetoplast
kDa	Kilodalton
mCherry	Monomeric cherry red

mNG	Monomeric neon green
MtQ	Microtubule quartet
ORF	Open reading frame
P	Posterior
PBS	Phosphate buffered saline
PFR	Paraflagellar rod
RNAi	RNA interference
sgRNA	Single guide ribonucleic acid
SF	Short flagellum
TEM	Transmission electron microscopy
TMDs	Transmembrane domains
UTR	Untranslated region

Chapter 1

Introduction

Declaration: Some aspects of this chapter was used as the basis of the flagellar pocket review, Halliday, C. *et al.* (2021) 'Trypanosomatid Flagellar Pocket from Structure to Function', *Trends in Parasitology*, 37(4), pp. 317–329. doi: 10.1016/j.pt.2020.11.005

1.1 *Leishmania* and leishmaniasis

Leishmania spp are protozoan parasites, which cause the infectious disease, leishmaniasis. Transmission of this disease between mammalian hosts occurs via the sand fly insect vector (Bates, 2007). Leishmaniasis can occur in three different forms, visceral, cutaneous (skin lesions) and mucocutaneous (affecting the nose, throat and mouth). Visceral leishmaniasis affects the liver, spleen and bone marrow and can be life threatening if untreated (Herwaldt, 1999; Bates, 2007). There are estimated to be between 200,000-400,000 visceral infections every year with 90% of those occurring in India, Bangladesh, Sudan, South Sudan, Brazil and Ethiopia. Cutaneous leishmaniasis infects between 700,000-1.2 million people every year, affecting a wider region including the Americas, the Mediterranean and Western Asia. Overall leishmaniasis is the 9th largest individual infectious disease burden in the world, with approximately 20-40,000 deaths every year (Alvar *et al.*, 2012).

1.1.1 *Leishmania* life cycle

Leishmania spp have a complex digenetic life cycle with developmental forms in both the mammalian host and insect vector. In order to adapt to the different environmental conditions of these ecological niches, *Leishmania* parasites have the ability to differentiate into different cell morphologies and cell types (Sunter and Gull, 2017). There are two main cell morphologies, which are the promastigote morphology, found in the sand fly with an elongated ovoid cell body and a long motile flagellum and the amastigote morphology, found in the mammalian host with a smaller, spherical cell body and a short immotile flagellum (**Fig 1.1**) (Sunter and Gull, 2017).

Leishmania parasites have a series of developmental forms in the sand fly, which occurs as a chain of events after uptake of amastigotes with the blood meal;

however, all are variations on the promastigote cell organisation. Amastigotes differentiate into procyclic promastigotes which then become nectomonad promastigotes (longer cell body) that migrate out of peritrophic matrix to attach themselves to microvilli in the midgut. Here, they differentiate into leptomonad promastigotes (shorter cell body) and then migrate to the stomodeal valve. Leptomonad promastigotes can differentiate to either haptomonad or metacyclic promastigotes. The metacyclic cell form is the mammalian infective form that is deposited into a bite site and taken up by a macrophage (Bates, 2007; Sunter and Gull, 2017). *Leishmania* morphological adaptation with different developmental morphologies is similar to other protozoan parasites, including the closely related species *Trypanosoma brucei* (Hoare and Wallace, 1966; Wheeler, Gluenz and Gull, 2013).

1.2 The flagellar pocket is critical for the determination of cell morphology in trypanosomatids

Despite different morphologies between trypanosomatids such as *Leishmania spp*, *Trypanosoma cruzi* and *Trypanosoma brucei*, they all share a number of important cellular architectural features. The overall shape of the parasite is determined by a sub-pellicular microtubule array, within which are positioned single copy organelles and structures, including the nucleus, kinetoplast (mitochondrial DNA), basal body, flagellum and flagellar pocket, an invagination of the cell membrane at the base of the flagellum (Sunter and Gull, 2017). It is the positioning of these organelles and structures that determines the shape and form of these parasites. For example, within the sand fly vector *Leishmania* have a promastigote morphology that has the basal body and kinetoplast positioned to the anterior of the nucleus with the flagellum emerging from the flagellar pocket at the anterior cell tip, which is not attached to the cell body beyond this point (**Fig 1.1**) (Sunter and Gull, 2017).

In contrast, *T. brucei* exhibits a trypomastigote morphology for the majority of its life cycle that has an elongated cell body with the basal body and associated kinetoplast, flagellum and flagellar pocket positioned to the posterior of the nucleus (**Fig 1.1**). Once the flagellum has exited the cell body it extends beyond the anterior cell tip

and is laterally attached to the cell body by flagellum attachment zone (FAZ) for the majority of its length (Krüger and Engstler, 2015). The repositioning of these organelles and structures is a key step in differentiation between different life cycle stages and morphological forms (Hoare and Wallace, 1966; Wheeler, Gluenz and Gull, 2013; Sunter and Gull, 2017).

The sub-pellicular microtubule array of these parasites is highly organised and runs from the anterior to posterior of the cell. The close positioning of the adjacent microtubules limits access to the cell membrane and therefore exo/endocytic processes can only occur at specific breaks in the array; hence, creating a highly polarised exo/endocytic system. The site of flagellum emergence from the flagellar pocket is one such break in the array in these parasites (Landfear and Ignatushchenko, 2001; Elias *et al.*, 2007; Field and Carrington, 2009; Ambit *et al.*, 2011). The flagellar pocket is a critical part of the exo/endocytic system and is involved in many cell roles such as acquisition of nutrients, secretion of proteins, immune evasion in addition to being of critical importance for cell division and determination of cell morphology (Field and Carrington, 2009). Studies have shown that FAZ assembly and structure is an important contributor to maintaining flagellar pocket architecture and therefore its function (Sunter *et al.*, 2019).

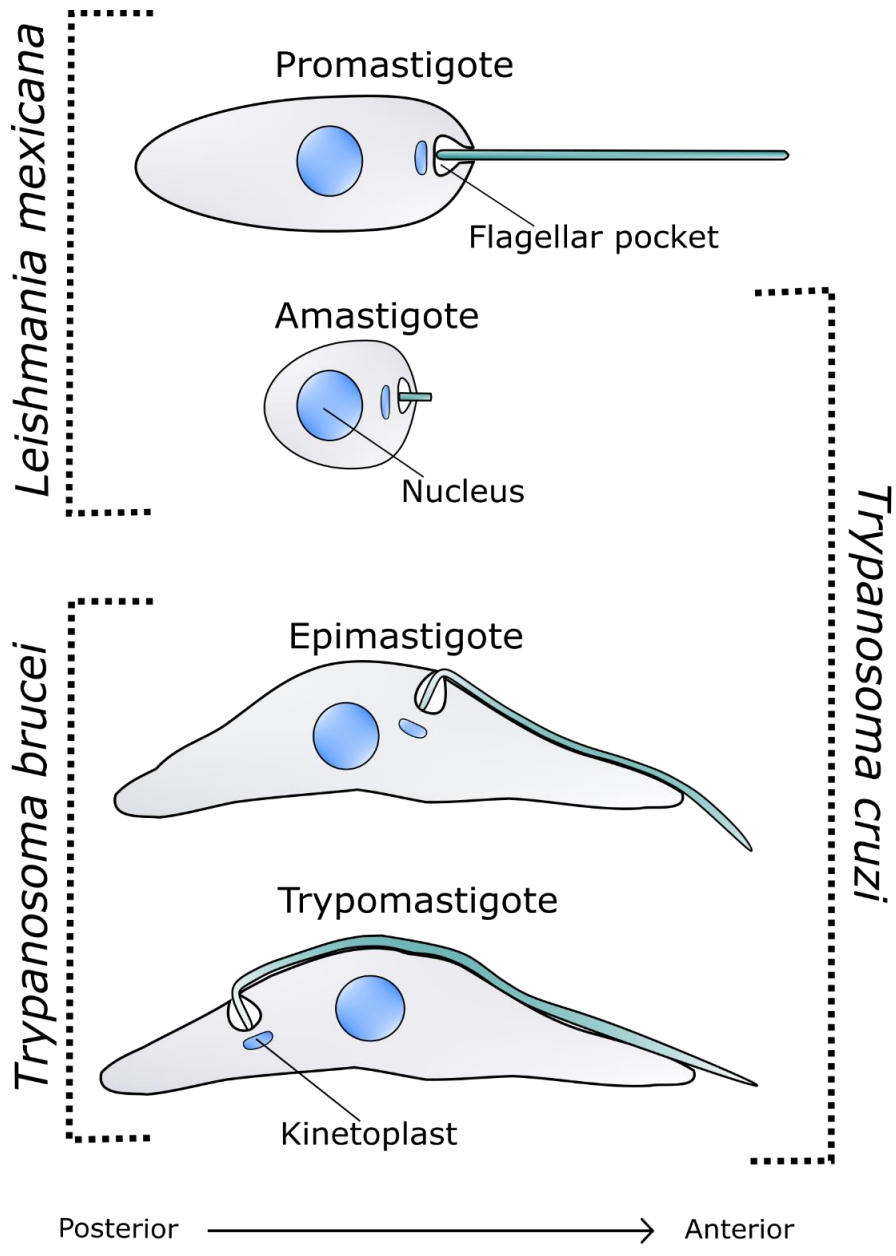


Figure 1.1: Morphology across trypanosomatids. The morphology is defined by positions of the nucleus, kinetoplast and flagellar pocket along the anterior-posterior axis. Promastigotes are found in *L. mexicana*, amastigotes are found in *L. mexicana* and *T. cruzi*. *T. cruzi* also share epimastigote and trypomastigote morphologies with *T. brucei*.

1.3 Flagellar pocket structure in *T. brucei* and *L. mexicana*

1.3.1 *T. brucei*

The *T. brucei* flagellar pocket is the best studied of the trypanosomatid flagellar pockets. It is an invagination of the cell membrane at the base of the flagellum that is shaped like a vase with two regions (**Fig 1.2**), the proximal bulbous region into which the exo/endocytic system connects and the distal neck region, which is surrounded by electron dense structures and at this point there is little gap between the flagellum and flagellar pocket neck membrane with the narrow gap restricting access of immune effector cells into the rest of the flagellar pocket (Field and Carrington, 2009; Wheeler, Sunter and Gull, 2016). The bulbous region is asymmetric with the anterior face larger than that of the posterior face. At base of the flagellar pocket is the basal body, which nucleates the flagellum that consists of a 9+2 microtubule axoneme structure (Lacomble *et al.*, 2009; Vaughan and Gull, 2016; Wheeler, Sunter and Gull, 2016). In close proximity to the flagellar pocket is the Golgi apparatus and a wide network of endoplasmic reticulum, highlighting the highly polarised nature of the *T. brucei* cell (Lacomble *et al.*, 2009).

The cell membrane can be split into four separate membrane domains, i) flagellum, ii) flagellar pocket bulbous, iii) flagellar pocket neck, iv) cell body and the boundaries between these different domains are located in the flagellar pocket (**Fig 1.2**) (Gadelha *et al.*, 2009). Around the base of the flagellum is a filamentous annulus called the collarette that has been described by electron microscopy. The collarette surrounds the flagellar membrane of transition zone region separating the flagellar pocket bulbous membrane from the flagellum membrane (Gadelha *et al.*, 2009; Lacomble *et al.*, 2009; Höög *et al.*, 2012). To date no collarette proteins have been identified. The boundary between the flagellar pocket bulbous membrane and the flagellar pocket neck membrane and then the cell body membrane is demarcated by the flagellar pocket collar and associated hook complex. The flagellar pocket collar is a horseshoe shaped cytoskeletal structure that is positioned distal to the flagellar pocket bulbous region cinching in the membrane, creating the two-part flagellar

pocket structure (**Fig 1.2**) (Angelopoulos, 1970; Field and Carrington, 2009; Gadelha *et al.*, 2009).

The best characterized component of the flagellar pocket collar is BILBO1 (Bonhivers *et al.*, 2008). *T. brucei* BILBO1 consists of an N-terminus domain (ubiquitin-like fold), EF hand motifs, a large coiled-coil domain in the C-terminus and a leucine zipper. BILBO1 is able to form homo-oligomers through its coiled-coil domain and the presence of calcium likely bound to the EF hands can change the conformation of a protein to form either circular or helical polymers (Florimond *et al.*, 2015; Vidilaseris *et al.*, 2015; Perdomo, Bonhivers and Robinson, 2016). The microtubule quartet (MtQ) a specialised set of four microtubules that are nucleated close to the basal bodies and wrap around the flagellar pocket pass through the gap in the flagellar pocket collar before extending along the cell body towards the anterior cell tip (**Fig 1.2**). The passage of the MtQ through the flagellar pocket collar creates a 'channel' within the neck region, which acts as an access route for material to enter the flagellar pocket bulbous lumen (Gadelha *et al.*, 2009; Lacomble *et al.*, 2009; S. Lacomble *et al.*, 2010; Sunter and Gull, 2016).

Just distal to the flagellar pocket collar is the hook complex, a cytoskeletal structure that forms a semi-circle around the flagellum with two arms that flank the proximal part of the MtQ and the flagellum attachment zone (FAZ) as these structures extend along the cell body (**Fig 1.2**). There is a growing list of hook complex proteins, including TbMORN1, TbLRRP1 and TbSmee and these proteins localise to either just one of the arms or one of the arms and the hook around the flagellum (Morriswood *et al.*, 2009; Zhou *et al.*, 2010; Esson *et al.*, 2012; Morriswood, 2015; Perdomo, Bonhivers and Robinson, 2016; Perry *et al.*, 2018). In trypanosomes the flagellum is attached for the majority of its length to the cell by the flagellum attachment zone (FAZ), which is a complex cytoskeletal structure (Vickerman 1969; Sherwin and Gull 1989; Höög *et al.* 2012; Sunter and Gull 2016).

1.3.2 *L. mexicana*

The *Leishmania* promastigote flagellar pocket is generally similar to that of *T. brucei* with both a bulbous region and a neck region (**Fig 1.2**); however, in *Leishmania* the neck is much longer than that of *T. brucei* and not as tightly opposed to the flagellum. In addition, both share important cytoskeletal structures including the MtQ, FAZ and the flagellar pocket collar (**Fig 1.2**). The *Leishmania* MtQ, like the one in *T. brucei*, runs along the pocket surface, in a left-handed helical path, which starts close to the basal body, crossing through a gap in the flagellar pocket collar which constituted by a double filament, unlike the single filament flagellar pocket collar seen in *T. brucei* (**Fig 1.2**) (Wheeler, Sunter and Gull, 2016).

In addition to the MtQ there is an electron dense FAZ filament similar to the *T. brucei* FAZ filament starting at the flagellar pocket collar and terminating with the MtQ in the neck region (Wheeler, Sunter and Gull, 2016). Within the *Leishmania* flagellar pocket neck region the flagellum is attached to the neck membrane; however, unlike in *T. brucei* the primary attachment region is not directly adjacent to the FAZ filament and MtQ and is instead located a quarter clockwise turn from them when viewed from the basal body. The *Leishmania* flagellum is only laterally attached within the flagellar pocket neck and this correlates with the 'free flagellum' morphology. Despite the radically different size of the FAZ, orthologs of FAZ proteins first identified in *T. brucei* localise to the FAZ in *Leishmania*. Moreover, *T. brucei* FAZ proteins were shown to localise to the FAZ in *L. mexicana* (Wheeler, Sunter and Gull, 2016).

In the mammalian host, the *Leishmania* promastigote is taken up by a macrophage where it differentiates into an amastigote form within the parasitophorous vacuole. This differentiation involves the restructuring of the long motile flagellum, transitioning from a 9+2 axoneme, to a short non-motile 9+0 axoneme (E. Gluenz *et al.*, 2010). The amastigote flagellar pocket organisation appears similar to the promastigote form but with key differences. The flagellar pocket neck region is narrower with a reduced gap to the flagellum and at the distal end of the neck is a constriction, which squeezes the flagellum at this point. This constriction and the

reduced gap between the flagellum and the neck will likely greatly restrict access to the flagellar pocket (Wheeler, Sunter and Gull, 2016). The rearrangement of the flagellar pocket neck structure involves a restructuring of the FAZ with proteins such as FAZ2 now localising to the neck constriction point. The width of the flagellar pocket bulbous region is larger minimising pocket surface area. The smaller surface area will likely reduce the uptake capacity of the pocket, which correlates with the slower growth of amastigotes plus there is now less surface area exposed to the environment of parasitophorous vacuole which is acidic and full of proteases (Antoine *et al.*, 1990, 1998; Wheeler, Sunter and Gull, 2016).

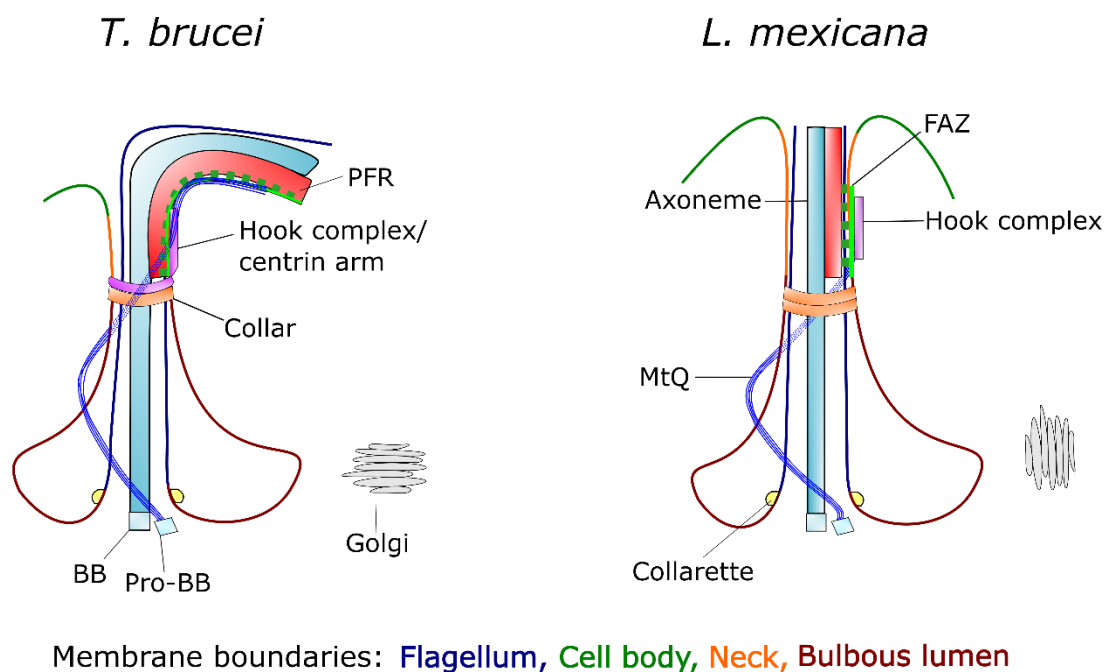


Figure 1.2 There are similarities and differences in *T. brucei* and *L. mexicana* flagellar pocket structure. *T. brucei* and *L. mexicana* share the following features; axoneme (cyan), PFR (red), basal bodies (light blue), collarette (yellow) and the collar (orange), MtQ (blue), FAZ (dotted green) and FAZ filament (green). The FAZ extends for the majority of cell length enabling the lateral attachment of the flagellum in *T. brucei*. Both pockets have four membrane boundaries (Flagellum, cell body, neck and bulbous lumen) indicated by colour. Adapted from (Halliday *et al.*, 2021)

1.4 Flagellar pocket shape is critical for its function

The correct formation and morphology of the flagellar pocket is vital for its exocytosis/endocytosis function and for cell survival. The knockdown of the flagellar pocket collar protein, BILBO1 by RNAi in procyclic form *T. brucei* prevented flagellar pocket formation and caused endo- and exocytosis defects as shown by cytoplasmic vesicle accumulation (Bonhivers *et al.*, 2008). The hook complex proteins, TbSmee and TbMORN1 are important for hook complex morphology and function. The depletion of TbSmee in *T. brucei* altered hook complex morphology resulting in a reduced rate of both fluid-phase and membrane marker uptake (Perry *et al.*, 2018). The RNAi knockdown of TbMORN1 in bloodstream form *T. brucei* caused an enlarged flagellar pocket (BigEye), which is associated with a mismatch in the delivery and recycling of membrane from the flagellar pocket. The loss of TbMORN1 caused a reduction in dextran uptake as expected with the BigEye phenotype; however, there was an additional phenotype with other larger uptake markers such as concanavalin A and bovine serum albumin (BSA) conjugated to gold unable to effectively access the flagellar pocket lumen, suggesting that hook complex has an important role in maintaining the flagellar pocket neck channel (Morriswood *et al.*, 2009; Morriswood and Schmidt, 2015).

1.5 FAZ is important for cell and flagellar pocket morphogenesis

The FAZ is a large interconnected set of fibres, filaments, junctional complexes linking flagellum skeleton through both flagellum and cell body membranes to the specialised FAZ filament and associated MtQ (Vickerman, 1969; Lacomble *et al.*, 2009; Sunter and Gull, 2016). In trypanosomes, the FAZ can be split into major structural domains; 1) FAZ flagellum domain, 2) FAZ intracellular domain and 3) cell body domain (**Fig 1.3**) (Sunter and Gull, 2016).

The first FAZ protein identified was gp72 in *T. cruzi* (Cooper, De Jesus and Cross, 1993; Rocha *et al.*, 2006). Gp72 discovery led to an identification of its ortholog, FLA1 in *T. brucei*, which is located in the FAZ intracellular domain (**Fig 1.3**) (Nozaki, Haynes and

Cross, 1996; Sun *et al.*, 2012). To date, 58 FAZ proteins were identified in *T. brucei* so far and some of these have been studied with FAZ domain location and specific function identified (**Table 1.1**).

Proteins located in the FAZ flagellum domain include ClpGM6, Flagellar Member 3 (FLAM3) and FAZ27, which all form a complex (**Fig 1.3**) and their depletion in *T. brucei* resulted in a similar phenotype; shortening of the FAZ with a transition from a trypomastigote to epimastigote-like morphology with the cells still able to proliferate in culture (Rotureau, Subota and Bastin, 2011; B. Rotureau *et al.*, 2014; Hayes *et al.*, 2014; Sunter *et al.*, 2015; An *et al.*, 2020). Whilst RNAi knockdown of proteins in the intracellular domain had a different phenotype. Depletion of FLA1 in *T. brucei* resulted in a reduction in FAZ length and flagellum detachment, leading to cell death (Lacount, Barrett and Donelson, 2002). The knockdown of the FLA1 associated protein FLA1 binding protein (FLA1BP) showed a similar phenotype although the cells continued to proliferate (Lacount, Barrett and Donelson, 2002). Depletion of FAZ10 caused defects in cell morphogenesis, flagellum attachment, positioning of kinetoplast/nucleus (Moreira *et al.*, 2017). FAZ5 on cell body membrane has flagellum attachment and cell morphology defects (Sunter *et al.*, 2015)

The knockdown of FAZ proteins located in the cell body domain had two distinct phenotypes (Sunter and Gull, 2016). The depletion of FAZ filament domain proteins, FAZ2 and coiled coil C2 domain containing protein (CC2D) (**Fig 1.3**) caused full length flagellum detachment and cell death (Zhou *et al.*, 2011; Q. Zhou *et al.*, 2015). On the other hand, depletion of another *T. brucei* FAZ filament protein, FAZ1, displayed only partial flagellum detachment with a disorganisation in FAZ structure (Vaughan *et al.*, 2008; Sunter and Gull, 2016). FAZ2 and CC2D are potentially located closer to the intracellular domain than FAZ1 and therefore their depletion had a similar phenotype as seen with the intracellular domain proteins, FLA1 and FLA1BP (**Fig 1.3**). However, FAZ9 a cell body domain protein located at the distal end of the FAZ does not fit with this pattern as its depletion in *T. brucei*, resulted in the generation of epimastigote-like cells without flagellum detachment or changes in FAZ length (McAllaster *et al.*, 2015; Sunter and Gull, 2016). Overall, these studies in trypanosomes have shown

that depletion of a FAZ protein causes alterations in cell shape and size and the FAZ is therefore described as a cellular ruler (Sunter and Gull, 2016).

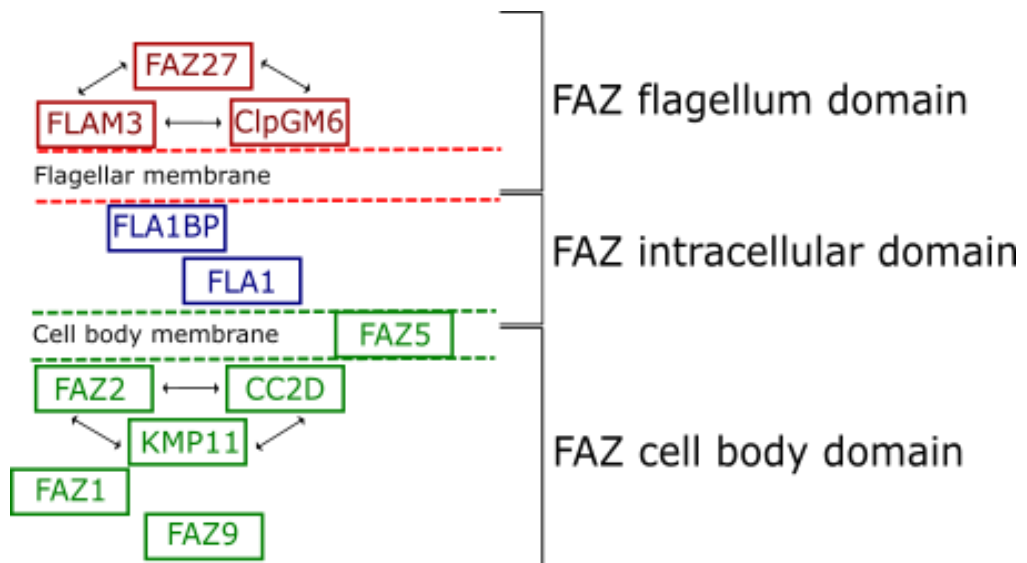


Figure 1.3 There are three main FAZ domains in trypanosomes. FAZ proteins are located within different domains- FAZ flagellum domain (in red), FAZ intracellular domain (in blue) and the cell body domain (in green). The locations of these proteins can be predicted by RNAi phenotype (Sunter and Gull, 2016).

Table 1.1 FAZ proteins identified in *T. brucei*.

Majority of proteins were identified in procyclics (insect form) but four were identified in the bloodstream form (BSF) as indicated next to protein name

Gene ID	Gene name	Known domain	RNAi Phenotype (if any)	FAZ localisation and characterisation references
Tb927.8.4010	FLA1	Intracellular	Flagellum detachment and cytokinesis defects	(Nozaki, Haynes and Cross, 1996; Lacount, Barrett and Donelson, 2002; Sun <i>et al.</i> , 2013)
Tb927.8.4060	FLA2 (BSF)	Intracellular		(Lacount, Barrett and Donelson, 2002)
Tb927.4.3740	FAZ1	FAZ filament	Flagellum attachment, cytokinesis and FAZ architecture defects	(Vaughan <i>et al.</i> , 2008)
Tb927.8.4780	FLAM3	Flagellum	Change from trypomastigote to epimastigote morphology, reduction in FAZ length and flagellum detachment	(Brice Rotureau <i>et al.</i> , 2014; Subota <i>et al.</i> , 2014; Sunter <i>et al.</i> , 2015; An and Li, 2018)
Tb927.10.2880	Ca ²⁺ channel (FAZ26)	Intracellular		(Oberholzer <i>et al.</i> , 2011; Zhou, An, <i>et al.</i> , 2018)
Tb927.4.2080	CC2D	FAZ filament	Inhibited FAZ filament assembly and cell morphogenesis defects	(Zhou <i>et al.</i> , 2011)
Tb927.11.13230	VAMP	FAZ-ER	Reduction in FAZ ER and in ER associated with FP	(Lacomble <i>et al.</i> , 2012)
Tb927.8.4050	FLA1BP	Intracellular	Change from trypomastigote to epimastigote morphology, reduction in FAZ and cell body length and flagellum detachment	(Sun <i>et al.</i> , 2013, 2018)
Tb927.8.4100	FLA1BP	Intracellular	Change from trypomastigote to epimastigote morphology, reduction in FAZ and cell body length and flagellum detachment	(Sun <i>et al.</i> , 2013, 2018)
Tb927.8.4110	FLA3 (BSF)	Intracellular		(Sun <i>et al.</i> , 2013)
Tb927.5.4570	FLA3 (BSF)	Intracellular	Flagellum detachment and cytokinesis defects	(Woods <i>et al.</i> , 2013)
Tb927.5.4580	FLA3 (BSF)	Intracellular	Flagellum detachment and cytokinesis defects	(Woods <i>et al.</i> , 2013)
Tb927.7.3330	FAZ10	Intracellular	Cell morphogenesis, flagellum attachment, K/N positioning and cleavage furrow defects	(Morriswood <i>et al.</i> , 2013; Moreira <i>et al.</i> , 2017)
Tb927.4.5340	FAZ11	Not known		(Morriswood <i>et al.</i> , 2013; Sunter <i>et al.</i> , 2015)
Tb927.11.1090	ClpGM6	Flagellum	Change from trypomastigote to epimastigote morphology, reduction in FAZ length and flagellum detachment	(Hayes <i>et al.</i> , 2014)
Tb927.1.4310	FAZ2	FAZ filament	Inhibited FAZ filament assembly, cell morphogenesis defects, flagellum detachment and cell death	(Q. Zhou <i>et al.</i> , 2015; Sunter <i>et al.</i> , 2015)
Tb927.11.12530	FAZ3	FAZ filament		(Sunter <i>et al.</i> , 2015)
Tb927.9.10530	FAZ4	FAZ filament		(Sunter <i>et al.</i> , 2015)
Tb927.10.8830	FAZ5	Intracellular	Attachment and cell morphology defects	(Sunter <i>et al.</i> , 2015)
Tb927.10.840	FAZ6	FAZ filament		(Sunter <i>et al.</i> , 2015)

Tb927.10.15390	FAZ7	FAZ filament		(Sunter <i>et al.</i> , 2015)
Tb927.4.2060	FAZ8	FAZ filament		(Qing Zhou <i>et al.</i> , 2015; Sunter <i>et al.</i> , 2015)
Tb927.10.14320	FAZ9	FAZ filament	Re-positioning of kinetoplast/nucleus	(McAllaster <i>et al.</i> , 2015; Sunter <i>et al.</i> , 2015)
Tb927.9.13820	KMP11	FAZ filament/ cell body	Flagellum detachment	(Q. Zhou <i>et al.</i> , 2015)
Tb927.9.13880	KMP11	FAZ filament/ cell body	Flagellum detachment	(Q. Zhou <i>et al.</i> , 2015)
Tb927.9.13920	KMP11	FAZ filament/ cell body	Flagellum detachment	(Q. Zhou <i>et al.</i> , 2015)
Tb927.11.2590	FAZ12	FAZ filament		(Hu, Zhou and Li, 2015b)
Tb927.3.1020	FAZ13	FAZ filament		(Hu, Zhou and Li, 2015b)
Tb927.8.6980	FAZ14	FAZ filament		(Hu, Zhou and Li, 2015b)
Tb927.11.3300	SAS-4	FAZ filament tip	Partial flagellum detachment, tryposmastigote to epimastigote like morphology, cytokinesis and growth defects	(Hu, Zhou and Li, 2015b)
Tb927.8.7070	FAZ15	Not known		(McAllaster <i>et al.</i> , 2015)
Tb927.5.3460	FAZ16	Not known		(McAllaster <i>et al.</i> , 2015; Hu <i>et al.</i> , 2019)
Tb927.10.7210	FAZ17	Not known		(McAllaster <i>et al.</i> , 2015)
Tb927.11.15800	TOEFAZ1	FAZ filament tip	Inhibits cytokinesis inhibition from anterior but triggers from cell posterior	(Sinclair-Davis, McAllaster and De Graffenried, 2017; Zhou, An, <i>et al.</i> , 2018; Hu <i>et al.</i> , 2019)
Tb927.10.12920	FAZ18	Not known		(Zhou, Hu and Li, 2016; Zhou, An, <i>et al.</i> , 2018; Hu <i>et al.</i> , 2019)
Tb927.3.3300	FAZ19	Not known		(Zhou, Hu and Li, 2016)
Tb927.11.9290	FAZ20	Not known		(Zhou, Hu and Li, 2016; Zhou, An, <i>et al.</i> , 2018)
Tb927.9.14290	CIF2	Not known		(Zhou, Hu and Li, 2016; Zhou, An, <i>et al.</i> , 2018)
Tb927.10.8240	CIF4	Not known	Inhibits cytokinesis initiation, disrupts CIF1 & FPRC localisation to new FAZ tip	(Hilton <i>et al.</i> , 2018; Hu <i>et al.</i> , 2019)
Tb927.10.13100	CIF3	Not known	Defective cytokinesis	(Kurasawa <i>et al.</i> , 2018; Zhou, An, <i>et al.</i> , 2018)
Tb927.8.6830	Kinesin	Not known		(Zhou, Lee, <i>et al.</i> , 2018; Hu <i>et al.</i> , 2019)
Tb927.7.5240	FAZ21	Not known		(Zhou, An, <i>et al.</i> , 2018; Hu <i>et al.</i> , 2019)
Tb927.10.9700	FAZ22	Not known		(Zhou, An, <i>et al.</i> , 2018; Hu <i>et al.</i> , 2019)

Tb927.3.4710	FAZ23	Not known		(Zhou, An, <i>et al.</i> , 2018)
Tb927.10.720	FAZ24	Not known		(Zhou, An, <i>et al.</i> , 2018)
Tb927.10.5870	FAZ25	Not known		(Zhou, An, <i>et al.</i> , 2018; Hu <i>et al.</i> , 2019)
Tb927.10.6360	FPRC	Not known	Cytokinesis and growth defects	(Zhou, An, <i>et al.</i> , 2018; Hu <i>et al.</i> , 2019)
Tb927.6.3840	Reticulon	FAZ-ER		(Zhou, An, <i>et al.</i> , 2018)
Tb927.10.13740	Synaptotagmin (FAZ35)	Not known		(Zhou, An, <i>et al.</i> , 2018)
Tb927.11.11480	Trichohyalin	Not known		(Zhou, An, <i>et al.</i> , 2018)
Tb927.10.870	Furrow 1 protein	Not known		(Zhou, An, <i>et al.</i> , 2018; Hu <i>et al.</i> , 2019)
Tb927.5.4380	KPP1	Not known		(Zhou, An, <i>et al.</i> , 2018)
Tb927.11.8350	KAT60a	Not known		(Zhou, An, <i>et al.</i> , 2018)
Tb927.9.9960	KAT80	Not known		(Zhou, An, <i>et al.</i> , 2018)
Tb927.8.4950	KLIF	Not known		(Zhou, An, <i>et al.</i> , 2018; Hu <i>et al.</i> , 2019)
Tb927.9.8180	FAZ31	Not known		(Hu <i>et al.</i> , 2019)
Tb927.11.3280	Kinesin-13 5	Not known		(Hu <i>et al.</i> , 2019)
Tb927.9.8350	FAZ27	Flagellum	Trypomastigote to epimastigote like morphology, reduction in FAZ and cell body length, flagellum detachment	(An <i>et al.</i> , 2020)

In *L. mexicana*, FAZ assembly and structure are less understood; however, Wheeler et al found that FAZ proteins could be separated into four classes based on their localisation patterns (Wheeler, Sunter and Gull, 2016). These are: 1) a short linear structure in the flagellum domain, 2) a short linear structure parallel to the flagellum (in the cell body domain), 3) a ring structure around the flagellum midway through the flagellar pocket or a 4) horseshoe/ring structure at the flagellum exit point (**Fig 1.4**) (Wheeler, Sunter and Gull, 2016).

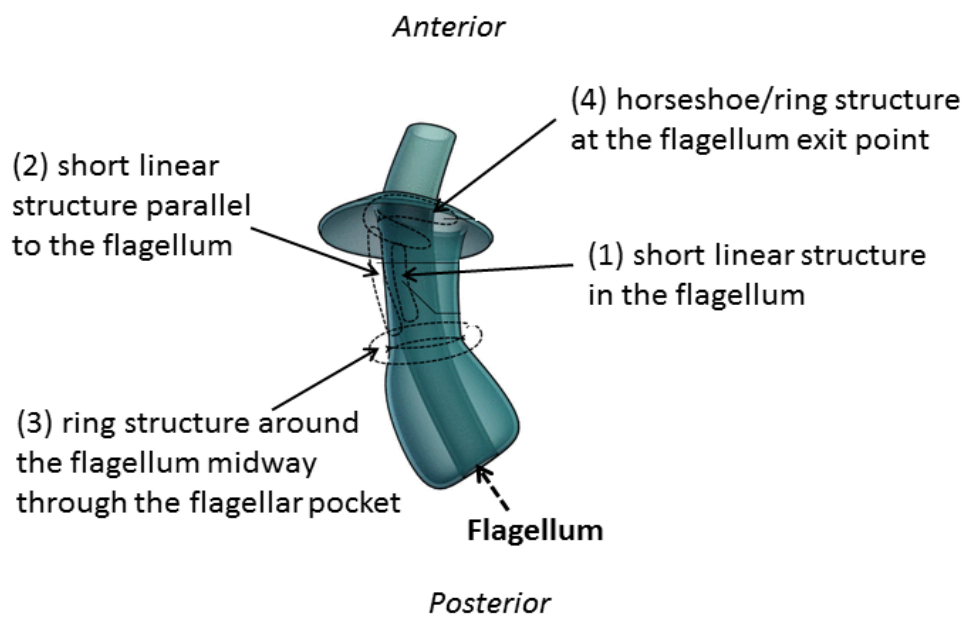


Figure 1.4 FAZ proteins in *L. mexicana* are split into classes based on localisation pattern. Four classes of FAZ protein localisation; 1) a short linear structure in the flagellum, 2) a short linear structure parallel to the flagellum (cell body side), 3) a ring structure around the flagellum midway through the flagellar pocket or a 4) horseshoe/ring structure at the flagellum exit point. Adapted from (Wheeler, Sunter and Gull, 2016)

The function of FAZ in *Leishmania* is also poorly understood; however, the first study by Sunter et al showed that FAZ5 in *Leishmania* is important for flagellar pocket architecture and function. In *L. mexicana* promastigotes the deletion of FAZ5 resulted in the shortening of flagellar pocket length and loss of attachment between the flagellum and the flagellar pocket neck region (Sunter *et al.*, 2019). These changes in

the flagellar pocket were associated with a reduced rate of endocytosis as observed with bulk, glycoprotein and plasma membrane uptake. In addition, the flagellar pocket of the FAZ5 null mutant amastigote had lost the typical two-part structure with the flagellar pocket neck region missing and only the constriction at the distal end of the flagellar pocket neck remaining. The flagellar pocket therefore only consisted of a large flagellar pocket bulbous domain. The changes to the FAZ and flagellar pocket neck in the FAZ5 null mutant were associated with a loss of pathogenicity in the mouse and an inability to develop and proliferate in the sand fly vector (Sunter *et al.*, 2019).

The deletion of FAZ2 a FAZ filament protein was found to cause anterior cell tip morphogenesis defects in *L. mexicana* (Halliday *et al.*, 2020). The membrane organisation at the anterior cell tip was disrupted, which resulted in FAZ mediated flagellum to flagellum connections causing delays in the late stage of cell cycle. This delay contributes the reduced growth rate demonstrating that FAZ2 is critical for cell segregation in *Leishmania*. Motility analysis showed there was a loss of directional movement in FAZ2 null mutant. Meanwhile they were unable to develop and proliferate in sandflies and unable to persist infection in mice (Halliday *et al.*, 2020). Most recently, a FAZ7 paralog, FAZ7B, which localises at the cell body side of FAZ was found to disrupt cell division, cell morphogenesis, flagellar pocket structure and function when deleted. The proliferation and pathogenicity of FAZ7B null mutant was also reduced (Corrales *et al.*, 2021).

1.6 The FAZ is intimately associated with flagellar pocket duplication and segregation

Flagellar pocket division is better understood in *T. brucei*. During the cell cycle, flagellar pocket division process begins with the nucleation of MtQ and biogenesis of new flagellum invading the existing flagellar pocket, while the pro-basal body matures (**Fig 1.5**) (S. Lacomble *et al.*, 2010; Wheeler, Gluenz and Gull, 2011). In *T. brucei*, upon maturation the new basal body rotates around the old basal body in an anti-clockwise direction (**Fig 1.5**). This results in the new basal body being positioned at the posterior side of the old. This move introduces a fold into the flagellar pocket

membrane around the old MtQ, which starts the flagellar pocket division process (**Fig 1.5**) (S. Lacomble *et al.*, 2010). However, during trypomastigote to epimastigote differentiation seen in tsetse fly, it was found that the flagellar pocket division was not dependent on the introduction of a fold facilitated by basal body rotation (Lemos *et al.*, 2019). Instead, the new flagellar pocket is formed before basal body rotation, which occurs later (Lemos *et al.*, 2019). With *L. mexicana*, the flagellar pocket division is not as well understood, but it is known that the basal body and kinetoplast segregation do not occur till later in the cell cycle, which suggests that the flagellar pocket division occurs later in a short time window (**Fig 1.5**) (Wheeler, Gull and Sunter, 2019). Due to the nature of the flagellar pocket position at the anterior end of the cell body, it is possible that basal body rotation might not be needed to initiate flagellar pocket segregation (**Fig 1.5**) (Wheeler, Gull and Sunter, 2019).

Once, the flagellar pocket divides, the formation of the cytokinetic furrow initiating cytokinesis occurs (Sherwin and Gull, 1989; S. Lacomble *et al.*, 2010). In *T. brucei*, the formation of new FAZ begins along the line of old FAZ during flagellum biogenesis. Next, the old and new FAZ along with their associated flagellar pockets separates by the insertion of new microtubules (Wheeler *et al.*, 2013). The cytokinesis furrow begins at the distal tip of the new FAZ mediated by TOEFAZ1/CIF1, CIF2, CIF3 and CIF4 (Zhou *et al.*, 2016; Zhou, Hu and Li, 2016; Sinclair-Davis, McAllaster and De Graffenried, 2017; Kurasawa *et al.*, 2018). Cytokinesis continues from the anterior to posterior axis, allowing the correct inheritance of organelles in daughter cells. Similarly, in *Leishmania* promastigotes, cytokinesis is initiated from the anterior and progresses to the posterior cell tip (Ambit *et al.*, 2011; Wheeler, Gluenz and Gull, 2011). The FAZ is therefore important for cytokinesis and with the ancestral morphology suggested to be a promastigote it is possible that the one of the key functions of the FAZ is providing positional information for cell division (Wheeler, Sunter and Gull, 2016).

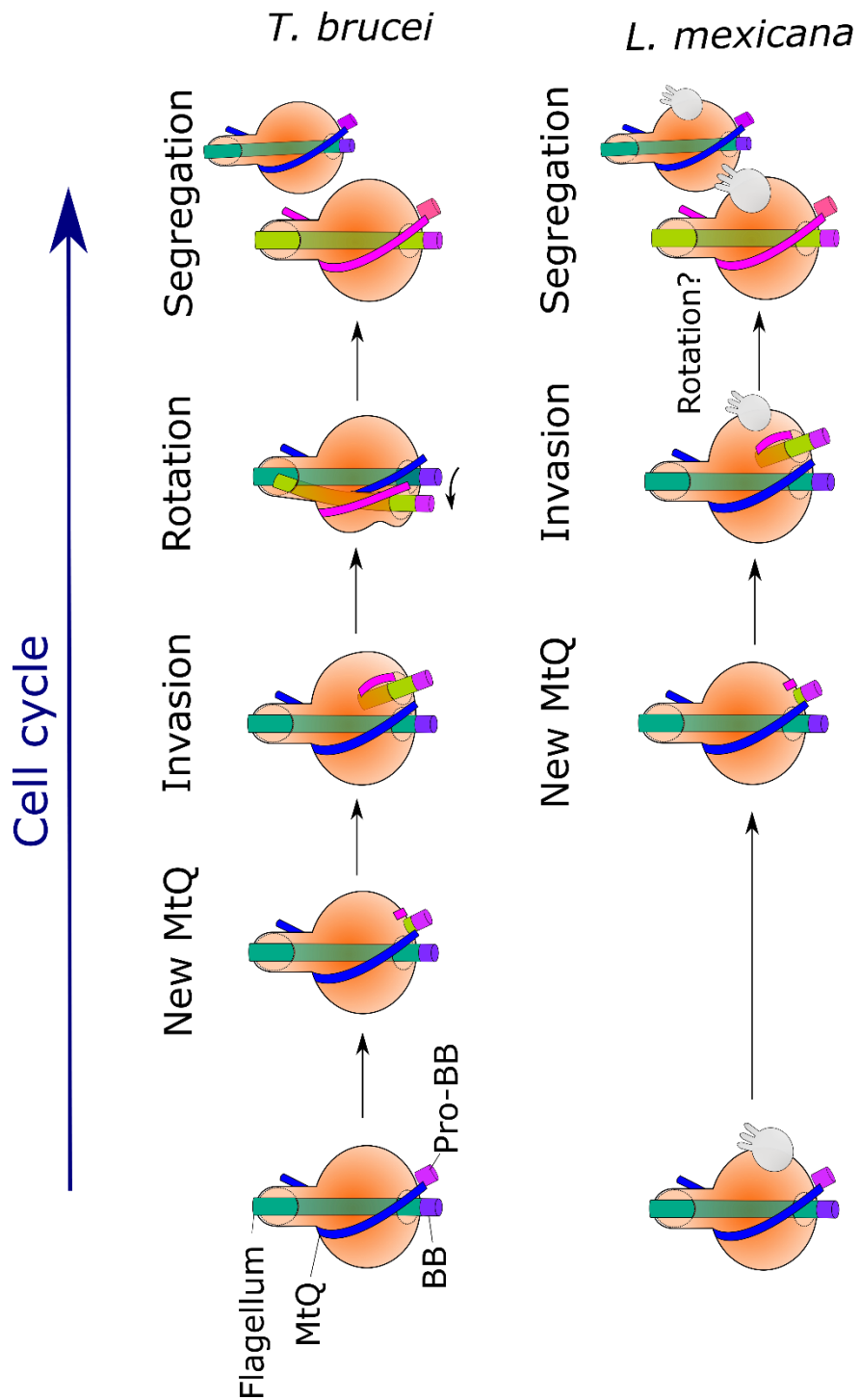


Figure 1.5 Flagellar pocket duplication in *T. brucei* and *L. mexicana*. Steps in flagellar pocket duplication and segregation includes 1) the formation of MtQ, 2) Invasion of new flagellum into existing flagellar pocket, 3) basal body mediated rotation followed by 4) flagellar pocket segregation. In *L. mexicana*, flagellar pocket division occurs later in cell cycle with the requirement for rotation unknown. Adapted from (Halliday *et al.*, 2021).

1.7 Flagellar pocket is important for pathogenicity

An important function for the flagellar pocket is as the site of endocytosis/exocytosis for nutrient uptake, immune evasion and secretory pathway with the secretory and endocytic machinery positioned close to the flagellar pocket (**Fig 1.6**). Many different protein families have roles in these exocytotic, endocytic, and recycling pathways (Field and Carrington, 2009).

1.7.1 Endocytosis, sorting and recycling

Endocytosis from the flagellar pocket is clathrin mediated (**Fig 1.6**) (Allen, Goulding and Field, 2003; Hung *et al.*, 2004). The effects of clathrin depletion was studied in *T. brucei*, which showed that bloodstream form cells developed a BigEye morphology with a rapid onset of cell death, whilst in procyclic form cells there was a slower onset of cell death with severe vesicle accumulation of transport vesicles (Allen, Goulding and Field, 2003). Clathrin mediated endocytosis has a number of steps, including nucleation, cargo selection, coat assembly, scission and uncoating (McMahon and Boucrot, 2011). These steps are dependent on phosphoinositides, derivatives of phosphatidylinositol lipids that in *T. brucei* are mainly concentrated in the flagellar pocket (Manna and Field, 2015). Studies have showed the importance of phosphatidylinositols for endocytosis in *T. brucei*, with the depletion of TbPIPKA, an enzyme with PIP kinase activity, which was located to the neck of the pocket, led to the absence of the phosphatidylinositol in the pocket, causing its enlargement and impairment of endocytosis (Demmel *et al.*, 2016). Phosphoinositides interact with adaptor protein 2 complex (AP2) for cargo selection to clathrin coated pits in many eukaryotes (**Fig 1.6**) (Gaidarov and Keen, 1999; Collins *et al.*, 2002; Kelly *et al.*, 2008). While AP2 is found across trypanosomatids, AP2 is not found in *T. brucei* (Field and Carrington, 2009; Manna, Kelly and Field, 2013) and this could be an evolutionary adaptation for efficient endocytosis and recycling of VSG (Field and Carrington, 2009; Manna, Kelly and Field, 2013). Many other proteins interact with clathrin, including the AP-1 complex, ENTH-domain family member, EpsinR, Soluble N-ethylmaleimide-sensitive factor attachment protein receptor proteins (SNAREs), Small Arf GTPase-activating protein (SMAP) and AP-2 associated kinase AAK1. These proteins localise

to the flagellar pocket and endomembrane system (Gabernet-Castello, Dacks and Field, 2009; Manna *et al.*, 2017).

1.7.2 Nutrient uptake

Trypanosomatids need haem for survival and they rely on the acquisition of this from their hosts via endocytosis in the flagellar pocket (Krishnamurthy *et al.*, 2005; Tripodi, Menendez Bravo and Cricco, 2011; Kořený, Oborník and Lukeš, 2013). In *Leishmania*, haemoglobin is taken up by the hexokinase haemoglobin receptor located in the flagellar pocket (Krishnamurthy *et al.*, 2005). In the *T. brucei* bloodstream form, haem uptake is mediated by the haptoglobin-haemoglobin receptor which is distributed over the plasma membrane (Vanhollebeke *et al.*, 2008). However, this receptor is not expressed in procyclic stage and instead another protein, the haem transporter protein, TbHrg is responsible for haem uptake and this protein is predominantly present in the flagellar pocket area of the cell (Horáková *et al.*, 2017). Rab7 was found to be important for uptake and degradation of hemoglobin (Patel *et al.*, 2008; Silverman *et al.*, 2011).

For *T. brucei* bloodstream form parasite survival, they need iron from the host. This iron is scavenged by a class of proteins, called transferrins, which is internalized by the parasite by receptor-mediated endocytosis, transferrin receptor (Schell, Borowy and Overath, 1991; Steverding *et al.*, 1995; Steverding, 2000). This was found to require the autophagy-related protein 24 (ATG 24), with a significant reduced receptor-mediated endocytosis of transferrin after ATG24 depletion. Loss of ATG24 also caused an enlargement of the flagellar pocket, due to a block of bulk endocytosis as concanavalin A was restricted to the enlarged pocket and did not enter the endocytic system (Brennand *et al.*, 2015).

1.7.3 Exocytosis

Exocytosis of post-Golgi/secretory vesicles is regulated by exocyst complex (**Fig 1.6**). This structure is made up of 9 subunits, Sec 3, 5, 6, 8, 10, 15, Exo 70, Exo 84 and Exo99 (Boehm *et al.*, 2017). Exo99 is a novel component of kinetoplastids, which suggests a unique role in export pathways. The exocyst complex interact with GTPases and

SNAREs. Exo99 and Sec 15 RNAi in *T. brucei* displayed an abnormally enlarged flagellar pocket, which filled a large proportion of cell volume, the 'BigEye' morphology. This showed the importance of the complex in maintaining membrane flow to/from the flagellar pocket (Boehm *et al.*, 2017).

1.7.4 The flagellar pocket is important for flagellum assembly

The flagellar pocket has an important role in the assembly of the flagellum as both the membrane and membrane proteins required for flagellum construction will pass through the flagellar pocket. However, we know little about this process. For example, flagellum membrane proteins may be sorted before delivery to the flagellar pocket or this sorting may occur within the flagellar pocket itself. In other organisms the BBSome (a multiprotein complex) has an important role in delivering flagellum membrane components (Wingfield, Lechtreck and Lorentzen, 2018). In *Leishmania* the deletion of BBS1 reduced the pathogenicity of the parasite in the mouse but had no gross effect on the flagellum, though there was an accumulation of vacuoles in the vicinity of the flagellar pocket, which also had a perturbed shape (Price *et al.*, 2013). Whilst the deletion of BBSome proteins in *T. brucei* perturbs endocytic trafficking and disrupts virulence no changes to the flagellum were observed (Langousis *et al.*, 2016). In addition to assembling the flagellum, these parasites must also assemble the FAZ, which has domains within both the cell body and flagellum. The site of assembly of the FAZ is at the proximal end of the flagellum, close to flagellar pocket and the membrane proteins involved in the FAZ assembly must be also trafficked through the flagellar pocket (Q. Zhou *et al.*, 2015; Sunter *et al.*, 2015; Sunter and Gull, 2016).

1.7.5. Secretion of molecules in the host

There is evidence that molecules are released into the extracellular environment with a purpose of interacting/manipulating the host and this release is likely to occur via the flagellar pocket. A number of mass spectrometry studies have been performed on the whole cell culture media in which these parasites have been grown or fractions of the media that have been enriched for extracellular vesicles. For

example, in the *T. brucei* secretome, proteins were identified with the potential for different functions such as heat shock protein acting as a mediator in intercellular signalling and purine salvage enzymes to recover host purines (Pellé, Schramm and Parkin, 1998; Calderwood, Mambula and Gray, 2007; Geiger *et al.*, 2010). Furthermore, ESAG9 protein has been shown to be released from bloodstream stumpy forms, generating the potential interaction with mammalian immune system or as a pre-adaption for parasite transmission (Barnwell *et al.*, 2010).

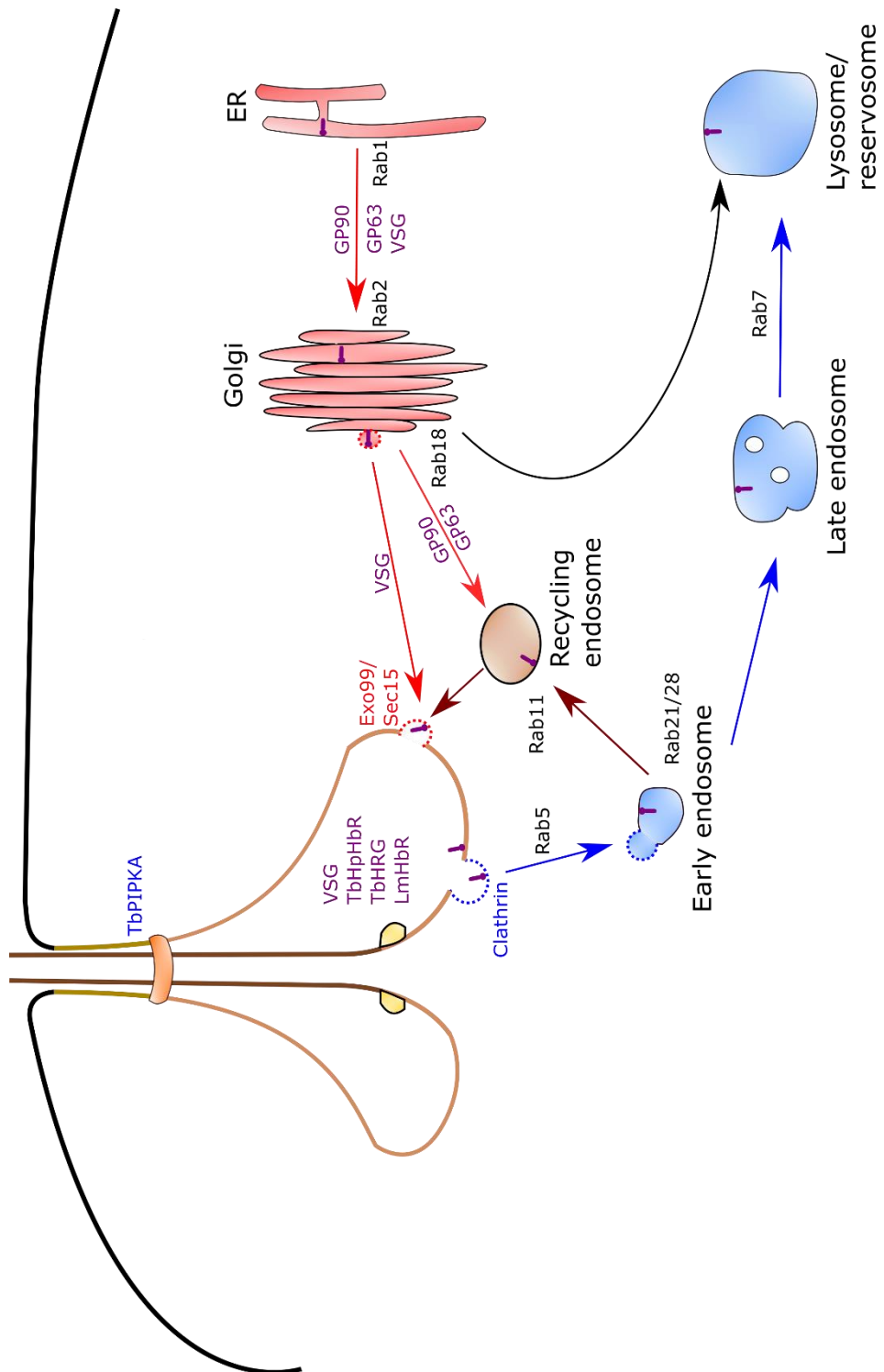


Figure 1. 6: Endocytosis and exocytosis pathways in *Trypanosomatids*. Endocytic (blue) and exocytic (red) pathways with trafficking routes of proteins (by arrows) are shown. Endocytosed proteins are sorted in endosomes for destinations in the lysosome, Golgi or recycled (brown) back to the pocket. Rab proteins have various roles within the endomembrane system.

1.8 Aims

L. mexicana has a highly defined cell organisation, which includes a flagellar pocket, an invagination of the cell membrane at the base of flagellum (Sunter and Gull, 2017). Here, the complex FAZ structure provides the attachment between the flagellum and cell body membranes and terminates at the exit point of the flagellar pocket neck (Wheeler, Sunter and Gull, 2016). *T. brucei* differs with an extension of FAZ organised in junctional complexes along the majority of the cell body length (Vickerman, 1969; Lacomble *et al.*, 2009; Sunter and Gull, 2016). While research into the FAZ has been heavily dominated by *T. brucei*, some work has begun in *L. mexicana*, which demonstrated that FAZ is important for cell morphogenesis and flagellar pocket function, including nutrient uptake and parasite pathogenicity (Sunter *et al.*, 2019; Corrales *et al.*, 2021; Halliday *et al.*, 2021). However, a poor understanding of FAZ structure organisation and the specific roles of the proteins within it remains.

This thesis aims to answer to two outstanding questions - 1) How is the molecular structure of the FAZ organised in *L. mexicana* and 2) What are the specific roles of the FAZ proteins in relation to FAZ assembly and cell morphogenesis? The specific aims of each chapter are as follows:

Chapter 3 - Identification of potential FAZ proteins using TrypTag and bioinformatics leading to the discovery of new FAZ proteins in *L. mexicana*.

Chapter 4 - Determination of potential functional groups based on FAZ localisation classes in *L. mexicana*.

Chapter 5 - Determination of the roles in *L. mexicana* of the flagellum FAZ domain proteins, FAZ27 and FAZ34 by the analysis of cell morphogenesis, FAZ assembly, overall flagellar pocket organisation and motility.

Chapter 6 - Determination of the role of the cell body FAZ domain protein, CC2D in *L. mexicana* and how it compares to its fellow cell body domain protein FAZ2 by the analysis of cell morphogenesis, FAZ assembly dependency relationships, overall flagellar pocket organisation and motility.

Chapter 2

Materials and Methods

2.1 Bioinformatics

2.1.1 Identifying FAZ proteins in *Trypanosoma brucei* using TrypTag

TrypTag; the *Trypanosoma brucei* genome wide resource was used to identify proteins with FAZ localisations (Dean, Sunter and Wheeler, 2017). By using the 'flagellum attachment zone' as the search term 96 proteins were identified and categorised into groups based on their localisation pattern.

2.1.2 Identifying protein ortholog in *Leishmania mexicana*

TriTrypDB; the Kinetoplastid genomics resource was used to identify FAZ orthologs in *L. mexicana* (Aslett *et al.*, 2009). Using orthoMCL 57 protein orthologs were identified and used for localisation screen.

2.1.3 Proteome analysis

TriTrypDB was used for the collection of protein sequences, molecular weight, isoelectric point and TMHMM (Transmembrane Helices; Hidden Markov Model) data on each listed FAZ proteins (Aslett *et al.*, 2009). The protein sequence of each FAZ protein was inserted into InterPro search tool to identify potential domains of interest (Mitchell *et al.*, 2019).

2.2 Molecular Biology

2.2.1 Generation of FAZ and flagellar pocket markers tagging constructs

FAZ orthologs in *L. mexicana* were endogenously tagged at either N or C-terminus. LeishGEdit, an online resource for CRISPR Cas9 T7 RNA polymerase gene editing in *L. mexicana* was used to extract primer sequences for use with pPLOT plasmids to create these tagging cassettes (Beneke *et al.*, 2017). Tagging primers are listed in **Appendix A**. pPLOT plasmids containing a drug resistance marker with a fusion fluorescent tag served as DNA templates for PCR amplification of tagging cassettes. pPLOT puro-mcherry-puro plasmids were used to generate FAZ domains marker, FLAM3, FLA1BP, FAZ5, FAZ2, CC2D, FAZ3 and FAZ10 and flagellar pocket marker

(LmxM.23.0060 and LmxM.06.0030) tagging cassettes. pPLOT blast-mNG-blast plasmids were used to generate FAZ ortholog tagging cassettes for the screen. These constructs were amplified using Expand High Fidelity (Hifi) polymerase (Sigma 4738276001). Each reaction contained 5 µl 10x Expand High Fidelity Buffer, final MgCl₂ concentration of 3 mM, 2% DMSO, 0.2 mM dTNPs, 25 ng pPLOT, 1 µM each of either upstream or downstream forward and reverse primers with 1 unit of HiFi polymerase made up in 50 µl. The thermocycling conditions used were 5 minutes of denaturation at 94°C, 35 cycles of 30 seconds denaturation at 94°C, 30 seconds of annealing at 60°C and 2 minutes of extension with further 7 minutes of final extension at 72°C.

For each gene, a single guide RNA (sgRNA) containing T7 RNA polymerase promotor, 20 bp target sequence and CRISPR CAS9 backbone were produced to introduce a double strand break at either upstream of ORF (5' end) for C-terminal tagging or downstream of ORF (3' end) for N-terminal tagging. sgRNA were amplified using Expand High Fidelity (Hifi) polymerase (Sigma 4738276001) with a common sgRNA primer sequence (G00) and either target specific forward or reverse primer as templates. Each reaction contained 2 µl 10x Expand High Fidelity Buffer, final MgCl₂ concentration of 1.5 mM, 0.2 mM dTNPs, 1 µM target specific primer and 1 µM G00 with 1 unit of HiFi polymerase made up in 20 µl. The thermocycling conditions used were 30 seconds of denaturation at 98°C, 35 cycles of 10 seconds denaturation at 98°C, 30 seconds of annealing at 60°C and 15 seconds of extension at 72°C.

Tagging cassettes and sgRNAs generated by PCR were loaded with purple dye (NEB B7024S) and run on SYBR safe (Invitrogen S33102) stained 0.8% agarose gel (Sigma A9539) in 1x TAE buffer at 90 volts for 35 minutes (Bio-Rad). The correct amplification of tagging cassettes was checked by their band size with a 1Kb DNA ladder (NEB N0552S) using SyngeneGBox transilluminator. Correctly amplified cassettes were precipitated with sodium acetate-100% ethanol and washed with 70% ethanol with centrifugation steps before resuspending the pellet in 20 µl sterile ddH₂O prior to transfection.

2.2.2 Generation of FAZ deletion constructs

pT plasmids containing a drug resistance marker served as DNA templates for PCR amplification of deletion cassettes (Beneke *et al.*, 2017). pT plasmids, pTBlast and pTNeo containing blasticidin and neomycin drug markers respectively were used to generate a knockout with double drug resistance.

These constructs were amplified using Expand High Fidelity (Hifi) polymerase (Sigma 4738276001). Each reaction contained 5 μ l 10x Expand High Fidelity Buffer, final $MgCl_2$ concentration of 3 mM, 2% dimethyl sulfoxide (DMSO), 0.2 mM dTNPs, 25ng pT, 1 μ M each of upstream forward and downstream reverse primers with 1 unit of Hifi polymerase made up in 50 μ l. The primers used for gene deletion are listed in **Appendix C**. The thermocycling conditions used were 5 minutes of denaturation at 94°C, 35 cycles of 30 seconds denaturation at 94°C, 30 seconds of annealing at 60°C and 2 minutes of extension with further 7 minutes of final extension at 72°C.

For each gene replacement, sgRNAs were produced to introduce a double strand break at both upstream and downstream of ORF. sgRNA were amplified using Expand High Fidelity (Hifi) polymerase (Sigma 4738276001) with a common sgRNA primer sequence (G00) and forward/reverse primer as templates. Each reaction contained 2 μ l 10x Expand High Fidelity Buffer, final $MgCl_2$ concentration of 1.5 mM, 0.2 mM dTNPs, 1 μ M target specific primer and 1 μ M G00 with 1 unit of HiFi polymerase made up in 20 μ l. The thermocycling conditions used were 30 seconds of denaturation at 98°C, 35 cycles of 10 seconds denaturation at 98°C, 30 seconds of annealing at 60°C and 15 seconds of extension at 72°C.

Correct amplification of deletion cassettes and sgRNAs generated by PCR were checked by gel electrophoresis using the same conditions as above (described in 2.2.1). Correctly amplified cassettes were precipitated with 0.5 M sodium acetate and 100% ethanol and washed with 70% ethanol with centrifugation steps before resuspending the pellet in 20 μ l sterile double distilled water (ddH₂O) prior to transfection.

2.2.3 The confirmation of null mutant cell lines

To confirm the loss of target gene in null mutant cell lines, genome DNA (gDNA) was extracted using DNEASY Blood & tissue kit (Qiagen 69506) according to manufacturer's instructions and eluted in 50 μ l ddH₂O. The concentration of gDNA was determined using Nanodrop spectrophotometer (ND-100, Lab Tech).

The primers were manually designed aimed to amplify a 500 bp region of target ORFs using Expand High Fidelity (Hifi) polymerase (Sigma 4738276001). An exception was made for LmxM.04.1100, which has a region of 400 bp targeted. List of primers used for confirmation PCR are listed in **Appendix D**. Each reaction contained 5 μ l 10x Expand High Fidelity Buffer, final MgCl₂ concentration range of 1.5-3 mM, 0-2% DMSO, 0.2 mM dTNPs, 200-300 ng gDNA, 0.1 μ M each of forward and reverse primers with 1 unit of HiFi polymerase made up in 50 μ l. The thermocycling conditions used were 5 minutes of denaturation at 94°C, 25 cycles of 30 seconds denaturation at 94°C, 30 seconds of annealing at 59°C and 30 minutes of extension with further 7 minutes of final extension at 72°C.

These PCR products were checked by gel electrophoresis (described in 2.2.1) alongside the parental gDNA and ddH₂O as positive and negative controls.

2.2.4 Generation of FAZ addback plasmids

For the generation of addback plasmids, the parental gDNA was extracted using DNEASY blood & tissue kit (Qiagen 69506) according to manufacturer's instructions and eluted in 50 μ l ddH₂O. This gDNA was used as template to generate addback genes for LmxM.04.0890, LmxM.33.2540, LmxM.18.1440 and its EF-hand pair domains (EF-1 and EF-2). The open reading frames were amplified by PCR with manually designed primers which contained XbaI and BamHI restriction sites listed in **Table 2.1** using Expand High Fidelity (Hifi) polymerase (Sigma 4738276001). Each reaction contained 5 μ l 10x Expand High Fidelity Buffer, final MgCl₂ concentration of 3 mM, 2% DMSO, 0.2 mM dTNPs, 2-10 ng parental gDNA, 1 μ M each of forward and reverse primers with 1 unit of HiFi polymerase made up in 50 μ l. The thermocycling conditions used were 5 minutes of denaturation at 94°C, 25 cycles of 30 seconds

denaturation at 94°C, 30 seconds of annealing at 57°C and target of 1 kb per minute of extension (e.g. 1.5 kb of gene = 90 seconds of extension time) with further 7 minutes of final extension at 72°C.

These PCR products were run on SYBR safe (Invitrogen S33102) stained 0.8% agarose gel (Sigma A9539) under the same conditions as above (described in 2.2.1) to check their size. Correctly amplified addback genes were extracted with a sterile blade and purified from the gel using Monarch gel extraction kit (NEB T1020) and eluted in 50 µl ddH₂O. All PCR products were digested with XbaI & BamHI with their supplied 10x buffer (NEB R0145 & R0136) making up to 50 µl digest mix and incubated for 1 hour at 37°C to generate 'sticky ends'. Digested PCR products were purified by Monarch DNA clean up kit (NEB T1030). Plasmid pJ1364 was digested with XbaI & BamHI with their supplied 10x buffer (NEB R0145 & R0136) making up to 50 µl digest mix and incubated for 1 hour at 37°C. The digested plasmid was run on SYBR safe (Invitrogen S33102) stained 0.8% agarose gel (Sigma A9539) under the same conditions. The digest plasmid was extracted with a sterile blade and purified from the gel using Monarch gel extraction kit (NEB T1020) and eluted in 50 µl ddH₂O. The digested and purified PCR products were ligated into the pJ1364 backbone (**Figure 2.1A**). All ligations were carried out for 2 hours at room temperature using T4 DNA ligase with the supplied ligation buffer (NEB M0202) in 10 µl mix.

After ligation, the plasmid was transformed into 25 µl *E. coli* SURE 2 competent cells (Agilent Technologies 200152) by heat shock for 1 minute at 42°C. They were spread evenly onto LB Agar plates (Melford L24030-2000) containing 100 µg/ml ampicillin (Melford 7177-48-2) for selection at 37°C for 16 hours. Bacterial colonies were picked using sterile pipette tips and grown in 4 ml LB medium (Melford L24060-5000) containing 100 µg/ml ampicillin in a shaking incubator set at 37°C overnight. The plasmids were extracted using Monarch Mini-Prep kit (NEB T1010) according to manufacturer's instructions and eluted in 50 µl ddH₂O. Nanodrop spectrophotometer (ND-100, Lab Tech) was used to determine plasmid concentration.

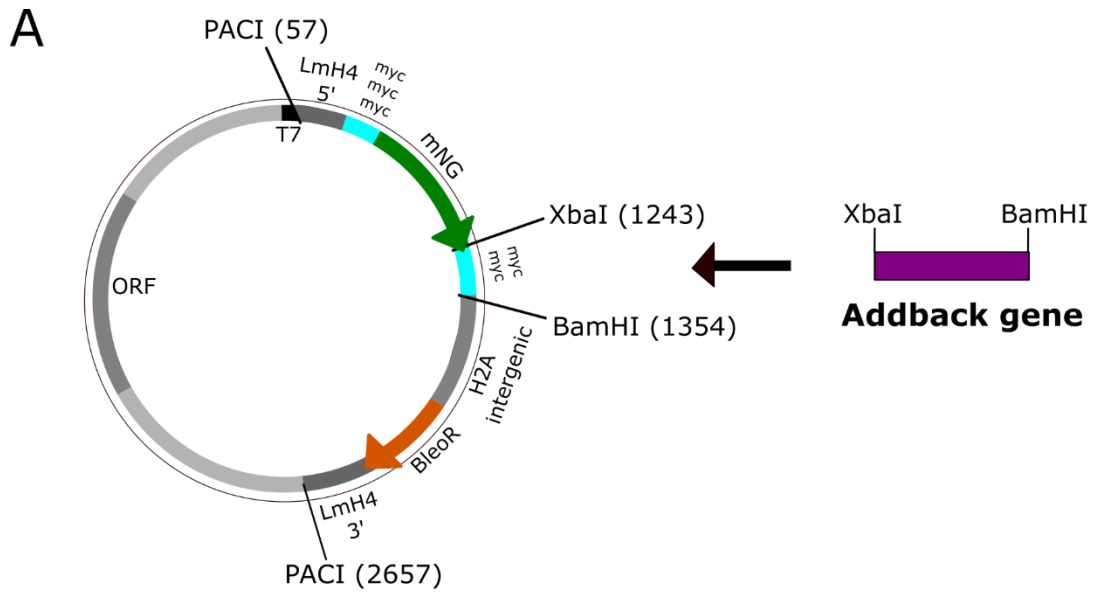
Modified plasmids were primarily checked by test digest and gel electrophoresis to confirm correct band sizes prior to sequencing check using Mix2Seq kit (Eurofins). Plasmids generated are listed in **Table 2.2**. When the correct sequences were confirmed, 10 µg of each plasmid was linearized with PacI (NEB R0547) (**Figure 2.1B**). The addback cassettes were precipitated with sodium acetate-100% ethanol and washed with 70% ethanol with centrifugation steps before resuspending the pellet in 20 µl sterile ddH₂O prior to transfection.

Table 2.1 Primers used for the generation of addback plasmids

Gene	Forward Primer with XbaI site	Reverse Primer with BamHI site
LmxM.33.2540	gaacattctagaATGTCCCGTATAGCACC CGTCGAC	cctaagggatccTACTGTAGCTCGTTGGA CGCCATG
LmxM.04.0890	gtacattctagaATGCTCGTCAACGCCGC CCCACGAG	cttgaaggatccTCACAGGTTGGTGGAGG TGCTGAAG
LmxM.18.1440	gtccagtctagaATGGGCGGCCGGATCTC GCGCGAG	gcattcggatccTCACATCAAATTCTTCATC TTCTC
LmxM.18.1440 _EF1	gtccagtctagaATGGGCGGCCGGATCTC GCGCGAG	gcattcggatccTCAATCCTCCTCTACCGC GTCTCC
LmxM.18.1440 _EF2	gtccagtctagaGGCATTGATTACTACGA TCACCTC	gcattcggatccTCACATCAAATTCTTCATC TTCTC

Table 2.2 Addback plasmids generated

Plasmid Name	mNG tag at N or C terminus
pJ1364_CC2DAB	N
pJ1364_FAZ27AB	N
pJ1364_FAZ34AB	N
pJ1364_FAZ34.EF1AB	N
pJ1364_FAZ34.EF2AB	N



pJ1364 plasmid

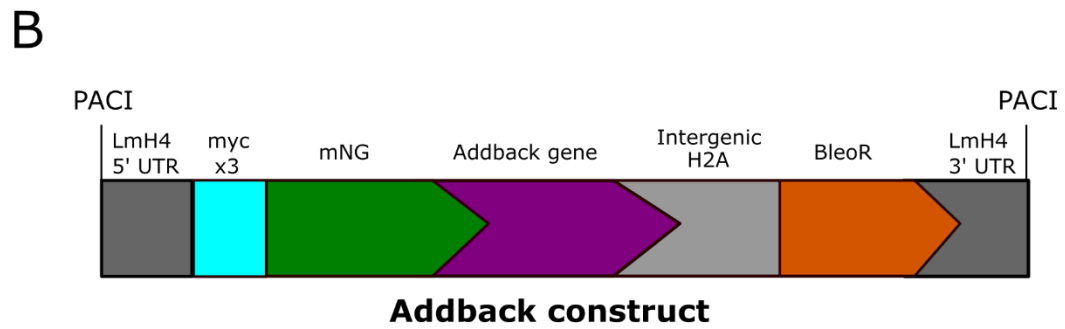


Figure 2.1 Generation of addback constructs. A) Addback ORF are inserted into XbaI and BamHI restriction enzyme sites of LmAB7 plasmid. B) An addback construct containing a mNG fusion tag was linearized by the restriction enzyme, PacI.

2.3 *L. mexicana* cell culture

2.3.1 Maintenance of cells

L. mexicana is listed by ACDP as a hazard category 2 pathogen. This organism was only maintained in culture form and kept in a category 2 laboratory. Lab coats and gloves were worn and removed prior to exit of the laboratory. Experiments were carried out in the microbiological safety cabinets (MBSCs) and when no longer in use this organism was killed by 2% virkon solution treatment for 1 hour. *L. mexicana* (WHO strain MNYC/BZ/1962/M379) promastigote cells used for this work were grown in M199 medium (Thermo-Fisher 31100019) with Earle's salts, L-glutamine, 10% FCS, 40 mM HEPES-NaOH (pH7.3), 26 mM NaHCO₃ and 5 µg/mL hemin at 28°C incubator. Logarithmic growth was maintained by regular sub-culturing.

2.3.2 Generation of tagging, null mutant and addback cell lines

The tagging, deletion and addback constructs were added into cuvettes with 1×10^7 cells resuspended in 1x Roditi buffer containing 200 mM Na₂HPO₄, 70 mM NaH₂PO₄, 15 mM KCl, 150 mM HEPES (pH 7.3) and 1.5 mM CaCl₂. Electroporation was carried out using programme X-001 on Amaxa Nucleofector II device. When electroporation was completed, the cells were transferred into 10 ml of M199 and incubated at 28°C. After 5-6 hours, transfected cells were selected with appropriate drug (**Table 2.3**), which were then kept incubated at 28°C for 5-14 days.

Table 2.3 Selection drugs

Transfections	Drugs	Selection
FLA1BP & FAZ2mCherry marker constructs	Puromycin (Melford)	20 µg/ml
Tagging constructs with mNG tag	Blasticidin (Melford)	5 µg/ml
Double deletion constructs	Blasticidin and G418 (Melford)	5 µg/ml and 20 µg/ml respectively
Addback constructs	Phelomycin (Melford)	25 µg/ml

2.3.3 Growth Curves

Cell counts were collected using Beckman Coulter Counter at 24 hour periods after sub-culturing the cell lines to 1×10^6 /ml. Data from 24, 48 and 72 hour time points were collected. A saw tooth growth curve was generated for parental, null mutant and addback cell lines for comparison.

2.4 Light Microscopy

2.4.1 Imaging the tagging, null mutant and addback cell lines

For tagged cell lines, transfectants grew back approximately 5 days post-transfection and for null mutant and addback cell lines, transfectants grew back approximately 10-14 days post-transfection. When the density of between 1×10^6 /ml and 1×10^7 /ml was reached 1 ml of cells were harvested and centrifuged at 1000 g for 3 minutes. After supernatant removal, the cells were washed in 1 ml DMEM (Gibco 31053028) with Hoechst 33342 ($1 \mu\text{g}/\text{ml}$) and then washed in 1 ml PBS and re-centrifuged two times before they were resuspended in 20-150 μl PBS, depending on cell number. 2.4 μl was transferred onto a super frost microscope slide and was mounted with a size 1.5 coverslip. The cells were observed on a Zeiss imager Z2 fluorescence microscope with ORCA Flash4 camera and x63 oil immersion objective lens. mCherry, GFP and DAPI channels were used to visualise the marker, mNG tagged protein and DNA in kinetoplast/nucleus, respectively. The images were captured using Zen Blue software and stored for analysis on Image J.

For imaging straight out of culture, when the density of between 1×10^6 /ml and 1×10^7 /ml was reached 2.4 μl of culture was taken straight out of a flask and transferred onto a super frost microscope slide prior to mounting with a coverslip. The cells were observed, and images captured at random on a Zeiss imager Z2 fluorescence microscope with ORCA Flash4 camera and x40 oil immersion objective lens.

2.4.2 Measurement of cell cycle position numbers and abnormalities

63x image fields were collected from each of three cell lines, parental, null mutant and addbacks. Kinetoplast/nuclei and flagella numbers were recorded from each cell observed and a percentage of each cell cycle positions were calculated. Cells with abnormalities were also counted.

40x image fields of cells straight from culture were collected from each of three cell lines, parental, null mutant and addbacks. 1F, 2F cells and cells with phenotypes were counted and a percentage of each were calculated.

2.4.3 Measurement of flagellum length and cell body length/width

Measurements of 100 1F1N1K cells were collected from each cell line. Each measurement was made using the line tool in ImageJ (Schneider, Rasband and Eliceiri, 2012). The length of the flagellum was measured from anterior cell tip to the distal flagellar tip (**Figure 2.2A**). The cell body length was measured from the posterior cell tip to the anterior cell tip and the width was measured from the top to bottom in line with the nucleus position (**Figure 2.2B-C**). The anterior end region was measured from the position of kinetoplast to the anterior cell tip (**Figure 2.2D**). The mean and standard deviation were calculated for each cell line.

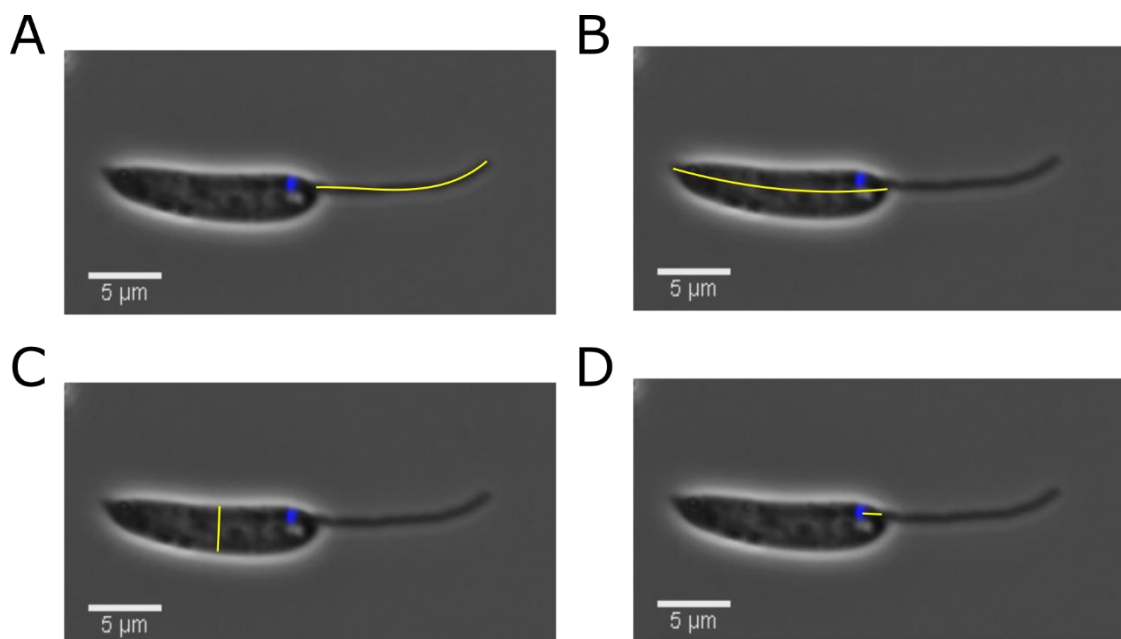


Figure 2.2 Measurements in ImageJ. A) Flagellum length. B) Cell body length. C) Cell body width length. D) Flagellar pocket length from Kinetoplast to anterior cell tip

2.4.4 Confirmation of flagellum loss by vortex

Observations of loose flagella were common in cell lines straight after transfection, so selected cell lines were tested at week one post-liquid nitrogen storage. When a density of between 1×10^6 /ml and 1×10^7 /ml was reached 2 x 1 ml cells from each cell line were harvested into microcentrifuge tubes. One tube from each pair was vortexed continuously for 30 seconds whilst the other tube was not. 2.4 μ l of culture was taken from a tube and transferred onto a super frost microscope slide prior to mounting with a coverslip. The cells were observed and captured at random on a Zeiss imager Z2 fluorescence microscope with ORCA Flash4 camera and x40 oil immersion objective lens. The counts from non-vortexed and vortexed were compared from images taken of parental and selected null mutant cell lines.

2.4.5 Motility assay

The cells at 1×10^7 /ml density were used for motility analysis. 5 μ l of cells were added into a gene frame on super frost microscope slide. The cells were imaged every 100 ms and recorded for 380 seconds through x10 lens of a Zeiss imager Z2 fluorescence microscope. Swimming tracks were analysed using a macro in ImageJ (Wheeler, 2017).

2.5 Methodology for Transmission Electron Microscopy

2.5.1 Fixing cells and single osmium preparation

Cells at the density of 1×10^7 were fixed by glutaraldehyde at the final concentration of 2.5%. This cell solution was mixed gently and fixed for 5 minutes before centrifugation at 800g for 10 minutes and washed in buffered fixative solution (0.1 M phosphate buffer with glutaraldehyde at 2.5%, pH 7.2). Cells were then resuspended in buffered fixative and left for 1 hour at room temperature. After a series of 3 washes in 0.1 M phosphate buffer, cells were incubated with 1% OsO₄ in 0.1 M phosphate buffer in the dark for 1 hour at 4°C. Post incubation cells were

washed twice in ddH₂O and embedded in 0.1 M phosphate buffer with 4% low melting point agarose. Pellet was then trimmed into smaller sections and incubated in 0.5% Uranyl acetate in the dark at 4°C overnight. Samples were then dehydrated in 30%, 50%, 70%, 90%, 100%, 2X absolute ethanol for 10 minutes each. Cells were incubated in ethanol/resin (TAAB 812 hard resin kit) ratios, starting with 3:1 ethanol/resin for 1 hour, 1:1 ethanol/resin for 2 hours, 1:3 ethanol/resin for 1 hour before being embedded in 100% resin overnight with gentle rotation. Next day, 100% resin was changed again and incubated for 6 hours before transfer to Beem capsules and polymerised at 60°C for 24 hours.

2.5.2 Thin sectioning and imaging

Samples embedded in resin were removed from Beem capsules with a razor blade and trimmed by PowerTome PT-PC microtome (Boeckeler) using a glass knife. A trapezium-shaped block face was produced and sectioned by ultramicrotomy, with sections set at 70 nm. Thin sections were embedded onto a copper grid (TAAB G200) and stained with Reynold's lead citrate prior to imaging on Joel-1400 Flash TEM with Gatan One View 16-megapixel camera.

2.6 Approach to data collection and analysis

To allow a fair measurement and analysis of cell lines used in this work all experiments were approached with a standard approach otherwise stated in figure legends (**Table 2.4**). When appropriate, statistical analysis in excel using t-test was used to calculate p values to determine significant differences between groups.

Table 2.4 Approach to data collection

Experiment	Approach
Localisation and deletion screens in Chapters 3 & 4	
Imaging cells	30 fields of views containing 20-100 cells each were taken. Representative image with the most typical phenotype and highest clarity was chosen.
Cell structure and cell cycle position numbers	30 fields of views containing 20-100 cells each were captured. A range of 100-151 cells were taken for cell cycle position analysis. Images containing ≤ 100 cell structures were taken straight from culture for cell structure analysis. Percentages of each group was calculated
Measurements of 1F1N1K cells	A range of 86-110 1F1N1K cells from each cell line was used for flagellum and cell body length analysis.
Analysis of FAZ27, FAZ34 and CC2D null mutants in Chapters 5 & 6	
Imaging cells	30 fields of views containing 20-100 cells each were taken. This was performed in 2x technical replicates on a weekly basis for 4 weeks
Cell structure and cell position numbers	30 fields of views containing 20-100 cells each were captured ≤ 100 cells were taken for cell cycle position analysis. Images containing ≤ 100 cell structures were taken straight from culture for cell structure analysis. Both carried out in 2x technical replicates
Measurements of 1F1N1K cells	A range of 67-141 1F1N1K cells from each cell line was used for flagellum and cell body length analysis in 2x technical replicates.
Measurement of flagellum loss by vortex	Images containing ≤ 100 cell structures were taken straight from culture for cell structure analysis in 2x technical replicates.
Loose flagella with kinetoplast attached analysis	Total of 114-122 loose flagella structures captured from weeks 1 and 2 in 2x technical replicates were used for analysis.
Motility analysis	360s captured in 3x technical replicates
TEM analysis	3x technical replicates were captured for each cell line. A representative image at appropriate orientation of cell at highest clarity was chosen.

Chapter 3

**Discovery of 28 FAZ proteins with 5 different FAZ
localisation classes in *L. mexicana***

3.1 Preface

L. mexicana parasites have a similar flagellar pocket structure to that of *T. brucei* and *T. cruzi* - the flagellar pocket has two domains, the bulbous and the neck region (Lacomble *et al.*, 2009; Alcantara *et al.*, 2014, 2017; Wheeler, Sunter and Gull, 2016). Within the neck region of *L. mexicana*, the FAZ provides attachment between the flagellum and cell body (Wheeler, Sunter and Gull, 2016). While, in *T. brucei* and *T. cruzi*, the attachment zone starts from within the neck and extends out along the cell body. In *T. brucei* and *T. cruzi*, the FAZ has a linear organisation with regularly spaced junctional complexes alongside the FAZ filament for the majority of the cell body length (Sherwin and Gull, 1989; Höög *et al.*, 2012; Sunter and Gull, 2016). *T. brucei* and *T. cruzi* can have a FAZ varying in length, dependent on its cell form (Rocha *et al.*, 2006; De Souza, 2009; Sunter and Gull, 2016). This organisation of the FAZ was not seen in *L. mexicana*, instead junctional complexes and the FAZ filament are separated within the flagellar pocket neck region (Wheeler, Sunter and Gull, 2016). Despite the differences, the FAZ of *L. mexicana* and *T. brucei* are clearly analogous to each other (Wheeler, Sunter and Gull, 2016).

A study conducted in 2016 identified seven FAZ proteins (FAZ1, FAZ2, FAZ5, FAZ8, CLPGM6, FLA1BP and FAZ10) in *L. mexicana*, by examining the localisation of the orthologs of known *T. brucei* FAZ-coding genes (Wheeler, Sunter and Gull, 2016). TrypTag.org, a genome wide protein localisation resource for *T. brucei* was completed in September 2019 (Dean, Sunter and Wheeler, 2017). Here, a list of proteins that localised to the FAZ of *T. brucei* as annotated by TrypTag was used to identify FAZ proteins in *L. mexicana* by determining whether the orthologs localised to the FAZ in *L. mexicana*.

3.2 58 orthologs of *T. brucei* FAZ proteins were identified in *L. mexicana*

A cohort of 96 FAZ proteins was identified in *T. brucei* by TrypTag (Dean, Sunter and Wheeler, 2017). These proteins were organised into seven categories based on their localisation patterns: 1) Full length (23 proteins), 2) Full length-distal enriched (18 proteins) 3) Full length-proximal enriched (3 proteins), 4) Distal only (17 proteins), 5) Proximal only (3 proteins), 6) FAZ-ER (9 proteins) and 7) Complex (23 proteins) (**Fig 3.1**). Full length applied to proteins with localisations along the entire length of FAZ, while full length with either distal or proximal enriched were for protein localisations along entire length of FAZ with stronger signal seen towards the distal/proximal end. Distal and proximal only were those with localisations restricted to the distal/proximal region of the FAZ. The *T. brucei* FAZ is closely associated with the ER through the MtQ and those with both an ER and FAZ signal were defined as FAZ-ER (Lacomble *et al.*, 2012). The complex category was assigned to those with additional localisations (except cytoplasm) or contain a combination of these FAZ localisation categories.

Information on protein properties and features (molecular weight, transmembrane domains and PFAM domains) were collated for the 96 *T. brucei* FAZ proteins (**Table 3.1**). Out of the 96 proteins, 39 had at least 1 PFAM domain. The majority of PFAM domains were restricted to individual proteins; however, one PFAM domain, a TerD domain which encodes calcium binding sites was found in both FAZ28 (Tb927.4.5000) and FAZ30 (Tb927.8.7420) (Anantharaman, Iyer and Aravind, 2012). Another domain, found in three proteins, CC2D (Tb927.4.2080), FAZ22 (Tb927.10.9700) and cAMP binding protein (Tb927.10.13740), was a C2 domain, which is important for in calcium-binding and membrane targeting processes (Davletov and Sudhof, 1993).

18 proteins were found to have transmembrane domains, which included two well-known FAZ proteins located in the intracellular domain, FLA1BP and FAZ5 (Sun *et al.*, 2013; Sunter *et al.*, 2015). Nine proteins with transmembrane domains were identified as FAZ-ER proteins, including VAMP associated protein (TbVAP) which was found to be important for FAZ and flagellar pocket ER domain maintenance (Lacomble *et al.*, 2012). The molecular weight was assessed but no correlation was

found across different categories, suggesting they have no role in determination of localisation patterns (**Table 3.1**).

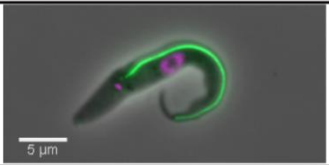

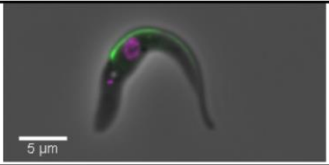
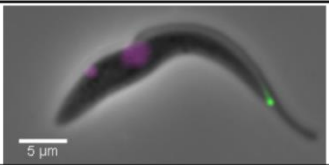
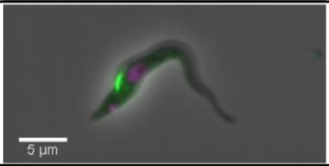

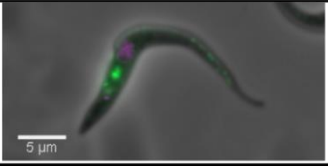
Type of FAZ localisation	No. of genes in <i>T. brucei</i>	Example image
Full length	23	
Full length-distal enriched	18	
Full length-proximal enriched	3	
Distal only	17	
Proximal only	3	
FAZ-ER	9	
Complex	23	

Figure 3.1 FAZ proteins in *T. brucei* were classified based on their localisation patterns. Categories are the following: Full length (example: FAZ8, Tb927.4.2060), Full length-distal enriched (example FAZ2, Tb927.1.4310), Full length-proximal enriched (example: FAZ19, Tb927.3.3300), Distal only (FAZ21, Tb927.7.5240), Proximal only (hypothetical protein, Tb927.9.8240), FAZ-ER (reticulum domain protein, Tb927.6.3840), Complex (Autophagy-related protein 27, Tb927.6.3940 with endocytic/FAZ signal). All protein localisations tagged with mNG were observed on TrypTag.org and assigned to groups based on their localisation patterns.

Table 3.1 FAZ proteins in *T. brucei* with orthologs in *L. mexicana* identified. Protein information including molecular weight (MW), TMHMM (containing transmembrane domains) and PFAM domains were obtained from TriTrypDB and InterPro (Aslett *et al.*, 2009; Blum *et al.*, 2021). *L. mexicana* orthologs were identified by OrthoMCL (Fischer *et al.*, 2011). Last updated: January 2020. *Tb927.9.13880 gene is not in current genome annotation.

Full Length						
Gene ID	Protein name	MW	TMHMM	PFAM domains	<i>L. mexicana</i> ortholog	FAZ related refs
Tb927.3.4710	Flagellum attachment zone protein 23	59.75	no			(Zhou, An, <i>et al.</i> , 2018)
Tb927.4.2060	Flagellum attachment zone protein 8	66.84	no		LmxM.33.2570	(Qing Zhou <i>et al.</i> , 2015; Sunter <i>et al.</i> , 2015)
Tb927.4.2080	C2 domain containing protein (CC2D)	104.88	no	C2 domain	LmxM.33.2540	(Q. Zhou <i>et al.</i> , 2011)
Tb927.4.3740	Flagellum attachment zone protein 1	192.57	no		LmxM.33.0690	(Vaughan <i>et al.</i> , 2008)
Tb927.4.5340	Flagellum attachment zone protein 11	94.70	no		LmxM.30.3110	(Morriswood <i>et al.</i> , 2013)
Tb927.6.840	Flagellum attachment zone protein 29	38.16	no	Glutathione S-transferase, N-terminal domain	LmxM.12.0360	
Tb927.8.4780	Flagellar Member 3 (FLAM3)	468.13	no	Clustered mitochondria & Translation initiation factor eIF3	LmxM.16.1660	(Rotureau <i>et al.</i> , 2014)
Tb927.8.7420	Flagellum attachment zone protein 30	96.39	no	TerD domain x2	LmxM.30.2590	
Tb927.9.2075	Flagellum attachment zone protein 44	302.50	no			
Tb927.9.8650	Flagellum attachment zone protein 32	12.29	no		LmxM.04.1100	
Tb927.9.9320	MAPK/MAK/MRK overlapping kinase, putative	41.76	no	Protein kinase domain	LmxM.34.5010	
*Tb927.9.13880	kinetoplastid membrane protein 11-2	11.08	no	Kinetoplastid membrane protein 11	LmxM.34.2221	
Tb927.10.2880	Flagellum attachment zone protein 26	303.77	22	Ion transport protein x4		(Oberholzer <i>et al.</i> , 2011)
Tb927.10.5870	Flagellum attachment zone protein 25	49.47	no			(Zhou, An, <i>et al.</i> , 2018)
Tb927.10.7210	Flagellum attachment zone protein 17	26.26	no			(McAllaster <i>et al.</i> , 2015a)
Tb927.10.8830	Flagellum attachment zone protein 5	66.66	7		LmxM.36.5970	(Sunter <i>et al.</i> , 2015)
Tb927.10.9700	Flagellum attachment zone protein 22	132.58	no	C2 domain x3	LmxM.36.4330	(Zhou, An, <i>et al.</i> , 2018)

Tb927.10.11360	Flagellum attachment zone protein 33	73.25	no	WD40/YVTN repeat-like containing domain superfamily, WD40-repeat-containing domain superfamily, protein phosphatase 2A regulatory subunit PR55		
Tb927.10.14320	Flagellum attachment zone protein 9	121.80	no	Armadillo-type fold	LmxM.31.0140	(Sunter <i>et al.</i> , 2015)
Tb927.11.1090	calpain-like protein, putative	663.06	no	Calpain family cysteine protease x2 & Calpain large subunit, domain III	LmxM.27.0490	(Hayes <i>et al.</i> , 2014)
Tb927.11.1110	calpain, putative	171.46	no	Calpain family cysteine protease	LmxM.27.0490	
Tb927.11.12530	Flagellum attachment zone protein 3	90.65	no		LmxM.09.0520	(Sunter <i>et al.</i> , 2015)
Tb927.11.12870	hypothetical protein, conserved	78.40	11			

Full length- Distal enriched						
Gene ID	Protein name	MW	TMHMM	PFAM domains	<i>L. mexicana</i> ortholog	Ref
Tb927.1.4310	Flagellum attachment zone protein 2	183.76	no		LmxM.12.1120	(Q. Zhou <i>et al.</i> , 2015; Sunter <i>et al.</i> , 2015)
Tb927.3.1020	Flagellum attachment zone protein 13	54.34	no			(Hu, Zhou and Li, 2015b)
Tb927.4.1960	Flagellum attachment zone protein 42	37.39	no			
Tb927.4.5000	Flagellum attachment zone protein 28	96.39	no	TerD domain x2	LmxM.30.2590	
Tb927.5.3460	Flagellum attachment zone protein 16	57.44	no	LysM domain		(McAllaster <i>et al.</i> , 2015a)
Tb927.7.3330	Flagellar attachment zone protein 10	502.65	no		LmxM.22.1320	(Morriswood <i>et al.</i> , 2013)
Tb927.8.4050	FLA1-binding protein	83.06	2		LmxM.10.0620	(Sun <i>et al.</i> , 2013)
Tb927.8.5350	Flagellar attachment zone protein 38	18.94	no			
Tb927.8.6980	Flagellum attachment zone protein 14	95.06	no		LmxM.30.3110	(Hu, Zhou and Li, 2015b)
Tb927.8.7070	Flagellum attachment zone protein 15	35.43	no			(McAllaster <i>et al.</i> , 2015a)
Tb927.9.8180	Flagellum attachment zone protein 31	70.84	no			(Hu <i>et al.</i> , 2019)
Tb927.9.8330	Flagellum attachment zone protein 39	52.61	no			
Tb927.9.8350	Flagellum attachment zone protein 27	66.85	no		LmxM.04.0890	(An <i>et al.</i> , 2020)
Tb927.9.10530	Flagellum attachment zone protein 4	118.72	no			(Sunter <i>et al.</i> , 2015)
Tb927.10.840	Flagellum attachment zone protein 6	195.48	no	WD domain, G-beta repeat x2	LmxM.21.1240	(Sunter <i>et al.</i> , 2015)

Tb927.10.12630	Flagellum attachment zone protein 34	25.14	no	EF-hand domain pair	LmxM.18.1440	
Tb927.11.2590	Flagellum attachment zone protein 12	121.14	no		LmxM.32.2460	(Hu, Zhou and Li, 2015b)
Tb927.11.3400	Flagellum attachment zone protein 41	34.88	no			

Full length- Proximal enriched

Gene ID	Protein name	MW	TMHMM	PFAM domains	<i>L. mexicana</i> ortholog	Ref
Tb927.1.5030	Flagellum attachment zone protein 37	80.77	no	Leucine Rich Repeat 1 & 6		
Tb927.3.3300	Flagellum attachment zone protein 19	89.20	no			(Zhou, Hu and Li, 2016)
Tb927.11.2070	Flagellum attachment zone protein 36	15.31	no		LmxM.27.1400	

Distal only

Gene ID	Protein name	MW	TMHMM	PFAM domains	<i>L. mexicana</i> ortholog	Ref
Tb927.2.2360	Ankyrin repeats (3 copies)/Zinc finger, C3HC4 type (RING finger), putative	74.5	no	Ankyrin repeats (3 copies), Zinc finger, C3HC4 type (RING finger)	LmxM.02.0140	
Tb927.6.3710	Hypothetical protein, conserved	78.29	no			
Tb927.7.5240	Flagellum attachment zone protein 21	53.49	no			(Zhou, An, <i>et al.</i> , 2018)
Tb927.8.6830	Kinesin, putative	198.66	no	Kinesin motor domain	LmxM.24.1430	(Zhou, Lee, <i>et al.</i> , 2018)
Tb927.10.5240	CAMP binding protein, putative	188.21	no	Cyclic nucleotide-binding domain & C2 domain x3	LmxM.36.0830	
Tb927.10.6360	FAZ-tip-localizing protein required for cytokinesis	55.52	no		LmxM.36.1920	(Zhou, An, <i>et al.</i> , 2018)
Tb927.10.8240	Cytokinesis initiation factor 4	42.85	no		LmxM.36.6960	(Hilton <i>et al.</i> , 2018)
Tb927.10.9720	RNA-editing-associated protein 1 (REAP-1)	64.38	no			
Tb927.10.12470	Flagellum attachment zone protein 40	58.39	no		LmxM.18.1560	
Tb927.10.12670	Hypothetical protein, conserved	58.47	no			
Tb927.10.12920	Flagellum attachment zone protein 18	112.87	no			(Zhou, Hu and Li, 2016)
Tb927.10.13100	Cytokinesis initiation factor 3	50.92	no			(Kurasawa <i>et al.</i> , 2018; Zhou, An, <i>et al.</i> , 2018)
Tb927.10.15390	Flagellum attachment zone protein 7	123.56	no	Kinesin motor domain superfamily	LmxM.19.0680	(Sunter <i>et al.</i> , 2015)

Tb927.11.5410	SUMO-interacting motif-containing protein	70.77	no			
Tb927.11.9290	Flagellum attachment zone protein 20	85.45	no	Protein kinase domain	LmxM.28.1650	(Zhou, Hu and Li, 2016)
Tb927.11.11240	Hypothetical protein, conserved	23.00	no			
Tb927.11.15800	Tip Of Extending FAZ protein 1	89.59	no		LmxM.31.2610	(Hu, Zhou and Li, 2015a; McAllaster <i>et al.</i> , 2015b)

Proximal only						
Gene ID	Protein name	MW	TMHMM	PFAM domains	<i>L.mexicana</i> ortholog	Ref
Tb927.3.5220	hypothetical protein, conserved	65.03	no			
Tb927.4.5330	Flagellum attachment zone protein 43	97.24	no			
Tb927.9.8240	hypothetical protein, conserved	55.58	no			

FAZ-ER						
Gene ID	Protein name	MW	TMHMM	PFAM domains	<i>L.mexicana</i> ortholog	Ref
Tb927.1.4420	ABC transporter, putative	104.68	no	ABC transporter	LmxM.12.1190	
Tb927.6.3840	Reticulon domain protein	21.07	3	Reticulon	LmxM.29.2580	(Zhou, An, <i>et al.</i> , 2018)
Tb927.7.3070	UAA transporter family, putative	54.85	8	UAA transporter family	LmxM.22.1010	
Tb927.7.3760	phosphatidylserine synthase, putative	57.60	8	Phosphatidyl serine synthase	LmxM.14.1200	
Tb927.10.13740	Flagellum attachment zone protein 35	67.31	3	C2 domain		(Zhou, An, <i>et al.</i> , 2018)
Tb927.11.5370	hypothetical protein, conserved	76.64	7		LmxM.24.0700	
Tb927.11.6060	major facilitator superfamily, putative	51.32	11	Major facilitator superfamily	LmxM.11.1320	
Tb927.11.13230	VAMP-associated protein, putative	23.91	1	MSP (Major sperm protein) domain	LmxM.09.1050	(Lacomble <i>et al.</i> , 2012)
Tb927.11.15870	Hypothetical protein, conserved	42.43	2		LmxM.31.2680	

Complex						
---------	--	--	--	--	--	--

Gene ID	Protein name	MW	TMHMM	PFAM domains	<i>L. mexicana</i> homolog	Ref
Tb927.1.4280	Hypothetical protein, conserved	75.28	no			
Tb927.4.3520	Amastin surface glycoprotein, putative	19.46	4	Amastin surface glycoprotein	LmxM.16.0490	
Tb927.6.3940	Autophagy-related protein 27, putative	39.21	3	Autophagy-related protein	LmxM.29.2670	
Tb927.7.5190	hypothetical protein, conserved	126.87	no			
Tb927.8.2030	Posterior and Ventral Edge protein 1	48.24	no		LmxM.23.0080	
Tb927.9.2760	EB1-like C-terminal motif containing protein, putative	57.00	no	EB1 C terminal domain, microtubule associated protein RP/EB, Calponin homology domain		
Tb927.9.11540	hypothetical protein, conserved	50.79	no		LmxM.34.3720	
Tb927.9.13820	kinetoplastid membrane protein 11-3	11.08	no	Kinetoplastid membrane protein 11	LmxM.34.2221	(Li and Wang, 2008; Li <i>et al.</i> , 2008)
Tb927.9.14290	Cytokinesis initiation factor 2	49.83	no			(Zhou, Hu and Li, 2016)
Tb927.10.1230	Enriched in surface-labeled proteome protein 23	37.68	5		LmxM.21.0940	
Tb927.10.1620	phosphoserine/threonine/tyrosine-binding protein, putative	59.94	no	Protein-tyrosine phosphatase-like	LmxM.21.0700	
Tb927.10.2480	hypothetical protein, conserved	105.08	3		LmxM.33.0060	
Tb927.10.2610	Domain of unknown function (DUF1935), putative	54.36	no	Domain of unknown function (DUF1935) x4	LmxM.33.0190	
Tb927.10.720	Flagellum attachment zone protein 24	118.09	no	PB1 domain	LmxM.21.1350	(Zhou, An, <i>et al.</i> , 2018)
Tb927.10.870	Furrow 1 protein	151.85	no		LmxM.21.1220	(Zhou, An, <i>et al.</i> , 2018)
Tb927.10.11650	Hypothetical protein, conserved	17.39	no		LmxM.32.1035	
Tb927.10.13010	cAMP-dependent protein kinase catalytic subunit 3 (PKAC3)	39.18	no	Protein kinase domain	LmxM.18.1080	
Tb927.10.14400	Hypothetical protein, conserved	125.26	1		LmxM.31.0220	
Tb927.10.14770	Associated kinase of Tb14-3-3	70.53	no		LmxM.19.0140	
Tb927.11.1640	Stumpy formation signalling pathway protein, putative	42.25	2		LmxM.27.1040	
Tb927.11.3280	Kinesin-13 5, putative	80.07	no	SAM domain (Sterile alpha motif) & Kinesin motor domain	LmxM.13.1610	(Hu <i>et al.</i> , 2019)
Tb927.11.3300	Spindle assembly abnormal 4	107.86	no	T-complex protein 10 C-terminus	LmxM.13.1590	(Hu, Zhou and Li, 2015b)
Tb927.11.11480	Trichohyalin, putative	78.97	no			(Zhou, An, <i>et al.</i> , 2018)

With *T. brucei* closely related to *Leishmania*, OrthoMCL identifier, an algorithm for protein ortholog groupings (Fischer *et al.*, 2011) was used to discover which of the 96 FAZ proteins identified in *T. brucei* were conserved in *L. mexicana*. Out of the 96 FAZ proteins identified in *T. brucei*, 61 were found to have orthologs in *L. mexicana* (Aslett *et al.*, 2009). However, 4 of the *L. mexicana* orthologs appeared twice on the list, shared with other FAZ proteins in *T. brucei*. These are LmxM.30.2590 orthologous to FAZ30 (Tb927.8.7420) and FAZ28 (Tb927.4.5000), LmxM.30.3110 orthologous to FAZ14 (Tb927.8.6980) and FAZ11 (Tb927.4.5340), LmxM.34.2221 orthologous to KMP-11-2 (Tb927.9.13880) and KMP-11-3 (Tb927.9.13820) and lastly, LmxM.27.0490 orthologous to calpain containing proteins (Tb927.11.1110) and ClpGM6 (Tb927.11.1090). This gives a total of 57 *L. mexicana* orthologs identified (**Table 3.1**).

Conservation analysis using orthoMCL was not limited to *L. mexicana*, but also was assessed across a diverse set of different kinetoplastid species, *T. cruzi* (Dm28c2017), *Paratrypanosoma confusum* (CUL13) and *Bodo saltans* (Lake Konstanz) (**Figure 3.2**). *P. confusum* is an early branching trypanosomatids and closely related to the free-living *B. saltans* (Flegontov *et al.*, 2013). With *T. cruzi* being most closely related to *T. brucei* it was unsurprising to see a high conservation of FAZ proteins (87/96). 53 of the 96 FAZ proteins were found to be conserved in *P. confusum*, similar to *L. mexicana*. Less (39/96) were seen for the distant relative *B. saltans*. Across all species, the highest conservation level was seen for FAZ proteins that localised along the full length of the FAZ in *T. brucei*. The lowest level of conservation across *L. mexicana*, *P. confusum* and *B. saltans* was seen for those that localise specifically to the proximal or distal region of the FAZ or have a stronger signal within that region (**Fig 3.2**). This suggests these FAZ proteins within these regions could be trypanosome specific with a role potentially related to their trypomastigote morphology, which is not found in other species. All species possess at least 78% of the genes localising to the FAZ and ER region in *T. brucei* (**Fig 3.2**). This demonstrates that FAZ-ER proteins are generally conserved across all kinetoplastids, which suggests that these FAZ-ER proteins may not be trypanosome specific.

The output from this orthoMCL algorithm changes as new data are added. Since this list was created in January 2020, there have been small changes (updated in May

2021). From this new list, three proteins, LmxM.30.3110, LmxM.21.1240 and LmxM.22.1320 were no longer identified as FAZ orthologs in *L. mexicana* (grey squares) (**Fig 3.2**). For the identification of FAZ proteins in *L. mexicana*, these orthologs were included in the localisation screen for completeness, so 57 orthologs were taken forward to the localisation screen.

<i>T. brucei</i>	<i>T. cruzi</i>	<i>L. mexicana</i>	<i>P. confusum</i>	<i>B. saltans</i>
Full Length				
Tb927.3.4710				
Tb927.4.2060				
Tb927.4.2080				
Tb927.4.3740				
Tb927.4.5340				
Tb927.6.840				
Tb927.8.4780				
Tb927.8.7420				
Tb927.9.2075				
Tb927.9.8650				
Tb927.9.9320				
Tb927.9.13880				
Tb927.10.2880				
Tb927.10.5870				
Tb927.10.7210				
Tb927.10.8830				
Tb927.10.9700				
Tb927.10.11360				
Tb927.10.14320				
Tb927.11.1090				
Tb927.11.1110				
Tb927.11.12530				
Tb927.11.12870				
Full length- Distal enriched				
Tb927.1.4310				
Tb927.3.1020				
Tb927.4.1960				
Tb927.4.5000				
Tb927.5.3460				
Tb927.7.3330				
Tb927.8.4050				
Tb927.8.5350				
Tb927.8.6980				
Tb927.8.7070				
Tb927.9.8180				
Tb927.9.8330				

<i>T. brucei</i>	<i>T. cruzi</i>	<i>L. mexicana</i>	<i>P. confusum</i>	<i>B. saltans</i>
Tb927.9.8350				
Tb927.9.10530				
Tb927.10.840				
Tb927.10.12630				
Tb927.11.2590				
Tb927.11.3400				
Full length- Proximal enriched				
Tb927.1.5030				
Tb927.3.3300				
Tb927.11.2070				
Distal only				
Tb927.2.2360				
Tb927.6.3710				
Tb927.7.5240				
Tb927.8.6830				
Tb927.10.5240				
Tb927.10.6360				
Tb927.10.8240				
Tb927.10.9720				
Tb927.10.12470				
Tb927.10.12670				
Tb927.10.12920				
Tb927.10.13100				
Tb927.10.15390				
Tb927.11.5410				
Tb927.11.9290				
Tb927.11.11240				
Tb927.11.15800				
Proximal only				
Tb927.3.5220				
Tb927.4.5330				
Tb927.9.8240				

<i>T. brucei</i>	<i>T. cruzi</i>	<i>L. mexicana</i>	<i>P. confusum</i>	<i>B. saltans</i>
FAZ-ER				
Tb927.1.4420				
Tb927.6.3840				
Tb927.7.3070				
Tb927.7.3760				
Tb927.10.13740				
Tb927.11.5370				
Tb927.11.6060				
Tb927.11.13230				
Tb927.11.15870				
Complex				
Tb927.1.4280				
Tb927.4.3520				
Tb927.6.3940				
Tb927.7.5190				
Tb927.8.2030				
Tb927.9.2760				
Tb927.9.11540				
Tb927.9.13820				
Tb927.9.14290				
Tb927.10.1230				
Tb927.10.1620				
Tb927.10.2480				
Tb927.10.2610				
Tb927.10.720				
Tb927.10.870				
Tb927.10.11650				
Tb927.10.13010				
Tb927.10.14400				
Tb927.10.14770				
Tb927.11.1640				
Tb927.11.3280				
Tb927.11.3300				
Tb927.11.11480				

Figure 3.2 FAZ protein conservation analysis across species. OrthoMCL identified conserved FAZ proteins in *T. cruzi*, *L. mexicana*, *P. confusum* and *B. saltans*. Black squares indicates an ortholog is present. Grey squares represents genes in *L. mexicana* that were no longer recognised as orthologs when this analysis was last updated in May 2021.

3.3 FAZ2 and FLA1BP were chosen as FAZ protein markers for resolution and clarity in localisation screen

The aim was to generate a cell line expressing a tagged FAZ protein that would add resolution to our protein localisation screen and provide spatial information about the FAZ structure. A potential set of markers were the FAZ proteins with a known localisation pattern from the Wheeler et al study (Wheeler, Sunter and Gull, 2016). Four of the following FAZ proteins, FAZ1, FAZ2, ClpGM6 and FLA1BP representing different FAZ domains were tagged with mCherry (**Figure 3.3**). The FAZ1 and FAZ2 fluorescent signal appeared as a short linear structure in the cell body parallel to the flagellum, but FAZ1 had an additional ring/horseshoe pattern at the collar region. ClpGM6 and FLA1BP localised to a short linear structure asymmetrically positioned within the flagellum. FAZ2 and FLA1BP representing two different localisations, gave the strongest, clearest signal. FLA1BP::mCherry was chosen as the main marker with mCherry::FAZ2 to be used for localisations from this screen as necessary.

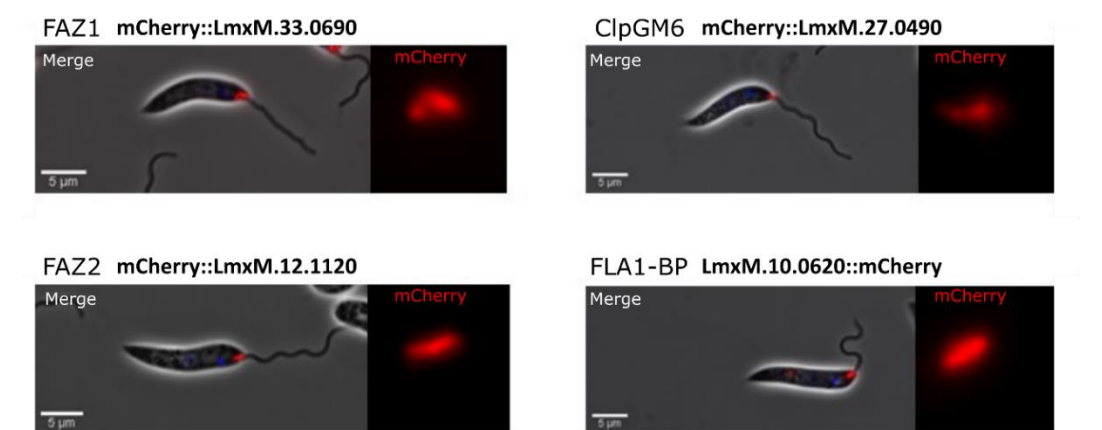


Figure 3.3 FAZ2 and FLA1BP were selected as FAZ markers. FAZ1 localised to both a linear structure on the cell body side and a ring/horseshoe structure at the pocket collar region, FAZ2 localised to a short linear structure on the cell body side, ClpGM6 and FLA1BP localised to a linear structure within the flagellum. FAZ2 and FLA1BP were selected due to the strength and clarity of signal. Scale bar = 5 µm.

3.4 Localisation screen identified 28 FAZ proteins categorised into five localisation classes

54 cell lines were successfully generated by endogenous tagging of the different FAZ protein candidates in *L. mexicana* with an mNG fluorescent protein at the N or C-terminus, in either the FLA1BP::mCherry or mCherry::FAZ2 marker cell line (See appendix A for primers list). Cell lines of two potential FAZ proteins- LmxM.36.4330 and LmxM.28.1650 were not generated due to a PCR and transfection failure, respectively (repeated three times). A total of 28 out of the potential 54 FAZ proteins examined were found to localise to the FAZ in *L. mexicana*.

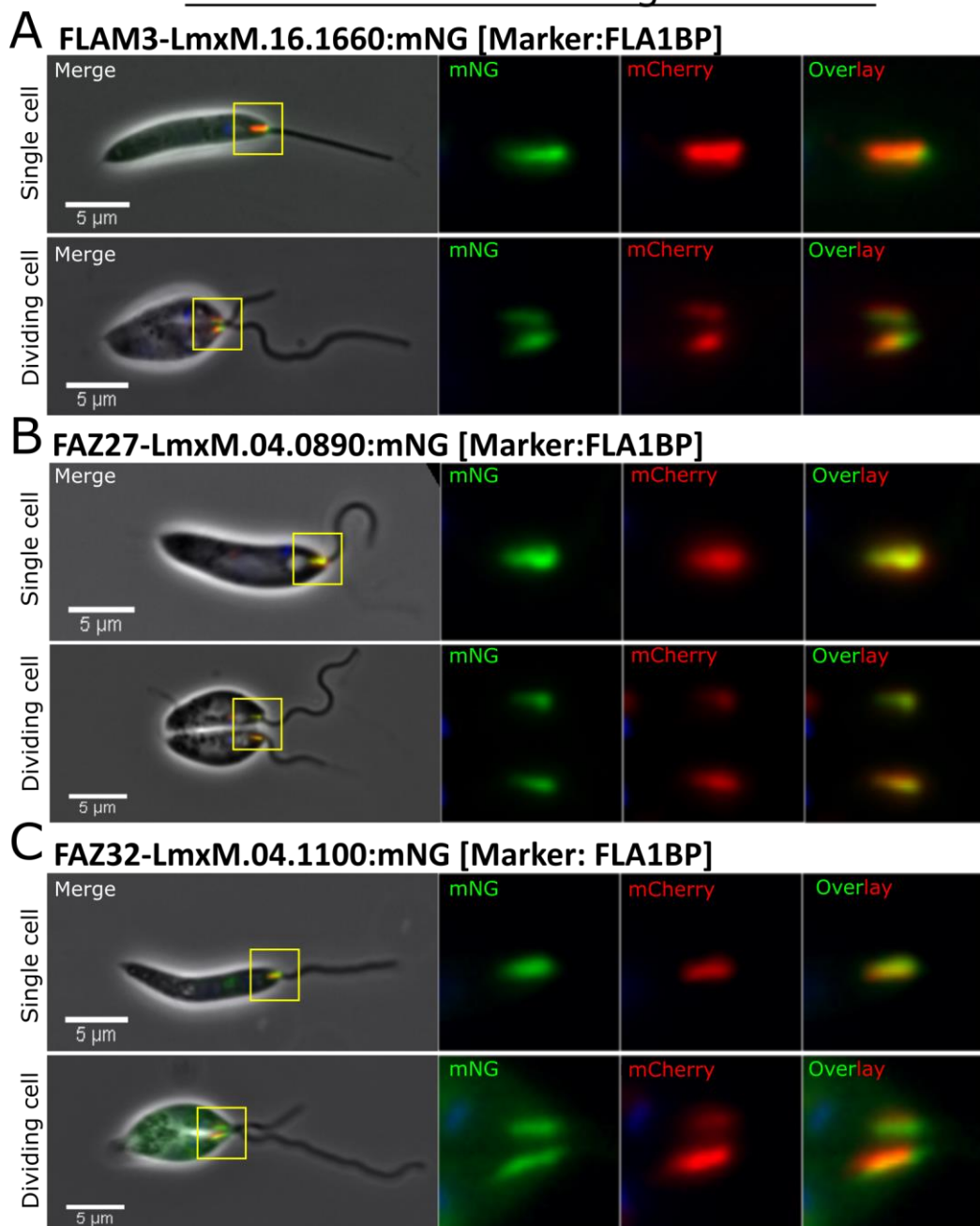
The 28 FAZ proteins were separated into five classes based on their localisation patterns in G1 cells (i.e. they have 1 flagellum, 1 nucleus and 1 kinetoplast): Class 1) Linear structure on the flagellum side, Class 2) Linear structure on the cell body side, Class 3) A ring/horseshoe structure distal to the pocket collar region, Class 4) A ring structure at the flagellum exit point, Class 5) Linear structure on the cell body side with a ring/horseshoe structure at the pocket collar region. Complex was given to those with additional localisations elsewhere for instance, a basal body or cell tip. However, for all the classes the dividing cells could potentially have a more complex localisation pattern due to the timing of FAZ duplication and flagellar pocket resolution.

Six proteins: FLAM3 (LmxM.16.1660), FAZ27 (LmxM.04.0890), FAZ32 (LmxM.04.1100), FAZ34 (LmxM.18.1440), cAMP binding protein (LmxM.36.0830) and ClpGM6 (LmxM.27.0490) along with the FLA1BP marker (LmxM.10.0620) were in class 1, which is a linear structure on the flagellum side, distal to the kinetoplast (**Fig 3.4**). Five proteins FLAM3, FAZ27, FAZ33, FAZ34, and cAMP binding protein were all expressed in the cell line expressing FLA1BP::mCherry as the marker (**Fig 3.4A-D&F**). To determine whether they were in the cell body or flagellum FAZ domain their localisation relative to FLA1BP was examined. All these proteins except cAMP binding protein co-localised with FLA1BP, showing that these proteins localise within the flagellum FAZ domain (**Fig 3.4A-D&F**). The cAMP binding protein signal appeared as a short line in the flagellum, which began at the distal end of the FLA1BP::mCherry

signal before extending a short distance along the flagellum (**Fig 3.4F**). ClpGM6 was expressed in the cell line with the FAZ2 marker and the ClpGM6 signal had a short linear appearance that was adjacent to FAZ2 marker, indicating that this protein was within the flagellum (**Fig3.4E**).

In dividing cells, all the FAZ proteins of this class expressed a similar pattern of two linear structures parallel to each other, distal to the kinetoplast (**Fig 3.4A-F**). One protein, FAZ32 also had this pattern except that the linear signal was longer than the FLA1BP signal extending beyond both sides of the FLA1BP signal (**Fig 3.4C**).

Class I: FAZ on the flagellum side



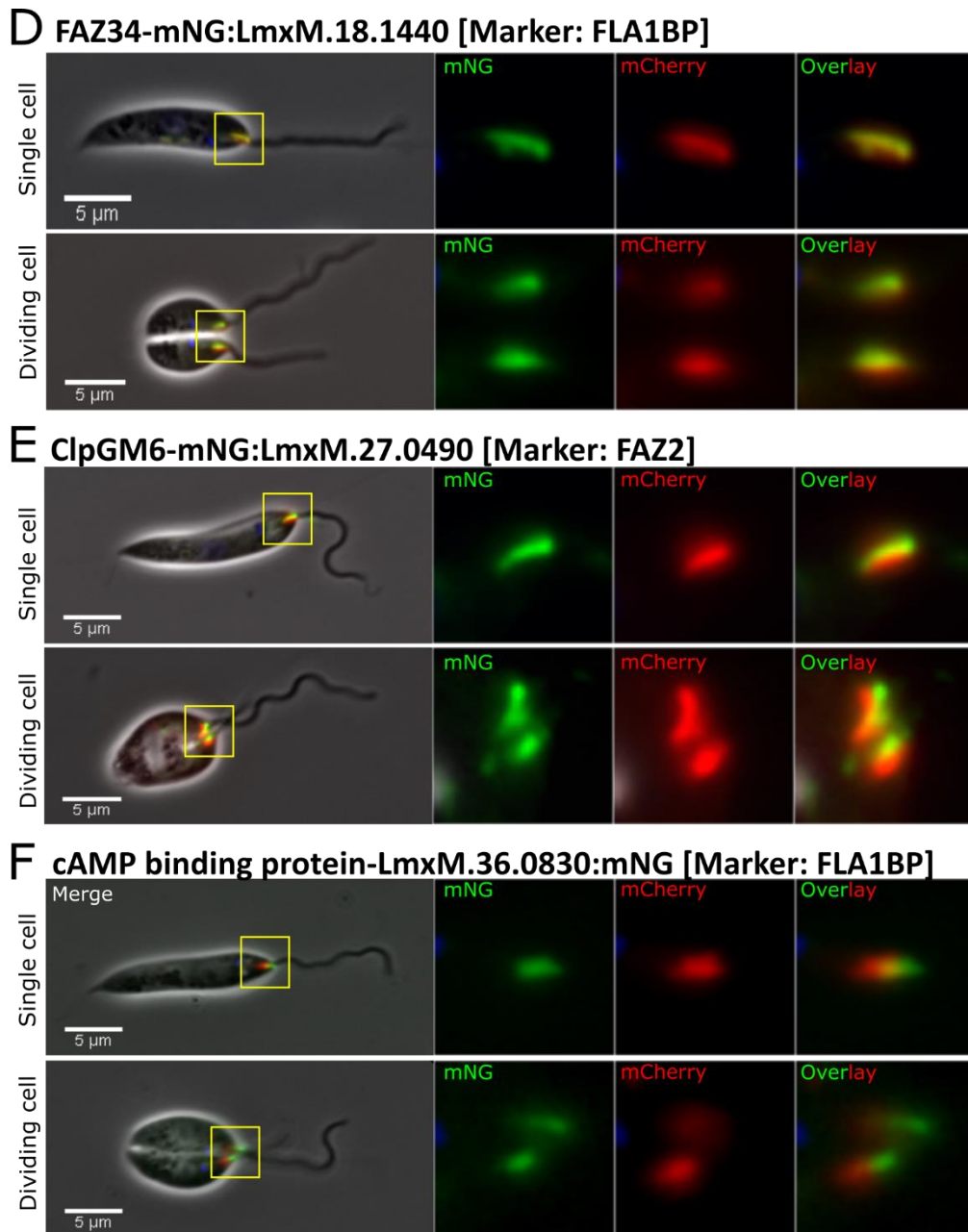


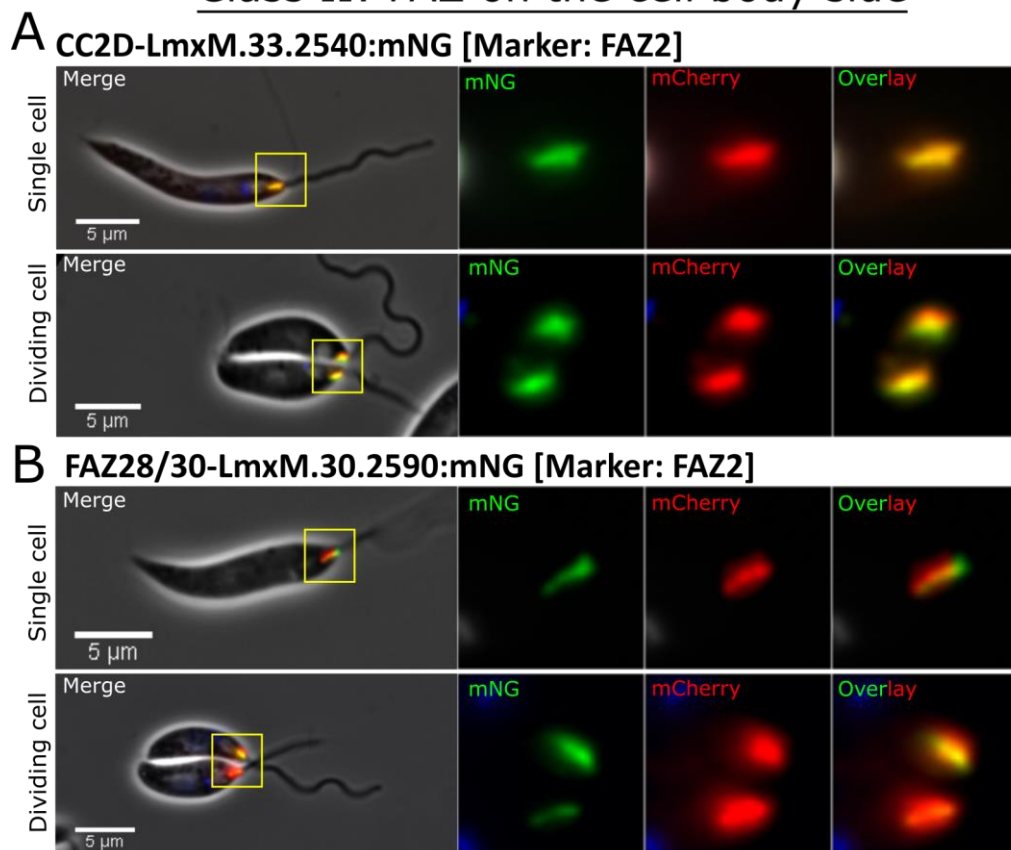
Figure 3.4 *Leishmania* FAZ proteins with Class 1; FAZ on flagellum side localisation

Widefield fluorescence images for each protein A) FLAM3, B) FAZ27, C) FAZ32, D) FAZ34, E) ClpGM6, F) cAMP binding protein in single and dividing cells are laid out in the same format: From left, an overlay of the phase contrast (grey), mNG tagged protein (green), mCh tagged marker (red) and Hoechst DNA (blue) then mNG only, and mCherry only, with the far right being the overlay of mNG AND mCh only. The protein name, gene fusion and FAZ marker are shown on top left (LmxM.X.XXXX::mNG for C-terminal tagging and mNG::LmxM.X.XXXX for N-terminal tagging).

Three proteins; CC2D (LmxM.33.2540), FAZ28/FAZ30 (LmxM.30.2590), FAZ5 (LmxM.36.5970) alongside FAZ2 marker (LmxM.12.1120) were in class 2, which is a linear structure on the cell body side, distal to the kinetoplast (**Fig 3.5**). All these proteins co-localised with FAZ2, showing that these proteins were within the cell body FAZ domain. The FAZ28/30 signal co-localised with FAZ2 marker but its signal extended beyond the distal end of FAZ2 marker (**Fig 3.5A**).

In the dividing cells a pattern of two linear structures parallel to each other was seen but only CC2D co-localised exactly with the FAZ2 marker (**Fig 3.5A**). The FAZ28/30 signal at the new flagellum was longer and less intense compared to the FAZ of the old flagellum (**Fig 3.5B**). Like 1F cells, both FAZ signals extended beyond the distal end of FAZ2 marker (**Fig 3.5B**). The FAZ5 signals in 2F cells were the same size and shape as FAZ2 marker (**Fig 3.5C**).

Class II: FAZ on the cell body side



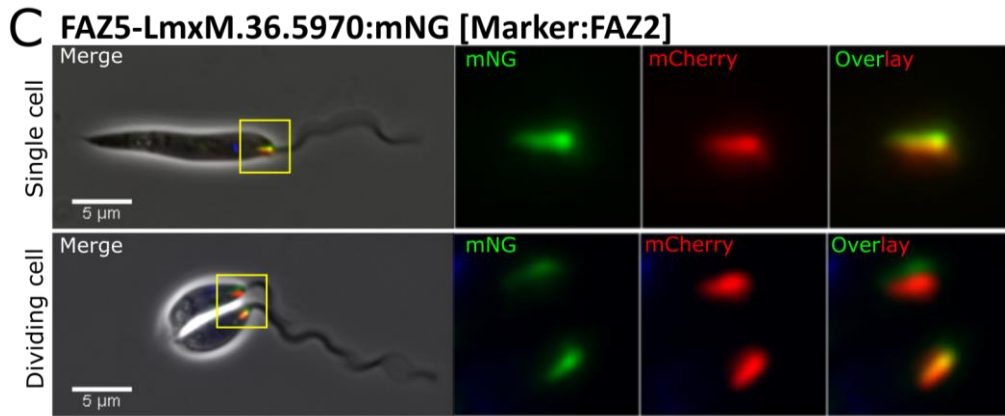


Figure 3.5 *Leishmania* FAZ proteins with Class 2; FAZ on cell body side localisation.

Widefield fluorescence images for each protein A) CC2D, B) FAZ28/30 and C) FAZ5 in single and dividing cells are laid out in the same format: From left, an overlay of the phase contrast (grey), mNG tagged protein (green), mCh tagged marker (red) and Hoechst DNA (blue) then mNG only, and mCherry only, with the far right being an overlay of mNG and mCherry only. The protein name, gene fusion and FAZ marker are shown on top left (LmxM.X.XXXX::mNG for C-terminal tagging and mNG::LmxM.X.XXXX for N-terminal tagging).

Only one protein, FAZ3 (LmxM.09.0520) was in class 3, which is a ring-like structure distal to the pocket collar region of the flagellar pocket. This localisation was clearly distinct from the FAZ2 marker (**Fig 3.6**). Whilst the FAZ2 marker was localised to the cell body FAZ domain, FAZ3 protein was localised with a ring-like shape surrounding the proximal half of FAZ2 marker. In dividing cells there were two structures labelled with FAZ3::mNG with one located on the old flagellum and another on the new flagellum side. These structures co-localised with the FAZ2 signal.

Class III: Ring/Horseshoe at collar region

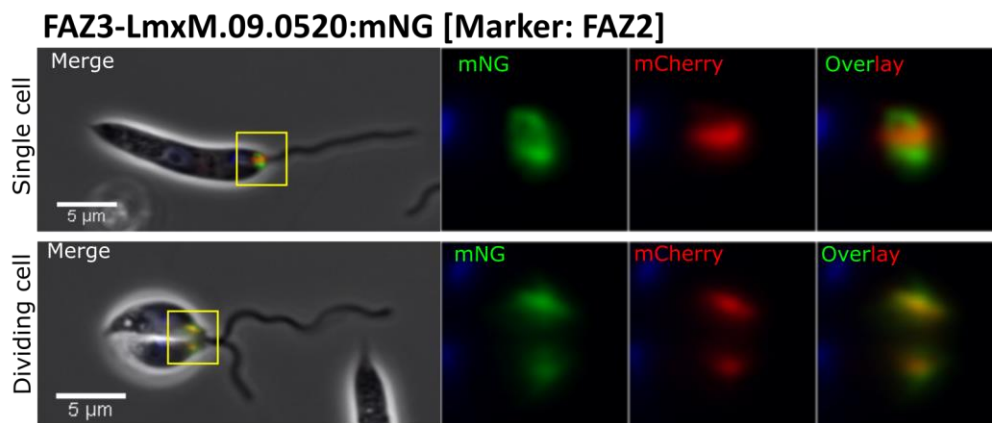
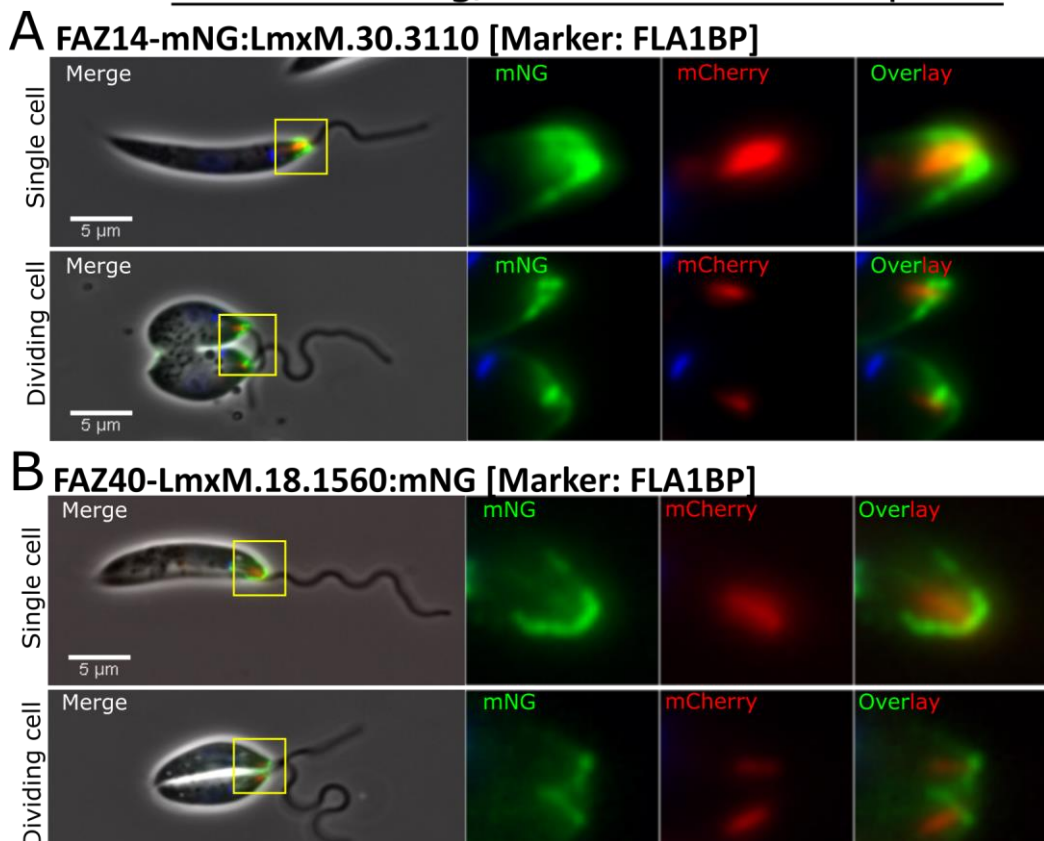


Figure 3.6 *Leishmania* FAZ protein with Class 3; FAZ ring/horseshoe at collar region localisation. Widefield fluorescence images for FAZ3 protein in single and dividing cells are laid out in the same format: From left, an overlay of the phase contrast (grey), mNG tagged protein (green), mCh tagged marker (red) and Hoechst DNA (blue) then mNG only, and mCherry only, with the far right being the overlay of mNG and mCherry only. The protein name, gene fusion and FAZ marker are shown on top left (LmxM.X.XXXX::mNG for C-terminal tagging and mNG::LmxM.X.XXXX for N-terminal tagging).

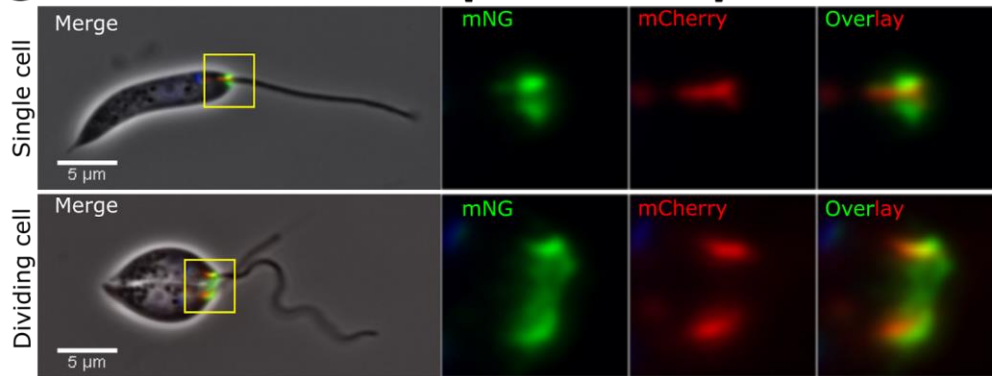
Six proteins; FAZ14 (LmxM.30.3110), FAZ10 (LmxM.22.1320), Kinesin (LmxM.24.1430), FAZ6 (LmxM.21.1240), FAZ40 (LmxM.18.1560) and FAZ12 (LmxM.32.2460) were in class 4, which is the flagellum exit point (**Fig 3.7**). FLA1BP::mCherry was used as the marker with the exit point localisation appearing on both sides of the distal end of the FLA1BP signal. The exit point localisations varied across these six proteins. There was a dome-like appearance seen with FAZ14 and FAZ40, which appeared to extend further into the cell body from the flagellum exit point compared to the marker (**Fig 3.7A&B**). Whilst FAZ10 was localised to both sides of the marker with a ring-like appearance as expected (Wheeler, Sunter and Gull, 2016) (**Fig 3.7C**). FAZ12, Kinesin protein and FAZ6 had a horseshoe/ring-like appearance across the exit point with the Kinesin protein showing a similar but weaker signal (**Fig 3.7D-F**).

The FAZ localisations of the dividing cells were all different to each other. FAZ14 and FAZ40 had a dome-like appearance on both old and new flagellum sides; however, FAZ14 displayed an additional short linear FAZ structure adjacent to the FLA1BP marker while FAZ40 appeared weaker (**Fig 3.7A&B**). FAZ10 localisation was seen across both anterior cell tips, with both signals partially co-localised with FLA1BP marker (**Fig 3.7C**). Kinesin protein and FAZ6 localised to one point at the distal end of FLABP marker on the old flagellum side and two points at distal end of FLA1BP marker on the new flagellum side (**Fig 3.7E&F**). The FAZ12 signal was a ring-like shape on both old and new flagellum sides (**Fig 3.7D**).

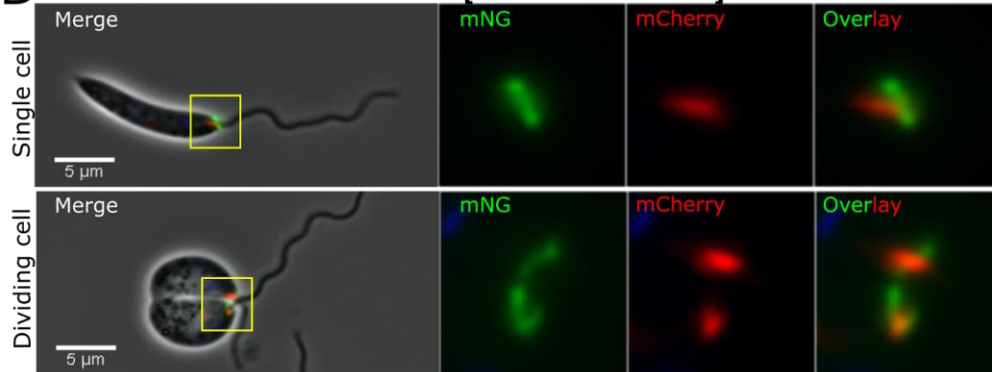
Class IV: Ring/Horseshoe at exit point



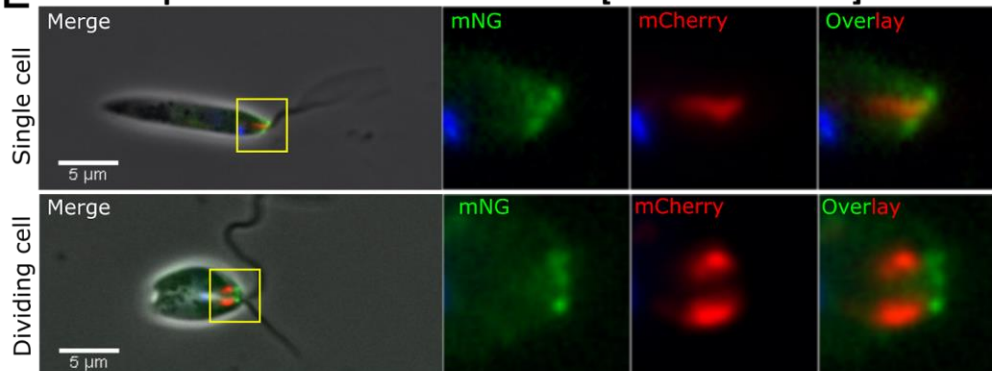
C FAZ10-mNG:LmxM.22.1320 [Marker: FLA1BP]



D FAZ12-LmxM.32.2460:mNG [Marker: FLA1BP]



E Kinesin protein-LmxM.24.1430:mNG [Marker: FLA1BP]



F FAZ6-mNG:LmxM.21.1240 [Marker: FLA1BP]

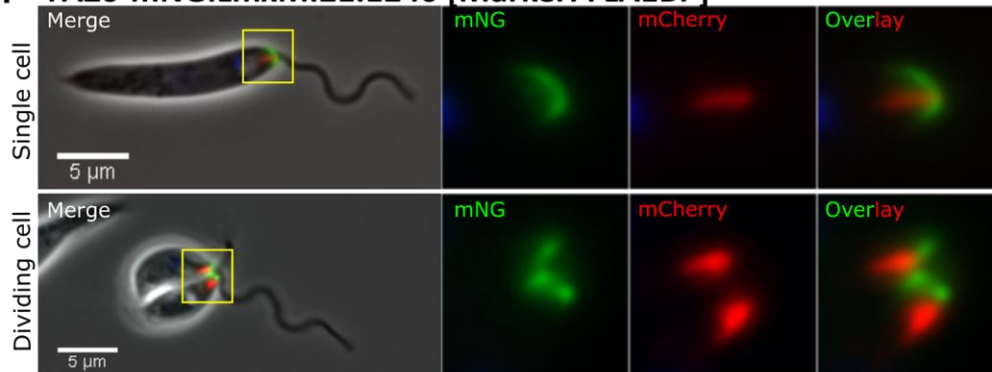
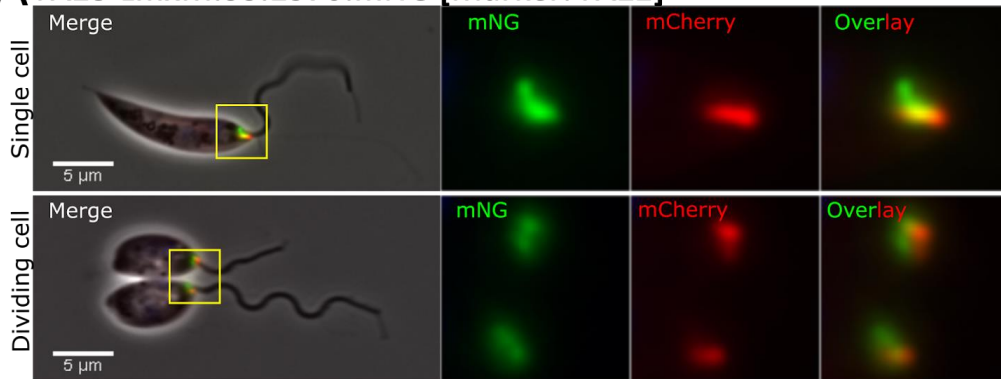


Figure 3.7 *Leishmania* FAZ proteins with Class 4; FAZ ring/horseshoe at exit point localisation. Widefield fluorescence images for each protein A) FAZ14, B) FAZ40, C) FAZ10, D) FAZ12, E) Kinesin protein and F) FAZ6 in single and dividing cells are laid out in the same format: From left, an overlay of the phase contrast (grey), mNG tagged protein (green), mCh tagged marker (red) and Hoechst DNA (blue) then mNG only, and mCherry only, with the far right being an overlay of mNG and mCherry only. The protein name, gene fusion and FAZ marker are shown on top left (LmxM.X.XXXX::mNG for C-terminal tagging and mNG::LmxM.X.XXXX for N-terminal tagging).

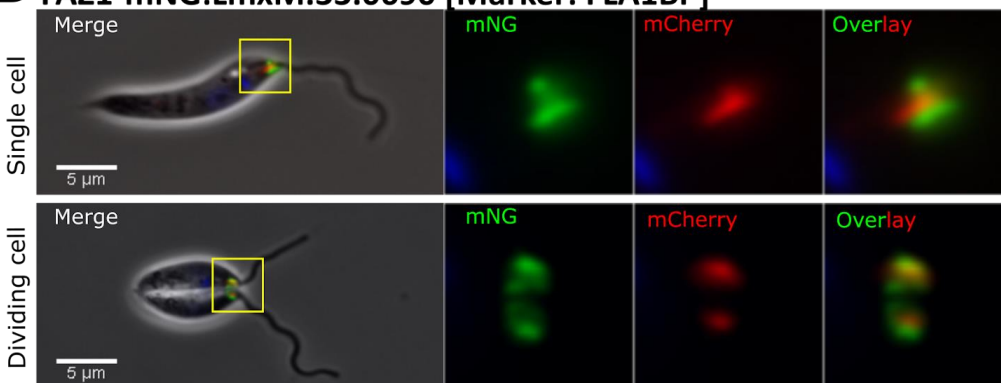
Four proteins; FAZ8 (LmxM.33.2570), FAZ1 (LmxM.33.0690), FAZ29 (LmxM.12.0360) and FAZ9 (LmxM.31.0140) were in class 5 which is short linear signal on the cell body side and a ring-like structure at the pocket collar region (**Fig 3.8**). This localisation pattern resembled an 'L' shape with long linear signal co-localising with FAZ2 marker as seen for FAZ8 and FAZ29 or appearing adjacent to FLA1BP marker as seen for FAZ1 and FAZ9 (**Fig 3.8**). In dividing cells, tagged FAZ1 localised to 'L' like structures on both the old and new flagellum sides (**Fig 3.8B**). FAZ8 and FAZ29 were localised at the proximal ends of the FAZ2 marker, in the pocket collar region without the presence of a linear structure in the cell body FAZ domain on both old and new flagellum sides (**Fig 3.8A&C**). FAZ9 localisation was different and complex, with a cross-like signal on the old flagellum side and linear points surrounding the FLA1BP marker on new flagellum side (**Fig 3.8D**).

Class V: FAZ on the cell body side and collar region

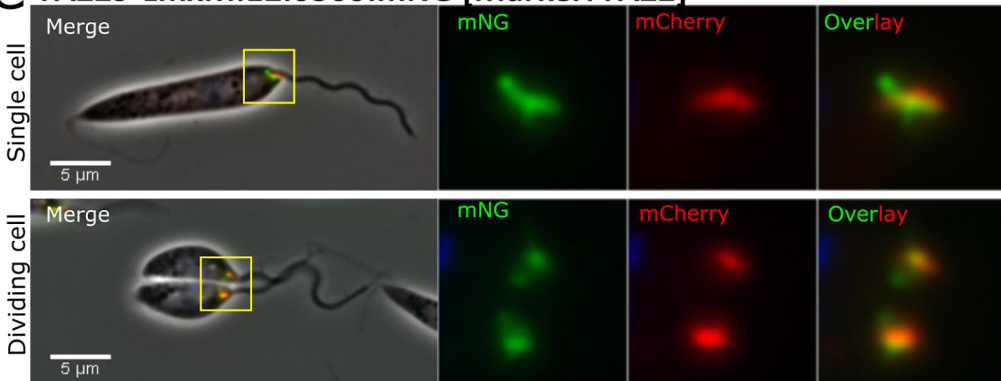
A FAZ8-LmxM.33.2570:mNG [Marker: FAZ2]



B FAZ1-mNG:LmxM.33.0690 [Marker: FLA1BP]



C FAZ29-LmxM.12.0360:mNG [Marker: FAZ2]



D FAZ9-mNG:LmxM.31.0140 [Marker: FLA1BP]

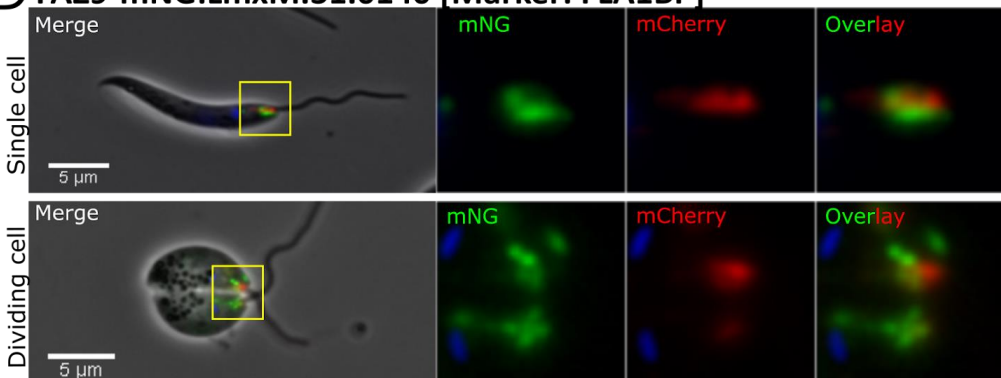


Figure 3.8 *Leishmania* FAZ proteins with Class 5; FAZ ring/horseshoe at exit point localisation. Widefield fluorescence images for each protein A) FAZ8, B) FAZ1, C) FAZ29 and D) FAZ9 in single and dividing cells are laid out in the same format: From left, an overlay of the phase contrast (grey), mNG tagged protein (green), mCh tagged marker (red) and Hoechst DNA (blue) then mNG only, and mCherry only, with the far right being an overlay of mNG and mCherry only. The protein name, gene fusion and FAZ marker are shown on top left (LmxM.X.XXXX::mNG for C-terminal tagging and mNG::LmxM.X.XXXX for N-terminal tagging).

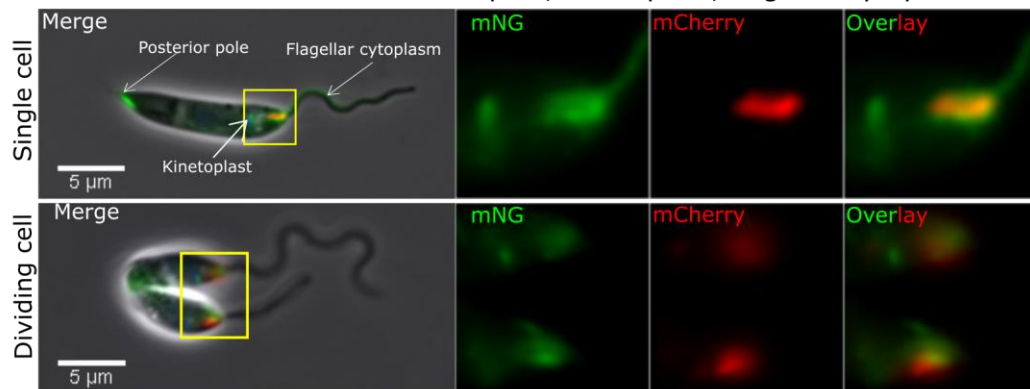
Six proteins; KMP11 (LmxM.34.2221), hypothetical protein (LmxM.32.1035), FAZ24 (LmxM.21.1350), Kinesin 13-5 (LmxM.13.1610), DUF1935 protein (LmxM.33.0190) and FAZ36 (LmxM.27.1400) were in class 6 - complex, a category for those with a FAZ signal and additional localisations elsewhere. KMP11 has a FAZ signal that co-localised with FLA1BP marker, a class 1 localisation along with signals in the flagellar cytoplasm, the posterior cell tip and at the kinetoplast. However, in dividing cells the kinetoplast signal was only seen in the old flagellum inheriting daughter cell (**Fig 3.9A**). The hypothetical protein, LmxM.32.1035 also had a FAZ signal that co-localised with FLA1BP marker but with a much shorter signal length. It was also present on the cytoskeleton at the anterior end of both 1F1N1K and dividing cells. A cleavage furrow signal was also seen in dividing cells with the FAZ signal found only on the old flagellum cell side. Meanwhile, the kinetoplast signal was seen on the new flagellum cell side (**Fig 3.9B**). FAZ24 had a class 2, linear FAZ on the cell body side signal and was found adjacent to the FLA1BP marker along with signals in the basal body and the posterior cell tip. In dividing cells, the FAZ signal appeared as a point on each side with the basal body signal being visible only on the old flagellum side of dividing cells, while posterior cell tip localisation disappeared (**Fig 3.9C**). The Kinesin 13-5 FAZ localisation was more complex with signals on both sides of the FLA1BP::mCherry marker and this signal was no longer visible in the dividing cells. Instead a cleavage furrow signal was present, which was stronger on the old flagellum side. A posterior cell tip signal was only seen in all 1F1N1K cells and the old flagellum side of dividing cells. (**Fig 3.9D**). DUF1935 protein had FAZ class 1 signal, co-localised with the FLA1BP marker with additional cytoplasm and flagellar cytoplasm signals. In dividing cells,

this FAZ signal also co-localised with the marker on the new and old flagellum side, but this signal appeared weaker on the old flagellum. The cytoplasm and flagellar cytoplasm signals were also still present (**Fig 3.9E**). FAZ36 had a FAZ class 2 appearance, adjacent to FLABP signal with additional kinetoplast, cytoplasm and flagellar cytoplasm signals. Whilst in dividing cells tagged FAZ36 was also found in the cleavage furrow in addition to the FAZ and cytoplasmic signals (**Fig 3.9F**).

Complex FAZ

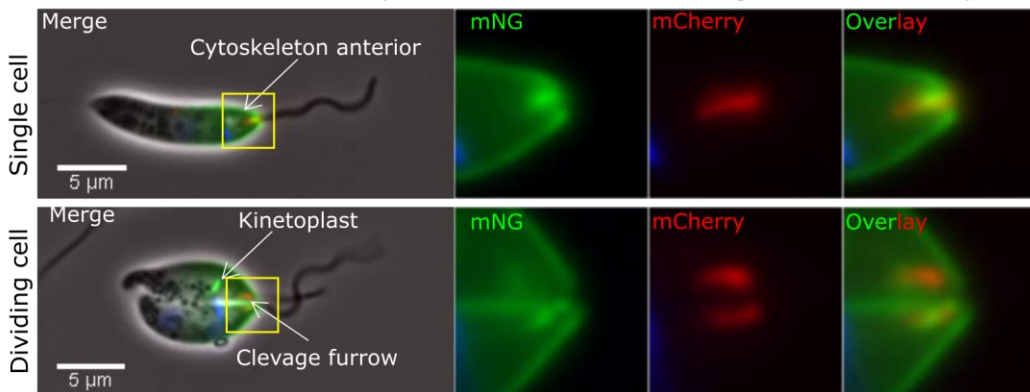
A KMP11- mNG:LmxM.34.2221 [Marker: FLA1BP]

Additional localisations: Posterior pole, kinetoplast, flagellar cytoplasm



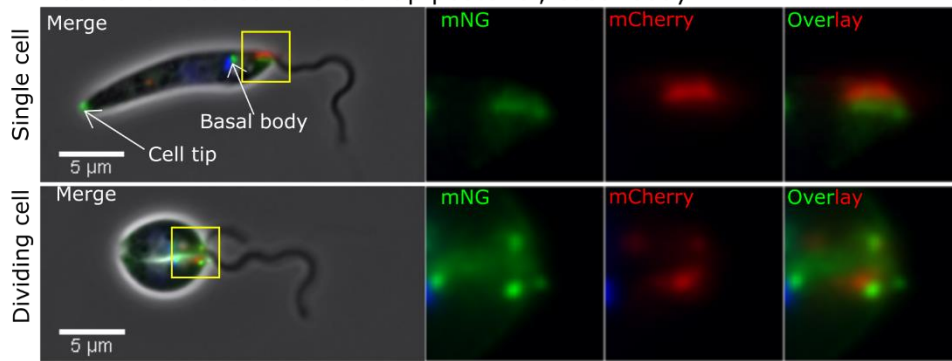
B Hypothetical protein- mNG:LmxM.32.1035 [Marker: FLA1BP]

Additional localisations: Cytoskeleton anterior, cleavage furrow, kinetoplast



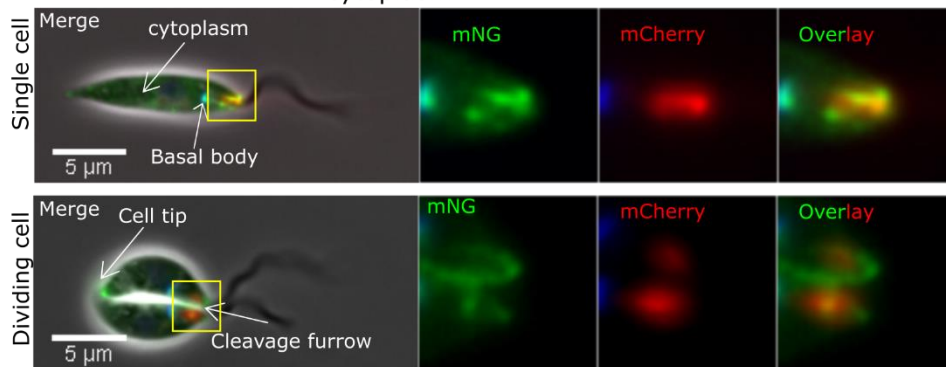
C FAZ24- mNG:LmxM.21.1350 [Marker: FLA1BP]

Additional localisations: Cell tip posterior, basal body



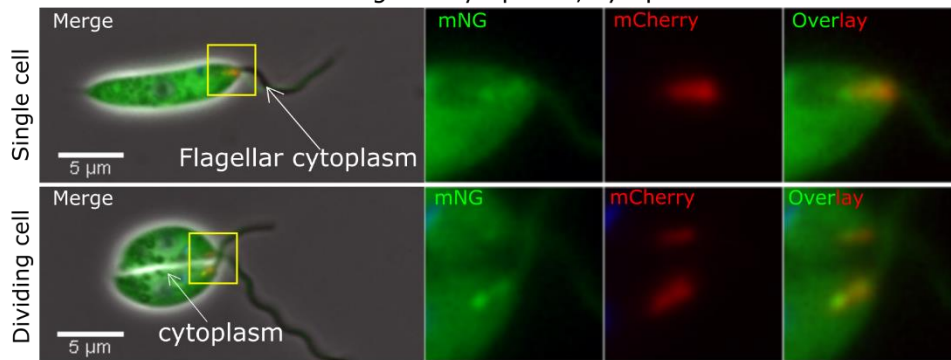
D Kinesin 13-5- LmxM.13.1610:mNG [Marker: FLA1BP]

Additional localisations: Cell tip posterior, basal body, cleavage furrow, cytoplasm



E DUF1935- mNG:LmxM.33.0190 [Marker: FLA1BP]

Additional localisations: Flagellar cytoplasm, cytoplasm



F FAZ36- mNG:LmxM.27.1400 [Marker: FLA1BP]

Additional localisations: Flagellar cytoplasm, cytoplasm, cleavage furrow, Kinetoplast

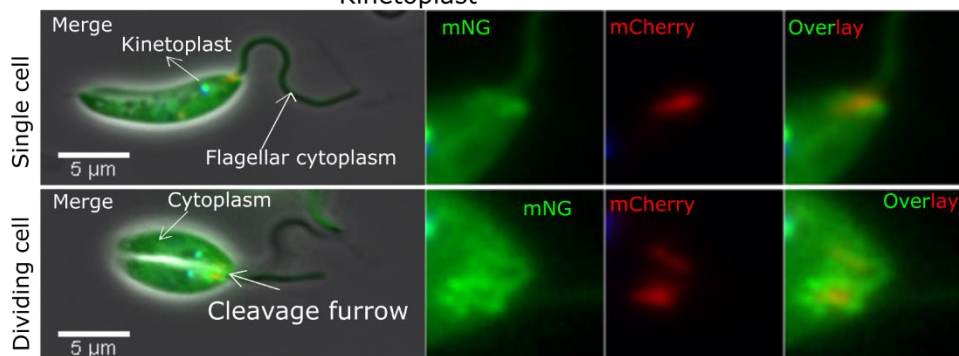


Figure 3.9 *Leishmania* FAZ proteins with Class 6; Complex FAZ localisations.

Widefield fluorescence images for each protein in single and dividing cells are laid out in the same format: From left, an overlay of the phase contrast (grey), mNG tagged protein (green), mCh tagged marker (red) and Hoechst DNA (blue) then mNG only, and mCherry only, with the far right being an overlay of mNG and mCherry only. The protein name, gene fusion and FAZ marker are shown on top left (LmxM.X.XXXX::mNG for C-terminal tagging and mNG::LmxM.X.XXXX for N-terminal tagging). Additional localisations are indicated beneath gene ids with arrows showing their location.

3.5 *T. brucei* FAZ protein localisation and domain pattern correlated with *L. mexicana* orthologs

To identify if there was a pattern and correlation in FAZ localisation classes between *L. mexicana* and *T. brucei*, the two datasets were compared (**Table 3.2**). The FAZ in *T. brucei* has three main structural domains, flagellum, intracellular and cell body (Sunter and Gull, 2016). Some of the domain localisations for the *T. brucei* FAZ proteins are known and indicated in Table 3.2, alongside their *T. brucei* FAZ localisation and the FAZ localisation class in *L. mexicana* (**Table 3.2**).

As previously shown, seven proteins were identified with a linear signal on the flagellum side of the neck in *L. mexicana*. Six of their orthologs in *T. brucei* localised along the full length of the FAZ while one, a cAMP binding protein was localised to the distal only region. All of the *L. mexicana* FAZ proteins of this class except for FLA1BP (LmxM.10.0620) do not have transmembrane domains. The presence of a transmembrane domain in FLA1BP suggests that this protein is likely to lie within the intracellular domain on the flagellum side. This correlates with its ortholog in *T. brucei*, known to be located in the intracellular domain (Sun *et al.*, 2013). Three other FAZ proteins in *T. brucei* within this group (FLAM3, FAZ27 and CLPGM6) were known to be in the flagellum domain (B. Rotureau *et al.*, 2014; Hayes *et al.*, 2014; An *et al.*, 2020). This suggests that there is correlation between Class I (Linear FAZ localisation on the flagellum side) in *L. mexicana* and full length FAZ localisation within the flagellum domain in *T. brucei*.

For *L. mexicana*, four proteins were identified with a linear signal in the cell body region of the neck. One of the proteins, FAZ5 (LmxM.36.5970) is a likely intracellular domain protein as it contains multiple transmembrane domains, which correlates with its ortholog in *T. brucei* (Sunter *et al.*, 2015, 2019). While the domain position of FAZ28/30 is unknown in *T. brucei*, it shares a full length localisation with FAZ2 (distal-enriched) and CC2D, known FAZ filament domain proteins (Zhou *et al.*, 2011; Sunter *et al.*, 2015). Similar to the previous class, it appeared that the linear FAZ signal seen in *L. mexicana* correlates with the full length FAZ signal seen in *T. brucei* but within the FAZ filament domain.

FAZ3, was the sole protein identified as a class III (ring/horseshoe signal at the collar region) in *L. mexicana*. Its ortholog in *T. brucei* was a full length FAZ shown to locate in the FAZ filament domain (Sunter *et al.*, 2015).

Class IV, a ring/horseshoe at the exit point in *L. mexicana* contains six proteins. All of the Class IV orthologs in *T. brucei* were full length with distal enrichment or distal only. Three proteins, FAZ14, FAZ6, FAZ12 were known FAZ filament domain proteins in *T. brucei* (Hu, Zhou and Li, 2015b; Sunter *et al.*, 2015); however, the FAZ10 ortholog in *T. brucei* was shown to localise to the intracellular domain (Moreira *et al.*, 2017). The domain localisation for FAZ40 and the kinesin in *T. brucei* is currently unknown. With the flagellum exit point in *L. mexicana* being at the distal end of the flagellar pocket neck and therefore the distal end of the FAZ, this suggests a link with these Class IV proteins and those with a distal FAZ localisation in *T. brucei*.

For Class V, four proteins including FAZ29, FAZ8, FAZ1 and FAZ9 were identified with a combination of a linear signal on the cell body side and a ring/horseshoe signal at the collar region. Their orthologs in *T. brucei* localised along the entire length of the FAZ, with three of those (FAZ8, FAZ1 and FAZ9) identified as FAZ filament domain proteins (Vaughan *et al.*, 2008; Sunter *et al.*, 2015). This suggests that the combination of linear FAZ on cell body side with horseshoe/ring at the collar region signals in *L. mexicana* correlates with the full length localisation within the FAZ filament in *T. brucei*. Together these results show that, each FAZ class in *L. mexicana* correlates with specific groups of localisations/FAZ domains in *T. brucei*.

Table 3.2 Comparison of FAZ localisations in *L. mexicana* and *T. brucei* Known FAZ domains of FAZ proteins in *T. brucei* are indicated below.

<i>L. mexicana</i>			<i>T. brucei</i>			
Gene ID	Protein name	TMDs	Gene ID	Localisation	Known FAZ domains	References
Linear on flagellum side						
LmxM.10.0620	FLA1BP	yes	Tb927.8.4050	Full-distal	Intracellular	(Sun <i>et al.</i> , 2013)
LmxM.16.1660	FLAM3	no	Tb927.8.4780	Full length	Flagellum	(Rotureau, Subota and Bastin, 2011)
LmxM.04.0890	FAZ27	no	Tb927.9.8350	Full-distal	Flagellum	(An <i>et al.</i> , 2020)
LmxM.04.1100	FAZ32	no	Tb927.9.8650	Full length	Not known	
LmxM.18.1440	FAZ34	no	Tb927.10.12630	Full-distal	Not known	
LmxM.27.0490	ClpGM6	no	Tb927.11.1090	Full length	Flagellum	(Hayes <i>et al.</i> , 2014)
LmxM.36.0830	cAMP binding protein	no	Tb927.10.5240	distal only	Not known	
Linear on cell body side						
LmxM.12.1120	FAZ2	no	Tb927.1.4310	Full-distal	FAZ Filament	(Sunter <i>et al.</i> , 2015)
LmxM.33.2540	CC2D	no	Tb927.4.2080	Full length	FAZ filament	(Qing Zhou <i>et al.</i> , 2011)
LmxM.36.5970	FAZ5	yes	Tb927.10.8830	Full length	Intracellular	(Sunter <i>et al.</i> , 2015)
LmxM.30.2590	FAZ28/30	no	Tb927.4.5000	Full length	Not known	
Ring/horseshoe at collar region						
LmxM.09.0520	FAZ3	no	Tb927.11.12530	Full length	FAZ filament	(Sunter <i>et al.</i> , 2015)
Ring at exit point						
LmxM.30.3110	FAZ14	no	Tb927.4.5340/ Tb927.8.6980	Full-distal	FAZ filament	(Hu, Zhou and Li, 2015b)
LmxM.21.1240	FAZ6	no	Tb927.10.840	Full-distal	FAZ filament	(Sunter <i>et al.</i> , 2015)
LmxM.32.2460	FAZ12	no	Tb927.11.2590	Full-distal	FAZ filament	(Hu, Zhou and Li, 2015b)
LmxM.22.1320	FAZ10	no	Tb927.7.3330	Full-distal	Intracellular	(Moreira <i>et al.</i> , 2017)
LmxM.18.1560	FAZ40	no	Tb927.10.12470	distal only	Not known	
LmxM.24.1430	Kinesin, putative	no	Tb927.8.6830	distal only	Not known	
Linear on cell body side & at collar region						
LmxM.12.0360	FAZ29	no	Tb927.6.840	Full length	Not known	
LmxM.33.2570	FAZ8	no	Tb927.4.2060	Full length	FAZ filament	(Sunter <i>et al.</i> , 2015)
LmxM.33.0690	FAZ1	no	Tb927.4.3740	Full length	FAZ filament	(Vaughan <i>et al.</i> , 2008)
LmxM.31.0140	FAZ9	no	Tb927.10.14320	Full length	FAZ filament	(Sunter <i>et al.</i> , 2015)

3.6 26 *L. mexicana* orthologs did not localise to the FAZ

26 candidate proteins were found not to localise to the FAZ but instead localised to the following; 9 in the cytoplasm, 4 in the ER, 7 to the cytoskeleton, 2 to the basal body/pro-basal body paired with cytoplasmic signals and 3 with complex signals, 1 with Endocytic/lysosome signal (**Table 3.3**). Examples are shown in (**Fig 3.10**). See appendix for full list of images (**Appendix B**).

In the examples shown, LmxM.31.2610, TOEFAZ1 localised to the nucleus and posterior cell tip in G1 cells; however, these localisations were not seen in dividing cells. Instead, a cleavage furrow signal was seen during cell division (**Fig 3.10A**). This cleavage furrow signal was also seen in LmxM.36.1920 (FAZ tip-localising protein) and LmxM.36.6960 (CIF4). This suggests these proteins known to initiate cytokinesis in *T. brucei*, are also likely important for cytokinesis in *L. mexicana* (Hilton *et al.*, 2018; Hu *et al.*, 2019). Of the non-FAZ orthologs in *L. mexicana*, six appeared to have a potential role in cytokinesis with either a cleavage furrow or anterior cytoskeleton localisation, which suggests the possibility of a different role for the FAZ in cytokinesis in *Leishmania* in comparison to *T. brucei*. LmxM.34.3720 localised to the cytoskeleton in the posterior region of both G1 and dividing cells (**Fig 3.10B**). LmxM.11.1320 had a web-like localisation, labelling the internal membranes throughout the central to anterior region of all cells, likely the endoplasmic reticulum (**Fig 3.10 C**). There were four orthologs with this localisation and all were FAZ-ER proteins in *T. brucei*, suggesting the ER localisation of these proteins is conserved between species. LmxM.19.0140 localised to the lysosome, but in the dividing cells there was an additional kinetoplast signal (mitochondrial DNA) (**Fig 3.10D**).

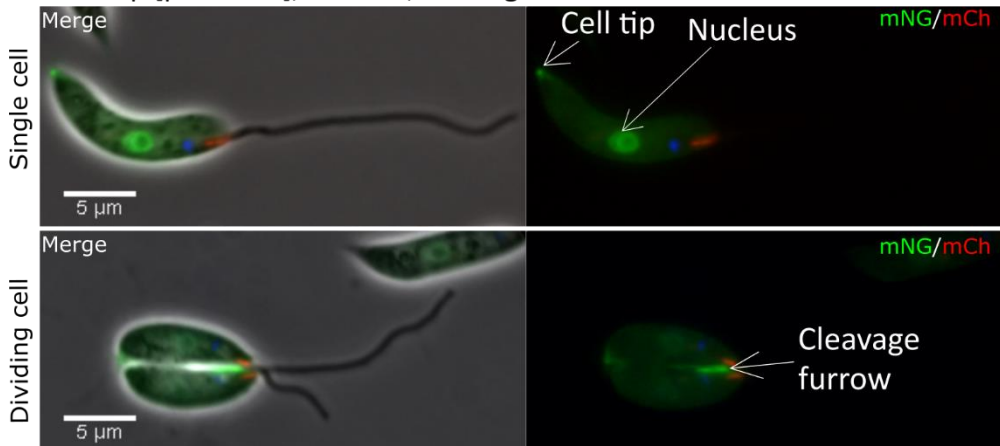
Table 3.3 Proteins with non-FAZ localisations. Localisations are listed below. Some localisations were specifically at the anterior end (A) or posterior end (P). Abbreviations: Basal body (BB), pro-basal body (pBB) and endoplasmic reticulum (ER).

<i>L. mexicana</i>			<i>T. brucei</i>	
Gene ID	Protein name	Localisations	Gene ID	Localisation
Cytoplasm				
LmxM.12.1190	ABC transporter	cytoplasm (weak)	Tb927.1.4420	FAZ-ER
LmxM.34.5010	mitogen-activated protein kinase	cytoplasm reticulated (weak)	Tb927.9.9320	Full Length
LmxM.33.0060	hypothetical protein, conserved	cytoplasm (points)	Tb927.10.2480	Complex
LmxM.24.0700	hypothetical predicted multi-pass transmembrane protein	cytoplasm posterior (points)	Tb927.11.5370	FAZ-ER
LmxM.14.1200	phosphatidylserine synthase	cytoplasm, lysosome	Tb927.7.3760	FAZ-ER
LmxM.02.0140	Ankyrin repeats (3 copies)/Zinc finger, C3HC4 type (RING finger)	cytoplasm	Tb927.2.2360	Distal only
LmxM.27.1040	Stumpy formation signalling pathway protein	cytoplasm (points)	Tb927.11.1640	Complex
LmxM.31.0220	hypothetical protein, conserved	cytoplasm (points)	Tb927.10.14400	Complex
LmxM.16.0490	Amastin surface glycoprotein	cytoplasm (points), lysosome	Tb927.4.3520	Complex
Cytoskeleton				
LmxM.29.2580	reticulon domain protein, 22 kDa potentially aggravating protein (pape22)	cytoskeleton (A), cytoplasm (points)	Tb927.6.3840	FAZ-ER
LmxM.18.1080	cAMP-dependent protein kinase catalytic subunit 3 (PKAC3)	cytoskeleton, cytoplasm	Tb927.10.13010	Complex
LmxM.36.1920	FAZ-tip-localizing protein required for cytokinesis	cytoskeleton (A), cleavage furrow	Tb927.10.6360	Distal only
LmxM.23.0080	Posterior and Ventral Edge protein 1	cytoskeleton (P)	Tb927.8.2030	Complex
LmxM.34.3720	hypothetical protein, conserved	cytoskeleton (P)	Tb927.9.11540	Complex
LmxM.36.6960	Cytokinesis initiation factor 4	cytoskeleton (A), cleavage furrow	Tb927.10.8240	Distal only
LmxM.21.0700	phosphoserine/threonine/tyrosine-binding protein	cytoplasm, cytoskeleton (A)	Tb927.10.1620	Complex
Complex				
LmxM.21.1220	Furrow 1 protein	Cell tip (P)/cytoplasm point	Tb927.10.870	Complex
LmxM.31.2610	Tip Of Extending FAZ protein 1	cell tip (P), cleavage furrow, nucleus	Tb927.11.15800	Distal only
LmxM.13.1590	Spindle assembly abnormal 4	Cell tip (A), BB, Kinetoplast, cytoskeleton (A)	Tb927.11.3300	Complex
LmxM.19.0680	Flagellum attachment zone protein 7A	cytoskeleton (A), BB, pBB	Tb927.10.15390	Distal only
LmxM.19.0140	Associated kinase of Tb14-3-3	cytoplasm, lysosome, kinetoplast	Tb927.10.14770	Complex
ER				
LmxM.22.1010	UAA transporter family	ER	Tb927.7.3070	FAZ-ER
LmxM.09.1050	MSP (Major sperm protein) domain containing protein	ER	Tb927.11.13230	FAZ-ER
LmxM.11.1320	major facilitator superfamily	ER	Tb927.11.6060	FAZ-ER
LmxM.31.2680	hypothetical protein, conserved	ER	Tb927.11.15870	FAZ-ER
Endocytic/lysosome				
LmxM.29.2670	Autophagy-related protein 27	endocytic, lysosome	Tb927.6.3940	Complex

Non FAZ examples

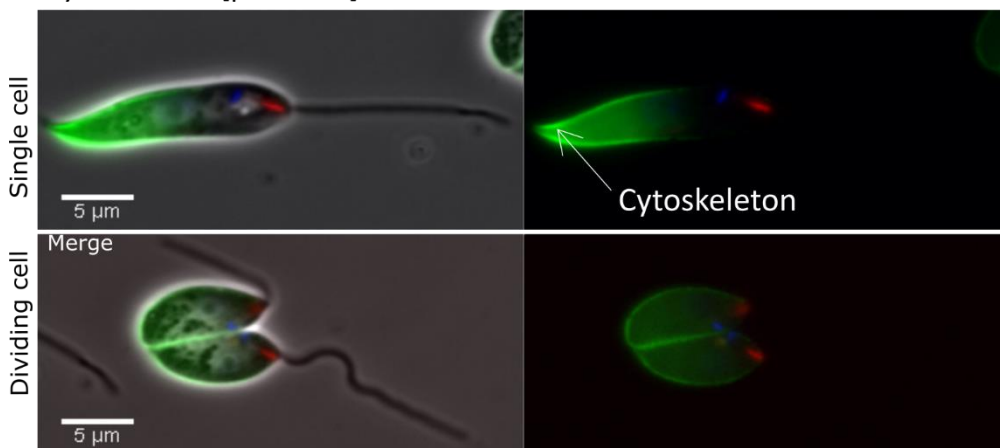
mNG:LmxM.31.2610 [Marker FLA1BP]

Cell tip [posterior], nucleus, cleavage furrow



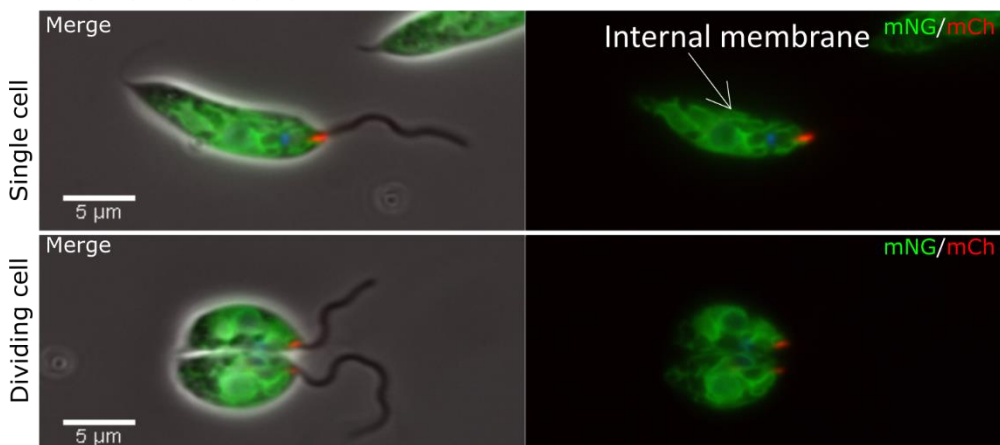
LmxM.34.3720:mNG [Marker FLA1BP]

Cytoskeleton [posterior]



mNG:LmxM.11.1320 [Marker FLA1BP]

Internal membrane



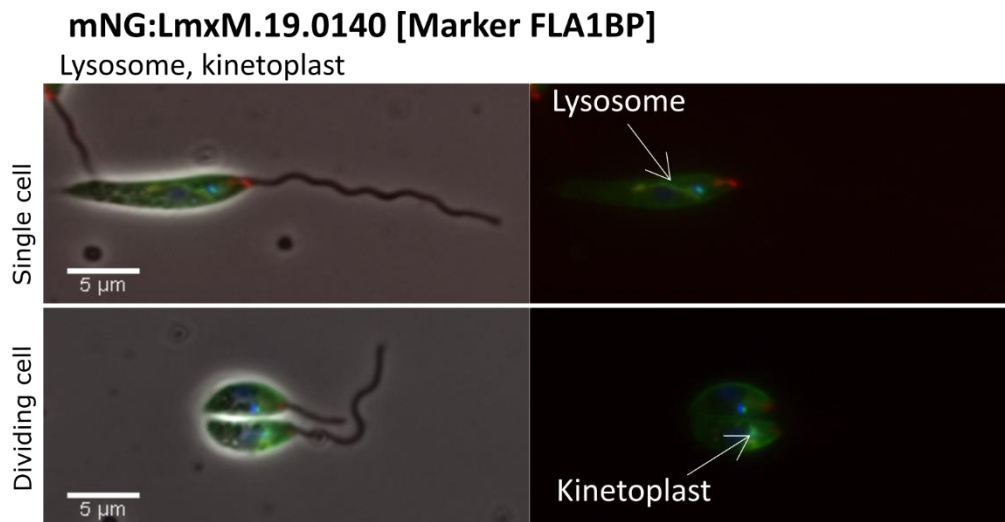


Figure 3.10 Non FAZ localisation examples. Widefield fluorescence images for each protein in single and dividing cells are laid out in the same format: Left, an overlay of the phase contrast (grey), mNG tagged protein (green), mCh tagged marker (red) and Hoechst DNA (blue) and right, the overlay of mNG AND mCh only. The protein name, gene fusion and FAZ marker are shown on top left (LmxM.X.XXXX::mNG for C-terminal tagging and mNG::LmxM.X.XXXX for N-terminal tagging). Annotations are displayed with arrows indicating their location.

3.7 All five FAZ localisation classes begin to assemble a new FAZ structure during early flagellum biogenesis

The mechanism of flagellar pocket duplication and segregation is unclear in *L. mexicana*, with the role and process of FAZ duplication during flagellar pocket duplication poorly understood. To understand how these classes duplicated throughout the cell cycle, proteins were selected that represent the different localisation classes. The following proteins were chosen; FLAM3 for the flagellum (Class I), FAZ2 for the cell body (Class II), FAZ3 for the collar (Class III) and FAZ10 (Class IV) for the exit point and each was tagged with the mCherry fluorescent protein tag (**Fig 3.11**). Due its complexity, Class V which contains both cell body and collar domain signals was not analysed, as the duplication events of the proteins with more restricted localisations needed to be understood first. The flagellum and cell body domains also include their respective regions of plasma membrane, so FLA1BP and

FAZ5 were selected to represent these membrane regions on the flagellum and cell body side respectively.

To gain an overview of how FAZ proteins from different classes progress through the cell cycle, images were taken from 3 different points of the cell cycle, 1F1N1K, 2F1N1K and 2F2N2K. 2F1N1K cells have a new flagellum that would have recently exited the flagellar pocket and 2F2N2K are cells with flagellar pockets that have already segregated and the cell has begun to divide. First, the focus was on the proteins with a linear localisation signal, FLAM3, FLA1BP, FAZ5 and FAZ2. As previously shown, in 1F1N1K cells they had a linear signal (**Fig 3.11A-D**). In 2F1N1K cells, a second but weaker linear signal, which were either shorter or same length as the first was seen for all four, FLAM3, FLA1BP, FAZ5 and FAZ2 proteins. These two linear signals, reduced in length in 2N2F2K cells (**Fig 3.11A-D**).

FAZ3 had a ring/horseshoe signal distal to the collar region as previously shown in 1F1K1N cells (**Fig 3.11E**). In 2F1N1K cells, there were two separate signals which were also present in 2F2N2K cells (**Fig 3.11E**). Like the linear FAZ proteins (FLAM3, FLA1BP, FAZ5 and FAZ2), both FAZ signals appeared to have reduced in size during duplication (**Fig 3.11E**). For FAZ10, a horseshoe/ring signal at the exit in 1F1N1K was seen, which was duplicated into two separate signals of the old and new flagella in 2F1N1K (**Fig 3.11F**). These signals remained in 2F2N2K cells (**Fig 3.11F**). To determine whether the FAZ3 and FAZ10 signals in 2F1K1N represented two separate horseshoe/ring structures each associated with a flagellum or a single enlarged structure encompassing two flagella TEM was carried out. This showed cells in which two flagella share one neck region prior to flagellar pocket segregation (**Fig 3.12**). This suggests that the separate signals seen for FAZ3 and FAZ10 at the distal to collar region and exit point in 2F1N1K cells are likely the result of an expansion of the structures containing these proteins within the existing flagellar pocket. From this (**Fig 3.11 and 3.12**), it seems that the critical time for new FAZ assembly occurred between the 1F1N1K and 2F1N1K stage and was completed by the 2F2N2K stage.

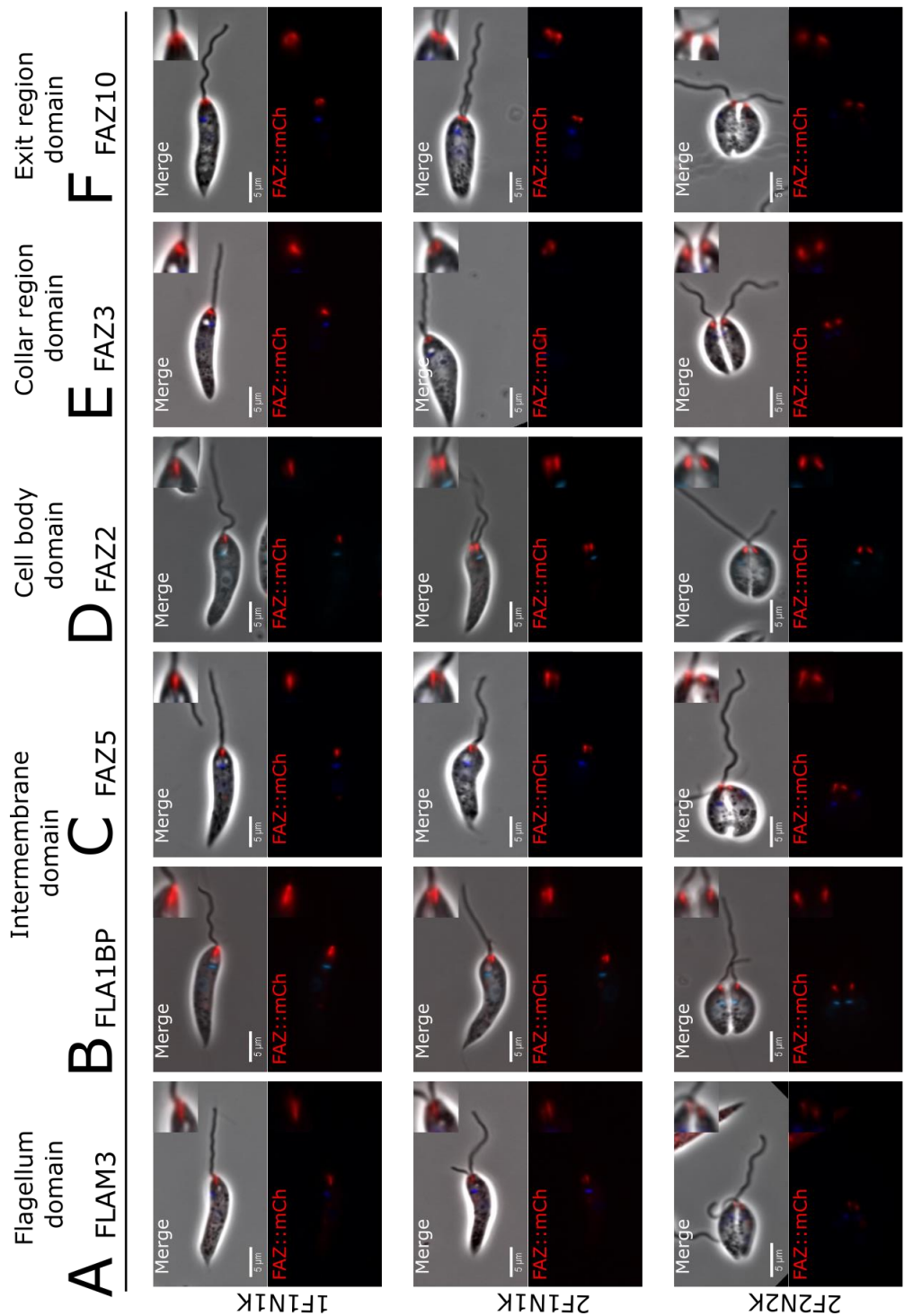


Figure 3.11 New FAZ begins to form by the time new flagellum emerges out of the flagellar pocket. Widefield fluorescence images for each representative domain protein A) FLAM3, B) FLA1BP, C) FAZ5, D) FAZ2, E) FAZ3 and F) FAZ10 in 1F1N1K, 2F1N1K and 2F2F2K cells. Top, an overlay of phase contrast (grey), mCh tagged protein (red) and Hoechst DNA (blue). Bottom, an overlay of mCh only. Both overlays have inserts at top right showing FAZ region in more detail.

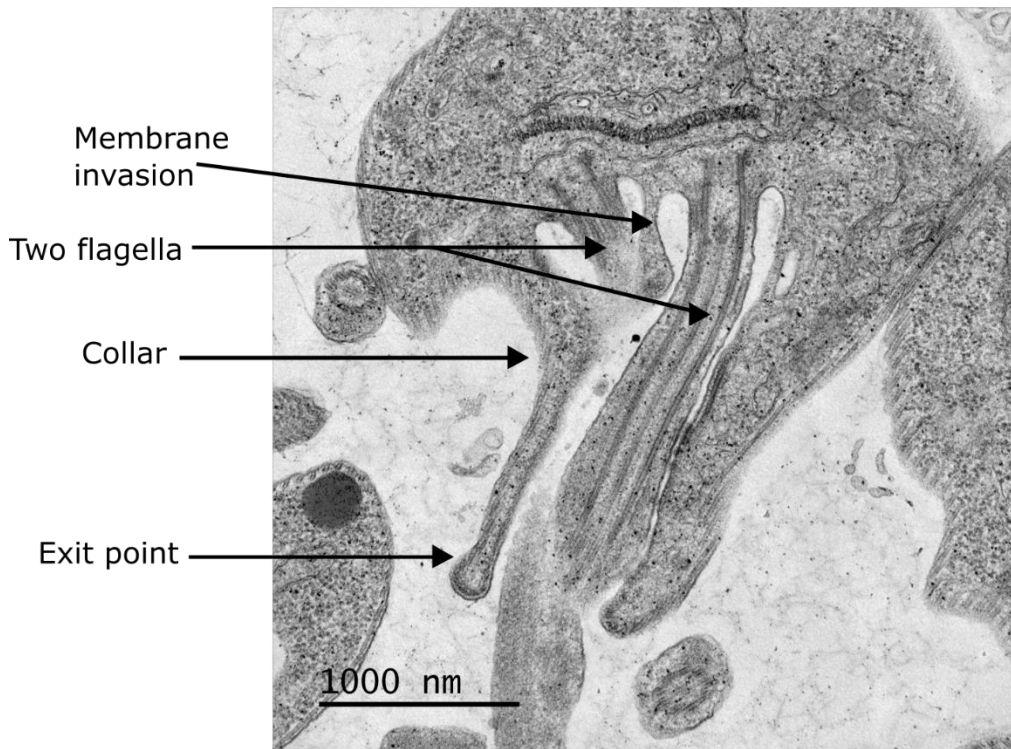


Figure 3.12 Two flagella were seen in the pre-existing flagellar pocket before segregation in *L. mexicana*. Image was taken by Edward Rea (Oxford Brookes University). Membrane invasion, flagella, collar and exit point are indicated by arrows.

3.8 Discussion

3.8.1 Five FAZ localisation classes were identified in *L. mexicana*

The localisation screen by endogenous tagging candidate proteins with the mNG fluorescent protein identified 28 FAZ proteins in *L. mexicana*, with five different FAZ classes defined on their localisation patterns (**Fig 3.13**). Following the FAZ classes through the cell cycle showed that the FAZ begins to duplicate by the 2F1N1K stage and is assembled fully by the 2F2N2K cell cycle stage, demonstrating that the new FAZ formation process begin during new flagellum assembly and is completed by flagellar pocket segregation.

Recently, a study on the kinesin FAZ7B (not localised in this study) demonstrated another potential localisation class with this protein localising as an asymmetric ring surrounding the majority of the flagellar neck region. FAZ7B was suggested to be

associated with specific microtubules such as cortical, cytoplasmic or pocket microtubules (Corrales *et al.*, 2021). The Class III protein FAZ3 differs from this, with a much narrower appearance with likeness a to the ring component of Class V localisation pattern, suggesting that FAZ3 is distinct to FAZ7B with likely different functions.

Interestingly, it appears that only proteins in the linear FAZ of the cell body side of the neck region can also be associated with the horseshoe/ring distal to the collar region, yet for example none of 23 FAZ orthologs here localise to both the neck region and the exit point, suggesting these two regions could be separate structures as mentioned by Wheeler 2016 (Wheeler, Sunter and Gull, 2016). Nevertheless, its important to be mindful that the FAZ proteins discovered here are limited to proteins conserved in *T. brucei*, therefore not *L. mexicana* specific. This analysis of FAZ proteins and their distinctive localisation classes; however, offers an opportunity to discover more FAZ partners through proteomic approaches, which may reveal *L. mexicana* or promastigote and amastigote specific FAZ proteins and give a further insight into FAZ biology of *L. mexicana*

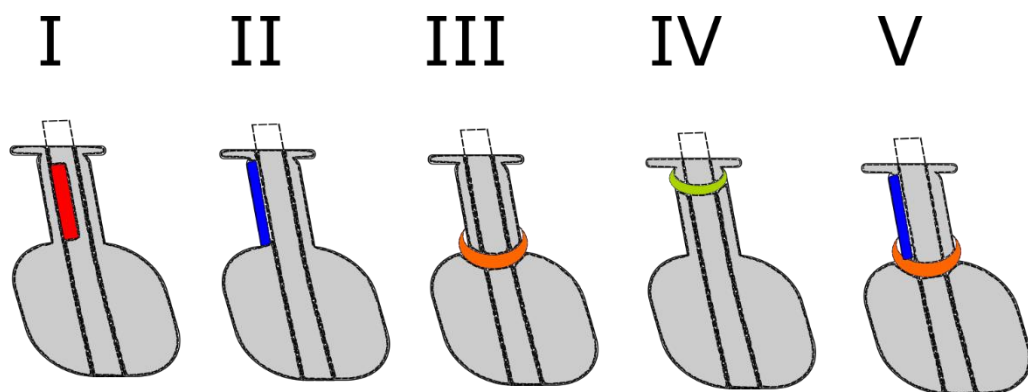


Figure 3.13 Five FAZ classes were defined by their localisation pattern in *L. mexicana*. I- Linear on the flagellum side, II- Linear on the cell body side, III- Horseshoe/ring distal to the collar region, IV- Horseshoe/ring at the exit point and V- Linear on the cell body side and horseshoe/ring distal to the collar region.

3.8.2 FAZ classes in *L. mexicana* correlate with specific groups in *T. brucei*

FAZ proteins possessing a full length localisation within the flagellum domain in *T. brucei* correlated with FAZ Class I linear localisation on the flagellum side in *L. mexicana*. This suggests that these two groups perform similar functions between species. If this is the case, it could mean that two unknown proteins with no transmembrane domains detected, FAZ32 (Tb927.9.8650) and FAZ34 (Tb927.10.12630) which produced full length FAZ signals are likely to be located within the flagellum FAZ domain in *T. brucei*. Furthermore, the FAZ Class II linear localisation on the cell body side in *L. mexicana* correlated with the full length localisation within the FAZ filament domain in *T. brucei*. With this similarity between species, the unknown domain protein FAZ28/30 with no transmembrane domains detected is therefore likely to be located within the FAZ filament domain in *T. brucei*.

FAZ3 was the sole protein of Class III, horseshoe/ring at the collar region identified in *L. mexicana*. Its ortholog was a full-length protein located within the FAZ filament domain in *T. brucei*. It was not possible to compare the pattern with just one protein but this divergence from commonly associated class II localisation suggests a likely change of function between species.

The FAZ class IV, a ring/horseshoe localisation at the exit point, distal of the neck in *L. mexicana* correlated with distal enriched/ distal only localisation in *T. brucei*. In *T. brucei*, three proteins, FAZ14, FAZ6 and FAZ12 were known FAZ filament proteins but FAZ10 was identified within the intracellular domain. This correlates with FAZ10 distinctive localisation restricting to the exit point only, while the other FAZ class IV proteins have dome-like appearance spanning the exit point and the anterior end of the cell. This suggests a potential difference in function with FAZ14, FAZ6 and FAZ12 connected to other parts of the cytoskeleton such as the sub-pellicular array, while FAZ10 is specific to the exit point. This also suggests that two unknown domain proteins, FAZ40 and the kinesin are likely to be in FAZ filament in *T. brucei*.

Class V, is more complex. The Class V linear localisation on the cell body side with horseshoe/ring at the collar region in *L. mexicana* appeared to correlate with full length localisations within FAZ filament domain in *T. brucei*. These proteins include FAZ1 and FAZ9, which were suggested to be located further away from the attachment region within the FAZ filament in *T. brucei* (Sunter and Gull, 2016). A recent study showed that while *L. mexicana* and *T. brucei* share the same core structures such as MtQ and filament, they displayed some differences. The neck region in *L. mexicana* and the proximal end of FAZ in *T. brucei* is similar, but in *L. mexicana* the FAZ filament is located separately from the junctional complexes connecting the flagellum to the cell body (Wheeler, Sunter and Gull, 2016). It is possible that Class V FAZ proteins in *L. mexicana* are linked to FAZ proteins located further away from the attachment area in *T. brucei*.

Based on the data shown, it appears that despite the differences in FAZ structure, both species show a correlation in their FAZ protein localisation patterns and groups; however, this correlation is limited to FAZ proteins in *L. mexicana* that are conserved in *T. brucei*. Identifying *L. mexicana* specific FAZ proteins will not only bring an insight into the extent of FAZ differences in both species, but also potential evolutionary adaptations that may have occurred.

3.8.3 20 *T. brucei* FAZ proteins are specific to trypomastigote and epimastigote morphology

Three proteins, the FAZ-tip localising protein, CIF4 and TOEFAZ1, were conserved across *T. cruzi*, *L. mexicana*, *P. confusum* and *B. saltans* and were localised to the distal only region of the FAZ in *T. brucei*. They were found to be important for cytokinesis (Hilton *et al.*, 2018; Hu *et al.*, 2019). However, in *L. mexicana*, they were not localised to the FAZ, but within the cleavage furrow in dividing cells. This suggests that the FAZ does not have the same role in initiating cytokinesis in *L. mexicana* as it does in *T. brucei*. Meanwhile, other proteins important for cytokinesis such as CIF2 and CIF3 in *T. brucei* were not conserved in *L. mexicana* but were conserved in *T. cruzi*, suggesting that the regulation of cytokinesis in *L. mexicana* differs to trypanosomes and these differences are potentially caused by the different

morphological requirements for the division of a promastigote versus trypomastigote cell.

Six FAZ proteins identified in *T. brucei* were either proximal enriched or proximal only, with five being conserved in *T. cruzi* but only one was conserved in *L. mexicana*. In *L. mexicana*, this one protein, a stumpy formation signalling pathway protein in *T. brucei* was localised to the cytoplasm. This suggests that the proximal based FAZ proteins have a distinctive function specific to *T. brucei* and *T. cruzi* which share similar morphologies, and may not be required in *L. mexicana* promastigote morphology. Meanwhile, nine FAZ-ER orthologs were all conserved in *T. cruzi*, and the eight conserved in *L. mexicana* were localised mostly in the cytoplasm or ER with no signals seen within the FAZ region. This is not surprising as ER is not located within the FAZ region in *L. mexicana* and serves to highlight the differences in structure and function of the FAZ between species (Wheeler, Sunter and Gull, 2016).

Chapter 4

Analysis of 23 FAZ proteins from 5 FAZ localisation classes revealed functional groups responsible for flagellum attachment and cell morphogenesis

Declaration: The results in this chapter were used to inform the work in Halliday, C. *et al.* (2020) 'Role for the flagellum attachment zone in Leishmania anterior cell tip morphogenesis', *PLoS Pathogens*, 16(10). doi: 10.1371/journal.ppat.1008494.

4.1 Preface

In the localisation screen (**Chapter 3**) 23 FAZ proteins from 5 different FAZ localisation classes were identified in *L. mexicana*. There were a further 6 proteins identified with a FAZ signal and additional localisations and/or a FAZ signal that was cell cycle dependent; therefore, these proteins were assigned as 'complex'.

The function of FAZ in *L. mexicana* has yet to be fully deciphered and only three proteins have been studied in detail. FAZ5 was found to be important for flagellar pocket shape and function, while FAZ2 is critical for cell tip morphogenesis (Sunter *et al.*, 2019; Halliday *et al.*, 2020). Recent findings showed that FAZ7B is required for cell morphogenesis and cell division (Corrales *et al.*, 2021). Studies in *T. brucei* showed that the RNAi knockdown phenotypes of FAZ proteins were found to be associated with their location within the FAZ structure, 1) FAZ flagellum domain, 2) FAZ intracellular domain and 3) cell body domain (Sunter and Gull, 2016). Each structural domain appears to have distinctive functions, for example, the flagellum domain is important for cellular morphology, while the intracellular domain is vital for flagellum attachment and the cell body domain is critical for either flagellum attachment or the correct positioning of kinetoplast/nucleus (Sunter and Gull, 2016).

The functional analysis of 23 FAZ proteins identified in the localisation screen offers the opportunity to determine protein function and correlate that with specific locations within the *L. mexicana* FAZ.

4.2 A pipeline was established for the functional analysis of FAZ null mutants

28 FAZ proteins in *L. mexicana* were identified in the localisation screen (**Chapter 3**), but six of these proteins, LmxM.34.2221, LmxM.32.1035, LmxM.21.1350, LmxM.13.1610, LmxM.33.0190 and LmxM.27.1400 were complex proteins, so given the focus on FAZ specific functional analysis they were not included in the functional screen. The focus was on the deletion of 23 FAZ proteins from the localisation classes 1-5 (**Table 4.1**). The two linear classes - Class I, linear on flagellum side, which has seven proteins and Class II, linear on the cell body side which has four proteins including two studied previously (FAZ5 and FAZ2) (Sunter *et al.*, 2019; Halliday *et al.*, 2020). The ring/horseshoe FAZ proteins are either in Class III, localised distal to the collar region (one protein) or Class IV, localised at the exit point (six proteins). Class V, the combination of linear FAZ on cell body side and ring/horseshoe distal to the collar region contains five proteins.

The generation of null mutants was carried out by replacing both alleles of the target gene of interest with two drug resistance markers in the FLA1BP::mCherry marker cell line, except for FLA1BP, which was deleted in the mCherry::FAZ2 marker cell line (**Chapter 2, 2.2.2 & 2.3.2**). The null mutants cell lines grew back ~ 10-14 days post-transfection and PCR was carried out to confirm the deletion of these genes. These null mutants were assessed by light microscopy within 2 weeks of cell growth post-transfection.

To assess for any possible phenotypes from gene deletion and to ensure fairness throughout, the following criteria was set and applied to all null mutants generated in this screen: 1) observation of atypical cell types and quantitation of cell types direct from culture if required, 2) analysis of cell cycle position numbers defined by F/N/K counts to assess effect on cell cycle 3) observation of change in FAZ marker localisation to determine importance in maintaining FAZ structure and 4) measurements of flagellum and cell body lengths in 1F1N1K cells to evaluate morphology.

Table 4.1 23 FAZ proteins taken forward for functional analysis screening in in *L. mexicana*.

Gene ID	Protein name
Class I: Linear on flagellum side	
LmxM.10.0620	FLA1 binding protein
LmxM.16.1660	Flagellar Member 3
LmxM.04.0890	FAZ27
LmxM.04.1100	FAZ32
LmxM.18.1440	FAZ34
LmxM.27.0490	ClpGM6
LmxM.36.0830	cAMP binding protein
Class II: Linear on cell body side	
LmxM.12.1120	FAZ2
LmxM.33.2540	CC2D
LmxM.36.5970	FAZ5
LmxM.30.2590	FAZ28/30
Class III: Ring/horseshoe distal to collar region	
LmxM.09.0520	FAZ3
Class IV: Ring/horseshoe at exit point	
LmxM.30.3110	FAZ14
LmxM.21.1240	FAZ6
LmxM.32.2460	FAZ12
LmxM.22.1320	FAZ10
LmxM.18.1560	FAZ40
LmxM.24.1430	Kinesin
Class V: Linear on cell body side & distal to collar region	
LmxM.12.0360	FAZ29
LmxM.33.2570	FAZ8
LmxM.33.0690	FAZ1
LmxM.32.0670	protein phosphatase 2A regulatory subunit
LmxM.31.0140	FAZ9

4.3 Class I

Class I FAZ proteins FLA1BP (LmxM.10.0620), FLAM3 (LmxM.16.1660), FAZ27 (LmxM.04.0890), FAZ32 (LmxM.04.1100), FAZ34 (LmxM.18.1440) and cAMP binding protein (LmxM.36.0830) were successfully deleted as confirmed by PCR (**Fig 4.1A-F**). Generation of the ClpGM6 (LmxM.27.0490) null mutant failed three times. ClpGM6 is a large gene (7.1 kb), which could make this difficult, so functional analysis was carried out on six of the seven proteins of this class.

4.3.1 Loose flagella and short flagellum cells were present in FAZ27, FAZ34 and FLA1BP null mutants

Upon initial observations of the null mutants by light microscopy, it was noticed that the FAZ27, FAZ34 and FLA1BP null mutants had atypical phenotypes including, loose flagella, short flagellum cells and cell rosettes (**Fig 4.2A**). To understand how prevalent these atypical cell structures were, quantitation of cell structures in the null mutants compared to the parental were assessed directly from culture. In the parental cultures, 78% and 21% of cells had 1F and 2F respectively. In the FAZ27 null mutant, short flagellum cells and loose flagella represented 22% and 20% of the population, respectively. Rosettes represented 1.5% of the population. 1F (43%) and 2F (13%) cell populations were much lower than the parental (**Fig 4.2B**). The FAZ34 null mutant showed a similar pattern, but with less atypical cell structure numbers. Short flagellum cells, loose flagella and rosettes represented 11%, 9% and 2% of the population, respectively. 1F and 2F cells were also reduced (65% and 12%). Meanwhile, rosettes were not detected in FLA1BP null mutant, but the population consisted of 18% short flagellum cells and 12% loose flagella. 1F cells were also reduced but the proportion of 2F cells was similar to the parental (**Fig 4.2C**).

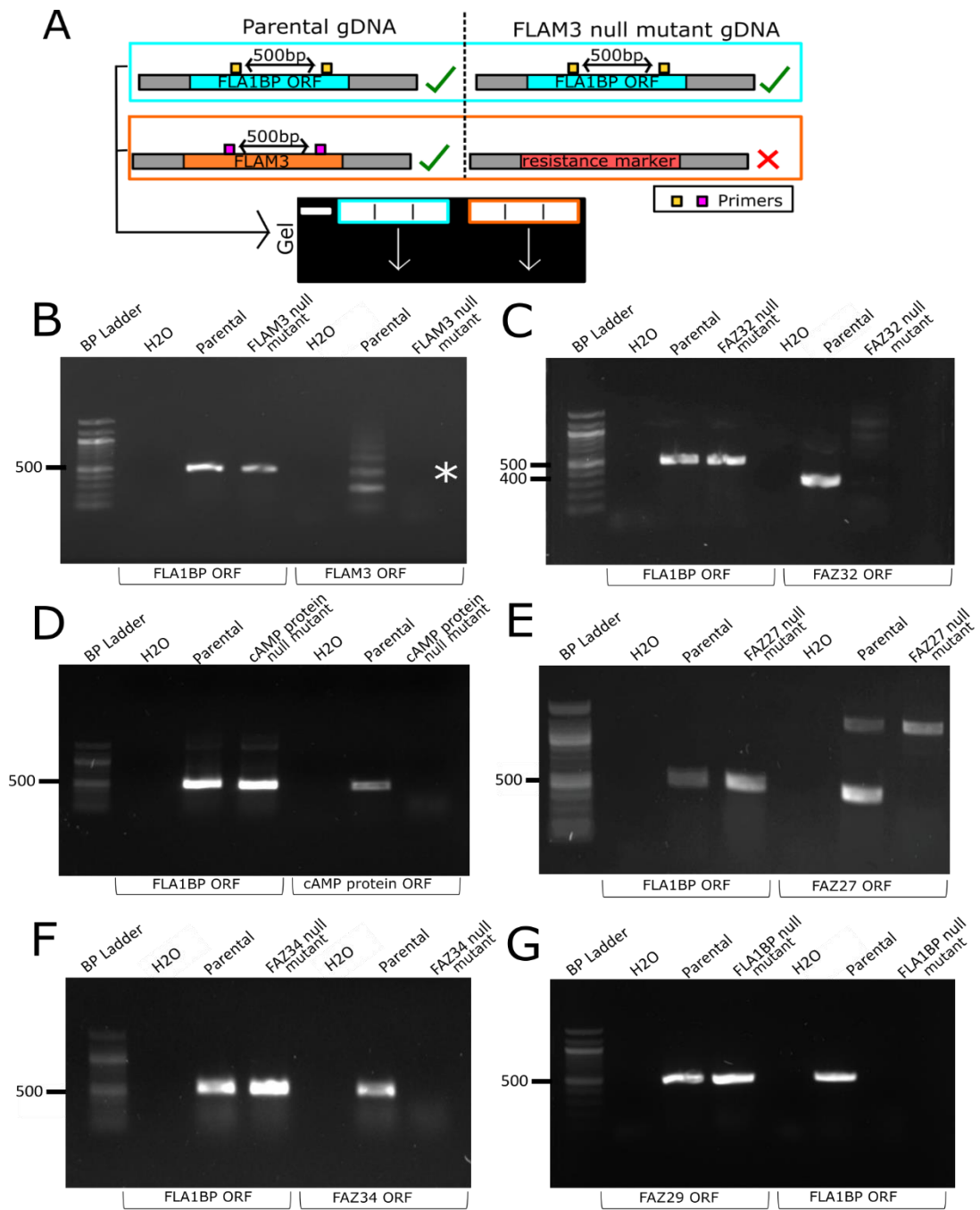


Figure 4.1 Diagnostic PCR confirmed gene deletion for Class I null mutants. A) Representative example for confirming FLAM3 deletion B) LmxM.16.1660 (FLAM3), C) LmxM.04.1100 (FAZ32), D) LmxM.36.0830 (cAMP protein), E) LmxM.18.1440 (FAZ27), F) LmxM.18.1440 (FAZ34) and G) LmxM.10.0620 (FLA1BP). gDNA were extracted from null mutants and tested alongside the parentals for confirmation of gene deletion. Extracted parental gDNA and targeted LmxM.10.0620 (FLA1BP) ORF were used as positive controls while water was used as a negative control. Meanwhile, for FLA1BP null mutant, LmxM.12.0360 (FAZ29) ORF was used as a positive control instead of LmxM.10.0620. The

primers were designed to amplify a 500 bp region from the ORF except for LmxM.04.1100, in which a 400 bp region was amplified. * indicates target band location.

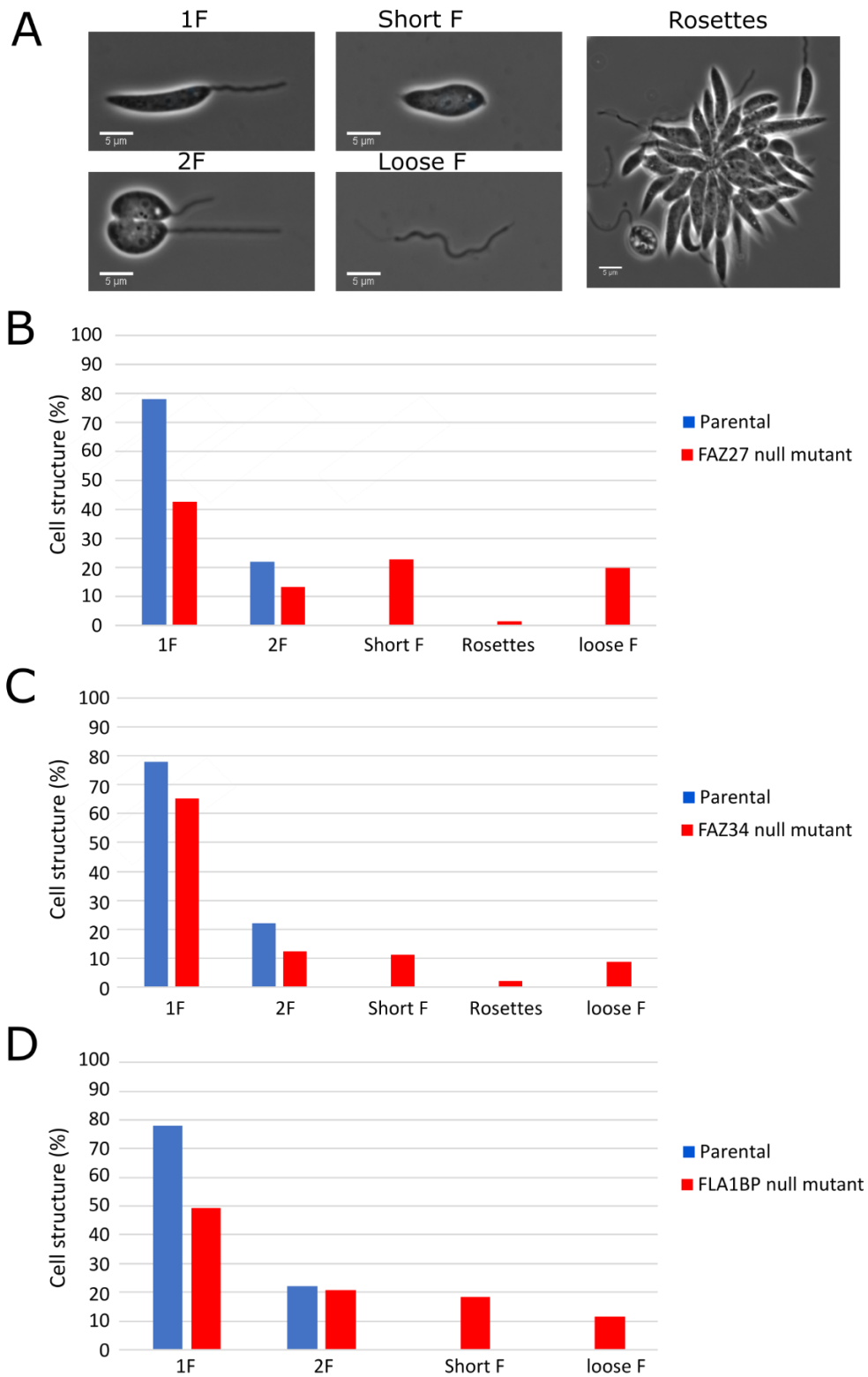


Figure 4.2 Deletion of FAZ27, FAZ34 and FLA1BP resulted in cells with short flagellum and loose flagella. A) Example images of 1F, 2F, cell with a short flagellum, loose

flagellum and rosettes observed. B-D) Quantitation of cell structure seen in B) FAZ27 null mutant, C) FAZ34 null mutant and D) FLA1BP null mutant. Scale bar = 5 μ m.

4.3.2 Cell cycle was only marginally altered in class I null mutants

Next, to determine whether there were changes in the cell cycle, the cell cycle position defined by their K/N/F status from each null mutant and the parental cell line was captured and recorded within two weeks of the cells recovering from transfection. The FLAM3 and cAMP binding protein null mutants cell cycle position numbers were similar to the parental, showing little change in cell cycle progression (**Fig 4.3A**). The FAZ32 null mutant had a larger proportion of 2F1N1K cells (30.8%) and lower proportion of 1F1N1K cells (60%), while later stage cells, 2F2N1K and 2F2N2K proportions were similar to the parental. This suggests that the FAZ32 null mutant spent a longer period in 2F1N1K configuration (**Fig 4.3A**).

For the FAZ27, FAZ34 and FLA1BP null mutants, short flagella were seen in 1F1N1K and 2F2N2K cells and recorded accordingly (**Fig 4.3A**). However, for the FLA1BP null mutant, short flagellum cells were not observed amongst 2F2N2K configuration and there was a smaller proportion of short flagellum cells with 1F1N1K configuration compared to FAZ27 and FAZ34 null mutants (**Fig 4.3A**). This shows that FLA1BP null mutant phenotype was not as severe as FAZ27 and FAZ34 null mutants. The cell cycle position numbers of the FAZ27, FAZ34 and FLA1BP null mutants were similar to the other null mutants and the parental cells when the short flagellum cell categories were taken into account and interpreted as belonging to either 1F1N1K or 2F2N2K cells (**Fig 4.3A**). The results showed there was limited change to the cell cycle and the null mutants were able to grow and divide.

4.3.3 Flagellar streamers are prevalent throughout the cell cycle of cAMP binding protein null mutant

During the cell cycle observations, it was noticed that streamers were associated with the flagellum of the cAMP null mutant in all cell cycle positions (**Fig 4.3B**). To assess how common flagellar streamers were in cAMP null mutant, cells with flagellar streamers were counted and the cell cycle position noted. Streamers were present

on cells throughout the cell cycle and were found on 11.4-35% of cells depending on the cell cycle stage (**Fig 4.3C**).

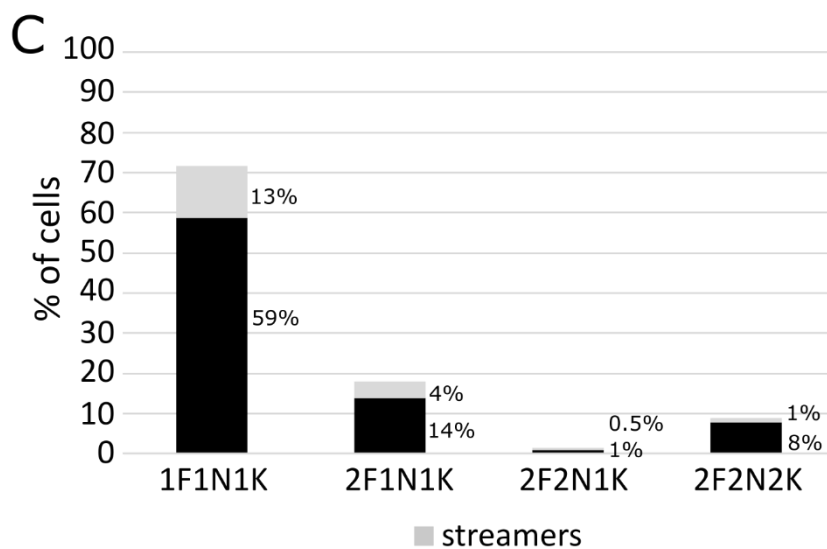
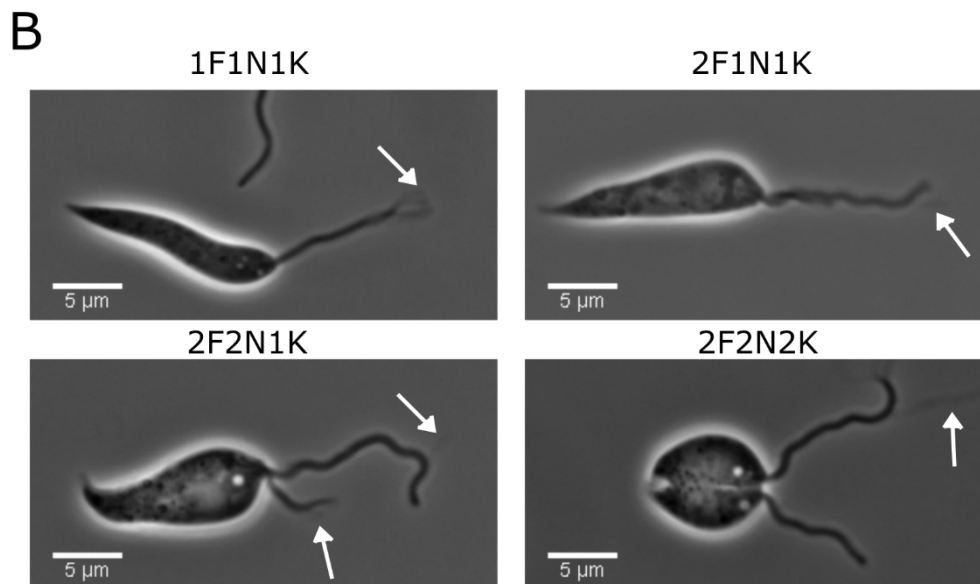
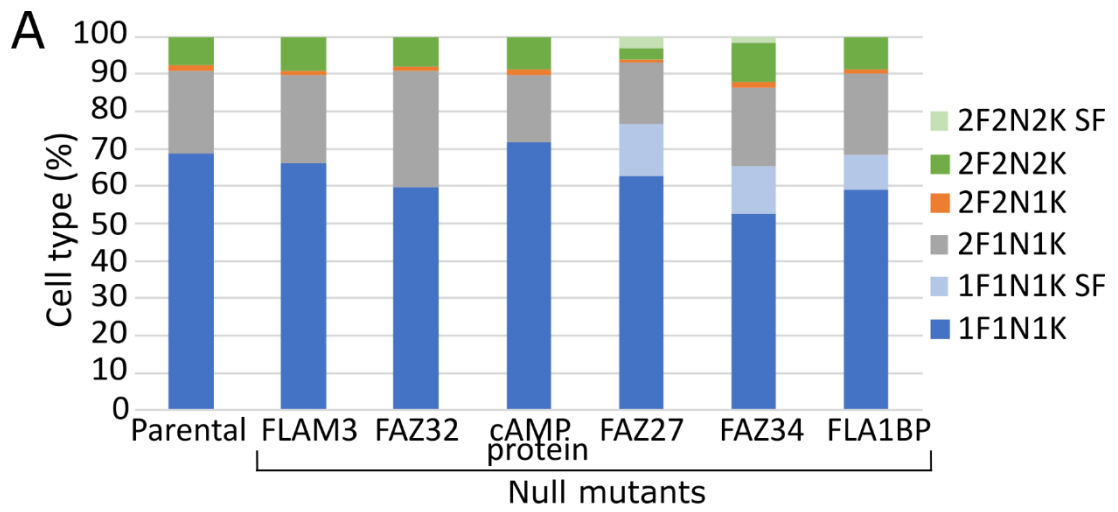


Figure 4.3 Deletion of Class I FAZ proteins did not affect the cell cycle. A) Quantitation of cell cycle positions seen in parental and FAZ null mutants. Cell cycle stages include 1F1N1K, 2F1N1K, 2F2N1K, 2F2N2K and 1F1N1K and 2F2N2K cells with short flagella. B) Examples of streamers seen in cAMP binding protein null mutant 1F1N1K, 2F1N1K, 2F2N1K and 2F2N2K cells indicated by white arrows. C) Quantitation of flagellar streamers seen in each cell cycle stage. Scale bar = 5µm.

4.3.4 FAZ assembly was affected in Class I null mutants

To gain an insight into the importance of Class I FAZ proteins for maintaining the molecular structure of the FAZ, the localisation of the FAZ proteins (mCh::FAZ2 or FLA1BP::mCh) was assessed. In the parental cells, FLA1BP::mCh and mCh::FAZ2 localised to linear structure in the flagellum and cell body side respectively (**Fig 4.4A**). For the FLAM3, FAZ32, cAMP binding protein, FAZ27 and FAZ34 null mutants the FLA1BP::mCh signal was noticeably shorter in 1F1N1K cells (**Fig 4.4 B-F**). This shorter signal was also seen in the short flagellum cells of the FAZ27 and FAZ34 null mutants (**Fig 4.4 E&F**). For the FLA1BP null mutant the mCh::FAZ2 signal was shorter in the 1F1N1K and short flagellum cells (**Fig 4.4G**). For both FLA1BP::mCh and mCh::FAZ2, the difference in signal length in 2F2N2K cells between parental and null mutants was less noticeable. This could be due to FLA1BP::mCh and mCh::FAZ2 signal being naturally shorter in the dividing parental cells (**Fig 4.4A-G**). Together, this suggests that Class I proteins are important for the assembly of a full length flagellar pocket neck FAZ structure.

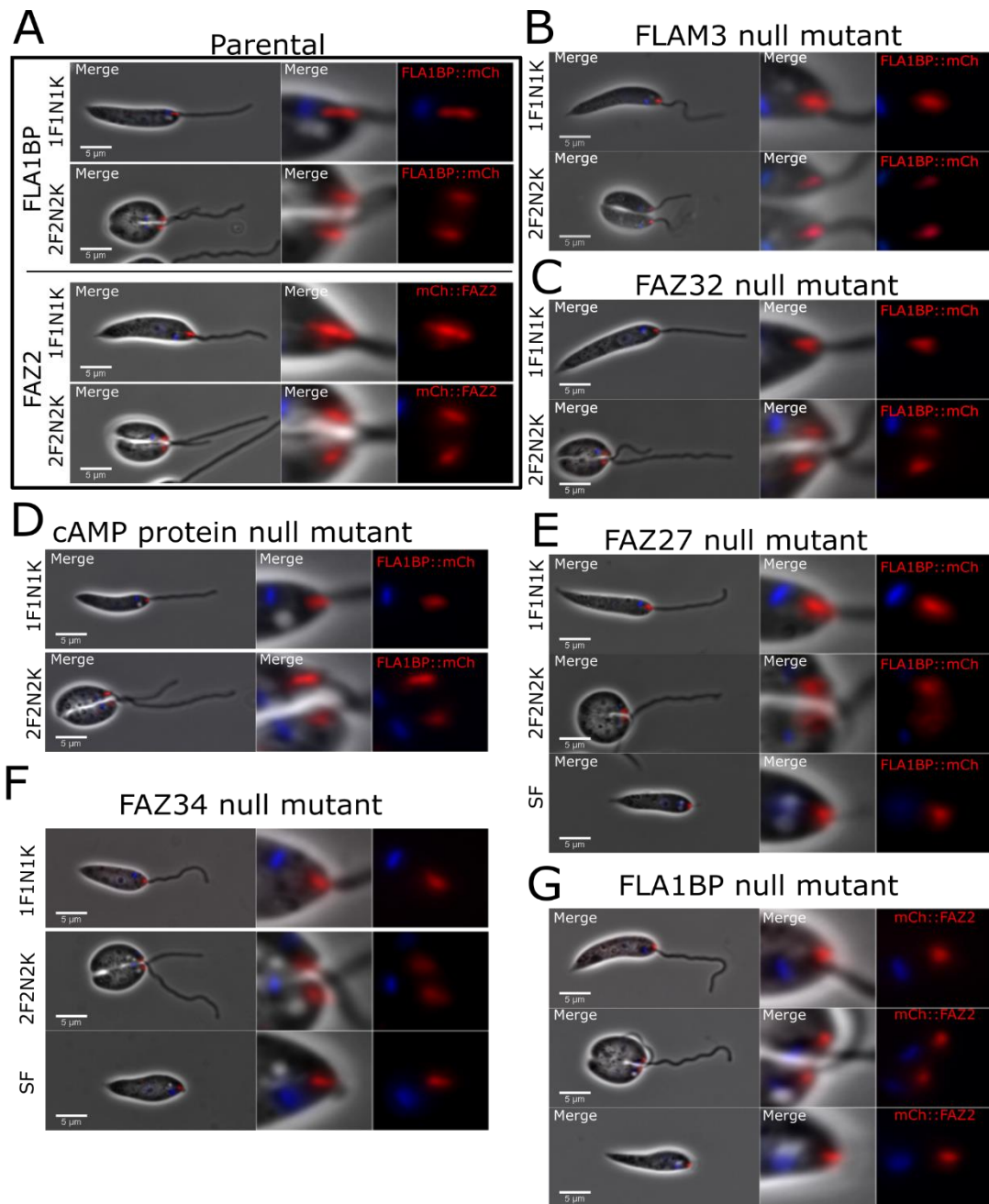


Figure 4.4 FAZ2 and FLA1BP localisation was affected in Class I null mutants. A) Parental marker cell lines, FLA1BP::mCh and mCh::FAZ2, B) FLAM3 null mutant, C) FAZ32 null mutant, D) cAMP protein null mutant, E) FAZ27 null mutant showing short flagellum (SF), F) FAZ34 null mutant showing short flagellum (SF). F) FLA1BP null mutant showing short flagellum (SF). All of the cell lines expressed FLA1BP::mCh except for the FLA1BP null mutant which expressed mCh::FAZ2. Images of cells (merge) contain phase (grey), mCherry (red) and Hoechst (blue). FAZ region insert image on the right contain both merge and mCherry (red) only. Top- 1F1N1K cell and bottom 2F2N2K cell. Scale bar = 5 μ m

4.3.5 FAZ27, FAZ34 and FLA1BP null mutants had shorter cell bodies

The FAZ has important roles in defining cell morphology (Sunter *et al.*, 2019; Halliday *et al.*, 2020; Corrales *et al.*, 2021). To assess any morphological changes, flagellum and cell body lengths were measured for 1F1N1K cells excluding those with a short flagellum. In the parental cells, flagellum length ranged from 8 - 23 μm with a mean of 13.4 μm (**Fig 4.5A**). For the FLAM3 (13.3 μm), FAZ32 (14.2 μm), FAZ27 (14 μm), FAZ34 (13.9 μm) and FLA1BP (14.2 μm) null mutants the mean flagellum length was similar to the parental (**Fig 4.5A**). However, for the cAMP binding protein null mutant the mean was 15.2 μm , higher than the parental (**Fig 4.5A**). These measurements show that flagellum length is unaffected in the majority of Class I null mutants except cAMP binding protein null mutant which had longer flagella.

For 1F1N1K cell body lengths, the parental cells ranged from 8 - 18 μm long with a mean of 13.6 μm (**Fig 4.5B**). For the FLAM3 (13.2 μm), FAZ32 (13.5 μm) and cAMP binding protein (13.4 μm) null mutants the mean cell body lengths were similar to the parental (**Fig 4.5B**). However, for the FAZ27 (12.5 μm), FAZ34 (12.4 μm) and FLA1BP (12.5 μm) null mutants the mean lengths in 1F1N1K cells were shorter by ~ 1 μm . As these null mutants also had short flagellum cells, measurements were also taken of short flagellum 1F1N1K cells to assess if the cell length is also affected in these cells. For the FAZ27, FAZ34 and FLA1BP null mutants the short flagellum cells with 1F1N1K configuration were even shorter, with a mean cell body length of 10.5 μm , 10.8 μm and 11.3 μm respectively. (**Fig 4.5C-E**). This shows that the cell morphology is altered in the FAZ27, FAZ34 and FLA1BP null mutants.

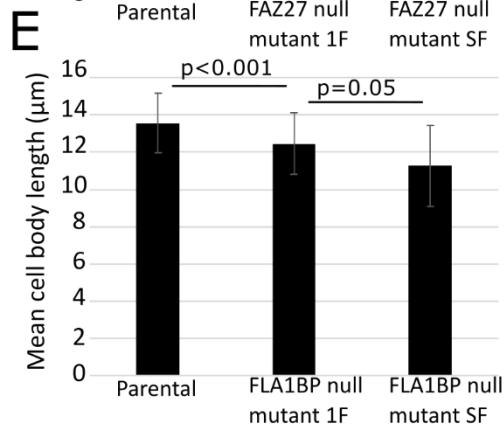
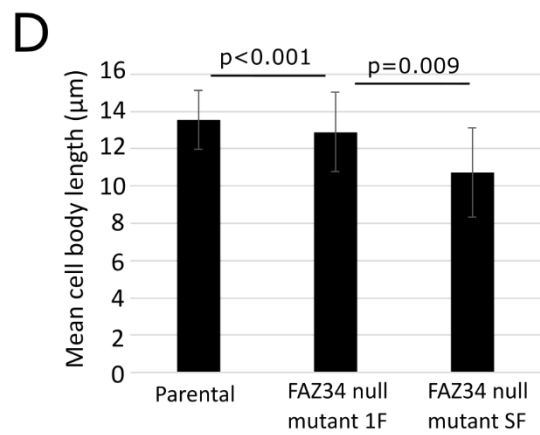
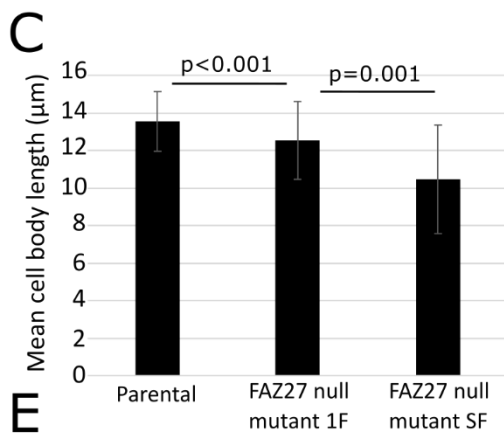
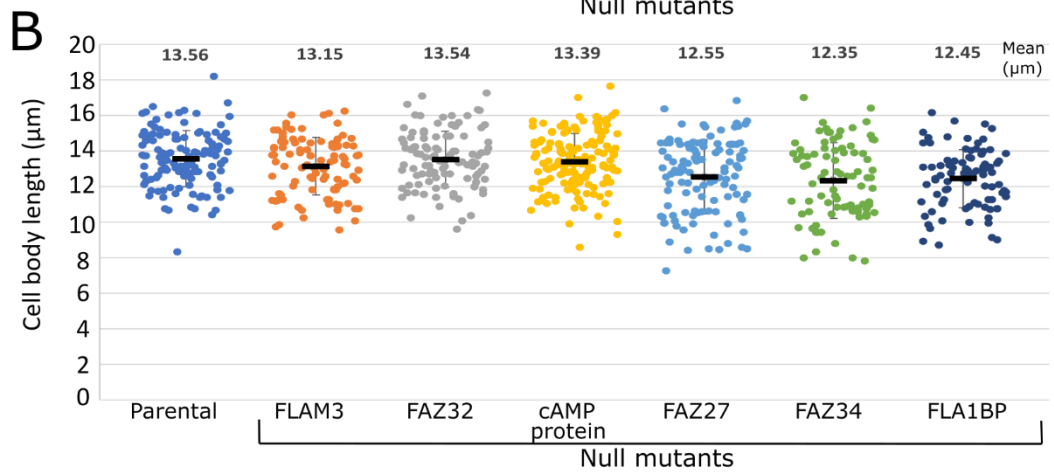
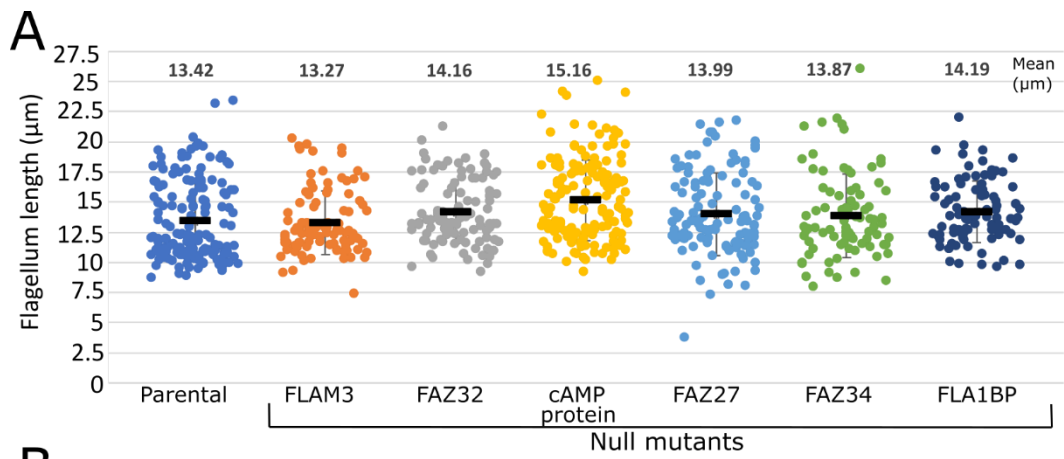


Figure 4.5 Cell body length was reduced in FAZ27, FAZ34 and FLA1BP null mutants.

A) Flagellum lengths of 1F1N1K cells (excluding short flagellum cells), B) Cell body lengths of 1F1N1K cells. Each dot represents the length measurement of an individual cell, and the mean (black bar) was calculated from these length measurements. C) Mean cell body length of the FAZ27 null mutant 1F1N1K and short flagellum (SF) cells, D) Mean cell body length of the FAZ34 null mutant 1F1N1K and short flagellum (SF) cells, E) Mean cell body length of the FLA1BP null mutant 1F1N1K and short flagellum (SF) cells.

4.4 Class II

The genes encoding the four Class II FAZ proteins, FAZ28/30 (LmxM.30.2590), FAZ5 (LmxM.36.5970), CC2D (LmxM.33.2540) and FAZ2 (LmxM.12.1120) were successfully deleted as confirmed by PCR (**Fig 4.6A-E**). Functional analysis was carried out on these four null mutants.

4.4.1 Loose flagella, short flagellum cells and flagellum to flagellum connections were observed in Class II null mutants

Upon initial observations by light microscopy, it was noticed that the FAZ5 null mutant had short flagellum cells, with loose flagella also seen, and the FAZ2 null mutant had atypical flagellum to flagellum connections, while the CC2D null mutant had a mix of both loose flagella, short flagellum cells and flagellum to flagellum connections (**Fig 4.7A**). To understand how prevalent these atypical cell structures were, the different cell types were assessed directly from culture within two weeks of the null mutants growing back post-transfection.

For the FAZ5 null mutant, there was a drop in 1F and 2F cells and this was matched by a large increase in the number of short flagellum cells and loose flagella, with only a small proportion of rosettes observed (**Fig 4.7B**). This phenotype of short flagellum cells and loose flagella was not seen in the published FAZ5 deletion study (Sunter *et al.*, 2019). For the FAZ2 null mutant, short flagellum cells and loose flagella were not seen. Instead, cells with flagellum to flagellum connections (F-F) were seen alongside rosettes, with a drop in 1F and 2F cells (**Fig 4.7C**). These

observations showed that the FAZ2 phenotype here resembled that previously reported (Halliday *et al.*, 2020).

In the CC2D null mutant, a mix of cell structures was observed. There was a drop in 1F and 2F cells with a large increase in short flagellum cells with loose flagella also seen those these were less common than seen for the FAZ5 null mutant. In addition, 13% of cells in the population had an F-F and 9.6% of the population were rosettes. (Fig 4.7D).

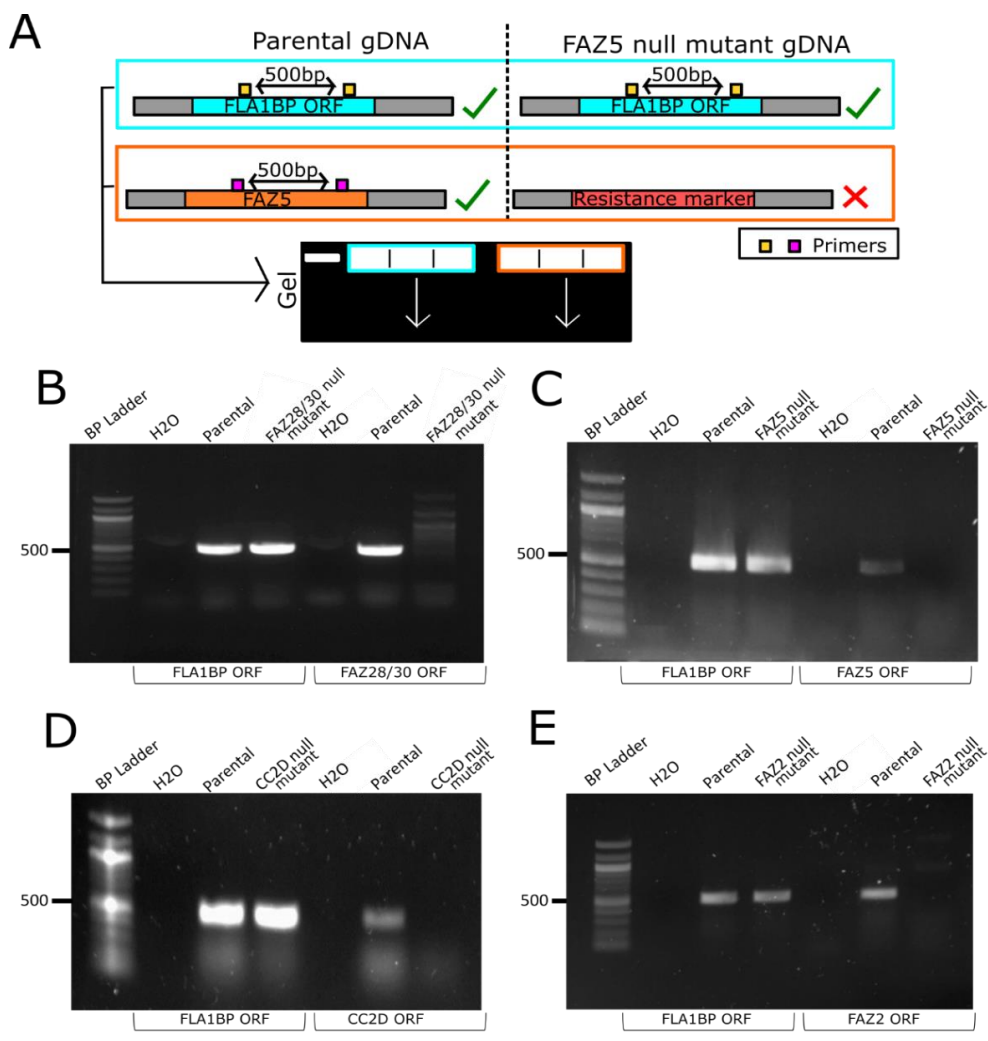


Figure 4.6 Diagnostic PCR confirmed gene deletion for Class II null mutants. A) Representative schematic example for confirming FAZ5 gene deletion. Deletion of the following genes were confirmed, B) LmxM.30.2590 (FAZ28/30), C) LmxM.36.5970 (FAZ5), D) LmxM.33.2540 (CC2D), E) LmxM.12.1120 (FAZ2). gDNAs were extracted from null mutants and tested alongside the parental for confirmation of gene deletion. Extracted parental gDNA and targeted LmxM.10.0620 (FLA1BP) ORF were used as positive controls while H₂O

was used as a negative control. The primers were designed to amplify a 500 bp region from the ORF.

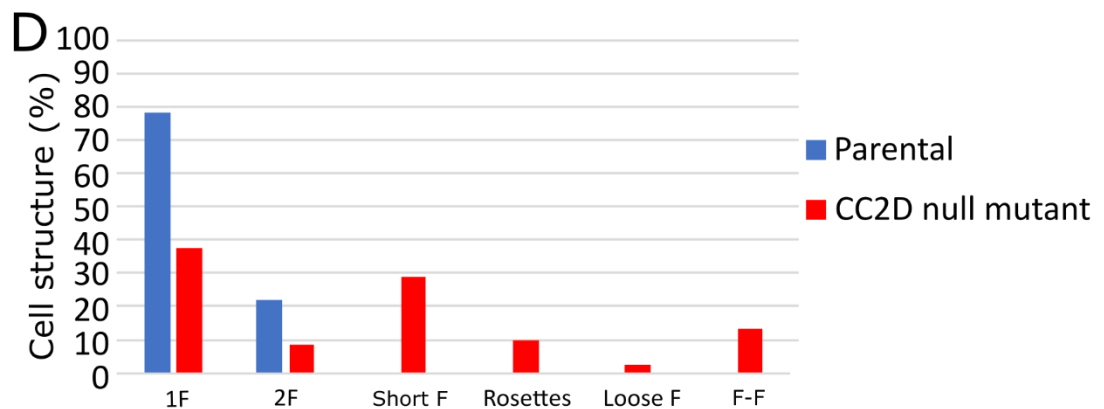
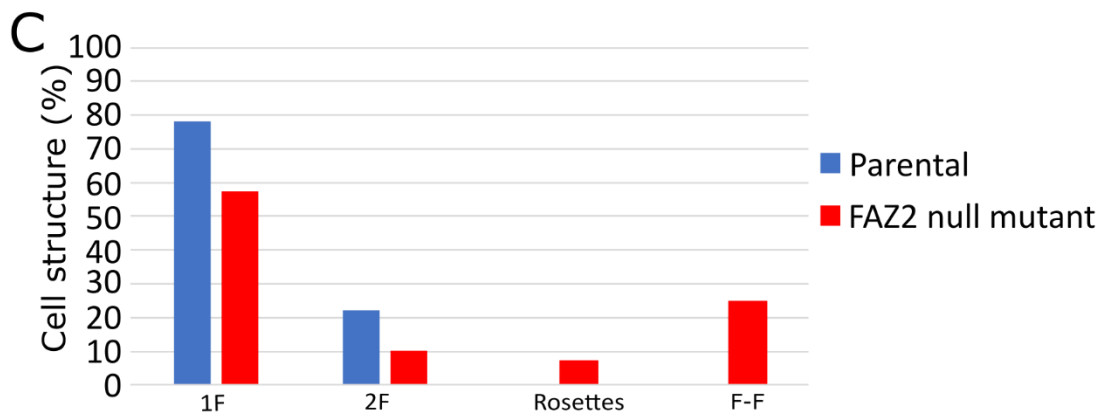
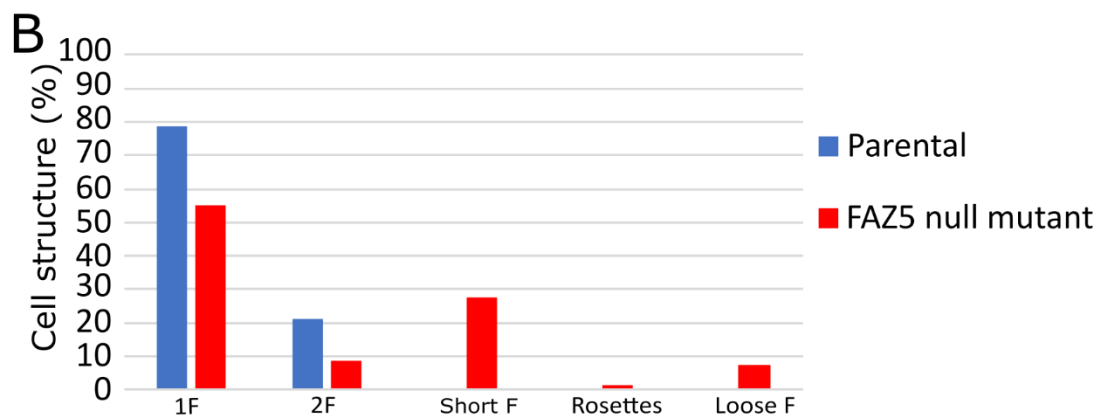
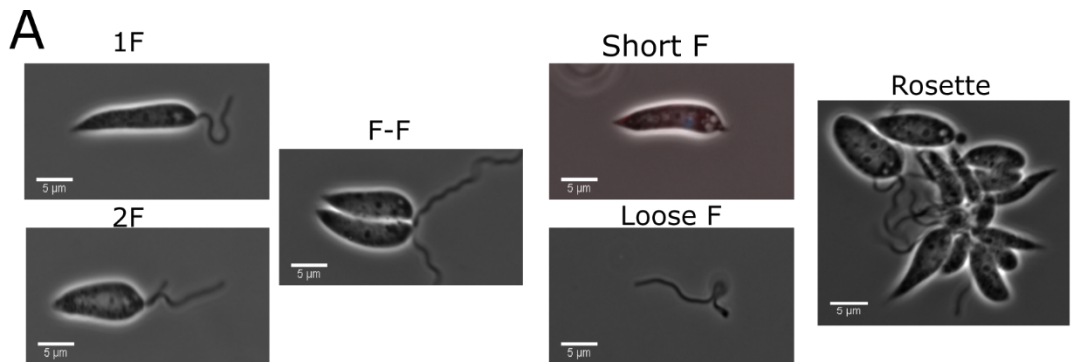


Figure 4.7 CC2D null mutant has loose flagella and short flagellum cells like FAZ5 and F-F connections like FAZ2. A) Example images of 1F, 2F, F-F, cells with a short flagellum, loose flagella and rosettes observed. B) Quantitation of cell structure seen in A) FAZ5 null mutant, B) FAZ2 null mutant and D) CC2D null mutant.

4.4.2 Deletion of FAZ5, FAZ2 and CC2D resulted in cell cycle changes

To determine whether there were changes in the cell cycle, the cell cycle position defined by the K/N/F status for each null mutant and the parental cell line was analysed.

The cell cycle of the FAZ28/30 null mutant was similar to that of the parental cells, with only a slight reduction in the number of 1F1N1K and 2F2N2K cells. For the FAZ5 null mutant there was a drop in 1F1N1K cells, but this was more than matched by an increase in 1F1N1K cells with a short flagellum. There was a large drop in 2F1N1K cells, while the proportions of 2F2N1K (2.6%) and 2F2N2K (8.2%) cells were similar to the parental with only a small number of 2F2N2K cells with a short flagellum seen (**Fig 4.8**). For the FAZ2 null mutant, 8.6% of cells had an F-F with a slightly lower percentage of cells in the other stages of the cell cycle seen (**Fig 4.8**) For the CC2D null mutant, F-F cells were also seen alongside short flagellum cells with 1F1N1K and 2F2N2K configurations. Compared to the parental, 1F1N1K, 2F1N1K, 2F2N1K and 2F2N2K cell numbers were reduced (**Fig 4.8**). These observations showed that while FAZ5 deletion had a mild cell cycle defect, both FAZ2 and CC2D deletion caused cell segregation defects.

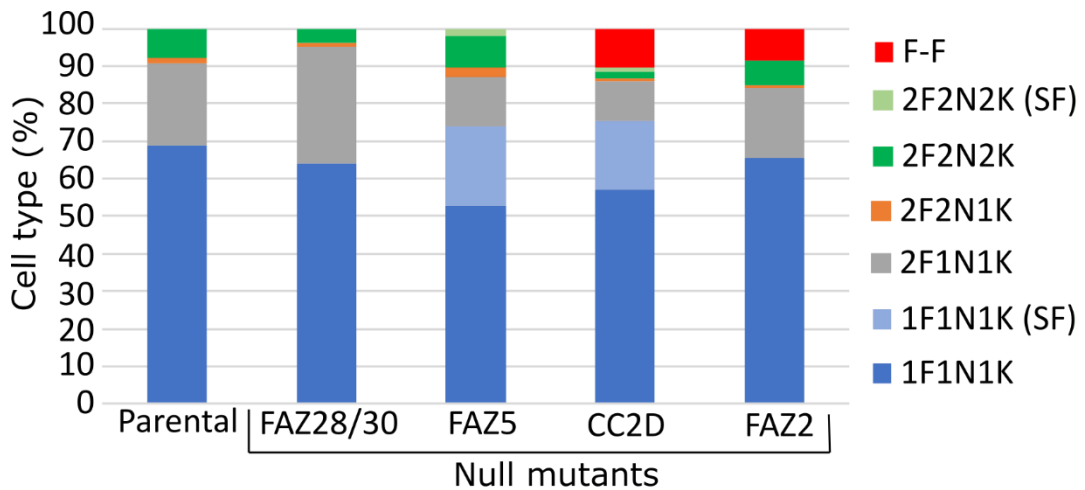


Figure 4.8 Cell cycle was affected in Class II null mutants. Quantitation of cell cycle positions seen in parental and FAZ null mutants. Cell cycle stages include 1F1N1K, 2F1N1K, 2F2N1K, 2F2N2K and 1F1N1K and 2F2N2K cells with short flagella.

4.4.3 FLA1BP localisation was affected in Class II null mutants

To gain insight into Class II FAZ protein importance for maintaining the molecular structure of the FAZ, the localisation of FLA1BP::mCh was assessed in the null mutants. In the parental cells, FLA1BP::mCh had a linear signal on the flagellum side of the FAZ (**Fig 4.9A**). For the FAZ28/30 null mutant the FLA1BP::mCh signal was noticeably shorter in 1F1N1K cells (**Fig 4.9B**). The parental FLA1BP::mCh signal in 2F2N2K cells was shorter and appeared to be similar to FAZ28/30 null mutant (**Fig 4.9A-B**). For the FAZ5, CC2D and FAZ2 null mutants, the FLA1BP::mCh protein was mislocalised to the region of the flagellum beyond the anterior cell tip in both 1F1N1K and 2F2N2K cells (**Fig 4.9 C-E**). Additionally, lysosomal signal was seen in these null mutants. The signal seen in the FAZ5 null mutant 1F1N1K configuration is similar to observations in the previous FAZ5 deletion study (Sunter *et al.*, 2019). Short flagellum FAZ5 and CC2D null mutant cells also followed this trend, where a short stub of marker signal was seen in the flagellum beyond the anterior cell tip with FLA1BP signal being much weaker in FAZ5 null mutant (**Fig 4.9C-D**). Meanwhile, for CC2D and FAZ2 null mutants the FLA1BP::mCh signal was also seen at the connection point between the flagella in F-F cells (**Fig 4.9D-E**). This FLA1BP::mCh localisation extending beyond the anterior tip and within the F-F contact point were similar to localisations

seen in the previously studied FAZ2 null mutant (Halliday *et al.*, 2020). These observations shows that Class II FAZ proteins are important for the correct localisation of Class I protein FLA1BP.

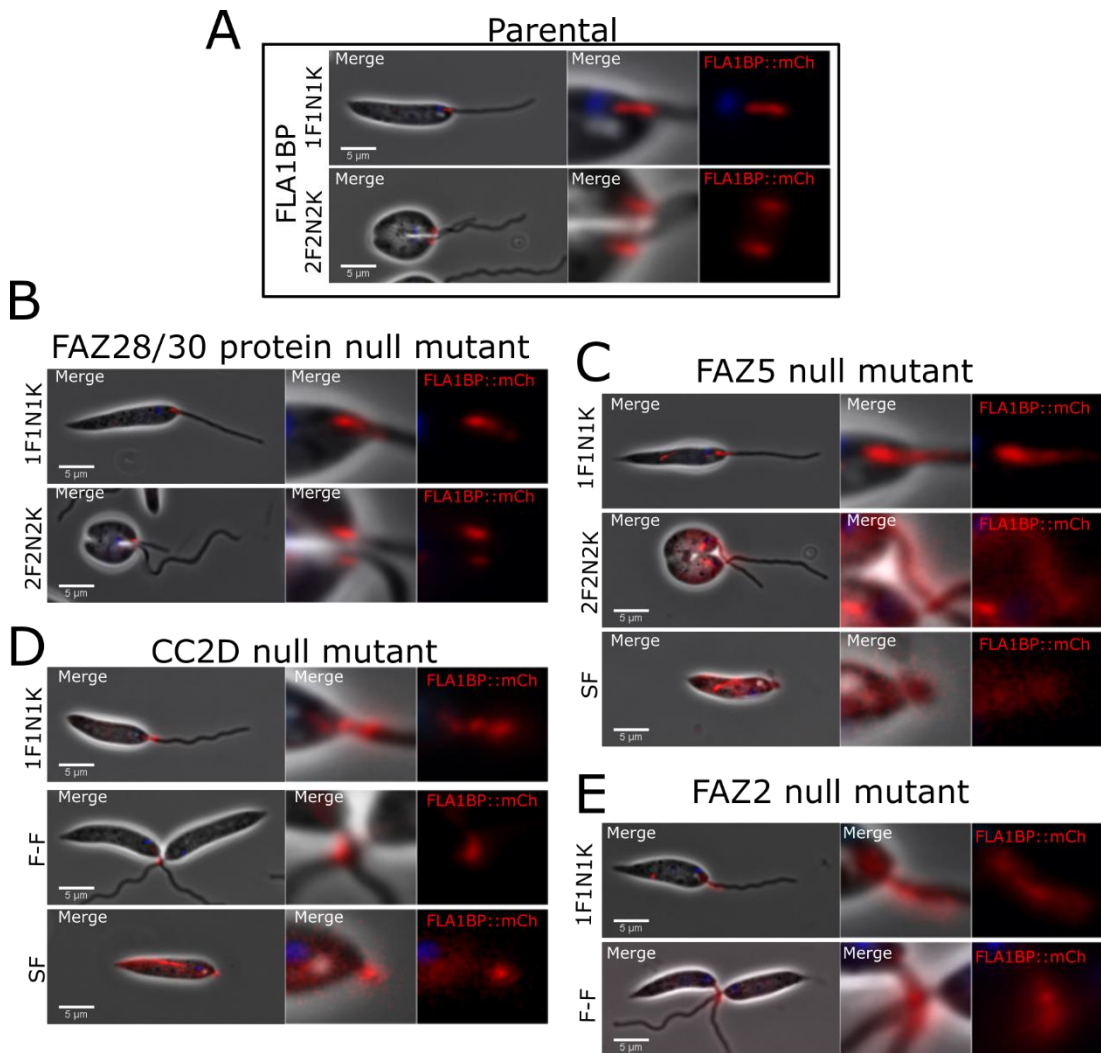


Figure 4.9 FLA1BP::mCh localisation was affected in Class II null mutants. A) Parental marker cell line, FLA1BP::mCh B) FAZ28/30 null mutant, C) FAZ5 null mutant including short flagellum (SF), D) CC2D null mutant including short flagellum (SF) and F-F cells, E) FAZ2 null mutant including F-F cells. All of the cell lines above contained FLA1BP::mCh marker. Images of cells (merge) contain phase (grey), mCherry (red) and Hoechst 33342 (blue). FAZ region insert image on the right contain both merge and mCherry (red) only. Top- 1F1N1K cell and bottom 2F2N2K cell. Scale bar = 5 μ m

4.4.4 Cell body length was reduced in FAZ5, CC2D and FAZ2 null mutants

To assess for morphological changes flagellum and cell body lengths were measured for 1F1N1K excluding short flagellum cells. In parental cells, the flagellum length ranged between 8 - 23 μm with a mean of 13.4 μm (**Fig 4.10A**). For the FAZ28/30, FAZ5, CC2D and FAZ2 null mutants, the mean flagellum lengths were 14.2 μm , 14.1 μm , 13.3 μm and 13.6 μm , respectively. These values are similar to the parental, showing that the flagellum length was unaffected in Class II null mutants.

For cell body lengths in 1F1N1K cells, the parental ranged from 8 - 18 μm with a mean of 13.6 μm (**Fig 4.10B**). For the null mutants, the cell body length in 1F1N1K cells was reduced by \sim 1-1.5 μm . Both FAZ5 and CC2D null mutants were previously shown to have atypical short flagellum cells so to assess if short flagellum cells with 1F1N1K configuration were affected measurements were taken. For the FAZ5 null mutant with a short flagellum the cell length was significantly reduced compared to both the parental and FAZ5 null mutant full length flagellum cells (**Fig 5.10C**). The CC2D null mutant also followed the same pattern with mean cell length of 10.2 μm for cells with a short flagellum (**Fig 5.10D**).

These results show that while the flagellum length was unaffected, the cell body length was reduced in Class II null mutants. The cell body length was reduced further in short flagellum cells of FAZ5 and CC2D null mutants. Deletion of genes encoding Class II FAZ proteins therefore affected the cell morphology.

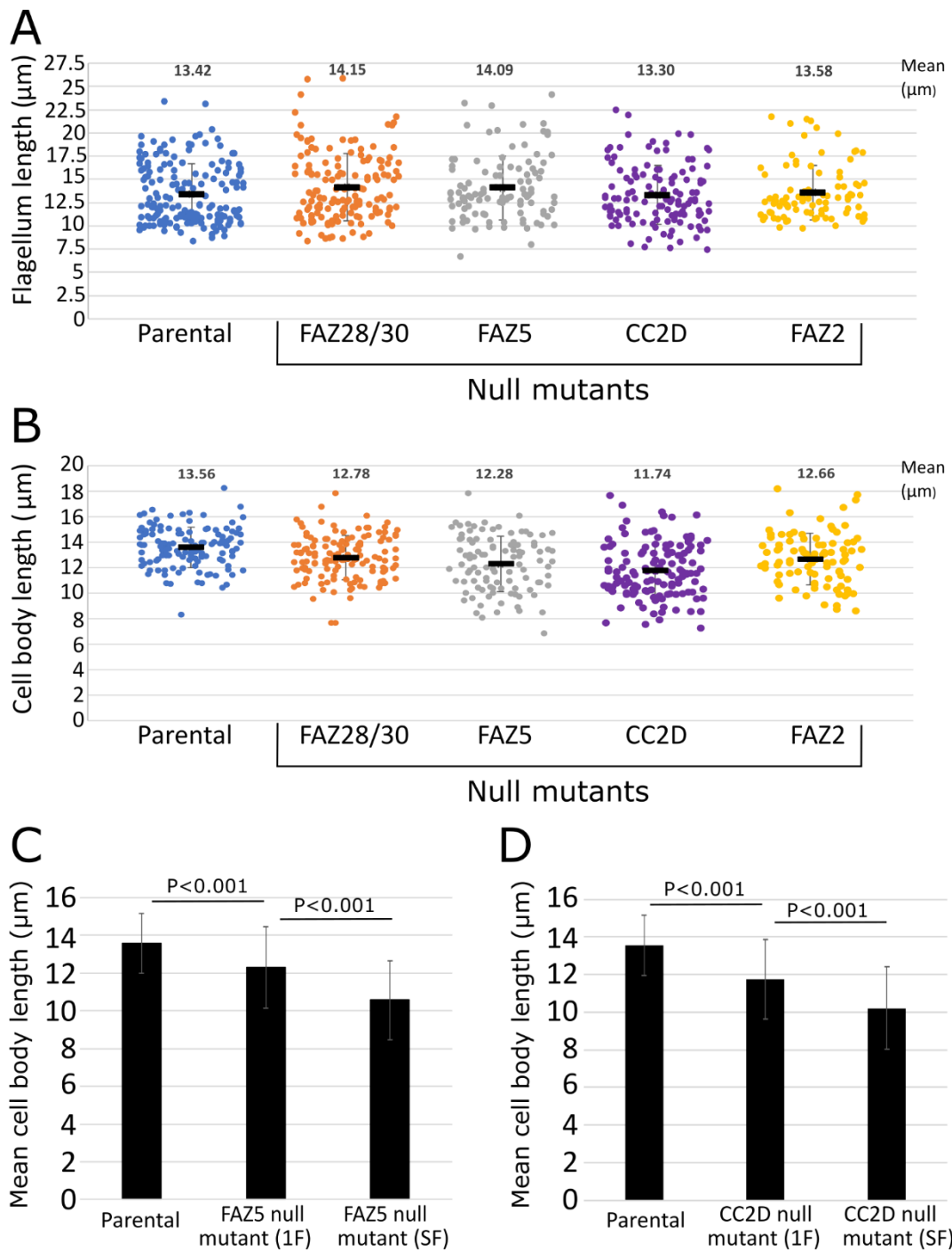


Figure 4.10 Cell body length was reduced in FAZ5, CC2D and FAZ2 null mutants. A) Flagellum lengths of 1F1N1K cells (excluding short flagella cells), B) Cell body lengths of 1F1N1K cells. Each dot represents the length measurement of an individual cell, and the mean was calculated from these length measurements. C) Mean cell body length of FAZ5 null mutant 1F1N1K and short flagellum (SF) cells, D) Mean cell body length of CC2D null mutant 1F1N1K and short flagellum (SF) cells.

4.5 Class III

The gene encoding the single Class III FAZ protein, FAZ3 was successfully deleted as confirmed by PCR (**Fig 4.11A**). Functional analysis was carried out on this null mutant.

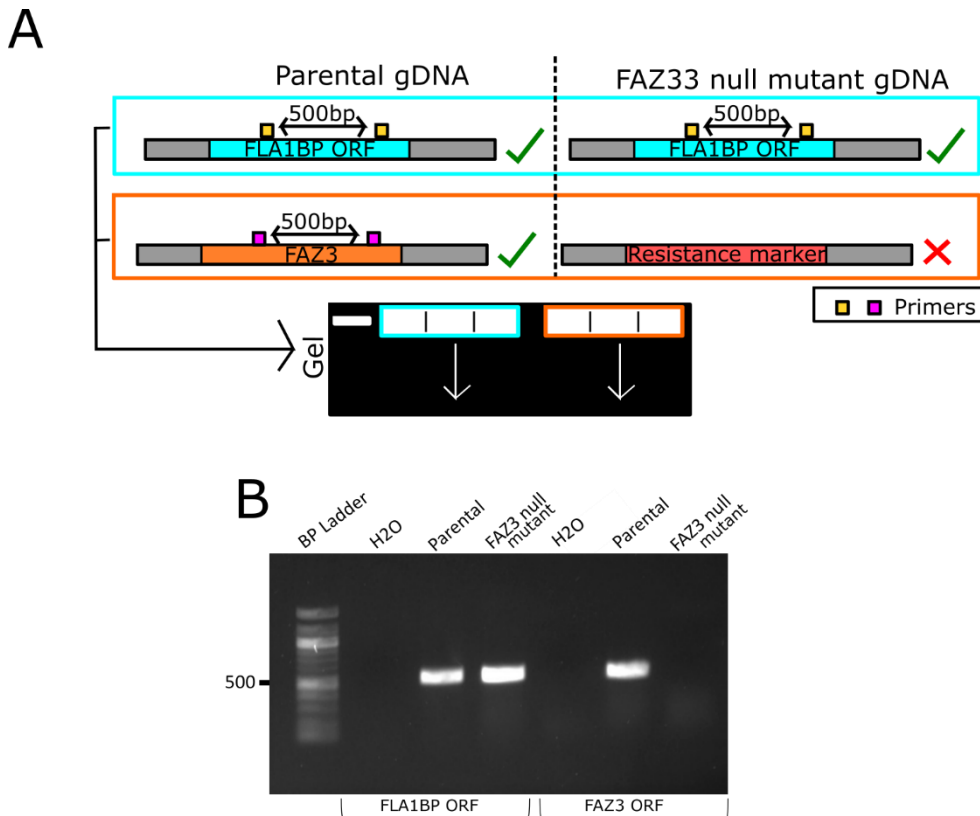


Figure 4.11 Diagnostic PCR confirmed gene deletion for Class III FAZ3 null mutant.

A) Representative example for confirming FAZ3 deletion. B) Deletion of FAZ3 was confirmed. gDNA were extracted from null mutants and tested alongside the parentals for confirmation of gene deletion. Extracted parental gDNA and targeted LmxM.10.0620 (FLA1BP) ORF were used as positive controls while H₂O was used as a negative control. The primers were designed to amplify a 500 bp region from the ORF.

4.5.1 FAZ3 null mutant phenotype was similar to parental

Initial observations by light microscopy showed that the FAZ3 null mutant had no obvious defects. The first step was to analyse if the cell cycle was affected. This was measured by determining cell cycle position numbers defined by the F/N/K status in the cell lines within two weeks of cell growth post-transfection. There were no large differences seen in the cell cycle position of the FAZ3 null mutant cells, with only slight increase in 2F1N1K cells with a matched decrease in 2F2K2N cells (**Fig 4.12A**).

Next, the effect of FAZ3 deletion on the localisation of the FAZ protein, FLA1BP::mCh was assessed. For the parental cells, the FLA1BP::mCh signal localised to a short line in the flagellum within the flagellar pocket neck in 1F1N1K cells, and two shorter linear signals on the old and new flagellum side in 2F2N2K cells (**Fig 4.12B**). For the FAZ3 null mutant, the FLA1BP::mCh signal was still linear but appeared slightly shorter in 1F1N1K cells. To assess this, FLA1BP::mCh localisation lengths were measured from 100 1F1N1K cells of both parental and FAZ3 null mutant. For FAZ3 null mutant, the mean length was 0.9 μm , which was significantly ($p < 0.001$) shorter than the parental (1.3 μm). Meanwhile, in 2F2N2K cells, the FLA1BP::mCh signal followed a similar pattern to the parental, displaying two shorter signals on the new and old flagellum side (**Fig 4.12C**). This shows that FAZ3 deletion affected FLA1BP::mCh localisation demonstrating FAZ3 is required for the recruitment and/or correct assembly of FLA1BP::mCh.

To assess any possible morphological changes in the FAZ3 null mutant, flagellum and cell body length measurements were carried out on 1F1N1K cells imaged within two weeks of cell growth post-transfection. The mean flagellum length of the FAZ3 null mutant was 13.4 μm , which was similar to the parental cells (**Fig 4.12D**). For the cell body length, the FAZ3 null mutant mean length was 13.3 μm which was similar to the parental mean length of 13.6 μm (**Fig 4.12E**). This demonstrates that deletion of FAZ3 had no morphological defects on the cell, with only possible subtle changes to the cell cycle and FLA1BP localisation.

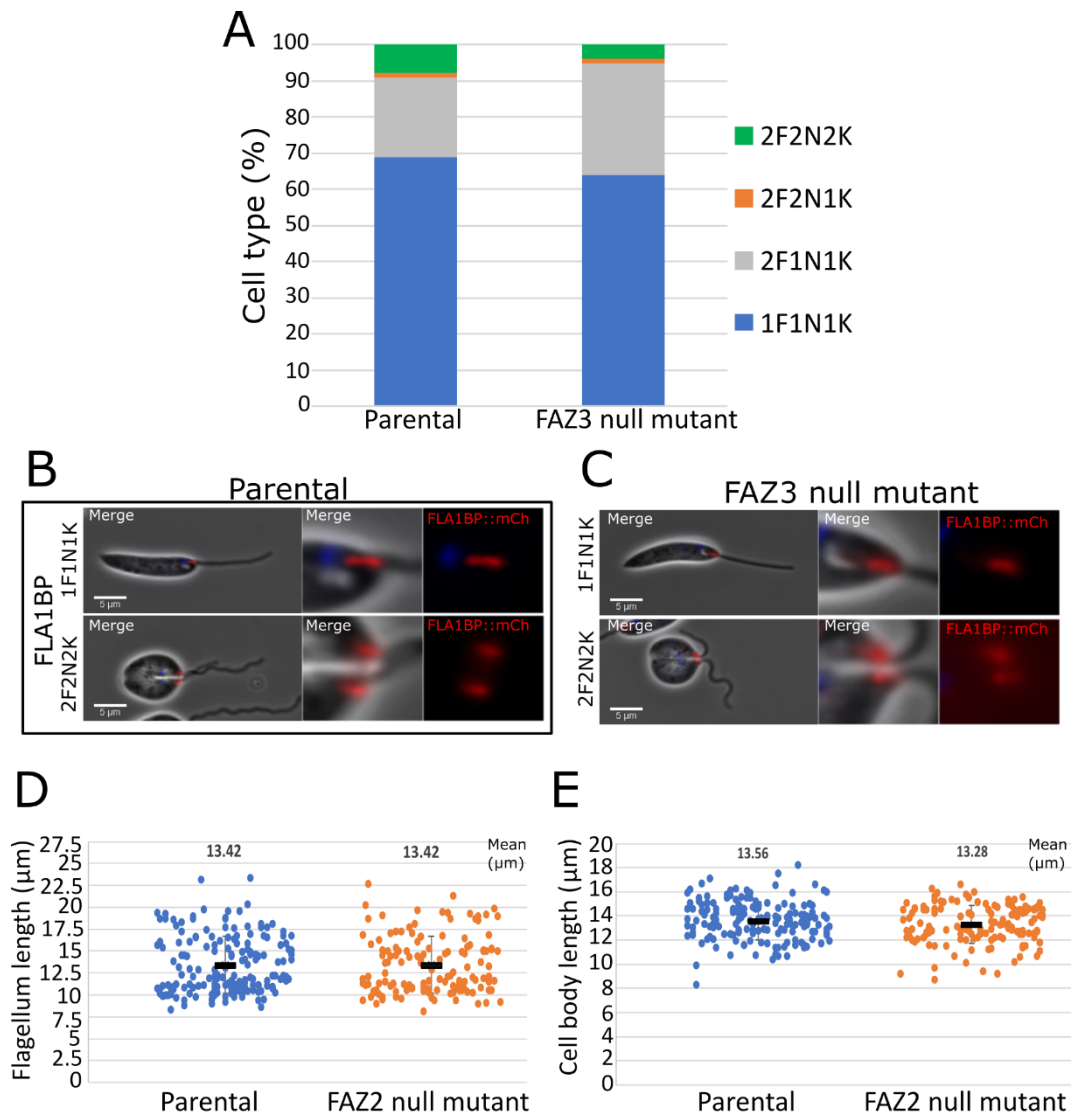


Figure 4.12 Deletion of class III, FAZ3 has no effect on cell cycle and morphology. A) Quantitation of cell cycle positions seen in parental and FAZ3 null mutant. Cell cycle stages include 1F1N1K, 2F1N1K, 2F2N1K and 2F2N2K, B) Parental marker cell lines, FLA1BP::mCh C) FAZ3 null mutant, D) Flagella lengths of 1F1N1K cells, E) Cell body lengths of 1F1N1K cells. Each dot represents the length measurement of an individual cell, and the mean was calculated from these length measurements. Scale bar = 5 µm

4.6 Class IV

The genes encoding the Class IV FAZ proteins, FAZ14 (LmxM.30.3110), FAZ6 (LmxM.21.1240), FAZ12 (LmxM.32.2460), FAZ40 (LmxM.18.1560), kinesin (LmxM.24.1430) and FAZ10 (LmxM.22.1320) were successfully deleted in the FLA1BP::mCh marker cell line as confirmed by PCR (Fig 4.13A-G). Functional analysis was carried out on these for six null mutants.

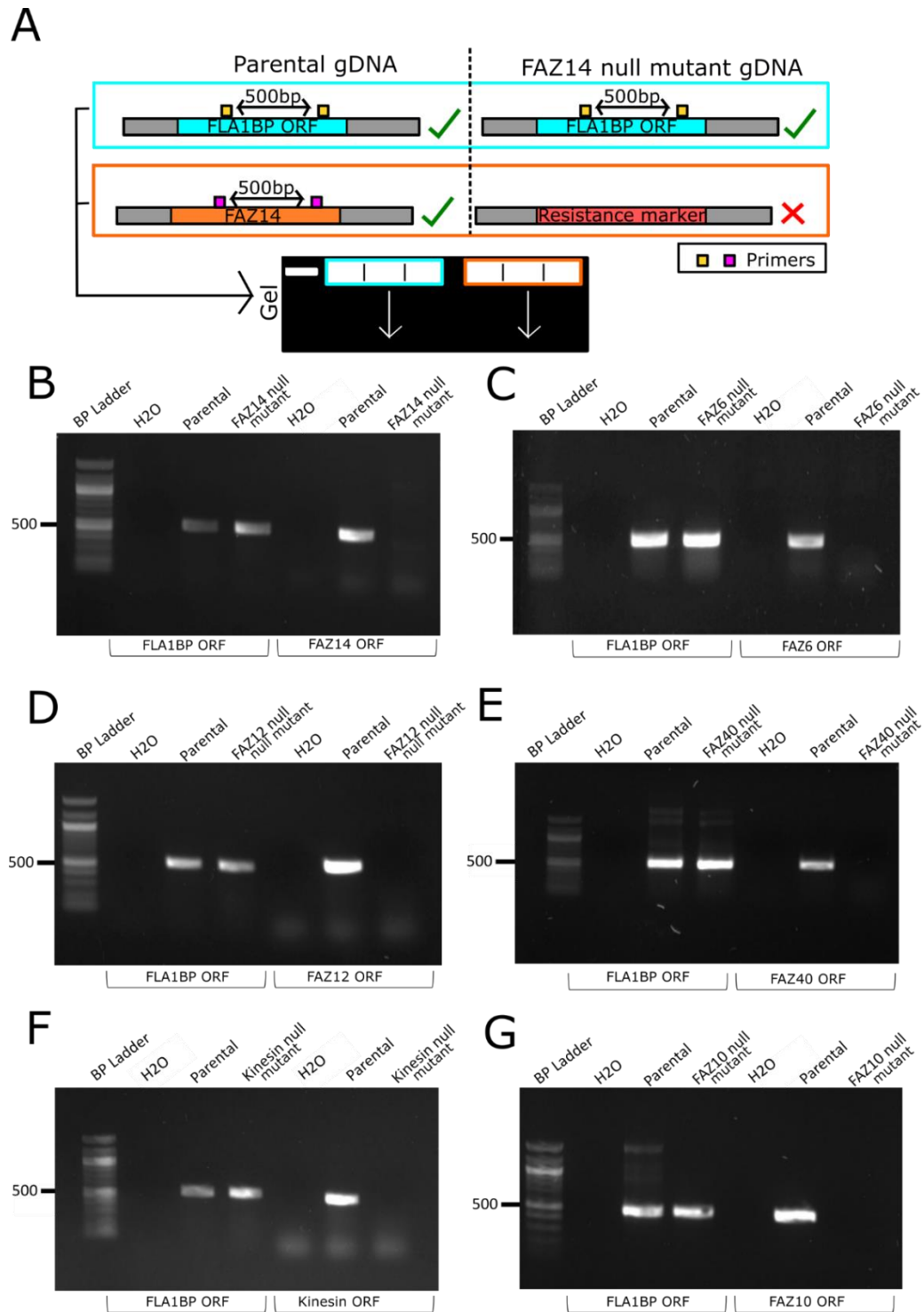


Figure 4.13 Diagnostic PCR confirmed gene deletion for Class IV null mutants. A) Representative example for confirming FAZ14 deletion. B) Deletion of the following genes B) LmxM.30.3110 (FAZ14), C) LmxM.21.1240 (FAZ6), D) LmxM.32.2460 (FAZ12), E) LmxM.18.1560 (FAZ40), LmxM.24.1430 (kinesin protein) and G) LmxM.22.1320 (FAZ10) are confirmed. gDNA were extracted from null mutants and tested alongside the parental for confirmation of gene deletion. Extracted parental gDNA and primers to the LmxM.10.0620 (FLA1BP) ORF were used as positive controls while H₂O was used as a negative control. The primers were designed to amplify a 500 bp region from the ORF.

4.6.1 Cell cycle was only marginally affected in Class IV null mutants

Initial observations by light microscopy showed that the Class IV null mutants had no obvious defects. Only 1F and 2F cells were observed in culture. The next step was to analyse if the cell cycle was affected. This was measured by determining cell cycle position numbers defined by the F/N/K status of cell lines imaged within two weeks of cell growth post-transfection. For the FAZ14 and kinesin null mutants, the cell cycle position numbers were very similar to the parental (**Fig 4.14**). This shows that the cell cycle was not affected in FAZ14 and kinesin protein null mutants. For FAZ6 and FAZ12 null mutants, there was a slight increase in 1F1N1K cells and for the later stages of cell cycle there was a drop in 2F1N1K in the FAZ6 null mutant, with a drop in the numbers of 2F2N1K and 2F2N2K cells in the FAZ12 null mutant (**Fig 4.14**). For the FAZ40 and FAZ10 null mutants, there was a decrease in 1F1N1K cells. While the FAZ40 null mutant showed a small raise in 2F2N2K cells, FAZ10 displayed a small increase across later stages of cell cycle, particularly 2F1N1K cells (**Fig 4.14**).

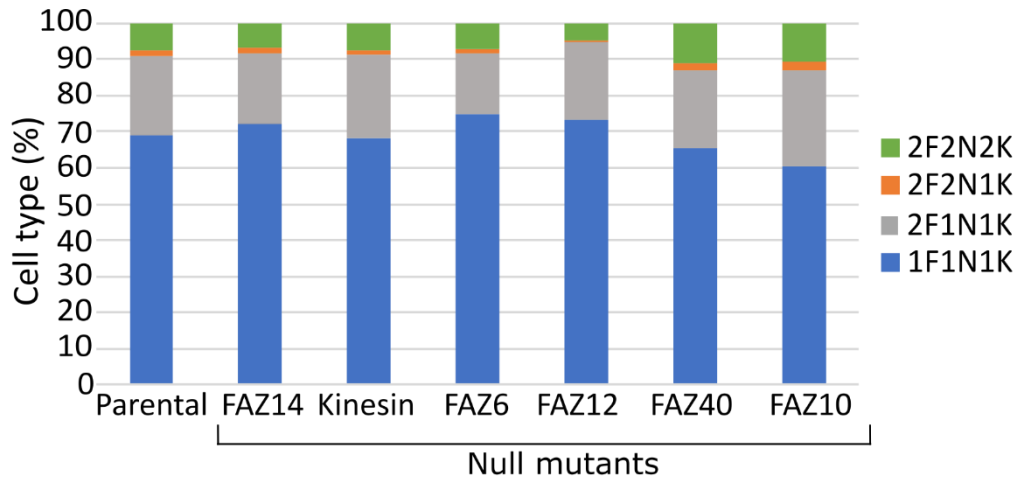


Figure 4.14 Little change in the cell cycle of Class IV null mutants. Quantitation of cell cycle positions seen in parental and Class IV null mutants. Cell cycle stages include 1F1N1K, 2F1N1K, 2F2N1K and 2F2N2K.

4.6.2 FLA1BP::mCh localisation was not affected in Class IV null mutants

To gain insight into the importance of Class IV FAZ proteins for maintaining the molecular structure of the FAZ, the localisation of FLA1BP::mCh was assessed in the captured images taken within two weeks of cell growth post-transfection. For the parental cells, FLA1BP::mCh localised to a linear structure on the flagellum side in 1F1N1K cells, and two shorter linear signals on the old and new flagellum side in 2F2N2K cells (**Fig 4.15A**). For the null mutants, the FLA1BP::mCh signal also showed a linear signal within the flagellum FAZ domain of 1F1N1K cells (**Fig 4.15B-G**). In 2F1N1K cells of the null mutants, two short FLA1BP localisation on the old and new flagellum sides were observed, showing no change from the parental (**4.15B-G**). These observations suggests that class IV proteins are not required for the correct localisation of FLA1BP::mCh

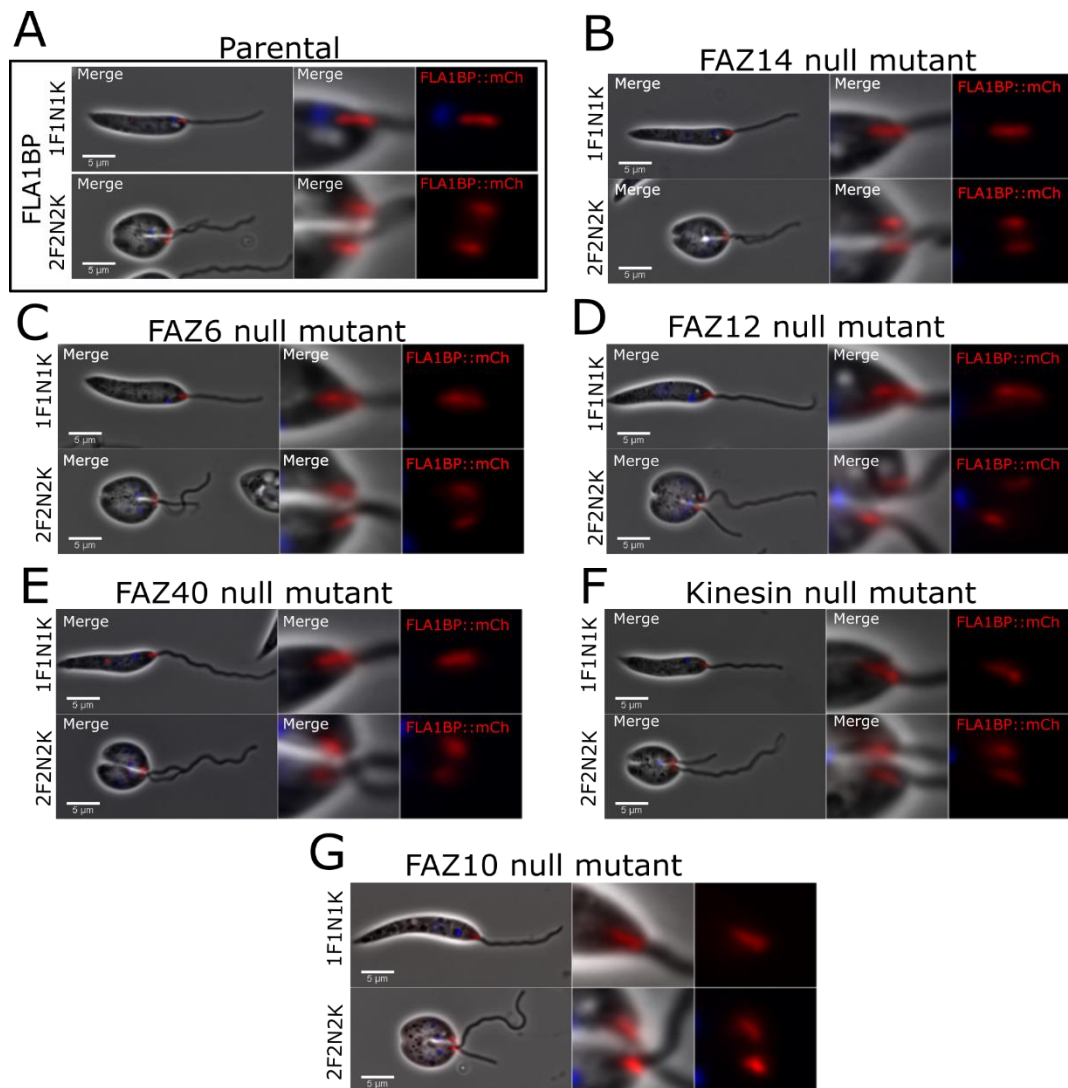
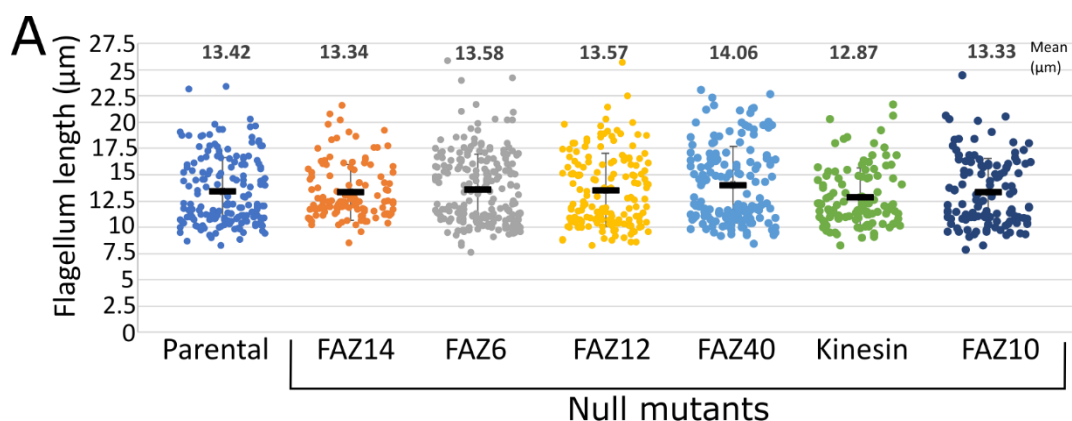


Figure 4.15 FLA1BP::mCh localisation was not affected in Class IV null mutants. A) Parental marker cell line, FLA1BP::mCh B) FAZ14 protein null mutant, C) FAZ6 null mutant, D) FAZ12 null mutant, E) FAZ40null mutant, F) kinesin protein null mutant and G) FAZ10 null mutant. All of the cell lines above contained FLA1BP::mCh marker. Images of cells (merge) contain phase (grey), mCherry (red) and Hoechst 33342 (blue). FAZ region insert image on the right contain both merge and mCherry (red) only. Top- 1F1N1K cell and bottom 2F2N2K cell.

4.6.3 Flagellum and cell body size was not affected in Class IV null mutants but FAZ10 had 'zip-like' flagella morphology

To assess any possible morphological changes in the Class IV null mutants, flagellum and cell body length measurements were carried out on 1F1N1K cells imaged within two weeks of cell growth post-transfection. The mean flagellum length for the parental cells was 13.4 μm (**Fig 4.16A**). All the null mutants mean flagellum lengths were within 0.7 μm of the parental, showing no significant change in flagellum length (**Fig 4.16A**). The mean cell body length for the parental cells was 13.6 μm (**Fig 4.16B**). All the null mutants mean cell body length were within 1 μm of the parental, showing no substantial change in cell body length (**Fig 4.16B**).

However, on a closer inspection of FAZ10 null mutant, it was noticed that on 7% of 2F1N1K cells there was a possible 'zip-like' connection between the two flagella beyond the anterior cell tip (**Fig 4.16C**). It was also noticed that 8% of 2F2N2K cells displayed damaged flagella and/or flagella streamers (**4.16D**). This suggests that FAZ10 deletion affects flagellar morphology. Given the localisation of FLA1BP to the F-F connections in the FAZ2 and CC2D null mutants the FLA1BP localisation in the FAZ10 null mutant was reassessed. However, the FLA1BP signal was not located within the connection region nor within the streamers/damage locations, which suggests this type of connection is different to that of FAZ2 and CC2D (**Fig 4.16 C&D**).



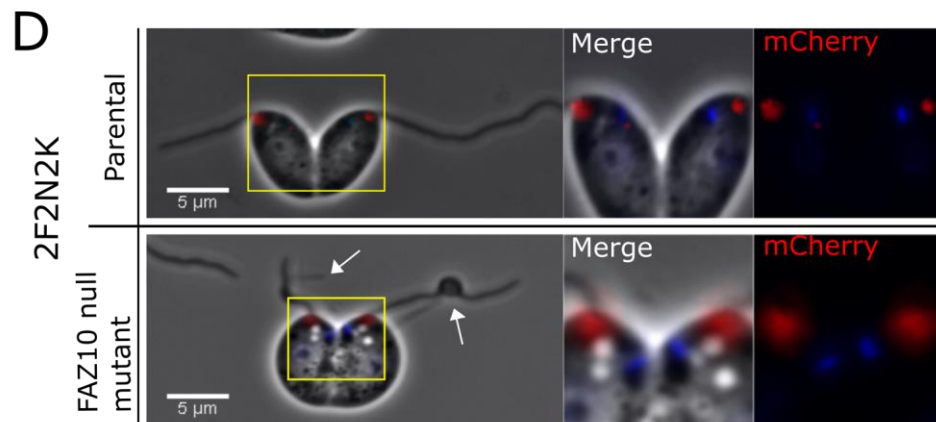
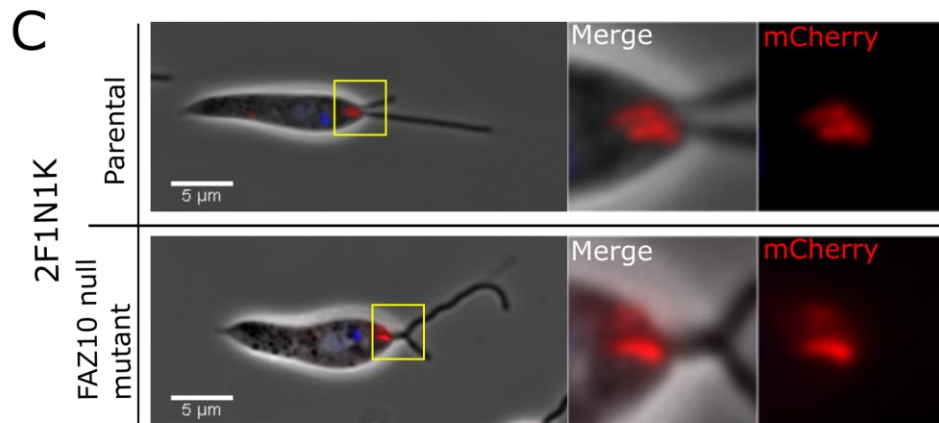
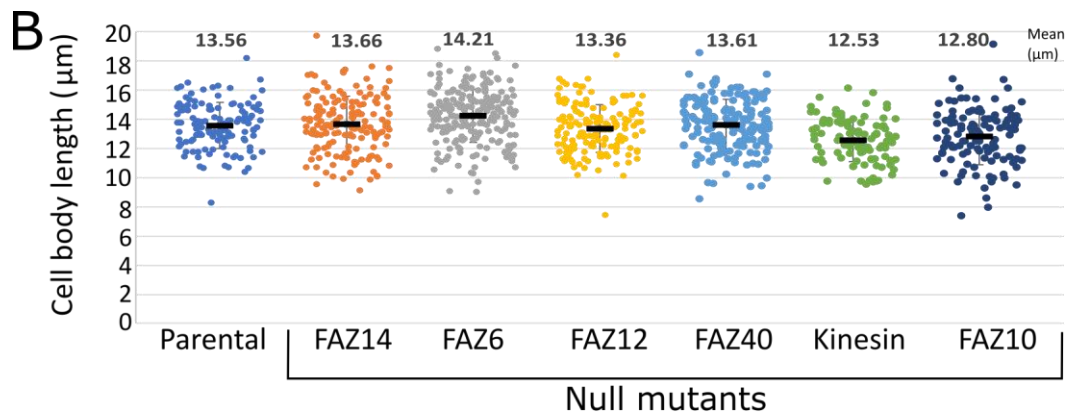


Figure 4.16 FAZ10 null mutant has flagellar morphology defects. A) Flagellum lengths of 1F1N1K cells, B) Cell body lengths of 1F1N1K cells. Each dot represents the length measurement of an individual cell, and the mean was calculated from these length measurements. C) Images of 1F1N1K cells for parental and FAZ10 null mutant. Right- Insert of anterior cell tip region. D) Images of 2F2N2K cells for parental and FAZ10 null mutant. FAZ region insert image on the right contain both merge and FLA1BP mCherry (red) only. Flagellar streamers are indicated by white arrows.

4.7 Class V

The genes encoding the Class V FAZ proteins, FAZ29 (LmxM.12.0360), FAZ8 (LmxM.33.2570), FAZ1 (LmxM.33.0690) and FAZ9 (LmxM.31.0140) were successfully deleted as confirmed by PCR (**Fig 4.17A-E**). Deletion of the gene encoding phosphatase 2A regulatory subunit protein (LmxM.33.0670) failed so functional analysis was carried out on four of the five proteins of this class.

4.7.1 Class V null mutants have no cell cycle or morphological defects

Initial observations by light microscopy showed that the Class V null mutants had no obvious defects. Only 1F and 2F cells were observed in culture. The next step was to analyse if the cell cycle was affected. This was measured by determining cell cycle position numbers defined by the F/N/K status in cell lines imaged within two weeks of cell growth post-transfection. The percentages of cells within each cell cycle position numbers in the null mutants showed little difference to the parental (**Fig 4.18A**). This demonstrates that the cell cycle was not affected in Class V null mutants.

Next, the effect of deletion of the Class V FAZ genes on the localisation of FLA1BP::mCh was assessed. In the parental cells FLA1BP::mCh had a linear signal on the flagellum within the flagellar pocket neck in 1F1N1K cells, and two shorter linear signals on the old and new flagellum side in 2F2N2K cells (**Fig 4.18B**). For the null mutants, the FLA1BP::mCh signal was still linear and of a similar length within flagellar pocket neck in 1F1N1K cells (**Fig4.18C-F**). In 2F2N2K cells, the FLA1BP::mCh signal followed a similar pattern to the parental, displaying two shorter signals on the new and old flagellum side (**Fig 4.18C-F**). This shows that FLA1BP::mCh localisation was not dependent on Class V FAZ proteins.

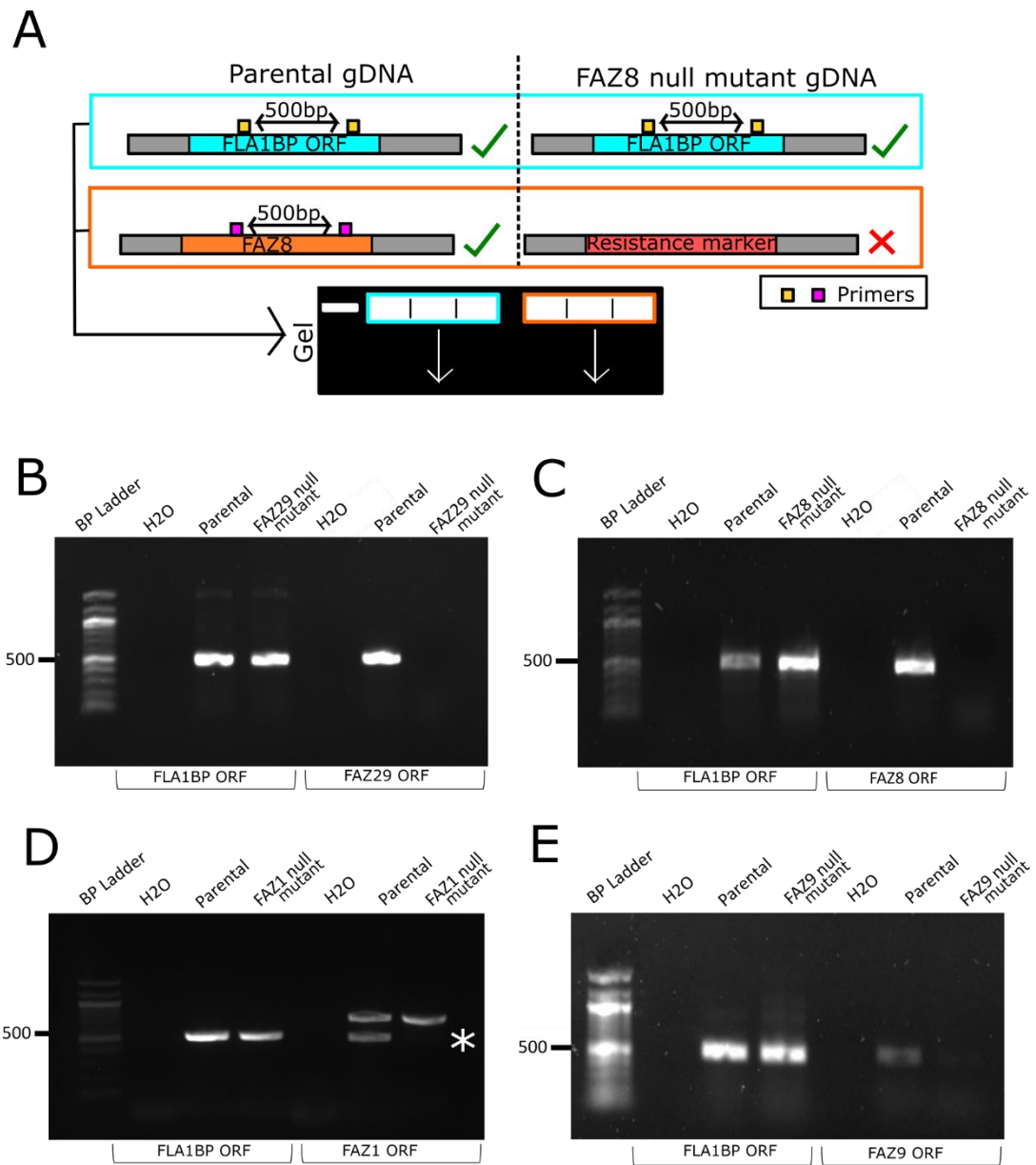


Figure 4.17 Diagnostic PCR confirmed Class V FAZ gene deletions. A) Representative example for confirming FAZ8 deletion. B) Deletion of the following genes B) LmxM.12.0360 (FAZ29), C) LmxM.33.2570 (FAZ8), D) LmxM.33.0690 (FAZ1) and G) LmxM.31.0140 (FAZ9) are confirmed. gDNA were extracted from null mutants and tested alongside the parental for confirmation of gene deletion. Extracted parental gDNA and primers targeting LmxM.10.0620 (FLA1BP) ORF were used as positive controls while H₂O was used as a negative control. The primers were designed to amplify a 500 bp region from the ORF. * indicates target band location.

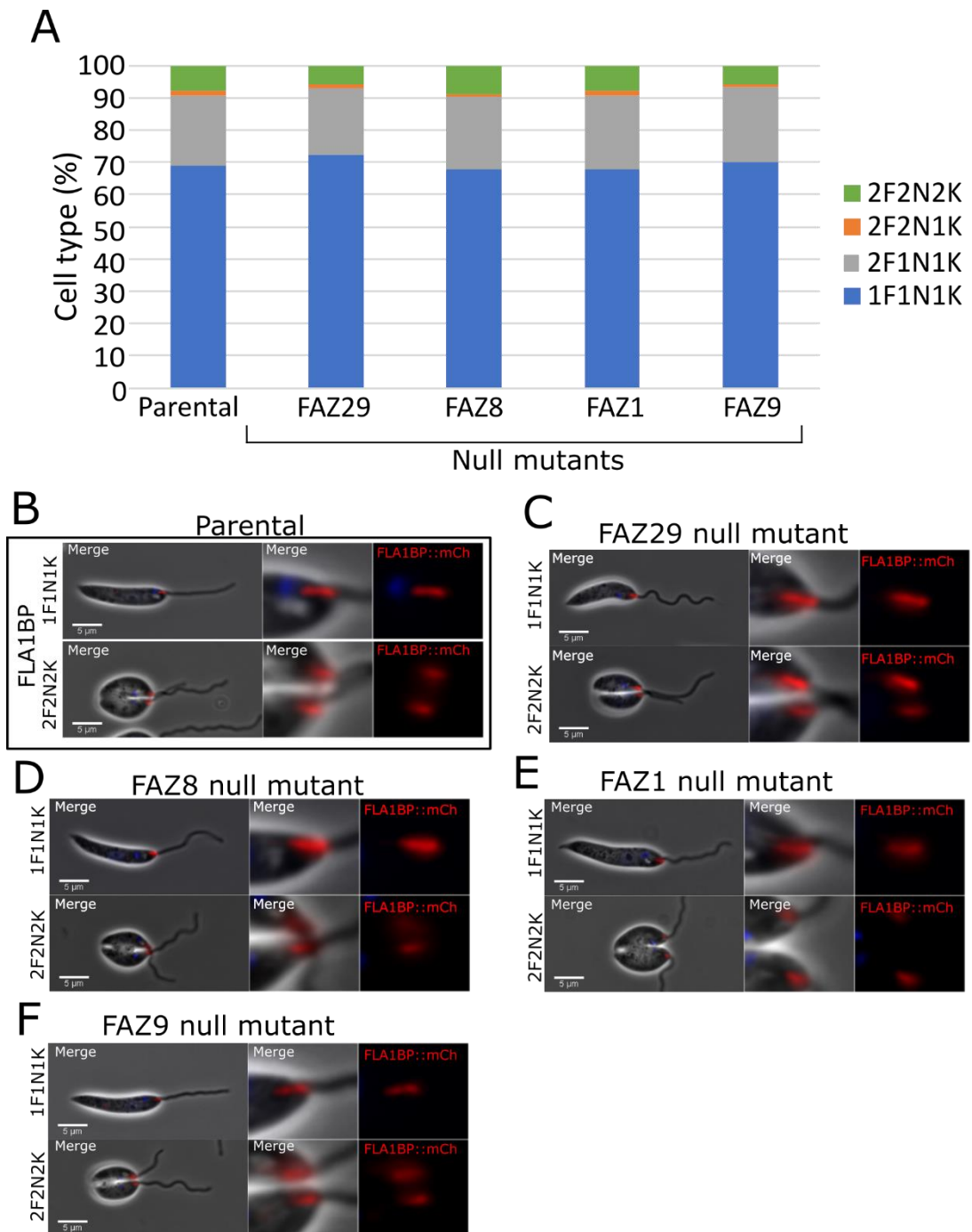


Figure 4.18 Cell cycle and FLA1BP::mCh localisation was not affected in Class V null mutants. A) Quantitation of cell cycle positions seen in parental and Class V null mutants. Cell cycle stages include 1F1N1K, 2F1N1K, 2F2N1K and 2F2N2K, B) Parental marker cell line, FLA1BP::mCh B) FAZ29 protein null mutant, C) FAZ8 null mutant, D) FAZ1 null mutant and E) FAZ9 null mutant. All of the cell lines above contained FLA1BP::mCh marker. Images of cells (merge) contain phase (grey), mCherry (red) and Hoechst (blue). FAZ region insert image on the right contain both merge and mCherry (red) only. Top- 1F1N1K cell and bottom 2F2N2K cell.

To assess any possible morphological changes in the Class V null mutants, flagellum and cell body lengths were measured in 1F1N1K cells imaged within two weeks of cell growth post-transfection. In the parental cells the mean flagellum length was 13.4 μm (**Fig 4.19A**). For the null mutants, the means ranged between 13.1 - 14.3 μm , similar to the parental (**Fig 4.19A**). For the cell body length, the parental mean length was 13.6 μm (**Fig 4.19B**). For the null mutants, the means were within 0.5 μm of the parental, suggesting that the cell body lengths in null mutants were unaffected (**Fig 4.19B**). This demonstrates that there were no major morphological changes after Class V FAZ gene deletion.

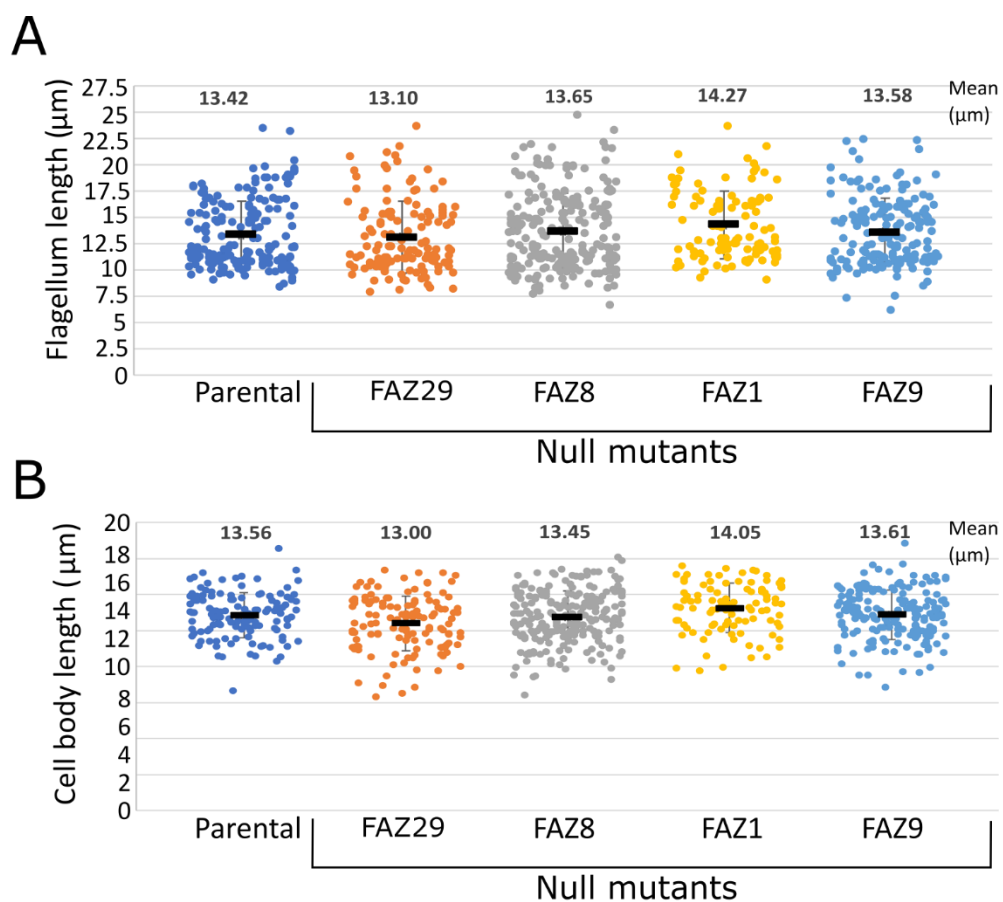


Figure 4.19 Flagella and cell body lengths were not affected in Class V null mutants.

A) Flagellum lengths of 1F1N1K cells, B) Cell body lengths of 1F1N1K cells. For group measurements, 1F1N1K cells of parental and null mutants were used. Each dot represents the length measurement of an individual cell, and the mean was calculated from these length measurements.

4.8 Discussion

4.8.1 Each FAZ localisation class represents a functional group with specific roles

The FAZ null mutants had a range of different phenotypes; however, there appeared to be a correlation between the phenotypes observed and the class in which the FAZ protein localised to. A similar effect was found in trypanosomes, in which the knockdown phenotype of a specific FAZ protein often correlated with their specific location within a FAZ domain (Sunter and Gull, 2016).

4.8.2 Class I is associated with flagellum attachment and cell morphology

Six proteins from Class I, a linear structure on the flagellum side were analysed. The null mutants of FAZ27, FAZ34 and FLA1BP had short flagellum cells and loose flagella in culture, which could be the consequence of the flagellum becoming detached from the cell body. This suggests that these FAZ proteins are important for flagellum attachment. Meanwhile, these null mutants were also found to have shorter cell bodies, suggesting these proteins have a role in maintaining the cell morphology. FLA1BP is found in the membrane of the flagellum in the intracellular domain, and with FAZ27 and FAZ34 having a similar phenotype, these proteins are potentially located close to the intracellular domain within the flagellum and hence have a similar function (**Fig.4.20**). This effect was similar to that observed for the knockdown of FAZ27 and FLA1BP in *T. brucei*; reduction in FAZ and cell body length, changes from trypomastigote to epimastigote morphology and flagellum detachment were observed for these RNAi cells (Sun *et al.*, 2013; An *et al.*, 2020). This shows that proteins within the flagellum and flagellar membrane domains of the FAZ in both species are comparable in terms of importance for cell morphology and flagellum attachment.

The cAMP binding protein null mutant did not have any flagellum attachment or morphology defects, instead flagellar defects were seen. The increase in flagellum

length and presence of membrane streamers suggests that cAMP binding protein has a separate function. The localisation of this protein described in chapter 3 showed an overlap of the distal end of FLA1BP and extending into the flagellum, which differs from what was seen for FAZ27 and FAZ34. Interestingly, previous studies showed that cAMP signalling is important for flagellum motility and sensing in *T. brucei* and *Leishmania* (Oberholzer, Saada and Hill, 2015; Mukhopadhyay and Dey, 2016; Salmon, 2018). The effect of flagella damage seen in cAMP binding protein null mutants also suggest that cAMP might be important for flagellum assembly.

FLAM3 did not have any obvious defects in flagellum and cell morphology, but affected the localisation of FLA1BP::mCh, which suggests that it could be important for correct localisation of FLA1BP and possibly other intracellular proteins. In trypanosomes, FLAM3 and ClpGM6 knockdown displayed similar morphological defects and localisation of these proteins was interdependent of each other, suggesting they form a complex (Brice Rotureau *et al.*, 2014; Hayes *et al.*, 2014; Sunter *et al.*, 2015; Sunter and Gull, 2016). Recent findings showed that the knockdown of FAZ27 caused a change from trypomastigote to epimastigote-like morphology in trypanosomes and therefore is involved in controlling cell morphogenesis similar to FLAM3 and ClpGM6. Moreover, FAZ27 was shown to form a complex with FLAM3 and ClpGM6 (An *et al.*, 2020). However, in *L. mexicana* deletion of FAZ27 caused a different phenotype to that of FLAM3, suggesting that the function of FAZ27 is distinct to FLAM3 and in *L. mexicana* these proteins may not form a complex.

4.8.3 Class II is associated with flagellum attachment, cell morphology and anterior cell tip morphogenesis

Four proteins from Class II, a linear structure on the cell body side were studied and showed a range of different phenotypes. Deletion of FAZ5 resulted in short flagellum cells with a reduced cell length and loose flagella in culture, suggesting that FAZ5 has an important role in flagellum attachment and cellular morphology. This is a similar phenotype to that observed with FLA1BP deletion, which is also found in the intracellular domain, suggesting this phenotype of short flagellum cells with a

reduced cell body length and loose flagella is common to proteins found in the intracellular FAZ domain. Deletion of FAZ5 has previously been studied and showed some similarities and differences to this chapter (Sunter *et al.*, 2019). Like this study, the FAZ5 null mutant showed reduction in cell body length and mis-localisation of FLA1BP::mCh (Sunter *et al.*, 2019). However, loose flagella were not reported in the original study (Sunter *et al.*, 2019). Interestingly, the number of loose flagella and short flagellum cells seen were found to decrease with time in FAZ27, FAZ34 and CC2D null mutants, possibly due to cellular adaptations that occur (**Chapters 5 & 6**). This phenomenon could be an explanation for the lack of these phenotypes in the original FAZ5 null mutant description. The morphological analysis within the original study also found a reduction in flagellum length, which could be due to the incorporation of the short flagellum cells into the measurements, whereas in this chapter the 1F1N1K cells with a short flagellum were excluded from the flagellum measurements.

FAZ2 deletion caused segregation defects, where F-F connections were observed in the dividing cells. This matches a recent study on FAZ2, which showed that F-F connections were the result of disruption to FAZ structure causing an extension of the anterior cell tip that breaks away forming a membranous structure between the flagella (Halliday *et al.*, 2020). This suggests a separate function for FAZ2 from FAZ5, a determination and maintenance of anterior cell tip morphology (Sunter *et al.*, 2019; Halliday *et al.*, 2020).

Deletion of CC2D resulted in a phenotype that combined elements of both the phenotypes observed for FAZ5 deletion (loose flagella, short flagellum cells and shorter cell body length) and FAZ2 deletion (F-F connections), suggesting that CC2D has multiple functions involving flagellum attachment and maintenance of cell tip morphogenesis. Proteins that directly affect flagellum attachment appear to localise predominately within the intracellular domain region, indicating that CC2D might localise in close proximity to the intracellular domain. Given that CC2D is important for both flagellum attachment and anterior cell tip morphogenesis, this might indicate that CC2D localises between FAZ5 and FAZ2 (**Fig 4.21**).

4.8.4 Class III could be important for correct FAZ assembly

FAZ3, the only protein identified in the region distal to the collar so far, showed little defect after deletion, with only the reduction in the length of the FLA1BP being observed. It is known that FAZ assembly starts at the proximal end of the FAZ structure (Q. Zhou *et al.*, 2015; Sunter *et al.*, 2015; Sunter and Gull, 2016). If this phenomenon is also applicable to the FAZ in *L. mexicana*, then FAZ3 a protein located at the proximal end of the FAZ structure could be the closest to the FAZ assembly site (**Fig 4.20**). It is therefore possible that FAZ3 is important for defining the start point of FAZ assembly and would be critical for assembly of the correct length of FAZ along the neck region.

4.8.5 FAZ10 has a role in cytokinesis

Deletion of the genes encoding the Class IV proteins, which form a horseshoe/ring at the exit point proteins deletion did not cause defects in cell morphology nor affected the recruitment and/or correct localisation of FLA1BP. However, the FAZ10 null mutant had a flagellum defect during the 2F1N1K cell configuration. The new flagellum was seen connecting to the old flagellum creating a zip-like appearance just beyond the anterior cell tip exit site. In trypanosomes, FAZ10 was found to be distributed along junctional complexes, otherwise known as intermembrane staples within the FAZ intracellular domain (Moreira *et al.*, 2017). It was suggested to be important for flagellum attachment and cleavage furrow positioning (Moreira *et al.*, 2017). In *L. mexicana* FAZ10 forms a distinct horseshoe/ring at the exit point only, while the majority of the other Class IV proteins have a dome-like appearance in different shapes and sizes surrounding the exit ring, which might indicate a role for them in connecting the exit point ring to the sub-pellicular microtubules (Wheeler, Sunter and Gull, 2016). This suggests that FAZ10 might have a specific role distinct from the other Class IV proteins. The cell cycle delay associated with an increase in 2F1N1K cells and the flagellar defects suggests that FAZ10 could be important for defining/regulating cleavage furrow ingression which likely occurs between the old and new FAZ at the anterior cell tip in *L. mexicana*.

4.8.6 Class V proteins likely located further away from the attachment region

Null mutants of Class V FAZ proteins, which localise to a linear structure in the flagellar pocket neck with a horseshoe ring at the collar had no obvious defects. Interestingly, Class V orthologs, FAZ1 and FAZ9 were found to have mild defects in trypanosomes despite being located in the cell body domain (Vaughan *et al.*, 2008; Sunter *et al.*, 2015; Sunter and Gull, 2016). FAZ1 knockdown was found to have a limited flagellum attachment defect, resulting in loops of unattached flagellum (Vaughan *et al.*, 2008; Sunter and Gull, 2016). While FAZ9 knockdown did not cause any attachment defects but was found to cause mis-positioning of the kinetoplast and nucleus (McAllaster *et al.*, 2015; Sunter *et al.*, 2015; Sunter and Gull, 2016). It was suggested therefore that FAZ1 and FAZ9 were located further away from the primary attachment area compared to CC2D/FAZ2 hence depletion causing milder defects. A recent study showed that while *L. mexicana* and *T. brucei* share the same core structures such as MtQ and collar, they were some differences. The neck region in *L. mexicana* and the proximal end of FAZ in *T. brucei* is similar, but in *L. mexicana* the structures that constitute the FAZ have a different organisation, with the FAZ filament not adjacent to the junctional complexes (Wheeler, Sunter and Gull, 2016). It is possible that with Class V proteins, no severe consequences were observed because these proteins are located further away from the primary attachment region and are associated with other roles in the flagellar pocket area that were not assessed (**Fig4.20**). Moreover, Class V FAZ proteins in *L. mexicana* are potentially those FAZ proteins located further away from the attachment area in *T. brucei*.

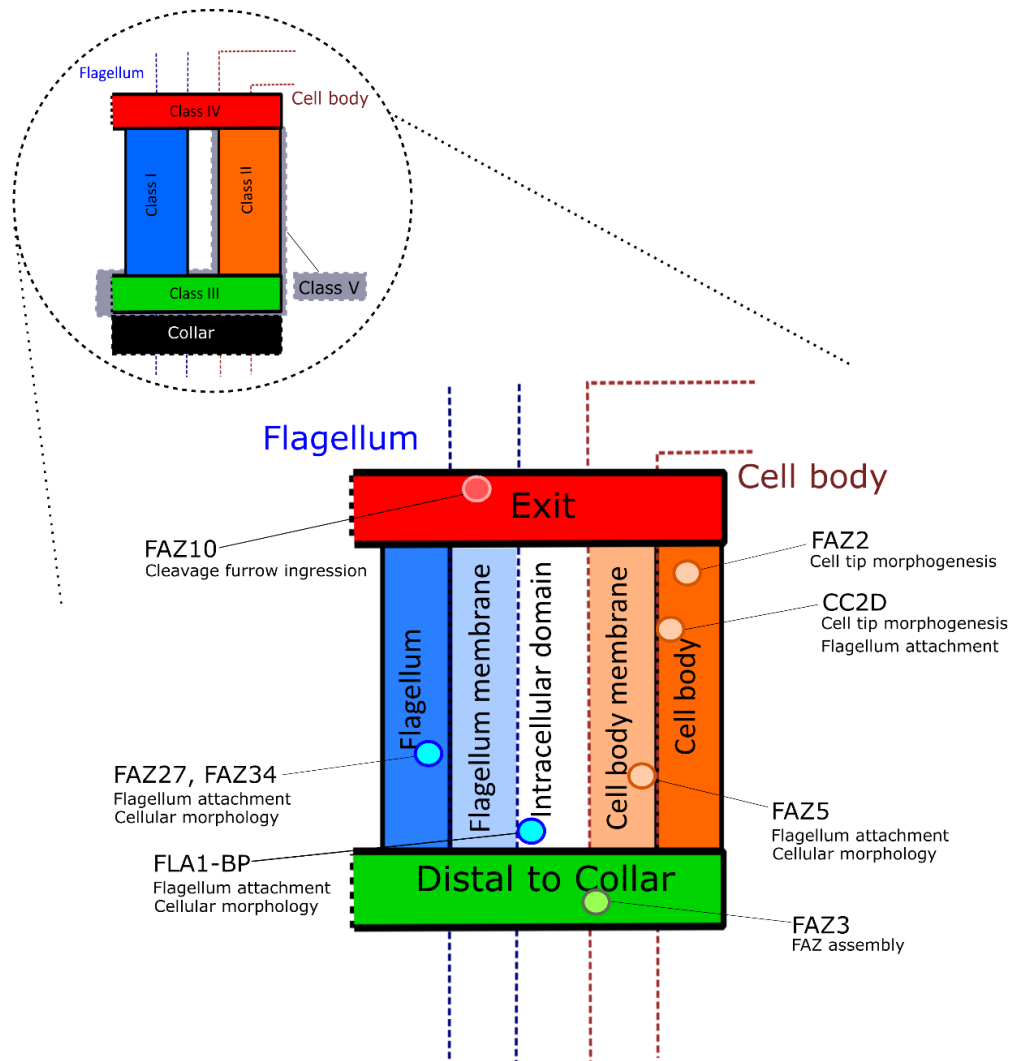


Figure 4.20 Potential roles of the different FAZ domains within the FAZ structure in *L. mexicana*. In insert image 5 FAZ localisation classes are shown: 1) Linear on flagellum side - blue, 2) Linear on the cell body side - orange, 3) distal to collar – green placed above the collar - black, 4) Exit - red, 5) Linear on cell body side and distal of the collar - grey. Flagellum (blue dotted lines) and cell body (red dotted lines) membranes are shown here. The localisation classes can be separated into sub-domains (main image) containing flagellum and flagellum membrane within class I, cell body and cell body membrane within class II and intracellular domain in between along with class III distal to collar and class IV exit domains. The locations of FAZ proteins can be predicted based on the following: known domains in *T. brucei* which correlate with localisation class in *L. mexicana* as determined in Chapter 3, transmembrane domains status, which indicates location within intracellular/membrane domains and functional analysis results. Typical patterns of phenotypes correlate with protein location suggesting each domain is a functional grouping of proteins with specific roles.

Chapter 5

Class I proteins FAZ27 and FAZ34 are important for flagellum attachment and flagellar pocket morphology

5.1 Preface

In the localisation screen (**Chapter 3**) FAZ27 and FAZ34 were identified as flagellum domain proteins (Class I), with a linear signal within the flagellar pocket neck. With no transmembrane domains detected, they were determined to be two of seven FAZ proteins proximal to the flagellum cytoskeleton.

Studies of flagellum domain FAZ proteins in trypanosomatids to date were in *T. brucei* (ClpGM6, FLAM3 and FAZ27). ClpGM6, FLAM3 and FAZ27 depletion caused the shortening of the FAZ and associated morphological changes (Rocha *et al.*, 2006; Rotureau, Subota and Bastin, 2011; Hayes *et al.*, 2014; J. D. Sunter *et al.*, 2015; An *et al.*, 2020). However, work on the flagellum domain of *L. mexicana* has not been carried out.

The deletion of three flagellum domain proteins, including FAZ27 and FAZ34 (**Chapter 4**) resulted in cells with a short flagellum and loose flagella in the media. As the *L. mexicana* FAZ organisation is different to that of *T. brucei*, and with the role of the flagellum domain proteins not known (Wheeler, Sunter and Gull, 2016), FAZ27 and FAZ34 proteins were therefore excellent candidates to explore the role of the flagellum FAZ domain for the morphogenesis of the FAZ and flagellar pocket.

5.2 Phenotype of FAZ27 and FAZ34 null mutants changes over time

To ensure the phenotypes previously seen in the deletion screen (**Chapter 4**) were reproducible, FAZ27 and FAZ34 null mutant cell lines were re-generated using the C9/T7 parental cell line. These cell lines grew back after the same length of time as previous null mutants, ~10 days post-transfection and PCR was carried out to confirm the deletion of these genes (**Fig 5.1A-C**). The FAZ27 and FAZ34 null mutant cells had the same phenotype as previously observed with loose flagella and cells with a short flagellum that are atypical in *L. mexicana* parental cells (**Fig 5.1C**).

During the observations of FAZ27 and FAZ34 null mutants post-transfection, it was noticed that the mutant phenotype appeared to change over time. To understand this phenomenon, the re-generated FAZ27 and FAZ34 null mutants alongside the parental cell line were taken out of liquid nitrogen storage at the exact same time for investigation. These cell lines were previously split once and frozen within three days of cell growth post-transfection (**Fig 5.1A**). To ensure an accurate and fair assessment of these cells, they were analysed at the same time point, in duplicates, every week over the period of 4 weeks (labelled as week 1, 2, 3 and 4) (**Fig 5.1A**).

To analyse cell growth, the cell counts of the mutant and parental cell lines were recorded at the same time point from the set density of 1×10^6 /ml every 24 hours during a 72 hour period in week 1 and 4 (**Fig 5.2A&B**). To assess any growth rate change over time the cell counts doubling time were calculated from the average 24-hour growth peak in week 1 and week 4. The parental doubling time was 5.81 hours in week 1 and 5.66 hours in week 4. This showed that parental growth rate did not change during the 4 weeks period. For the FAZ27 null mutant, the doubling time was much slower, 9.78 hours in week 1. However, in week 4, the doubling time reduced by 2.5 hours to 7.33 hours (**Fig 5.2A**). For the FAZ34 null mutant, the doubling time was 8.12 hours and 7.37 hours in week 1 and 4, respectively, showing a slight reduction (**Fig 5.2B**). The reduction in doubling time for both null mutants at week 4 shows that the cells growth rate increased during the first four weeks post-transfection.

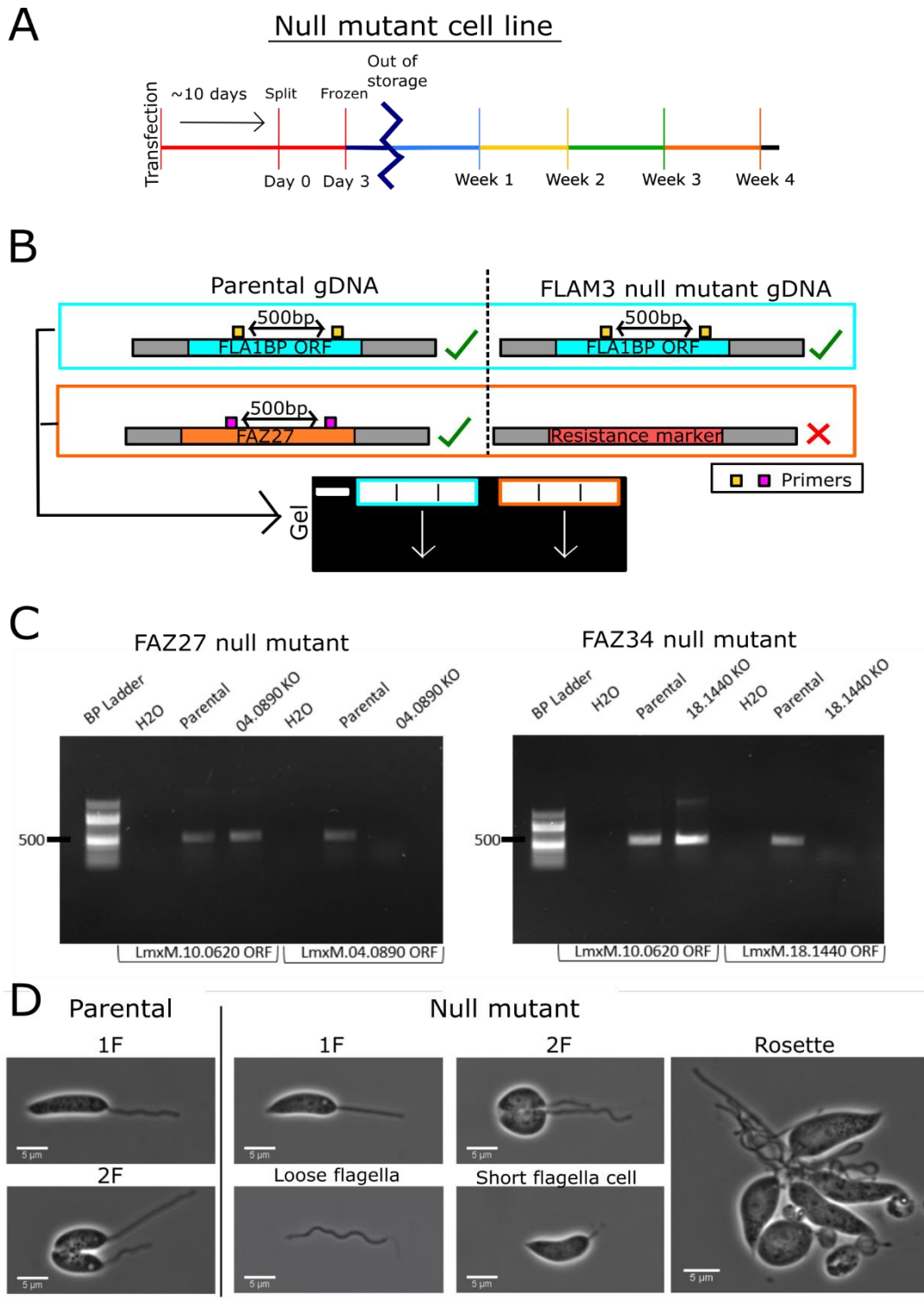


Figure 5.1 FAZ27 and FAZ34 null mutants were successfully re-generated. A) Timeline of null mutant cells life, which started from transfection with the null mutants growing back after ~10 days and stored within 3 days of growth. Post-storage null mutants were analysed at weeks 1, 2, 3 and 4. B) Schematic of PCR and gel layout to confirm gene deletion C) Gels showing the diagnostic PCR carried out on the extracted gDNA from the null mutants confirmed gene deletion. D) Re-generated null mutants presented mutant phenotypes seen previously, loose flagella, short flagellum cells and rosettes.

For further analysis, these cell lines were imaged directly from cell culture to measure the cell structures observed. To determine whether there were changes in the cell cycle, the cell cycle position defined by their K/N/F status from each cell line were also captured and recorded at the same time. In the parental cell line, for cells directly out of culture there was a slight increase in 1F cells (75.9% and 76.6% in week 1 to 81% and 85.3% in week 4). While 2F cells decreased from 24.1% and 23.4% in week 1 to 19.1% and 14.7% in week 4 (**Fig 5.2C&D**). The analysis of cell cycle position demonstrated that the decrease in 2F cells was exclusively in the 2F1N1K cell type, with the mean reduced from 19.3% in week 1 to 14.3% in week 4 (**Fig 5.2D**). This reduction in 2F cells, and more specifically in 2F1N1K suggests that less time was spent in this configuration.

In the FAZ27 null mutant cell line, when analysed directly from cell culture, the percentage of loose flagella reduced from 11.1% and 19.4% in week 1 to 3.7% and 7.4% in week 4 (**Fig 5.2E**). Cells with a short flagellum were seen less often as the time progressed, reducing substantially from week 1 to week 2 (12.5% and 18.37% to 8.23% and 3.3%) and remaining relatively stable into week 4 (**Fig 5.2E**). A similar trend for both loose flagella and short flagellum cells was seen in the K/N/F counts analysis (**Fig 5.2F**). Whilst there was a reduction in loose flagella and short flagellum cell numbers, the presence of rosettes remained consistent at low levels throughout (**Fig 5.2E**). In concert with the reduction in loose flagella and cells with a short flagellum, the numbers of 1F and 1F1N1K cells increased over time (**Fig 5.1E&F**). The 2F cell type also increased steadily and remained consistent into week 4 (**Fig 5.1E&F**).

FAZ34 null mutants behaved in a similar way, with a decrease in loose flagella and short flagellum cell numbers matched by an increase in 1F and 2F cells over the time

period. When analysing directly out of culture, it was shown that loose flagella decreased dramatically from week 1 (12.7% and 23.5%) to week 2 (6.1% and 9.8%) and continued with a steady decline thereafter (**Fig 5.2G**). Short flagellum cell numbers also steadily decreased (**Fig 5.2G**) and the cell cycle position analysis confirmed this steady trend starting with 7.87% and 11.32% in week 1 reducing to 5.5% and 4.4% in week 4. (**Fig 5.2H**). Similar to the FAZ27 null mutant cell line, the decrease in these cell types correlated with an increase in 1F and 2F cells over the 4-week period (**Fig 5.2G&H**). This shows that the severity of the mutant phenotype decreases with time.

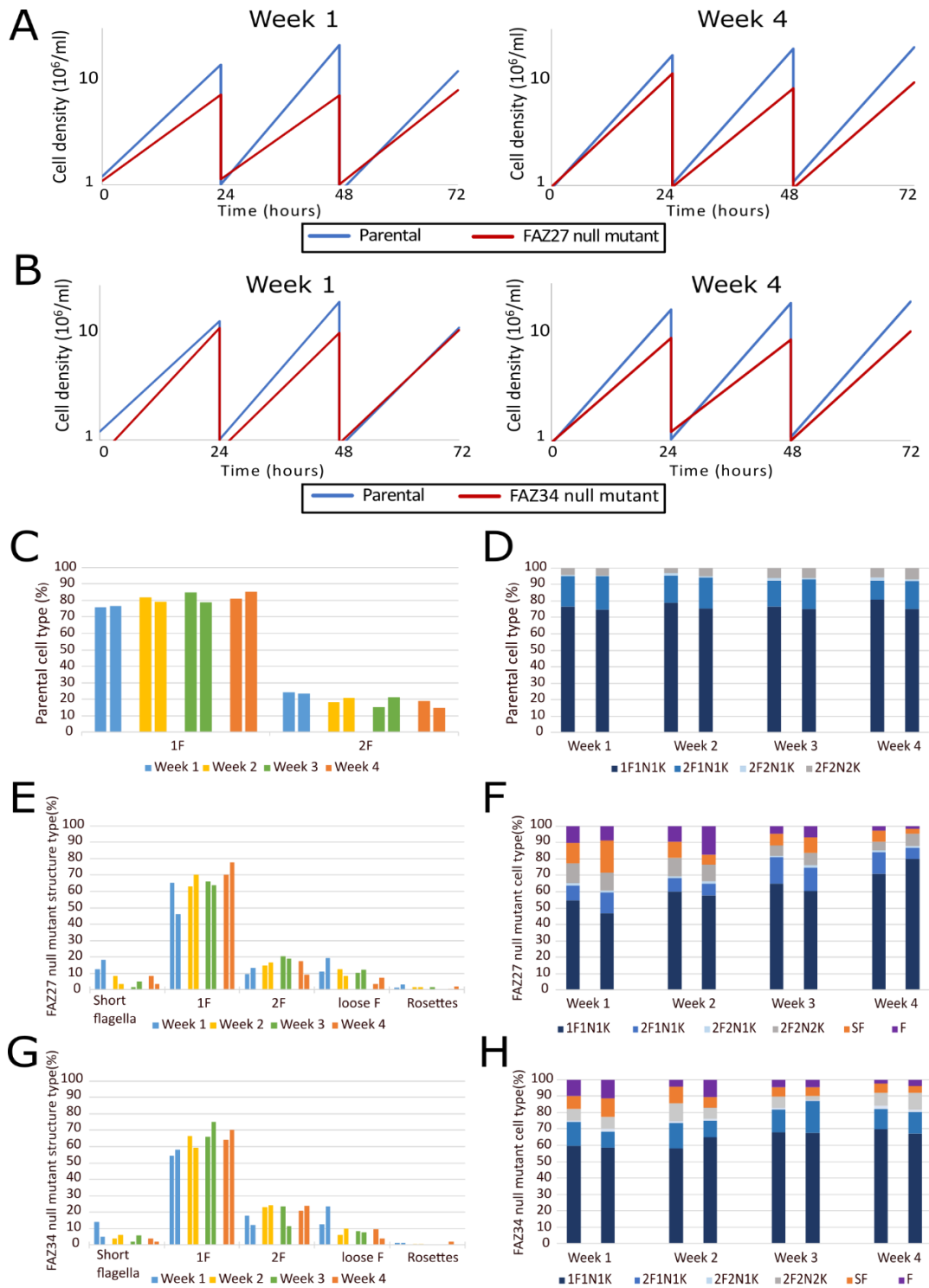


Figure 5.2 Phenotype of FAZ27 & FAZ34 null mutant cells changed over time. A) Growth curves for FAZ27 null mutant recorded in week 1 and 4, B) Growth curves for FAZ34 null mutant recorded in week 1 and 4, C) % of cell type seen in culture for parental. D) % of cell cycle counts for parental. E) % of cell structures seen in culture for FAZ27 null mutant. F) % of cell cycle counts for FAZ27 null mutant. G) % of cell structures seen in culture for FAZ34 null mutant. H) % of cell cycle counts for FAZ34 null mutant. SF- short flagellum, F- loose flagella.

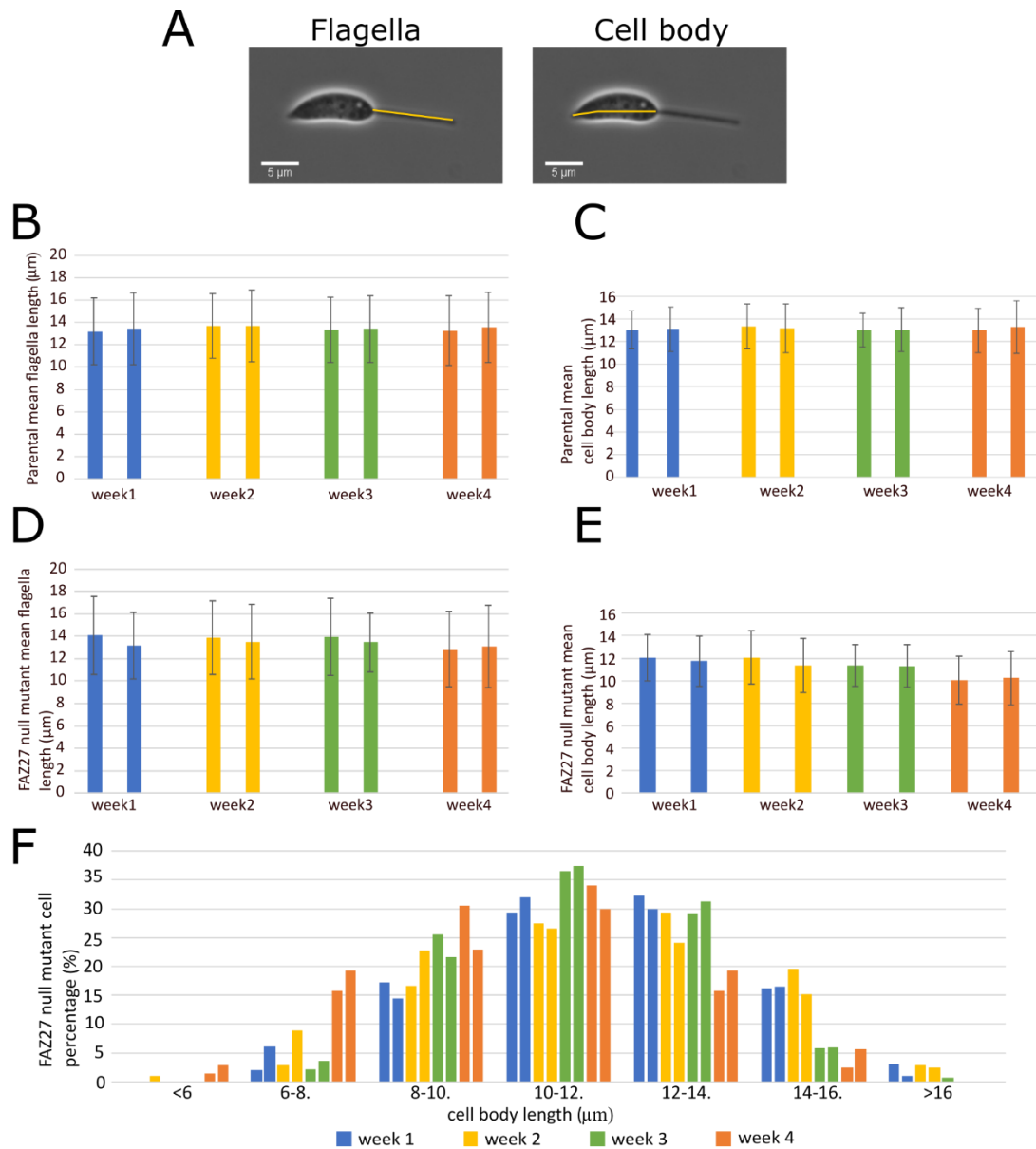
It was demonstrated that for both FAZ27 and FAZ34 null mutants, the severity of mutant phenotype declines and becomes more similar to the wildtype appearance over time. As the null mutants had disrupted cell cycles and morphological defects, the next step was to investigate the morphology in detail. To assess this, the morphology was analysed by measuring flagellum and cell body lengths of 1F1N1K cells (**Fig 5.3A**), which were captured at the same time point, in duplicates on the weekly basis over the same 4 week period. The mean of both set of lengths were calculated for both groups of 90-100 1F1N1K cells (excluding short flagellum cells) from each week.

The parental cell line was analysed over the course of 4 weeks, with the mean flagellum length ranging from 13.2 - 13.7 μm . These lowest and highest values were derived from week 1 and 2, respectively (**Fig 5.3B**). For the cell body lengths, the mean ranged from 13.0 - 13.3 μm , observed in week 3 and 2 respectively (**Fig 5.3C**). These narrow ranges with no distinctive pattern show that there are no significant changes in flagella and cell body lengths of the parental cell line over this time period.

The FAZ27 null mutant mean flagellum lengths were calculated, showing a range of 12.9 - 14.1 μm over 4 weeks with no pattern of increase or decrease (**Fig 5.3D**). For the cell body lengths, there was a gradual reduction in mean length of $\sim 2 \mu\text{m}$ from week 1 (12.1 μm , 11.7 μm) to week 4 (10.1 μm , 10.2 μm) (**Fig 5.3E**). The distribution of cell body lengths showed that the highest proportion of shorter lengths, $< 10 \mu\text{m}$ were associated with week 4 and the highest proportion of longer lengths $> 14 \mu\text{m}$ was associated with weeks 1 and 2 (**Fig 5.3F**).

For the FAZ34 null mutant, the flagellum length also showed no large changes with the mean range varying from 13.7 - 14.5 μm (**Fig 5.3G**). Like the FAZ27 null mutant, the mean cell body length reduced significantly from 12.2 μm , 12.3 μm in week 1 to 10.2 μm , 10.2 μm in week 4, giving a similar reduction of $\sim 2 \mu\text{m}$ in total (**Fig 5.3H**). The distribution of cell body length measurements showed that highest proportion of $> 12 \mu\text{m}$ lengths were from weeks 1 and 2, while lower lengths ($< 10 \mu\text{m}$) were associated with weeks 3 and 4 (**Fig 5.3I**). The cell body length reduction occurred during the same time window as there was a reduction in the number of loose flagella

and cells with a short flagellum. The decrease in cell length also correlates with an increase in growth rate which suggests the possibility of reduction in cell body length as an adaptation to enable faster growth.



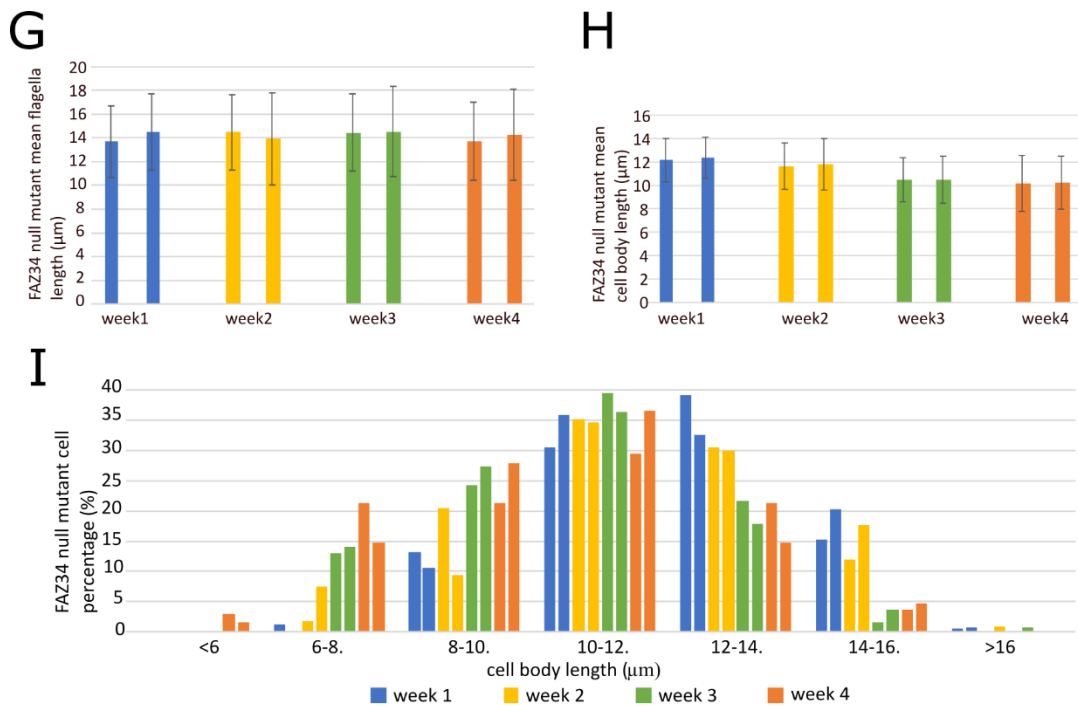


Figure 5.3 Cell body length in FAZ27 & FAZ34 null mutants reduced over time. A) Example measurements for flagellum (proximal to distal tip) and cell body (posterior to anterior cell tip). B) Mean flagellum lengths in Parental. C) Mean cell body lengths in Parental. D) Mean flagellum lengths in FAZ27 null mutant. E) Mean cell body length in FAZ27 null mutant. F) Cell body length distribution in FAZ27 null mutant. P-values between week 1 and week 4 were <0.001 . G) Mean flagellum lengths in FAZ34 null mutant. H) Mean cell body lengths in FAZ34. I) Cell body distribution in FAZ34 null mutant.

5.3 Likelihood of flagellum loss correlated with increasing flagellum length

A likely explanation for the presence of loose flagella and cells with a short flagellum in the FAZ27 and FAZ34 null mutants was that there was a weakened flagellum attachment which was more readily broken due to the mechanical stress of the flagellum beating, releasing the flagellum. To determine if the flagellum attachment was weakened and susceptible to mechanical stress the mutants were subjected to a defined period of vortexing and the different cell types before and after were counted. As previously shown, null mutants had a greater number of detached loose flagella in week 1, so for an extreme test of ‘flagella loss’ these cell lines were

assessed in week 1 after defrosting. Images were captured prior to vortex and again after 30s of vortexing to measure and compare the cell types observed.

As a control, the parental cell line was used, and it was observed that the proportion of cell types consisting of 1F (~75%) and 2F (~25%) cells did not change before and after 30s of vortex (**Fig 5.4A**). For the FAZ27 null mutant, the proportion of 1F cells reduced substantially to 42% from 65% after 30s vortex, which was matched by an increase in short flagellum cells and loose flagella from 12% and 11% to 20% and 24%, respectively (**Fig 5.4B**). A similar trend was seen in FAZ34 null mutant, that after 30s vortex, the percentage of 1F cells was reduced from 54% to 40%. Short flagellum cells and loose flagella increased from 14% to 25% and 13% to 20% respectively (**Fig 5.4C**). For both mutants, there was an insignificant difference in 2F and rosettes levels (**Fig 5.4B & C**).

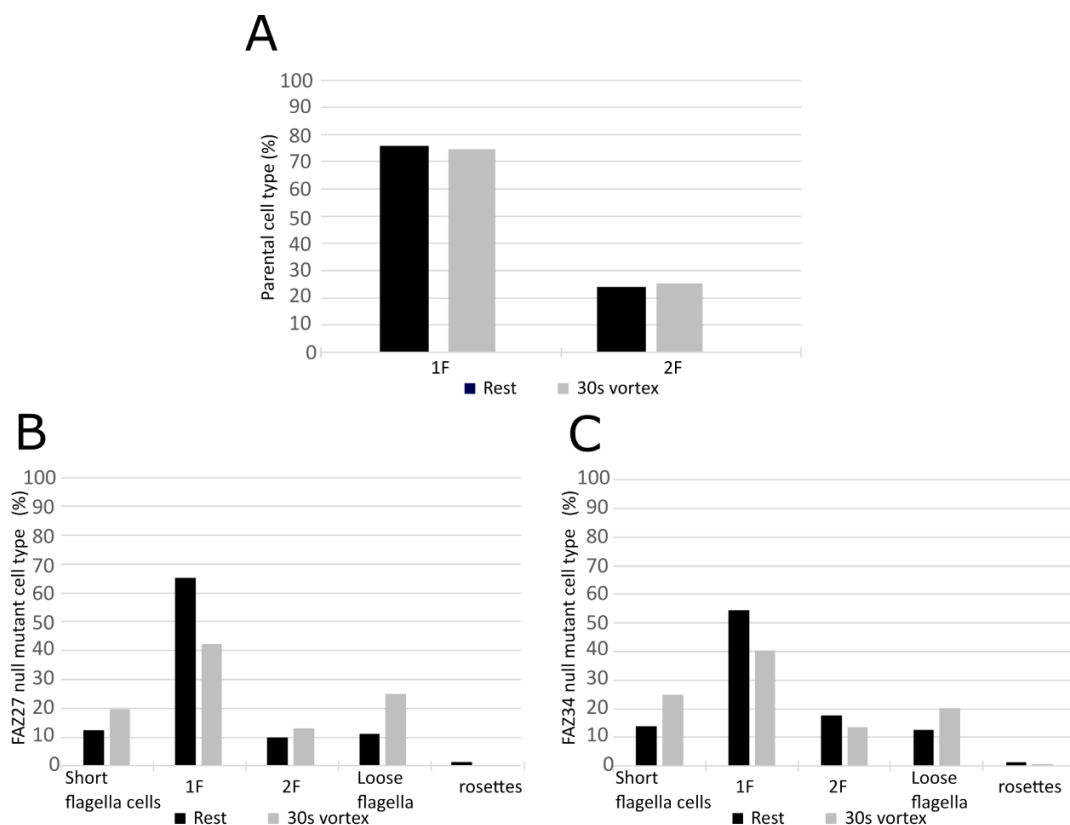


Figure 5.4 Mechanical stress from vortexing caused flagellum loss. A) Parental. B) FAZ27 null mutant. C) FAZ34 null mutant. % Of cell types measured at rest and after 30s vortex. 1ml of cell lines were tested in 1.5ml Eppendorf tubes and each experiment was performed in duplicate. The representative data from one experiment is shown.

The increase in short flagellum cells and loose flagella demonstrated that mechanical stress can contribute to flagellum loss in the null mutant cells. The longer the flagellum the greater the force it can exert on the cell body and FAZ and therefore flagellum length may be a critical contributing factor to this flagellum loss phenotype. To assess whether there was a relationship between flagellum length and flagellum loss the length of the flagellum in 1F cells and loose flagella was measured.

Previously, it was shown that in weeks 1 and 2 there were higher levels of loose flagella with little change in 1F flagellum length. This provided a reliable and consistent set of images to measure the loose flagella and attached flagellum lengths (**Fig. 5.5**).

For the FAZ27 null mutant, the mean loose flagellum length was 17.2 μm and 19.0 μm , which was significantly longer than the attached flagellum length (14.1 μm and 13.2 μm) (**Fig 5.5A**). The same result was seen for the FAZ34 null mutant, with the mean length of the loose flagella of 18.4 μm and 21.4 μm and 13.7 μm and 14.5 μm for the attached flagellum (**Fig 5.5B**). With a mean difference of approximately 4-5 μm between the two types of flagellum, the distribution of flagellum lengths was investigated. For both the FAZ27 and FAZ34 null mutants, it was clear that the loose flagella were longer than those attached to cells, with the highest proportion seen for longest lengths of 20 - 22 μm and <22 μm , respectively (**Fig 5.5C & D**). The highest proportion of attached flagellum length were seen in the length group of 12 -14 μm , and as the lengths increased, the proportion became progressively smaller until it was almost non-existent at <22 μm (**Fig 5.5C & D**). This demonstrated that as the length increased, the likelihood of flagellum loss increased.

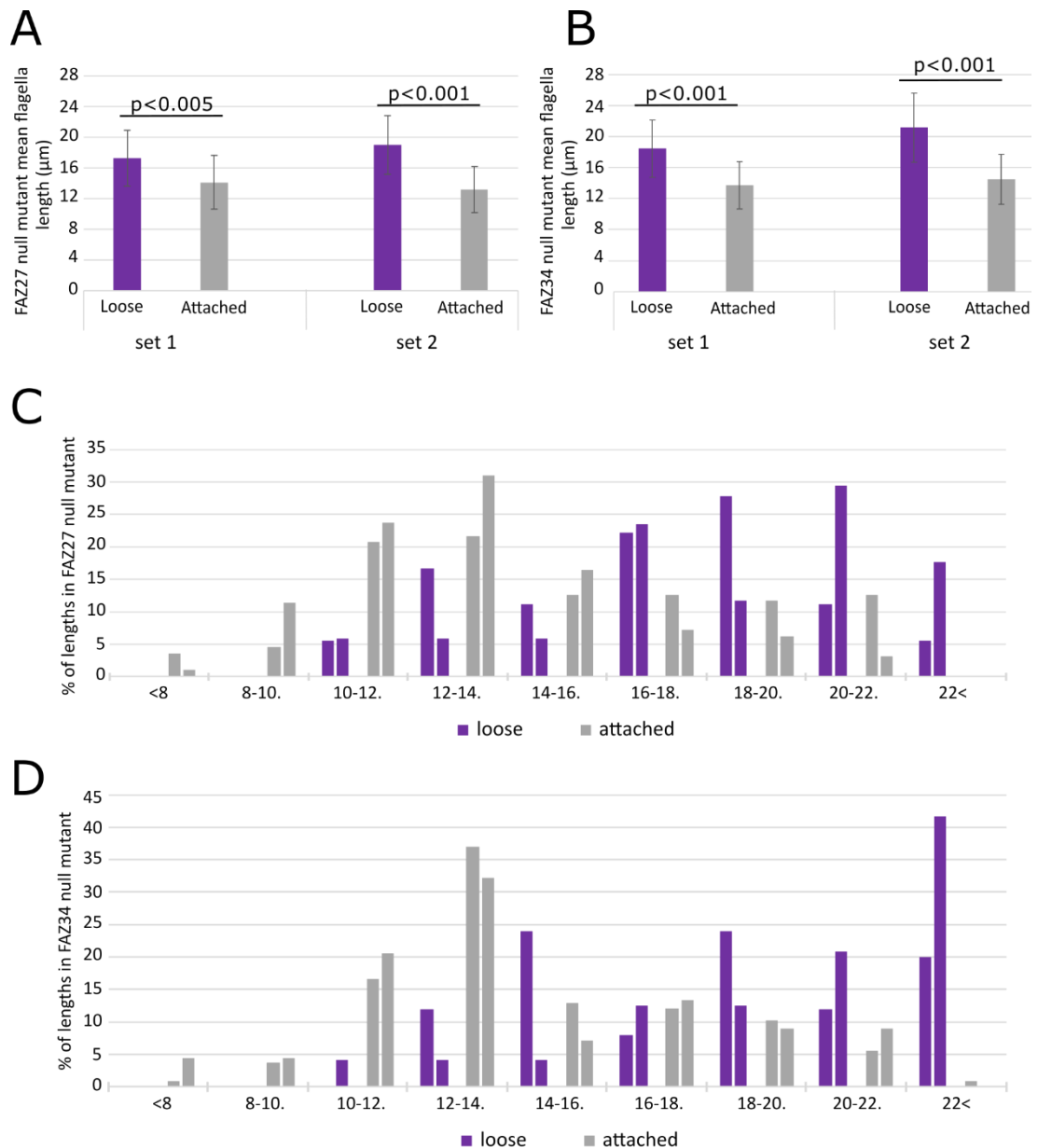
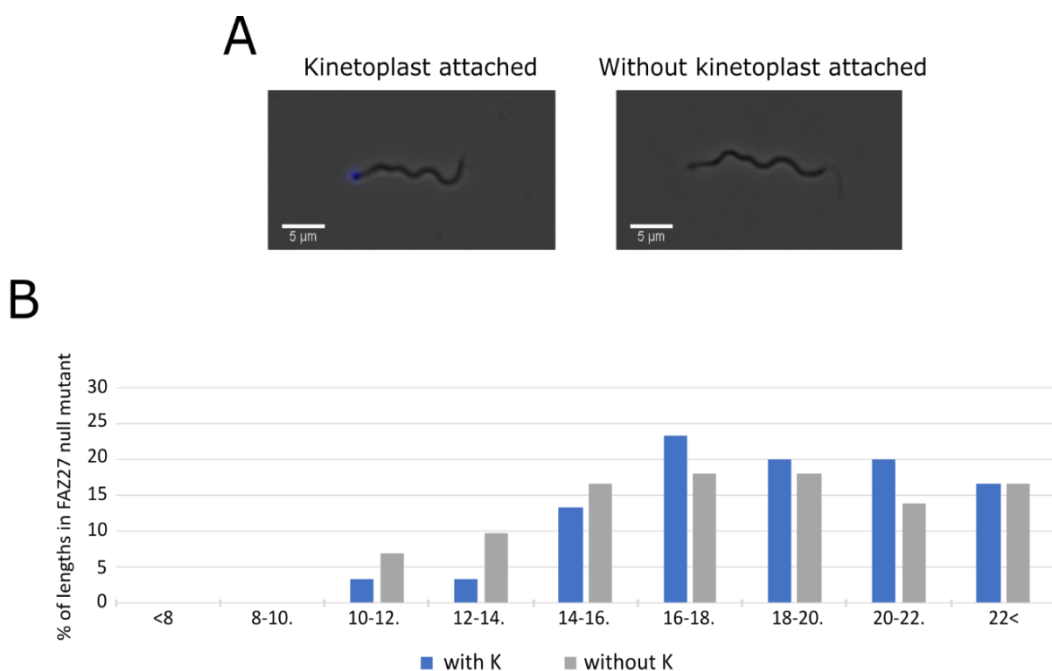


Figure 5.5 Likelihood of flagellum loss increased with increasing flagellum length. Mean length for loose vs attached flagella in A) FAZ27 null mutant and B) FAZ34 null mutant. The mean of flagellum length was calculated from ≥ 100 loose flagellum and attached flagellum measurements C) Histogram of loose and attached flagellum lengths in FAZ27 null mutant. D) Histogram of loose and attached flagellum lengths in FAZ34 null mutant.

It was noticed that a number of the loose flagella had a kinetoplast attached, as indicated by a Hoechst 33342 stained structure at one end (**Fig 5.6A**). 42% and 35% of loose flagella had an attached kinetoplast in the FAZ27 and FAZ34 null mutants, respectively in week 1 and 2 average. To determine whether kinetoplast attachment was related to flagellum length, the measurements of loose flagellum length were split into two groups, with kinetoplast and without kinetoplast. The mean flagellum length for the subset with the kinetoplast attached was slightly longer than for those without a kinetoplast (18.72 μm and 19.64 μm versus 17.85 μm and 17.54 μm for the FAZ27 and FAZ34 null mutants, respectively).

To investigate this small difference further, the loose flagellum lengths were distributed into flagellum length groups for comparison (**Fig 5.6B&C**). For the FAZ27 null mutant, there seemed to be little difference in the proportions of lengths between loose flagella with and without kinetoplast attached (**Fig 5.6B**). However, for the FAZ34 null mutant, higher proportions of longer lengths (>18 μm) seemed to be associated with kinetoplast attached loose flagella and equally, higher proportions of shorter lengths (<18 μm) were seen for loose flagella without kinetoplast attachment (**Fig 5.6C**). It was previously demonstrated that for FAZ27 and FAZ34 null mutants, flagella loss correlates with increasing flagella length, but there was no clear relationship between flagellum length and retention of the kinetoplast during flagellum loss.



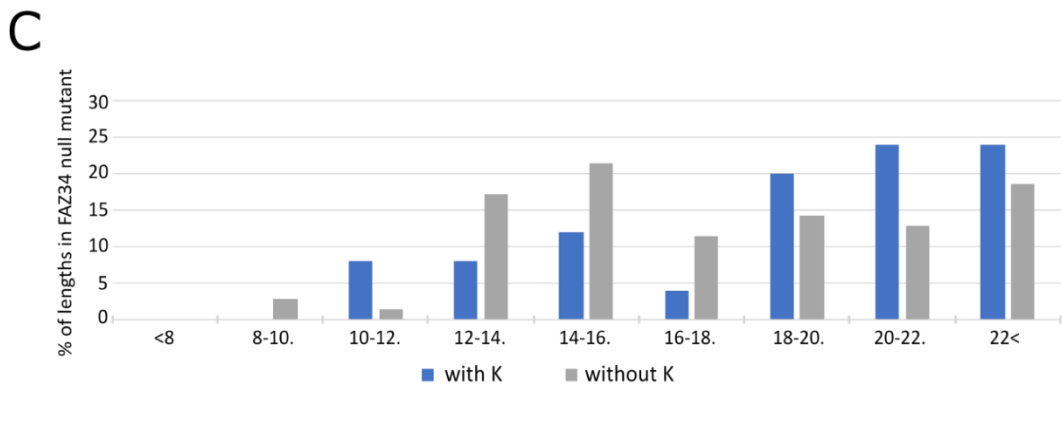


Figure 5.6 Kinetoplast attachment correlated with flagellum length in FAZ34 null mutant. A) Example images of loose flagella observed with and without kinetoplast. Kinetoplast was stained with Hoechst 33342. Histogram of loose flagellum lengths with and without kinetoplast in FAZ27 null mutant B) and FAZ34 null mutant.

5.4 Re-introduction of FAZ27 and FAZ34 genes confirmed flagellum loss was directly related to FAZ27 and FAZ34 deletion

To confirm the mutant phenotype of loose flagella and cells with a short flagellum was the consequence of FAZ27 and FAZ34 deletion, add-back cell lines were generated. The add-back constructs were created by cloning the FAZ27 and FAZ34 ORF into a constitutive expression plasmid (See section 2.2.4 for the generation of FAZ add-back plasmids). The add back plasmids were transfected into the appropriate null mutant cell lines, with the add-back cell lines growing back 10 days post transfection, before being split once and frozen within 3 days (**Fig 5.7A**). The add-back cell lines expressed FAZ27 and FAZ34 tagged at the N-terminus with mNG fluorescent protein. On inspection by microscopy, the mNG tagged FAZ27 and FAZ34 protein in the add-back cells was observed at the FAZ throughout the cell cycle as expected (**Fig 5.7B**).

To check that the add-back cell lines restored the parental phenotype, the parental, FAZ null mutants and add-back cell lines were compared. As previously shown, the mutant phenotype was at its least severe in week 4 post storage and with the add-backs having gone through additional selection pressures, it was logical to measure the true extent of the FAZ gene add-back in restoring the parental phenotype when all cell lines were 4 weeks post-storage. These cell lines were imaged directly from cell culture to assess the levels of cell types observed.

For the FAZ27 add-back, cells with a short flagellum and loose flagella were not observed (**Fig 5.7C**). Meanwhile, the 1F and 2F cell populations increased from 70% to 75% and 17% to 24%, respectively. The percentages of 1F and 2F cells observed in the add-backs was close to the parental. (**Fig 5.7C**). For the FAZ34 add-back, cells with a short flagellum and loose flagella were also eliminated entirely (**Fig 5.7D**), with the percentages of 1F and 2F cells increased to 80% and 20% respectively. The proportions of cell types observed was overall very similar to the parental cell line (**Fig 5.7D**). This demonstrated that the add-back of the deleted protein restored the parental phenotype, indicating that the phenotype observed was the consequence of FAZ27 and FAZ34 loss. To assess the functions of FAZ27 and FAZ34 specifically, the add-backs will be included alongside the parental for further analysis of the null mutants.

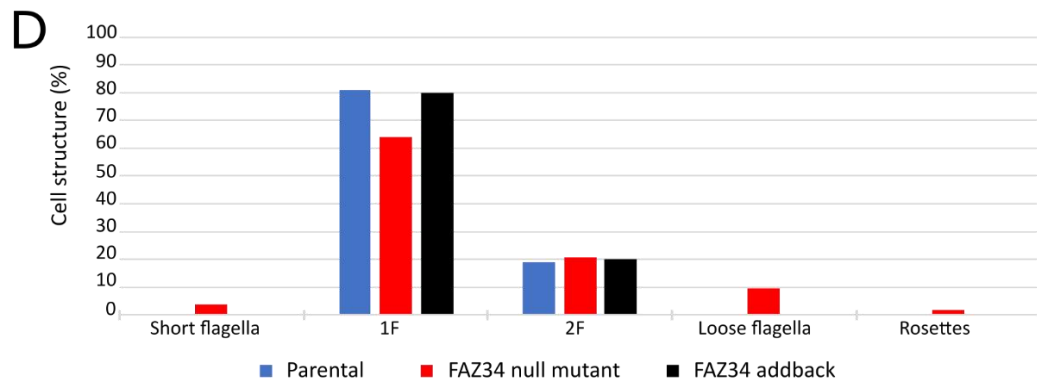
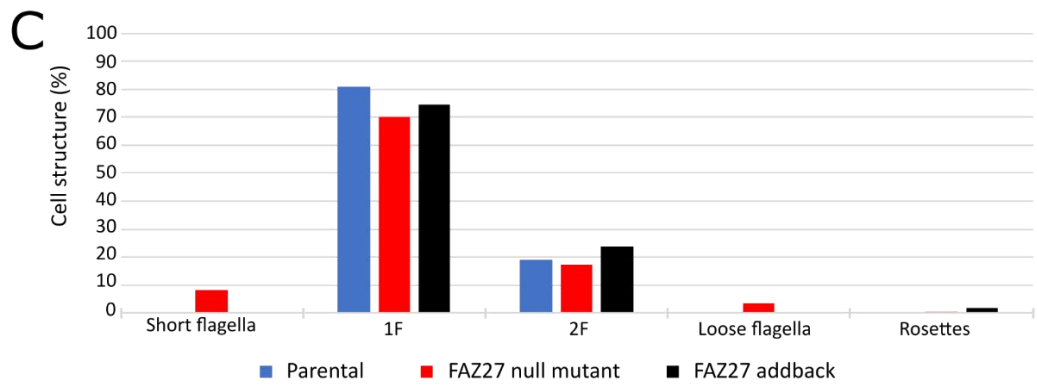
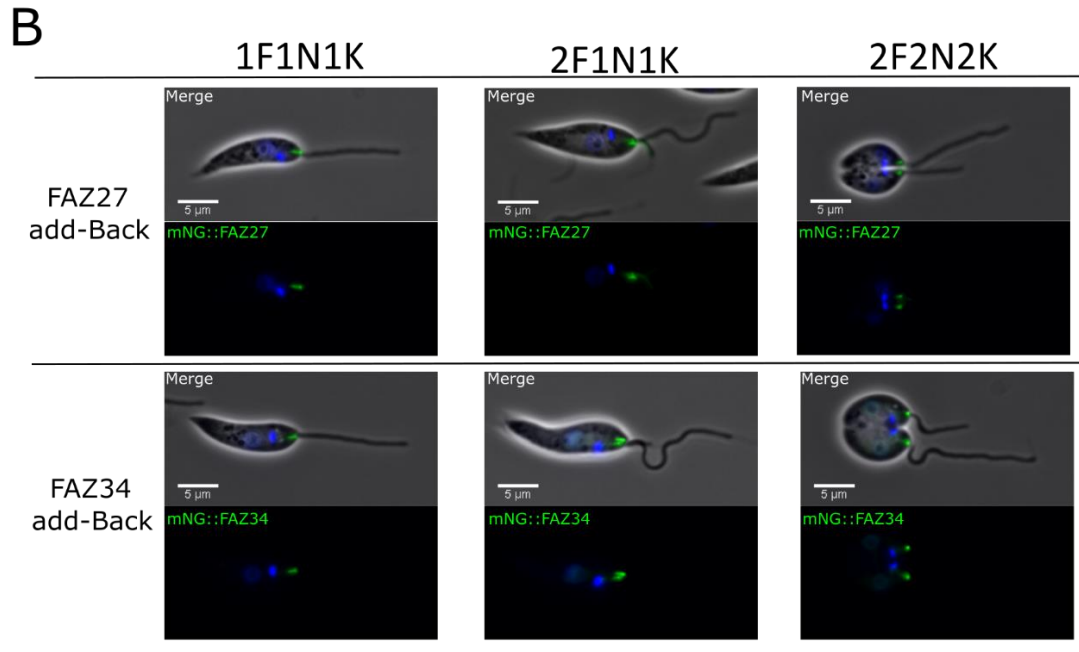
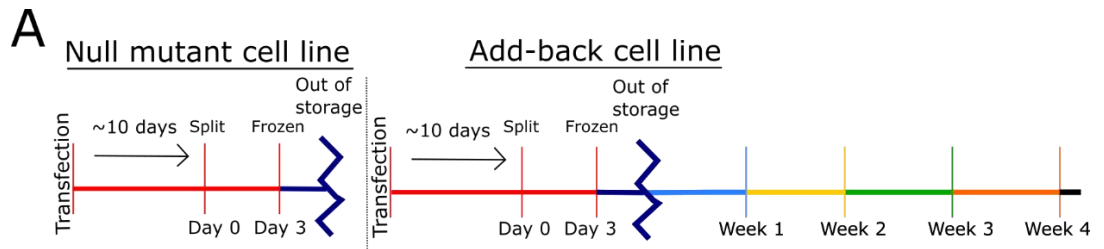


Figure 5.7 FAZ27 and FAZ34 null mutant phenotype was the consequence of protein loss. A) A time-line of add-back life, which started with transfection to generate null mutant cell lines. Post-storage transfection occurred to generate add-back cell lines. Post-storage add-backs were analysed at weeks 1 and 4. B) FAZ27 and FAZ34 add-backs tagged with mNG were observed with linear signal in the FAZ region throughout the cell cycle. C) Quantitation of cell types observed in parental, FAZ27 null mutant and FAZ34 addback in week 4. D) Quantitation of cell types observed in parental, FAZ34 null mutant and FAZ34 addback in week 4. Each experiment was performed in duplicate and the representative data from one experiment is shown.

5.5 Both EF1 and EF2 domains of FAZ34 were required for maintaining flagellum attachment

It was previously shown (**Chapter 3**) that the FAZ34 protein has a pair of EF-hand domains. FAZ34 is 229 amino acids long, and the first EF-hand domain (EF-1) was predicted to run from amino acids 4 to 60 and the second (EF-2) was from amino acids 139 to 214 (**Fig 5.8A**). To understand if these domains are important for the function of FAZ34, truncation mutations were analysed.

To permit evaluation of these domains separately, truncated add-backs, containing either EF-1 or EF-2 were generated (**Fig 5.8A**). The truncated add-backs were expressed with mNG fluorescent protein at their N-terminus, using a constitutive expression plasmid. (See section 2.2.4 for the generation of FAZ add-back plasmids). The truncated add-backs EF-1 and EF-2 grew back at the same rate, 10 days post-transfection and were split once and then frozen.

The initial observations of EF-1 and EF-2 add-back cell lines by fluorescence microscopy showed a weak mNG signal in the cytoplasm with no indication of a signal in the FAZ region (**Fig 5.8B**). This demonstrated that the individual EF-1 and EF-2 domains of FAZ34 were unable to localise to the FAZ.

To investigate if EF-1 or EF-2 expression could alleviate the phenotype of the FAZ34 null mutant, the growth curves were recorded for EF-1, EF-2, full FAZ34 add-backs

alongside the null mutant and parental cell lines over a period of 72 hours. As previously shown, the growth rates were more stable in week 4, so for the reliability all cell lines were assessed at the same time, at 4 weeks post-storage. The FAZ34 null mutant was found to be the slowest growing with a doubling time of 7.37 hours and the full length add-back displayed a completely restored growth rate comparable to the parental (5.60 and 5.66 hours respectively) (**Fig 5.8C**). EF-1 and EF-2 truncated add-backs did not have as fast growth as the parental and full length add-back, but they were not as slow growing as the null mutant. It is possible that the additional selection and recovery of these cell lines could contribute to their increased growth rate. Additionally, there was little difference in growth rate between EF-1 and EF-2 with the doubling time of 6.61 and 6.13 hours, respectively (**Fig 5.8C**).

To further evaluate the role of EF-1 and EF-2 the different cell types observed directly from culture were quantitated at week 4 post-storage. For the EF-1 and EF-2 add-backs, the proportion of loose flagella observed were 3% and 4.5% respectively while short flagellum cells were almost non-existent (<1%). These numbers were lower than 9.4% and 3.7% seen in FAZ34 null mutant, respectively. (**Fig 5.8D**). This demonstrated that while the individual EF-1 and EF-2 domains were able to restore the parental phenotype to a small degree, possibly due to additional selection but both are required for correct FAZ34 function and localisation.

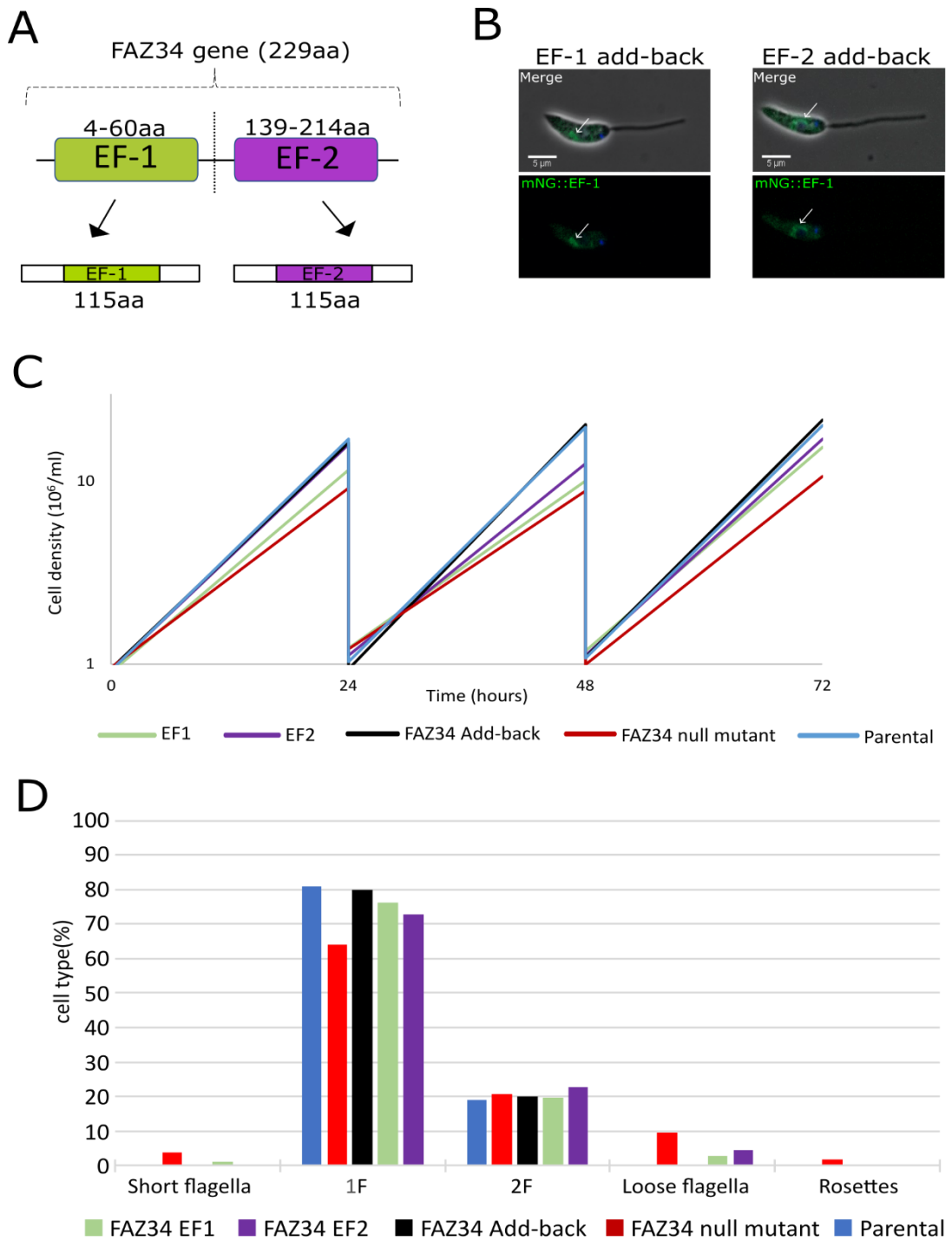


Figure 5.8 EF-1 and EF-2 domains are both important for FAZ34 function. A) Schematic diagram of EF-1 and EF-2 add-back constructs. B) Images of EF-1 and EF-2 addbacks tagged with mNG signal observed in the lysosome (as indicated by white arrows) of FAZ34 null mutant cell line. C) Growth curves and D) Histogram of cell types observed in EF-1, EF-2 and FAZ34 add-backs, FAZ34 null mutant and parental.

5.6 The deletion of flagellum domain proteins FAZ27 and FAZ34 disrupted FAZ organisation

FAZ27 and FAZ34 deletion resulted in flagellum loss, which indicates that the eponymous function of the FAZ to maintain flagellum attachment was impacted. To understand the causes of this loss of flagellum attachment, the molecular structure of the FAZ was investigated. The FAZ contains the following domains, flagellum, cell body, collar region, flagellum exit point, and intracellular (both flagellum and cell body side) and proteins representing these domains were tagged with mCherry fluorescent protein in FAZ27 and FAZ34 null mutants and imaged for comparison with the parental for any changes. The following proteins were chosen to represent each domain; FLAM3 for the flagellum domain, FLA1BP and FAZ5 for the flagellum and cell body side of intracellular membrane domain respectively, FAZ2 for the cell body domain, FAZ3 for the collar domain and FAZ10 for the exit domain (**Fig 5.9A-F**).

The short flagellum cells were compared to 1F1N1K cells for potential changes, which could give an insight to the source of flagellum loss. For the FAZ27 null mutant, in cells with a short flagellum and 1F, instead of expressing a linear localisation parallel to the cell body domain as seen in the parental cells, FLAM3 was mis-localised to the distal end of the flagellum side of the FAZ and appeared to extend beyond the anterior cell tip (**Fig. 5.10A**). FLAM3 signal was also seen close to the kinetoplast in both short flagellum and 1F1N1K cell types. FLA1BP and FAZ5, the intermembrane proteins changed from a linear to a short stub-like signal which appeared at the distal end of the neck close to flagellum exit point (**Fig 5.10B&C**). In both short flagellum and 1F1N1K cells, FAZ2 was also stub-like, at the anterior tip of the cell body but it localised slightly away from the anterior cell tip (**Fig 5.10D**). Meanwhile FAZ3 and FAZ10 signals showed no change with their ring/horseshoe signals at the collar region and exit point, respectively in both short flagellum and 1F1N1K cells (**Fig 5.10E&F**). These FAZ3 and FAZ10 signals were consistent throughout the cell cycle with similar pattern to those seen in the parental (**Fig 5.10E&F**).

For the FAZ34 null mutant, all but one followed the same pattern as the FAZ27 null mutant. The molecular composition of the intracellular domains (FLA1BP and FAZ5),

cell body domain (FAZ2), collar domain (FAZ3) and exit domain (FAZ10) appeared identical to that of FAZ27 null mutant (**Fig 5.10&5.11**). FLA1BP and FAZ5, the intermembrane proteins and FAZ2, the cell body displayed a short stub-like signal in short flagellum and 1F1N1K cells (**Fig 5.11B-D**). Horseshoe/ring localisations of FAZ3 at the collar and FAZ10 at the exit showed no change from the parental in shorten flagella and 1F1N1K cells (**Fig 5.11E&F**). However, the flagellum domain protein, FLAM3 signal was not seen anywhere within or close to the FAZ region. Instead, it had a localisation pattern consistent with the lysosome and endocytic system (**Fig 5.11A**). These localisations were consistent throughout the cell cycle. It was also appeared that there were no differences between the cells with a short flagellum and 1F cell type (**Fig 5.11**).

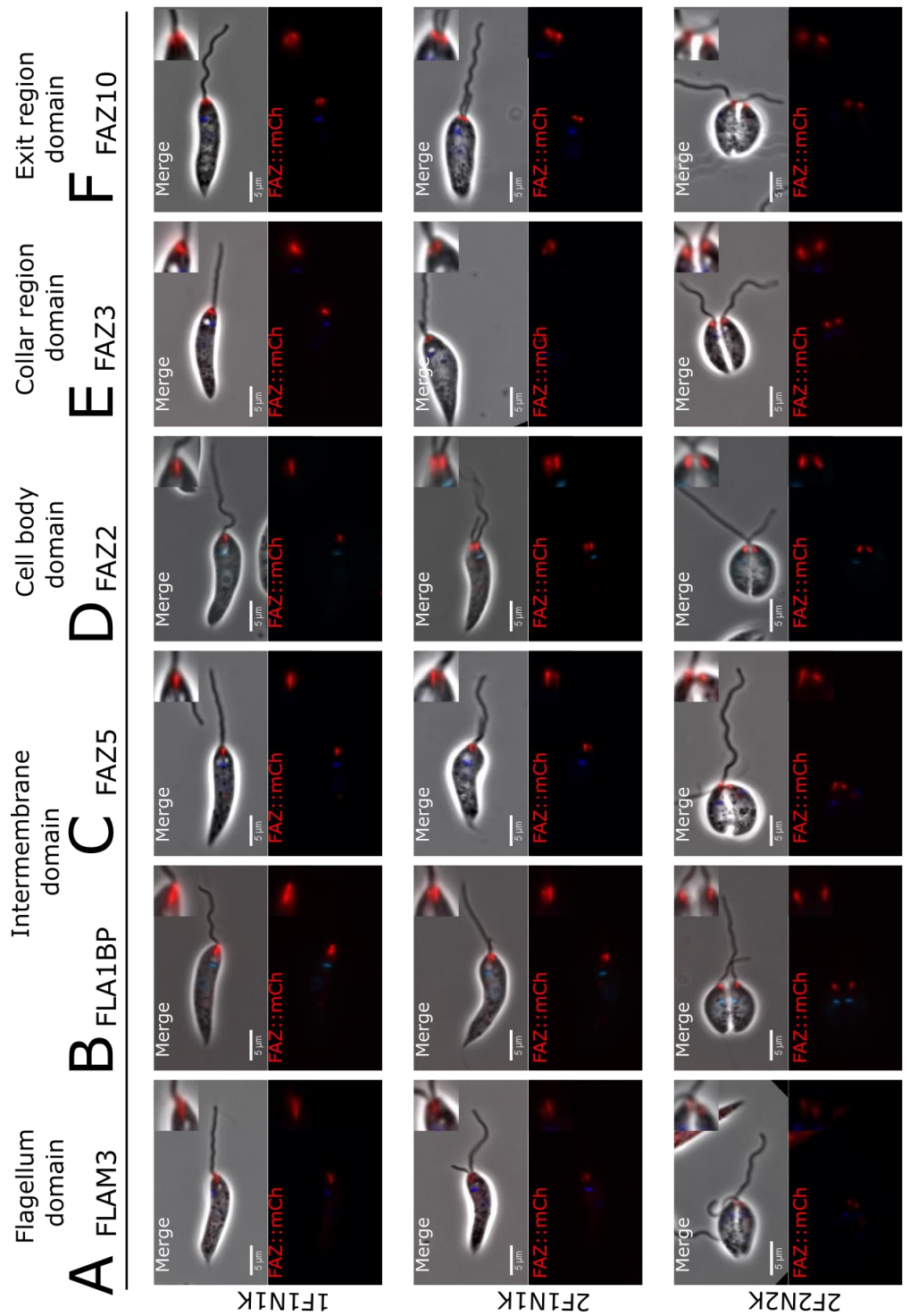


Figure 5.9 Localisations of six proteins representing different FAZ domains in the parental cell line. A) The following proteins, A) FLAM3, B) FLA1BP, C) FAZ5, E) FAZ2, F) FAZ3 and G) FAZ10 were tagged with mCherry and transfected in C9/T7 cell line. Images shown are from 1F1N1K, 2F1N1K and 2F2N2K stages of the cell cycle. Top- merge containing phase (grey), mcherry (red) and Hoechst 33342 (blue) and bottom- mcherry (red) and Hoechst 33342 (blue) only. Inserts included shows an enlarged image of FAZ region.

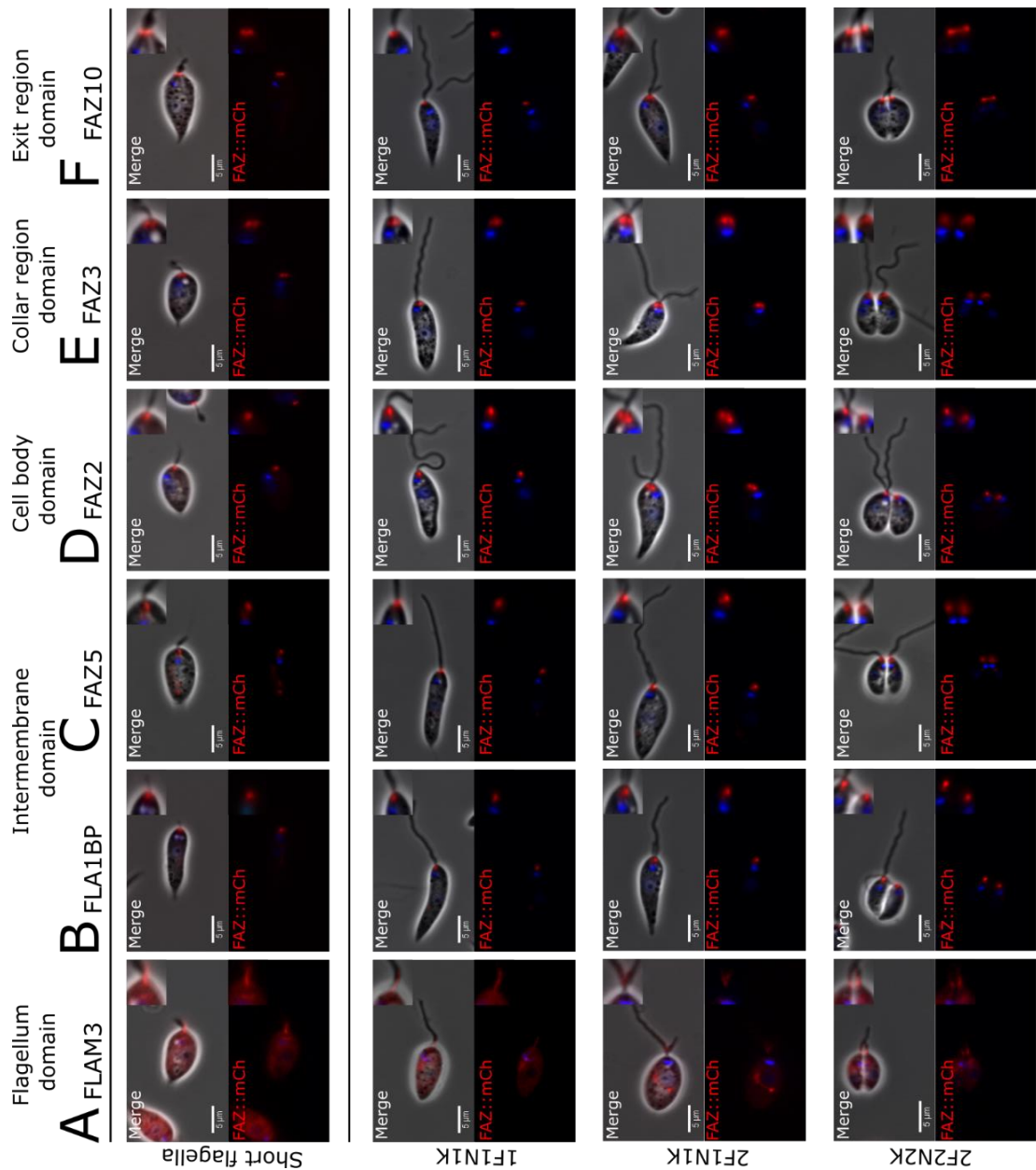


Figure 5.10 Deletion of FAZ27 affected the localisation of flagellum, intermembrane, and cell body FAZ domain proteins. The following proteins, A) FLAM3, B) FLA1BP, C) FAZ5, D) FAZ2, E) FAZ3 and F) FAZ10 were tagged with mCherry and transfected into FAZ27 null mutant cell line. Images shown are from short flagella, 1F1N1K, 2F1N1K and 2F2N2K cells. Top- merge containing phase (grey), mCherry (red) and Hoechst 33342 (blue) and bottom- mCherry (red) and Hoechst 33342 (blue) only. Inserts included shows an enlarged image of FAZ region.

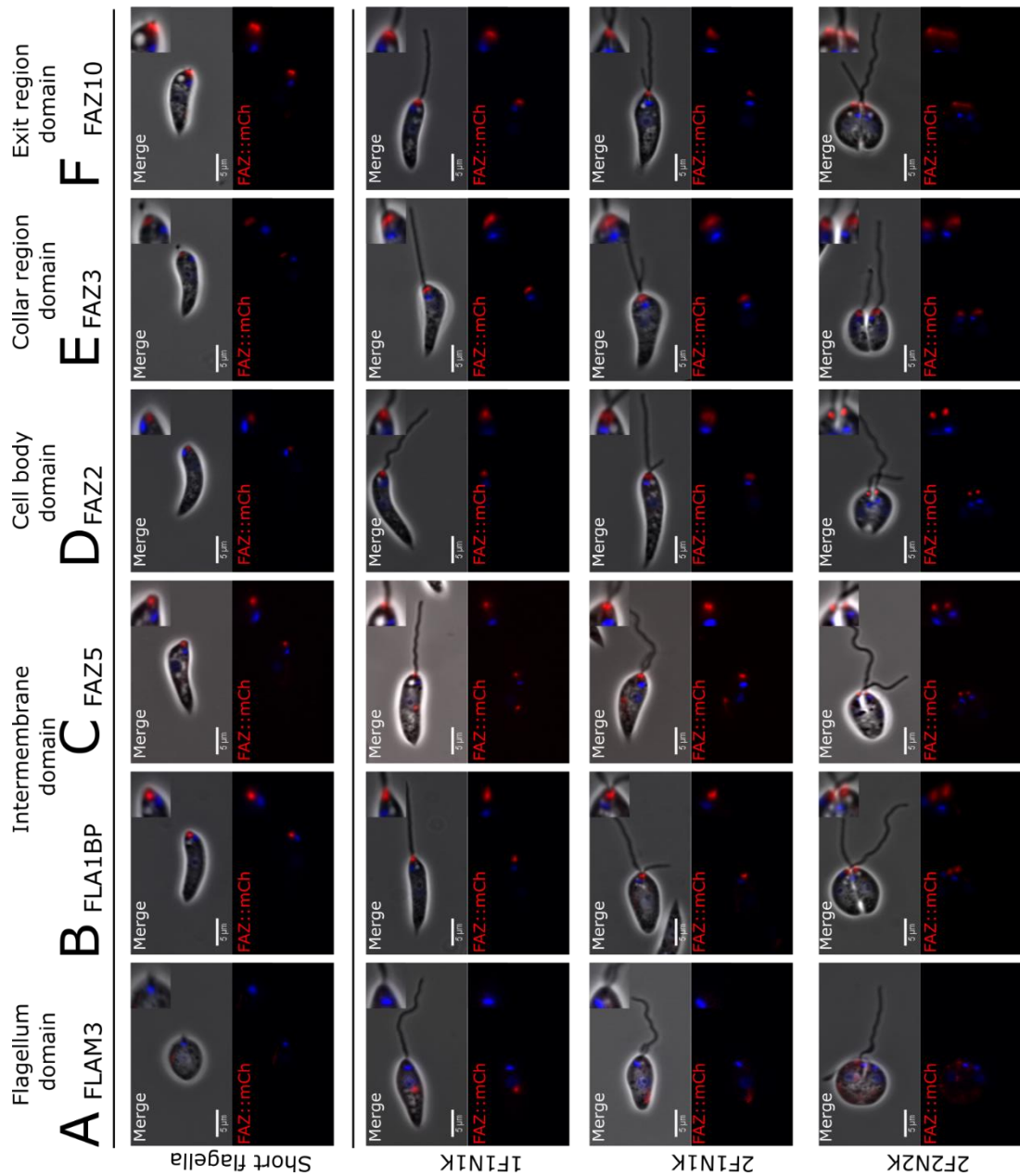


Figure 5.11 Deletion of FAZ34 affected the localisation of flagellum, intermembrane, and cell body FAZ domain proteins. The following proteins A) FLAM3, B) FLA1BP, C) FAZ5, D) FAZ2, E) FAZ3 and F) FAZ10 were tagged with mCherry and transfected into FAZ34 null mutant cell line. Images shown are from short flagella, 1F1N1K, 2F1N1K and 2F2N2K cells. Top- merge containing phase (grey), mCherry (red) and Hoechst 33342 (blue) and bottom- mCherry (red) and Hoechst 33342 (blue) only. Inserts included shows an enlarged image of FAZ region.

5.7 Disruption of FAZ organisation reduces attachment and alters flagellar pocket size and shape

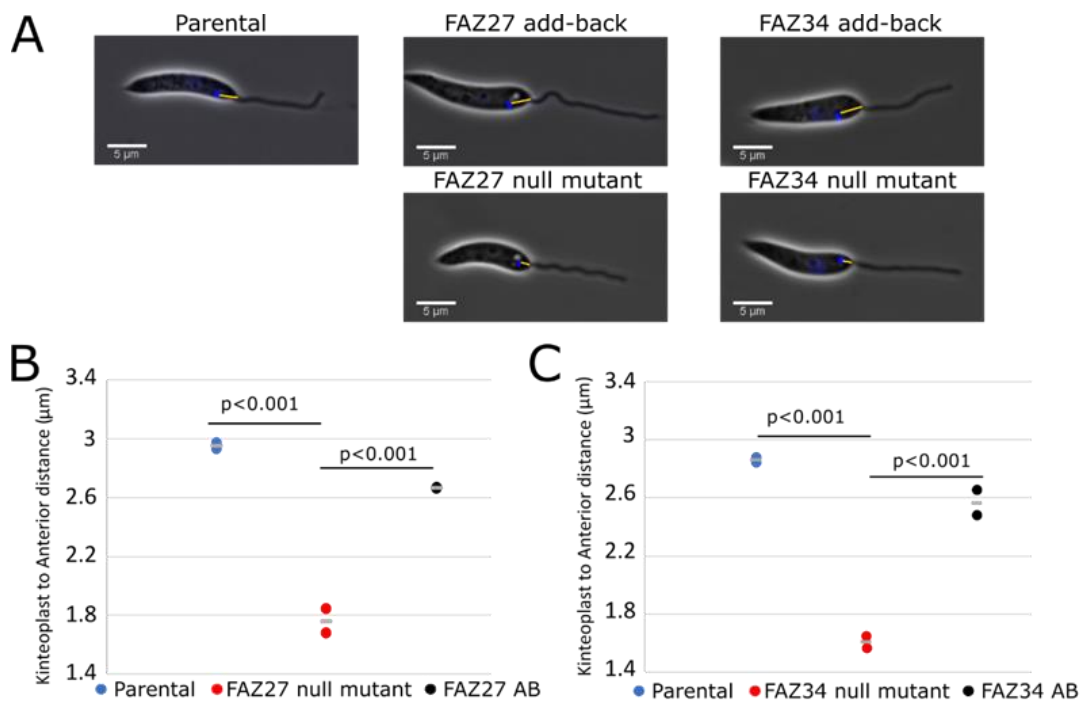
The changes to the flagellum, intracellular, and cell body FAZ in FAZ27 and FAZ34 null mutants could cause a reduction in the size of the attachment interface between the flagellum and the flagellar pocket neck, leading to flagellum loss. Previous studies in FAZ5 and FAZ2 deletion cell lines showed that the flagellar pocket size was reduced (Sunter *et al.*, 2019; Halliday *et al.*, 2020). To assess if FAZ27 and FAZ34 loss caused the same effect, the distance between the kinetoplast and the anterior cell tip was measured. It was previously shown that both null mutants cell body lengths were significantly shorter than the parental and they continued to decrease in size over time. For this reason, all cell lines were assessed at 4 weeks post-storage. Light microscopy appeared to show that the kinetoplast was positioned closer to the anterior cell tip in null mutants compared to the parental and add-backs (**Fig 5.12 A**).

To confirm this, the kinetoplast-anterior cell tip distances were measured in 1F1N1K cells from each cell line and the mean was calculated for each set. The mean distance for the parental cells was 3 μm (**Fig 5.12B& C**). However, the distance in the FAZ27 null mutant was ~ 1 μm shorter, while in the FAZ27 add-back cells the distance was similar to the parental cells (**Fig 5.12B**). The kinetoplast-anterior cell tip distance was also reduced by a similar amount in the FAZ34 null mutant (1.7 μm) with its add-back restoring this distance almost completely (**Fig 5.12C**). The reduction in kinetoplast to anterior cell tip distance as result of FAZ27 and FAZ34 loss suggests that the length of the flagellar pocket was reduced in the null mutants.

To look at the flagellar pocket in more detail, the flagellar pocket markers, LmxM.23.0630 and LmxM.06.0030 were used (Sunter *et al.*, 2019). These markers were expressed with a mCherry tag at their C-terminus in the parental and null mutants. LmxM.23.0630 was localised to the bulbous domain and LmxM.06.0030 was localised to the neck domain in the parental cells as expected (**Fig 5.12D**). In the null mutants, it was consistently observed that LmxM.23.0630 signal was still present, and instead of being located distal of the kinetoplast they appeared adjacent to the kinetoplast (**Fig 5.12D**). However, for LmxM.06.0030, the signal was no longer

seen within the flagellar pocket region of both null mutants (**Fig 5.12D**), indicating that FAZ27 and FAZ34 loss disrupts the flagellar pocket neck region.

Thin section transmission electron microscopy (TEM) was carried out to visualise the flagellar pocket of the FAZ27 and FAZ34 null mutants. ≥ 12 longitudinal images of 1F cells each were analysed. The two-part domain structure of the flagellar pocket, the bulbous lumen, and the neck region were present in FAZ27 and FAZ34 null mutants, but their flagellar pocket length appeared reduced compared to the parental (**Fig 5.13**). This correlates with reduced kinetoplast to anterior length observed by light microscopy. There was less contact between the flagellum and the cell body, particularly in FAZ34 null mutant was also observed, suggesting that the attachment was reduced (**Fig 5.13**).



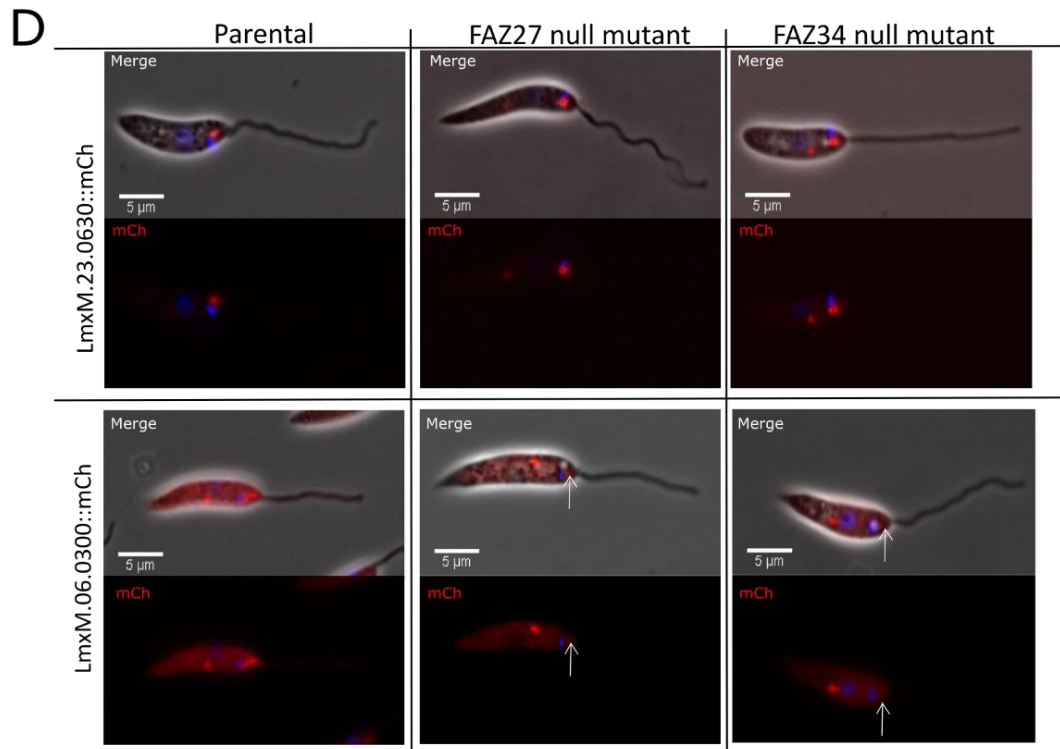


Figure 5.12 FAZ27 and FAZ34 loss disrupted flagellar pocket shape and organisation. A) Example images of kinetoplast to anterior cell tip distances in the null mutants compared to the parental and add-back cells. Distances were measured in ImageJ. Mean kinetoplast to anterior cell tip distances were calculated for B) FAZ27 and C) FAZ34 null mutants which were compared to the parental and add-back cell lines. ≥ 100 1F1N1K cells in duplicates were used to measure the means and p-values were calculated from two sets of lengths together. D) Widefield images showing FP markers tagged with mCherry in parental and null mutants. Top- overlay of phase (grey), Hoechst (Blue) and mCherry (red) combined and bottom- overlay of Hoechst 33342 (blue) and mCherry (red) only.

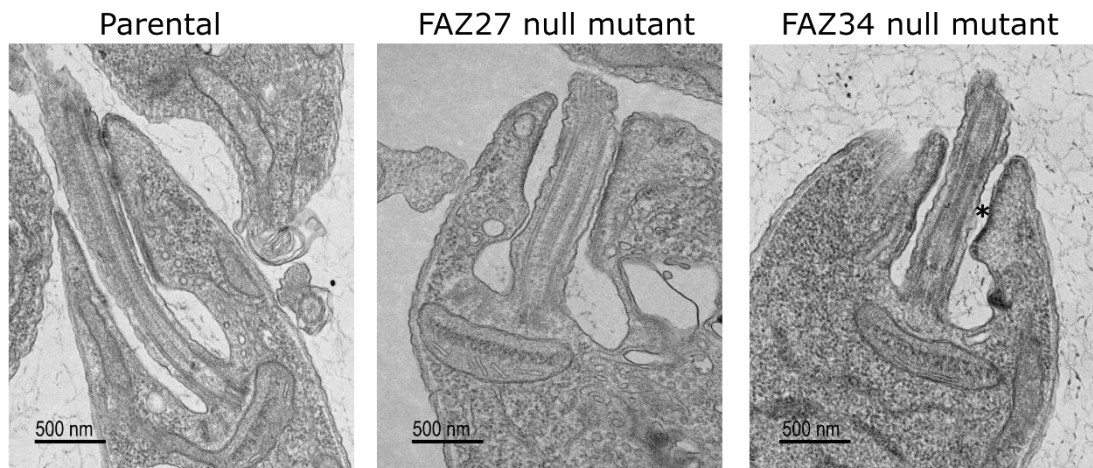


Figure 5.13 Flagellar pocket size and attachment was reduced in FAZ27 and FAZ34 null mutants. Representative TEM images of longitudinal section through the flagellar pocket of a parental cell, FAZ27 and FAZ34 null mutant cells Scale bar is 500 nm. * indicates a loss of contact between flagellum and cell body in FAZ34 null mutant

5.8 Change in FAZ organisation and attachment affected cell motility

The loss of FAZ27 and FAZ34 caused flagellar pocket morphogenesis and flagellum attachment defects, which might also impact cell motility as previously observed for FAZ5 and FAZ2 null mutants (Sunter *et al.*, 2019; Halliday *et al.*, 2020). To assess the effect of FAZ27 and FAZ34 deletion on cell motility, movies of swimming tracks were taken from cell lines 4 weeks post storage. The parental, null mutants and add-backs were tested directly from culture of equal density (1×10^7) and repeated three times.

The tracks and speed/persistence data combined showed that the FAZ27 null mutant were not as directionally progressive as the parental cells. The swimming tracks showed less directional persistence (**Fig 5.14A-C**). While the motility of the FAZ27 add-back was similar to the parental cells (**Fig 5.14A-C**). For the FAZ34 null mutant, the reduction in directional persistence were similar for the FAZ27 null mutant while again the add-back restored the motility almost to parental levels (**Fig 5.15A-C**).

There was a reduction in directional persistence seen in FAZ27 and FAZ34 null mutant which suggests that the mutants had lost their ability to engage in progressive movement as a direct result of FAZ27/FAZ34 loss. These data were collected at the

time when the severity of mutant phenotype was dramatically reduced, with the presence of loose flagella and short flagellum cells becoming rare. This indicates that the result of reduced motility was likely to be caused by changes in the FAZ and associated structures rather than by complete flagellum loss.

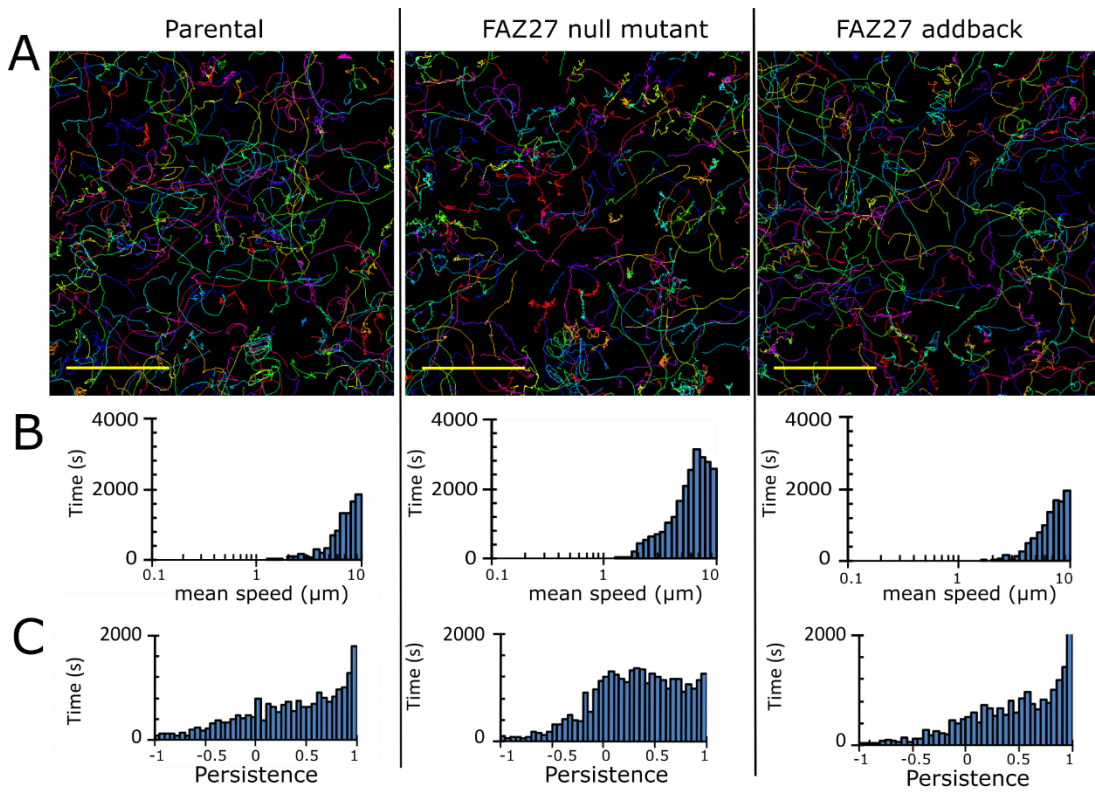


Figure 5.14 FAZ27 loss reduced swimming speed and progressive movement. A) Plots of the swimming tracks for the parental, FAZ27 null mutant and FAZ27 add-back cells (Scale bar, 100 μm). B) Histograms of the mean speed and C) directional persistence. This was repeated three times and data shown are representative of one experiment.

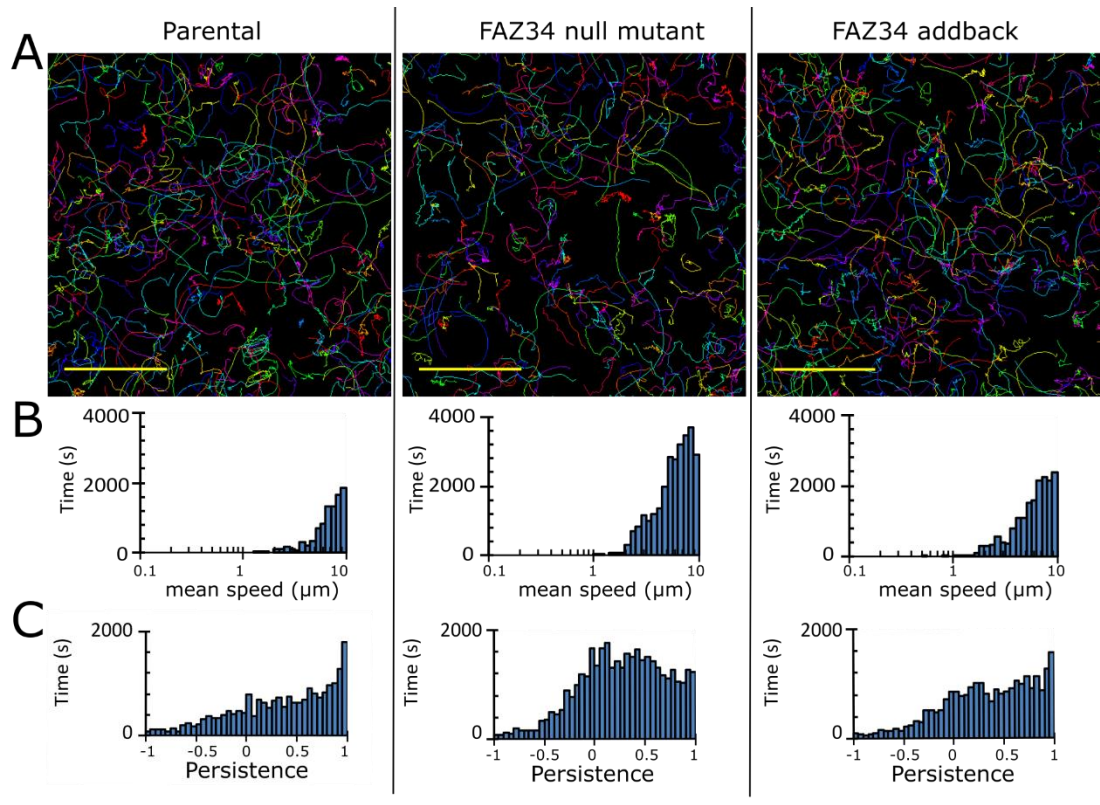


Figure 5.15 FAZ34 loss reduced swimming speed and progressive movement. A) Plots of the swimming tracks for the parental, FAZ27 null mutant and FAZ27 add-back cells (Scale bar, 100 μm). B) Histograms of the mean speed and C) directional persistence. This was repeated three times and data shown are representative of one experiment.

5.9 Discussion

The discoveries of FAZ27 and FAZ34 as Class I proteins within the FAZ flagellum domain in *L. mexicana* offered the opportunity to explore the role of Class I proteins within the FAZ structure and the overall flagellar pocket architecture. With this specific part of the FAZ complex not being investigated before, the results of this study opened new insights into the importance of the FAZ for flagellum attachment and maintenance of flagellar pocket shape in *L. mexicana*.

5.9.1 FAZ has a key role in flagellum attachment

FAZ27 and FAZ34 loss resulted in the disruption of FAZ molecular structure (**Fig 5.16**). The losses of these flagellum domain proteins affected the localisation of other proteins from this domain as well as the cell body and intracellular domains proteins. The flagellum domain protein FLAM3 was mislocalised and absent in FAZ27 and FAZ34 null mutants, respectively (**Fig.5.16B&C**). It shows that while correct FLAM3 localisation relies on the presence of both, FAZ27 and FAZ34, its recruitment is dependent on FAZ34. This shows a hierarchy of assembly of FAZ34 being required for FLAM3 assembly. This differs to what was seen for *T. brucei*, which demonstrated that FAZ27 and FLAM3 are interdependent for assembly to the FAZ (An *et al.*, 2020). In the null mutants, the cell body and intracellular proteins FAZ2, FAZ5 and FLA1BP did not have clear linear signals which indicates their assembly is dependent on the correct assembly of FAZ27 and FAZ34 (**Fig.5.16B&C**).

The reduced length of the linear FAZ from all three structural domains as observed by light microscopy and TEM potentially explains the weakened flagellum attachment as there is a reduced attachment area that can now more easily break with the mechanical stress induced during vortex. Slender-body theory shows that lateral movement by shear forces increase with length (Batchelor, 1970). A longer flagellum therefore experiences more drag and hence the point of attachment to the cell experiences a greater force. This could explain why longer flagella are more breakable. An alternative hypothesis is that as the flagella length continue to grow over several cell cycles and therefore length is an indication of age, the accumulation

of FAZ damage could build overtime leading to an increasing likelihood of flagella breaking off.

5.9.2 FAZ organisational structure is important for flagellar pocket shape

The reduction in kinetoplast to anterior distance combined with the re-positioning of the bulbous lumen marker demonstrates that FAZ27 and FAZ34 are important for flagellar pocket morphogenesis. The further observation of the flagellar neck marker being absent, probably caused by the disruption of the neck region as indicated by FAZ signal length and TEM, suggests that the flagellum domain is important for the organisation of the flagellar pocket. This is supported by TEM images which showed a reduction in flagellar pocket length which correlated with the reduced length of Class I and II proteins in FAZ27 and FAZ34 null mutants (**Fig 5.16B&C**).

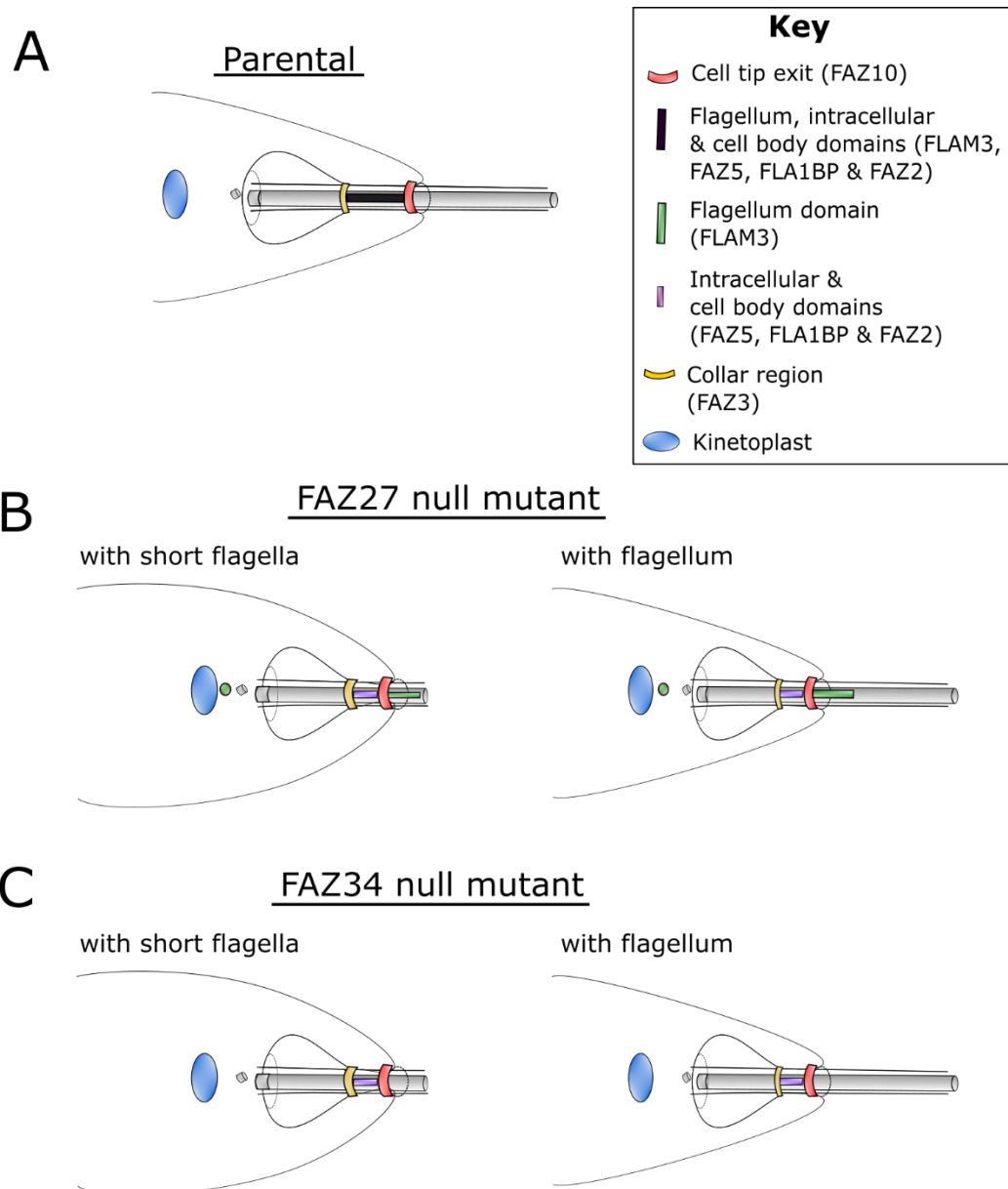


Figure 5.16 FAZ molecular structure is disrupted in FAZ27 and FAZ27 null mutants.

Organisation of FAZ domains in 1F1N1K with short and long flagellum cells of A) the parental, B) FAZ27 null mutant and C) FAZ34 null mutant. The following proteins FLAM3 (Class I on flagellum side), FLA1BP and FAZ5 (intracellular proteins), FAZ2 (cell body), FAZ3 (Class III, distal to collar) and FAZ10 (Class IV, exit) were used for the all cell lines.

5.9.3 FAZ attachment and flagellar pocket shape is important for directional movement

The motility analysis demonstrated that the deletion of FAZ27 and FAZ34 caused a reduction in directional persistence and importantly this was not due to examining cells without a flagellum as this cell type only made up a small proportion of the population when this analysis was performed. FAZ5 deletion, which demonstrated a motility phenotype of little processive movement, similar to FAZ27 and FAZ34 deletion was found to have a lack of coordination in flagellum beating (Sunter *et al.*, 2019). Though not tested here, but this could be an explanation to FAZ27 and FAZ34 reduced directional movement. Studies on FAZ2 and FAZ5 also found that flagellar pocket shape is important for motility (Sunter *et al.*, 2019; Halliday *et al.*, 2020). Moreover, for FAZ2 and FAZ5 null mutants, reduced motility was found to affect proliferation and development in sandfly (Sunter *et al.*, 2019; Halliday *et al.*, 2020). This has not been tested for FAZ27 and FAZ34 null mutants; however, it is likely a similar effect would be seen. Equally, the effect of flagellar pocket disruption on its function as a site of endocytosis/exocytosis for nutrient uptake, immune evasion and secretory pathway, important for pathogenicity was not tested. The FAZ5 null mutant showed a reduction in endocytosis and demonstrated a connection between flagellar pocket architecture and nutrient uptake, which affected the parasites ability to persist in mice (Sunter *et al.*, 2019). A similar phenotype in the case of the FAZ27 and FAZ34 null mutants could not be ruled out.

5.9.4 FAZ27 and FAZ34 function is similar to FLA1BP and FAZ5

Work described in Chapter 4 revealed a similarity in phenotype between the FAZ27, FAZ34 and FLA1BP null mutants, with loose flagella and short flagellum cells. This work described in chapter 4 demonstrated that this phenotype was a consequence of flagellum loss caused by a reduction in attachment in FAZ27 and FAZ34 null mutants, indicating that FAZ27 and FAZ34 are important for flagellum attachment. Furthermore, it is therefore likely that FLA1BP also shares a role in flagellum attachment.

FAZ27 and FAZ34 null mutants had a shorter cell body length, similar to the FLA1BP null mutant (**Chapter 4**), which shows their function in cell morphogenesis. This decrease in cell body length correlated with the increasing growth rate, which suggests this could be a modification to allow faster growth. A role for both flagellum attachment and cell morphogenesis have parallels to what has been seen for FAZ27 and FLA1BP in *T. brucei*. The knockdown of FAZ27 and FLA1BP caused a reduction in FAZ and cell body length, changes from trypomastigote to epimastigote morphology and flagellum detachment (Sun *et al.*, 2013; An *et al.*, 2020). This shows that proteins within the flagellum and flagellar membrane domains of the FAZ in both species are comparable in terms of importance for cell morphology and flagellum attachment.

Another intracellular protein, FAZ5 from the cell body side also had a similar phenotype in *L. mexicana* of flagellum loss (short flagellum cells and loose flagella) and shorter cell length (**Chapter 4**). However, a study on FAZ5 deletion in *L. mexicana* by Sunter and colleagues did not observe short flagellum cells and loose flagella (Sunter *et al.*, 2019). This difference could potentially be explained by the phenomenon of null mutant phenotype changing over time as seen with FAZ27, FAZ34 (this chapter) and CC2D (**Chapter 6**) null mutants. Here, the impact of FAZ5 deletion on flagellum loss was lower than compared to FAZ27, FAZ34 and FLA1BP (**Chapter 4**), so this phenotype would have become more subtle over time. This also reflects the hierarchy of FAZ protein importance for flagellum attachment and cell morphogenesis, where flagellum domain proteins have higher importance while intracellular proteins particularly cell body membrane have less impact.

Chapter 6

Class II protein CC2D is required for flagellum attachment and anterior cell tip morphogenesis

6.1 Preface

In the localisation screen (Chapter 3) CC2D was identified as cell body domain protein (Class II localisation), with a linear signal within the flagellar pocket neck. CC2D is one of four proteins (FAZ2, FAZ5 and FAZ28/30) in this domain.

Recent studies of FAZ2 and FAZ5 in *L. mexicana* showed some differences. FAZ5, an intracellular domain protein within the cell body was shown to be critical for maintaining the flagellar pocket shape and pathogenicity (Sunter *et al.*, 2019). While, FAZ2, a FAZ protein within the cell body domain was shown to be important for anterior cell tip morphogenesis in *Leishmania* (Halliday *et al.*, 2020). However, work described in Chapter 4 showed that the deletion of CC2D resulted in cells with a shorter cell body and loose flagella along with flagellum-to-flagellum connections. This demonstrates CC2D is potentially important for both roles, maintaining the flagellar pocket shape and anterior cell tip morphogenesis. The function of FAZ2, FAZ5 and CC2D orthologs have been studied in *T. brucei*. FAZ2 and CC2D knockdown caused full length flagellum detachment and cell death (Zhou *et al.*, 2011; Q. Zhou *et al.*, 2015). FAZ5, an intracellular domain protein knockdown resulted in loops of detached flagella at the proximal end of the flagellum (Sunter *et al.*, 2015).

As the *L. mexicana* FAZ organisation is different to that of *T. brucei*, and with the role of Class II being more diverse in *L. mexicana* (Wheeler, Sunter and Gull, 2016; Sunter *et al.*, 2019; Halliday *et al.*, 2020), CC2D protein was therefore an excellent candidate to explore more about the function of Class II FAZ proteins and their contribution to the FAZ and flagellar pocket structures.

6.2 Phenotype of CC2D null mutant changes over time

To ensure the phenotype previously seen in the deletion screen (Chapter 4) was reproducible, the CC2D null mutant cell line was re-generated using the C9/T7 parental cell line. The new CC2D null mutant grew back after the same length of time as the previous null mutant, ~10 days post-transfection and PCR was carried out to confirm the deletion of CC2D (**Fig 6.1A-C**). The CC2D null mutant had the same phenotype as previously observed with loose flagella, cells with a short flagellum and flagellum-to flagellum connections that are atypical in *L. mexicana* parental cells (**Fig 6.1D**).

During the observations of CC2D null mutant over time post-transfection, it was noticed that like FAZ27 and FAZ34 null mutants (Chapter 5) the mutant phenotype appeared to change. The study of FAZ27 and FAZ34 null mutants showed that mutant phenotype severity reduced with time. To assess if this also applied to the CC2D null mutant, the re-generated CC2D null mutant alongside the parental cell line were taken out of liquid nitrogen storage at the exact same time for investigation. The CC2D null mutant cell line was previously split once and frozen within three days of cell growth post-transfection (**Fig 6.1A**). To ensure an accurate and fair assessment of these cells, they were analysed at the same time point, in duplicates, every week over a period of 4 weeks (labelled as week 1, 2, 3 and 4) (**Fig 6.1A**).

To analyse cell growth, the cell counts of the CC2D null mutant and parental cell lines were recorded at the same time point from the set density of 1×10^6 /ml every 24 hours during a 72-hour period in week 1 and 4 (**Fig 6.2A**). To assess if any growth rate change over time the doubling time was calculated from the average 24-hour growth peak from three 24-hour periods within 72-hours in week 1 and week 4. The parental doubling time was 5.81 hours in week 1 and 5.66 hours in week 4. This showed that parental growth rate only changed slightly during the 4 week period. For the CC2D null mutant, the doubling time was much slower, 9.43 hours in week 1. However, in week 4, the doubling time reduced by 1.3 hours to 8.1 hours (**Fig 6.2A**). The reduction in doubling time for CC2D null mutant at week 4 showed that the growth rate increased during the first four weeks post-transfection.

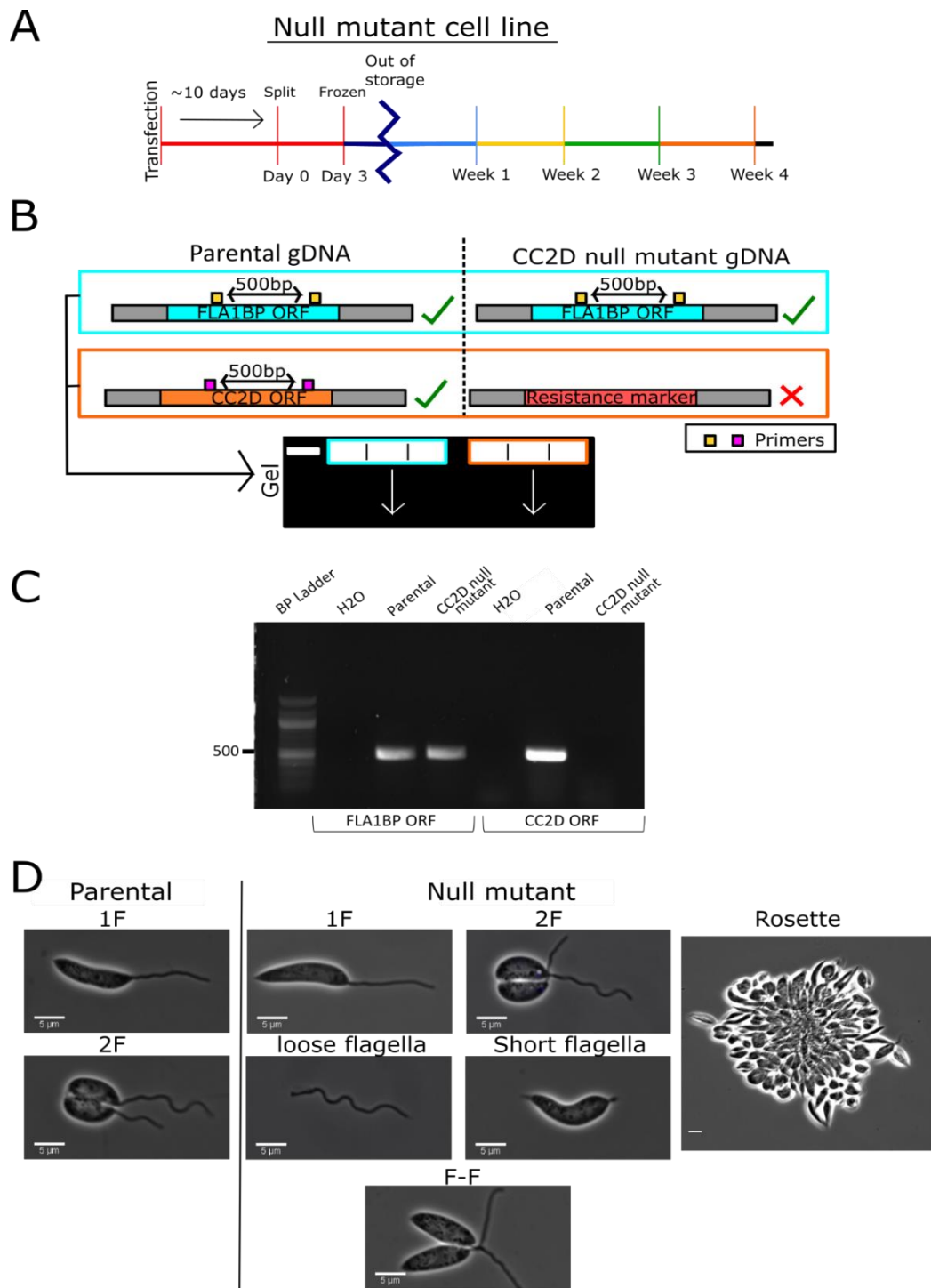


Figure 6.1 CC2D null mutant was successfully re-generated. A) Timeline of null mutant life, which started from transfection with the null mutants growing back after ~10 days and stored within 3 days of growth. Post-storage CC2D null mutant was analysed at weeks 1, 2, 3 and 4. B) Schematic of PCR and gel layout to confirm gene deletion. C) Gel showing the confirmation of CC2D deletion. D) Re-generated CC2D null mutant presented mutant phenotypes seen previously, loose flagella, short flagellum cells, cells with flagellum to flagellum (F-F) connections and rosettes

For further analysis, these cell lines were imaged directly from cell culture to measure the cell types observed. To determine whether there were changes in the cell cycle, the cell cycle position defined by their K/N/F status from each cell line was also captured and recorded at the same time. In the parental cell line, for cells directly imaged from culture there was an increase in 1F cells from week 1 to week 4, while 2F cells decreased from week 1 to week 4 (**Fig 6.2B&C**). The analysis of cell cycle position demonstrated that the decrease in 2F cells was exclusively in the 2F1N1K cell type, with the mean reduced from 19.3% in week 1 to 14.3% in week 4 (**Fig 6.2C**). This reduction in 2F cells, and more specifically in 2F1N1K suggests that less time was spent in this configuration.

In the CC2D null mutant cell line, when analysed directly from cell culture, the percentage of loose flagella reduced steadily from 15.2% and 11.1% in week 1 to 8.8% and 9.4% in week 4 (**Fig 6.2D**). Cells with a short flagellum reduced substantially from 21.2% and 17.5% in week 1 to 1.5% and 1.9% in week 4 (**Fig 6.2D**). While 2F cells and rosettes remained constant throughout the 4 week period, 1F cells increased from 43.9% and 42.9% in week 1 to 58.8% and 62.3% in week 4. Interestingly, flagellum-to-flagellum connections increased from 4.5% and 9.5% in week 1 to 10.3% and 18.9% in week 4 (**Fig 6.2D**).

A similar trend for loose flagella, short flagellum and F-F cells was seen in the K/N/F counts analysis (**Fig 6.2E**). 1F cells increased steadily from week 1 to week 4. (**Fig 6.2E**). 2F1N1K-2F2N2K configurations remained constant throughout while loose flagella and short flagellum cells decreased to low proportions by week 4 (**Fig 6.2E**). F-F connections steadily increased from ~2% to ~6% average over the 4 weeks (**Fig 6.2E**). Imaging of the cells for this cell cycle analysis involved a number of washes and centrifugation steps, which might break the F-F connections resulting in a lower number of this cell type in comparison to the analysis of cells direct from culture.

The growth rate and cell type analysis showed the phenotype changed over time with number of loose flagella and short flagellum cells decreasing, similar to FAZ27 and FAZ34 null mutants (Chapter 5), while the presence of the F-F connection became more common.

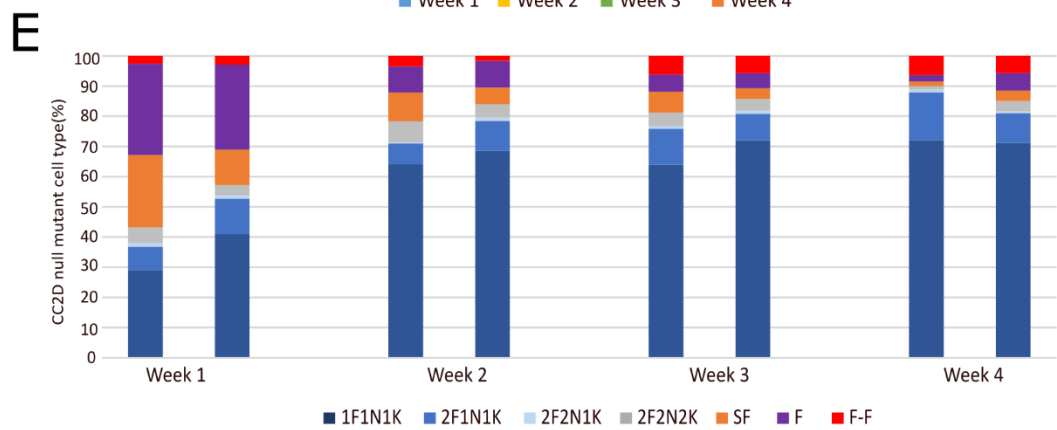
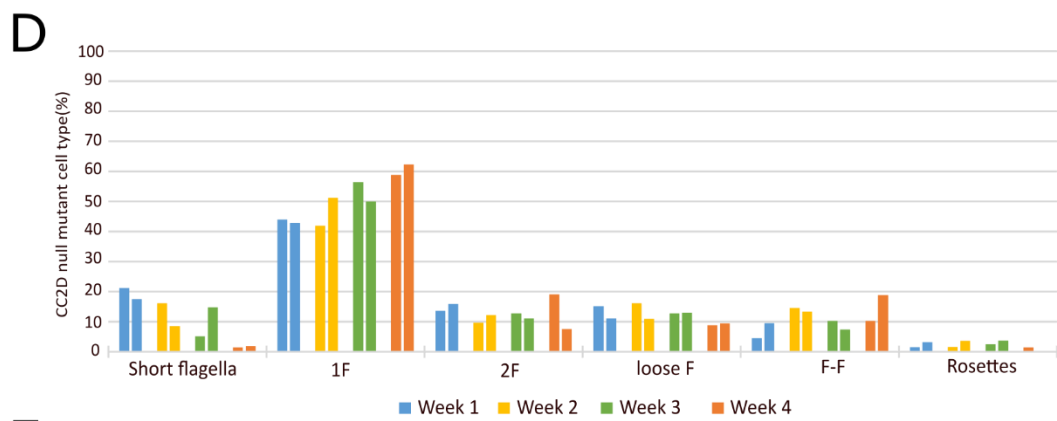
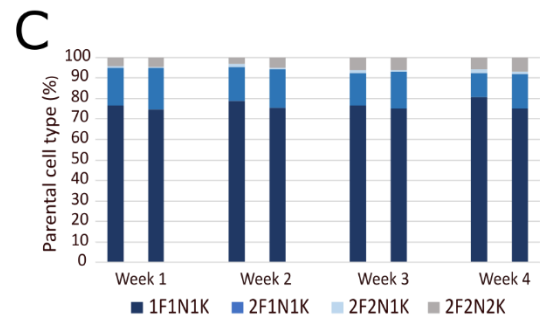
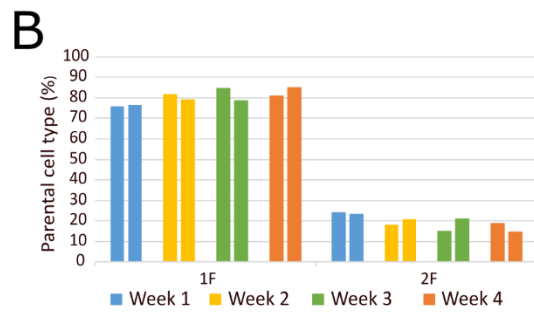
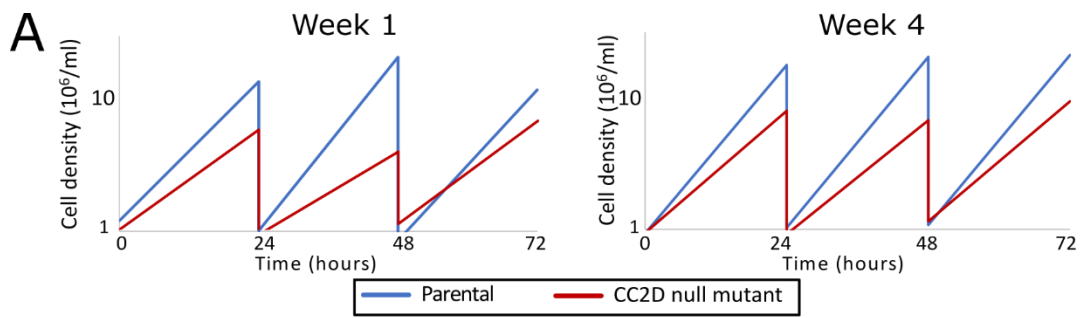


Figure 6.2 Change in CC2D null mutant phenotype occurs over time. A) Growth curves for CC2D null mutant recorded in week 1 and 4, B) % of cell types seen in culture for parental. C) % of cell cycle counts for parental. D) % of cell types seen in culture for CC2D null mutant. E) % of cell cycle counts for CC2D null mutant. SF- short flagellum, F- loose flagella, F-F- flagellum-to-flagellum connections.

It was demonstrated that for CC2D null mutant mutants, the phenotype changes over-time with an increase in F-F connections. As the CC2D null mutant had a disrupted cell cycle and morphological defects, the next step was to investigate the morphology in detail. To assess this, the morphology was analysed by measuring flagellum and cell body lengths of 1F1N1K cells (**Fig 6.3A**), which were captured at the same time point, in duplicates on the weekly basis over the same 4 week period. The mean of both set of lengths were calculated for both groups of 90-100 1F1N1K cells from each week.

For the parental cell line the mean flagellum length ranged from 13.2 - 13.7 μm (**Fig 6.3B**) and for the cell body length, the mean ranged from 13.0 - 13.3 μm (**Fig 6.3C**). These narrow ranges with no distinctive pattern showed that there were no significant changes in flagellum and cell body lengths of the parental cell line over this time period.

The CC2D null mutant mean flagellum lengths ranged from 12.8 - 14.3 μm with no pattern of increase or decrease (**Fig 6.3D**). For the cell body lengths, a lower mean range of 11.1 - 11.8 μm was measured compared to the parental, suggesting that CC2D is important for cell morphogenesis. However, unlike FAZ27 and FAZ34 null mutants (chapter 5), there was with no change over time in cell body length, which remained shorter than the parental cell (**Fig 6.3E**). The distribution of cell body lengths confirmed there was no correlation in length versus time (**Fig 6.3E**).

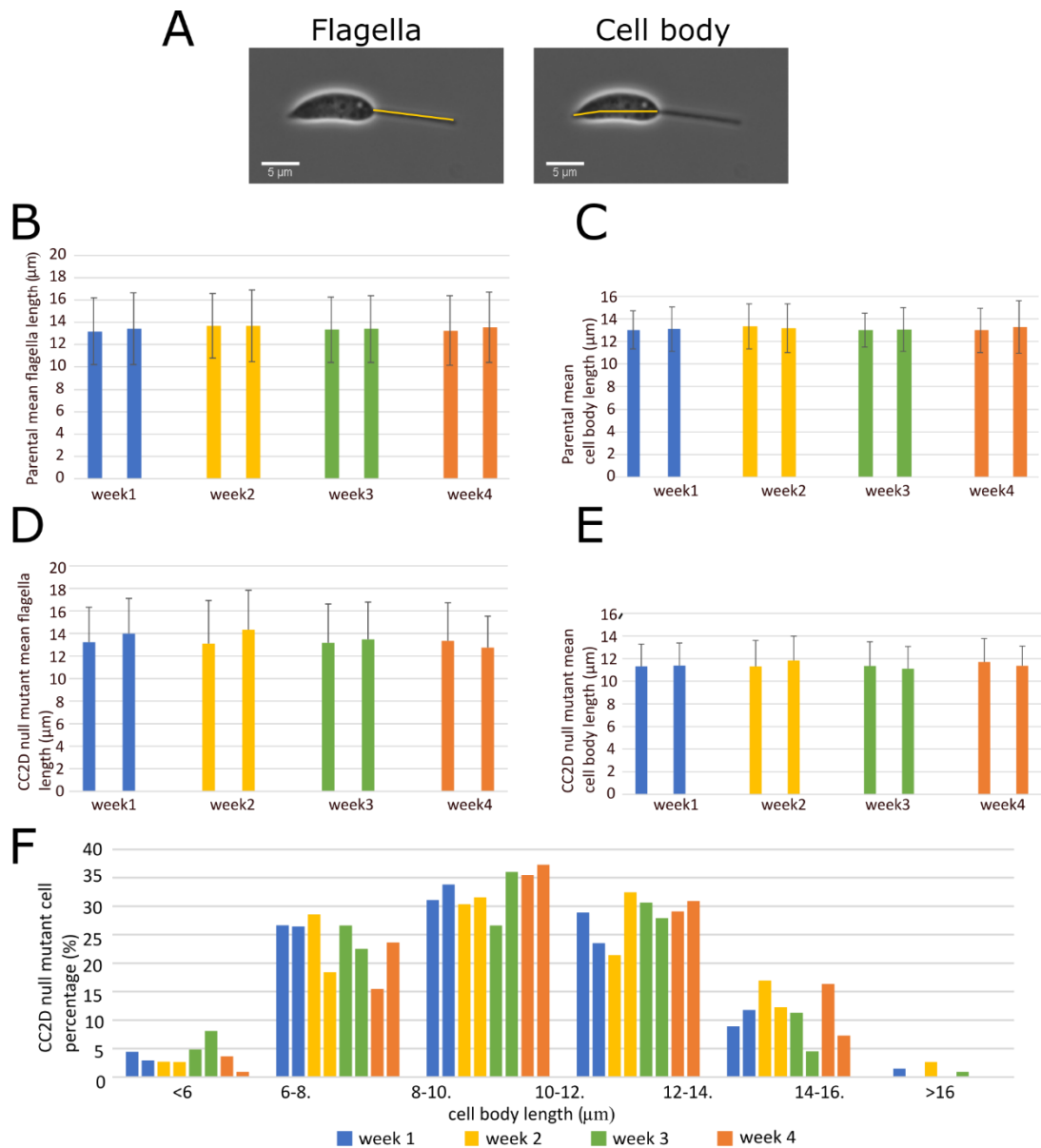


Figure 6.3 No morphological changes were detected in CC2D null mutant over time.

A) Example measurements for flagellum (proximal to distal tip) and cell body (posterior to anterior cell tip). B) Mean flagellum lengths in Parental. C) Mean cell body lengths in Parental. D) Mean flagellum lengths in CC2D null mutant. E) Mean cell body length in CC2D null mutant. F) Cell body length distribution in CC2D null mutant.

6.3 Flagellum in CC2D null mutant was hard to detach by shear force, but the likelihood increased with length

An explanation for the presence of loose flagella and cells with a short flagellum in the FAZ27 and FAZ34 null mutants was a weakened flagellum attachment that was more readily broken due to the mechanical stress of the flagellum beating, releasing the flagellum as shown by the differences between loose flagella/short flagellum cells before and after 30s of vortexing (chapter 5).

As previously shown, the CC2D null mutant had a greater number of detached loose flagella in week 1, so for an extreme test of 'flagella loss' these cell lines were assessed in week 1 after defrosting. Images were captured prior to vortex and again after 30s of vortexing to measure and compare the cell types observed.

As a control, the parental cell line was used, and it was observed that the proportion of cell types consisting of 1F (~75%) and 2F (~25%) cells did not change before and after 30s of vortex (**Fig 6.4A**). For the CC2D null mutant, the proportion of 1F cells did not change after 30s vortex, which was paired with no to little increase in short flagellum cells and loose flagella (**Fig 6.4B**). For short flagellum cells, the proportions were similar, 21.2% and 18.7% seen at rest and after vortexing, respectively, while loose flagella levels were 15.2% and 17.3% at rest and after vortexing, respectively (**Fig 6.4B**). This suggests that the flagellum in the CC2D null mutant was not readily detached by shear force, unlike FAZ27 and FAZ34 null mutants. However, the proportion of F-F cells was 4.6% at rest and 1.3% after vortexing, which suggested the F-F connection was disruptable by shearing. (**Fig 6.4B**).

The results demonstrated that the flagellum was not easily detached in the CC2D null mutant, but the flagellum length may still play a role in the loose flagella phenotype as witnessed in FAZ27 and FAZ34 null mutants (Chapter 5). To assess if this is the case, the relationship between flagellum length and loose flagella was analysed by measurements of loose and attached flagellum length in 1F1N1K cells. Previously, it was shown that in week 1 there were higher levels of loose flagella with little change in 1F flagellum length. This provided a reliable and consistent set of images to

measure the loose flagella and attached flagellum lengths (**Fig. 6.4C-D**). In the CC2D null mutant, the mean lengths for loose flagella were 17.5 μm and 16.9 μm , which was significantly higher than the attached flagella (13.3 μm and 14 μm) (**Fig 6.4C**). The histogram shows that longer lengths $\geq 18 \mu\text{m}$ were associated with loose flagella, while shorter lengths $\leq 10 \mu\text{m}$ were only seen for attached flagella (**Fig 6.4D**). This suggests that increasing flagellum length plays a role in loose flagella presence.

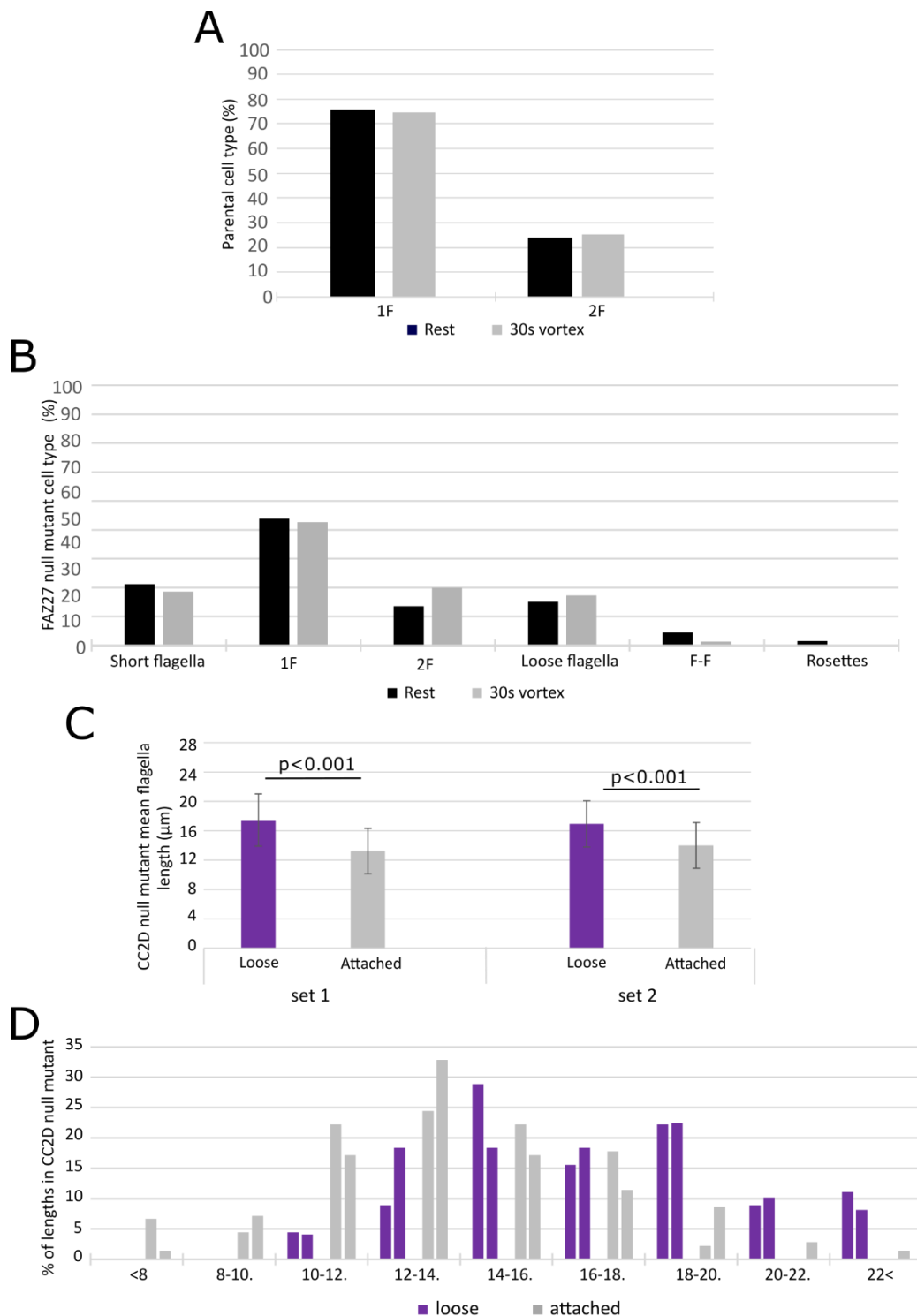


Figure 6.4 Loose flagella are longer than the attached flagella in CC2D null mutant.

% of cell types measured at rest and after 30s vortex in A) Parental, B) CC2D null mutant. 1 ml of cell lines were tested in 1.5 ml Eppendorf tubes and each experiment was performed in duplicate shown here. The representative data from one experiment is shown, C) Mean length for loose vs attached flagella in CC2D null mutant and D) Histogram of loose and attached flagellum lengths in FAZ27 null mutant. The mean flagellum length was calculated from loose flagella and attached flagella measurements.

6.4 Add-back of *CC2D* gene confirms CC2D null mutant phenotype was directly related to CC2D deletion

To confirm the mutant phenotype of loose flagella and cells with a short flagellum and F-F connections was the consequence of CC2D deletion, an add-back cell line was generated. The add-back construct was created by cloning the CC2D ORF into a constitutive expression plasmid (See section 2.2.4 for the generation of FAZ add-back plasmids). The add-back plasmid was transfected into CC2D null mutant cell line, with the add-back cell line growing back 10 days post transfection, before being split once and frozen within 3 days (**Fig 6.5A**). The add-back cell line expressed CC2D tagged at the N-terminus with mNG fluorescent protein. On inspection by microscopy, the mNG tagged CC2D protein in the add-back cells was observed at the FAZ throughout the cell cycle as expected (**Fig 6.5B**).

To check that the add-back cell lines restored the parental phenotype, the parental, CC2D null mutant and CC2D add-back cell lines were compared. As previously shown, the mutant phenotype was at its least severe in week 4 post storage and with the add-backs having gone through additional selection pressures it was logical to measure the true extent of the FAZ gene add-back in restoring the parental phenotype when all cell lines were 4 weeks post-storage. These cell lines were imaged directly from cell culture to assess the levels of cell types observed.

For the CC2D add-back, loose flagella, short flagellum cells and cells with F-F connections were no longer seen. 1F and 2F cells were restored to similar levels seen

in the parental (**Fig 6.5C**). This demonstrated that the add-back of the CC2D protein restored the parental phenotype, indicating that the phenotype observed was the consequence of CC2D loss. This also confirmed that tag did not interfere with CC2D function.

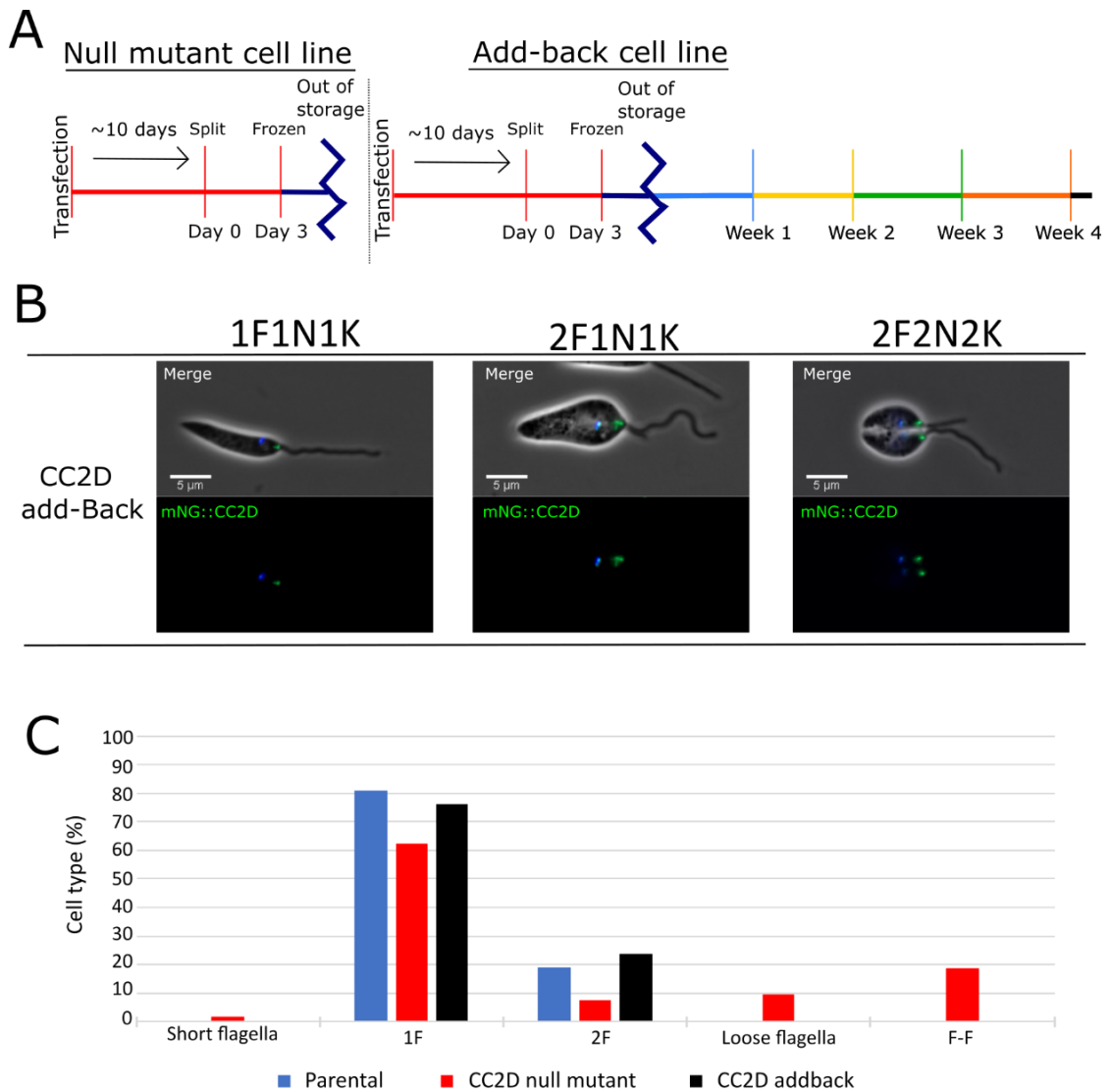


Figure 6.5 CC2D null mutant phenotype was the consequence of CC2D deletion. A)

A time-line of add-back life, which started with transfection to generate null mutant cell lines. Post-storage transfection occurred to generate add-back cell lines. Post-storage add-backs were analysed at week 4. B) CC2D add-back tagged with mNG were observed with linear signal in the FAZ region throughout the cell cycle. C) Quantitation of cell types observed in parental, CC2D null mutant and CC2D addback in week 4. Each experiment was performed in duplicate and the representative data from one experiment is shown.

6.5 The deletion of CC2D disrupts FAZ organisation

CC2D deletion resulted in loose flagella and short flagellum cells likely caused by the flagellum becoming detached, indicating that the role of the FAZ role in maintaining flagellum attachment was impacted. To understand the causes of phenotype, the molecular structure of the FAZ was investigated. The FAZ contains different domains that include the flagellum, intracellular and cell body domains and horseshoe/ring at the collar and exit regions, proteins that localise to these domains were tagged with mCherry fluorescent protein in CC2D null mutant and imaged for comparison with the parental for any changes. The following proteins were chosen to represent each class; FLAM3 for the flagellum side, FLA1BP and FAZ5 for the flagellum and cell body side of intracellular membrane domain respectively, FAZ2 for the cell body side, FAZ3 for the collar class and FAZ10 for the exit class (**Fig 6.6A-F**).

The short flagellum cells were compared to 1F1N1K cells for changes, which could give an insight to the source of flagellum loss. For the CC2D null mutant, in cells with a short flagellum and 1F, instead of expressing a linear localisation parallel to the cell body domain as seen in the parental cells, FLAM3 was mis-localised to the distal end of the flagellum side of the FAZ and extended beyond the anterior cell tip (**Fig 6.7A**). FLAM3 signal was also seen at the kinetoplast in 1F1N1K configuration but disappeared by 2F2N2K/F-F configuration (**Fig 6.7A**). The intracellular proteins, FLA1BP and FAZ5 also followed this pattern, where a long signal was seen within the flagellum beyond the anterior cell tip but no signal at the kinetoplast was seen (**Fig 6.7B&C**). In both short flagella and 1F1N1K cells, FAZ2 was stub-like, at the anterior tip of the cell body with an additional cytoplasmic signal, which remained throughout the cell cycle (**Fig 6.7D**). This suggests that not all of FAZ2 was integrated into a shorter FAZ. Meanwhile FAZ3 and FAZ10 signals showed no change with their ring/horseshoe signals at the collar region and exit point, respectively in both short flagellum and 1F1N1K cells (**Fig 6.7E&F**). These FAZ3 and FAZ10 signals were consistent throughout the cell cycle with similar pattern to those seen in the parental (**Fig 6.7E&F**). Throughout the cell cycle, FLAM3, FLA1BP and FAZ5 remained beyond the anterior cell tip and appeared within the F-F connection region of dividing cells (**Fig 6.7A-C**).

This demonstrates that CC2D deletion caused the mis-localisation of Class I protein FLAM3 on the flagellum side and intracellular proteins FLA1BP and FAZ5, which appeared to mediate the F-F connection. A similar phenomenon was seen in FAZ2 null mutants (Halliday *et al.*, 2020).

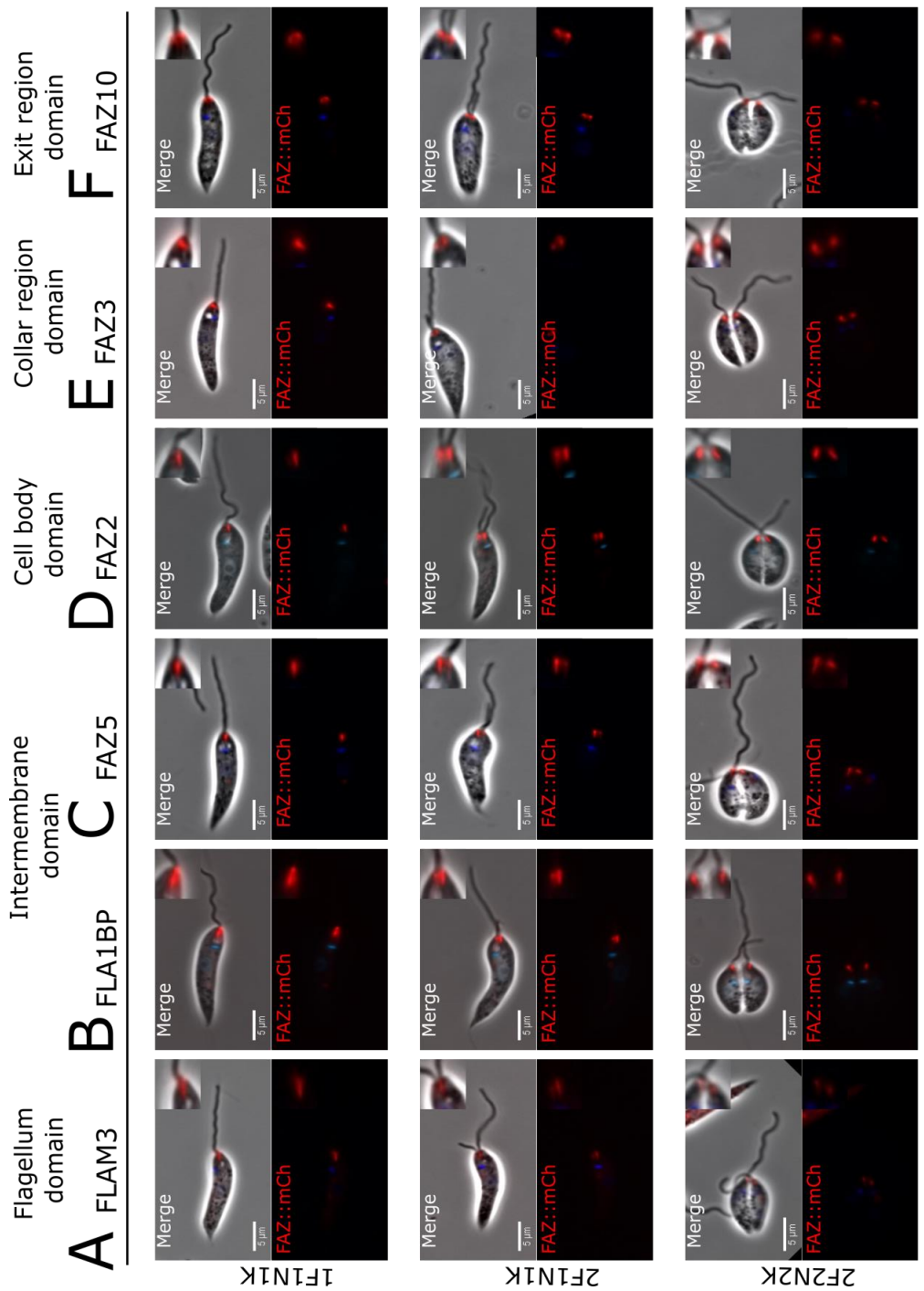


Figure 6.6 Localisations of six proteins represents different domains in the parental cell line. This figure was reproduced from Figure 5.9 in Chapter 5 for clarity here. A) The following proteins, A) FLAM3, B) FLA1BP, C) FAZ5, E) FAZ2, F) FAZ3 and G) FAZ10 were tagged with mCherry and transfected in C9/T7 cell line. Images shown are from 1F1N1K, 2F1N1K and 2F2N2K stages of the cell cycle. Top- merge containing phase (grey), mCherry (red) and Hoechst 33342 (blue) and bottom- mCherry (red) and Hoechst 33342 (blue) only. Inserts included shows an enlarged image of FAZ region.

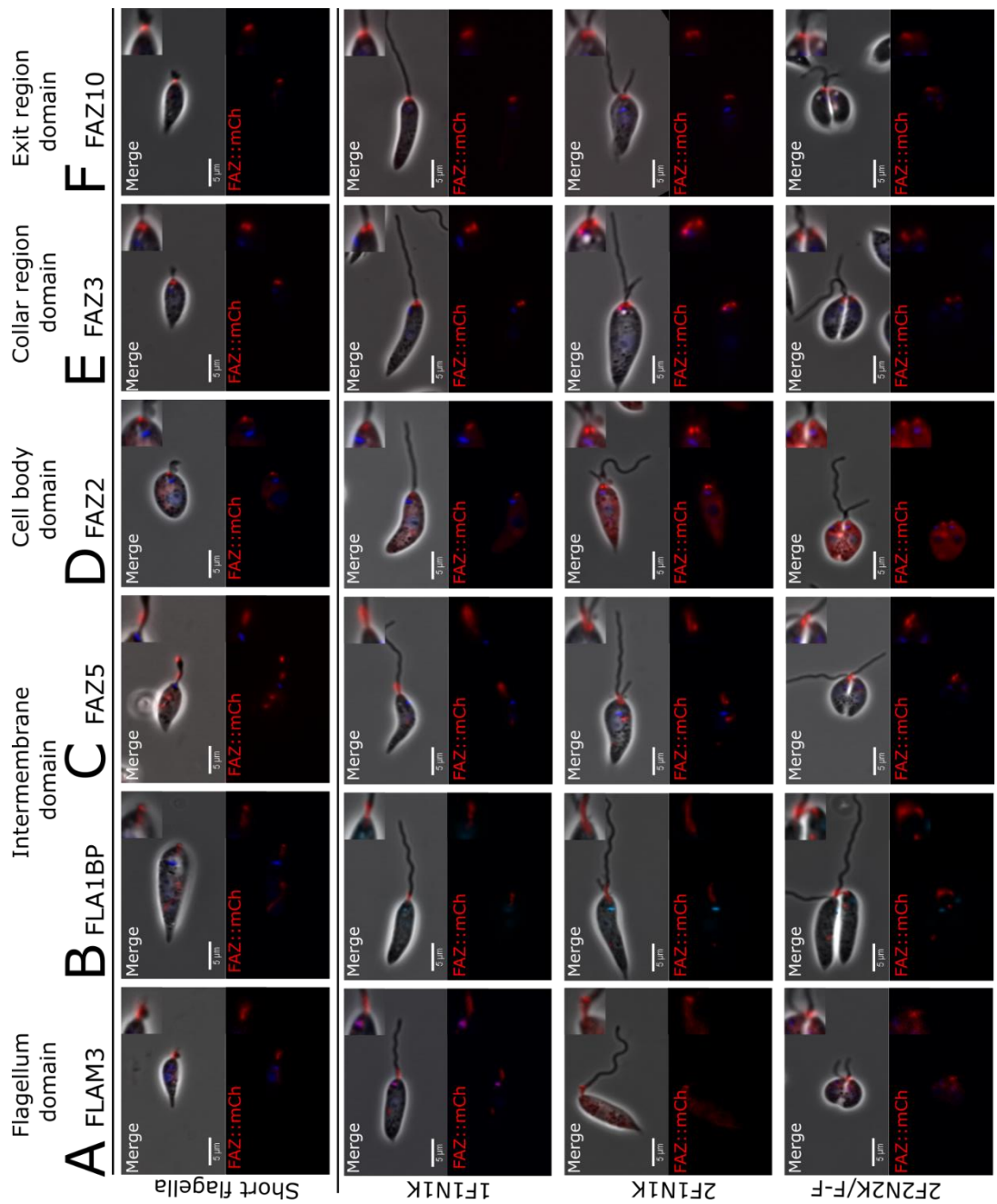


Figure 6.7 Deletion of CC2D affected the localisation of flagellum, intermembrane, and cell body FAZ domain proteins. The following proteins, A) FLAM3, B) FLA1BP, C) FAZ5, D) FAZ2, E) FAZ3 and F) FAZ10 were tagged with mCherry and transfected into CC2D null mutant cell line. Images shown are from short flagella, 1F1N1K, 2F1N1K and 2F2N2K/F-F cells. Top- merge containing phase (grey), mCherry (red) and Hoechst 33342 (blue) and bottom- mCherry (red) and Hoechst 33342 (blue) only. Inserts included shows an enlarged image of FAZ region.

6.6 FAZ2 necessary for assembly of CC2D into *L. mexicana* FAZ

CC2D and FAZ2 are cell body FAZ domain proteins and share a phenotype of F-F connections on deletion. In *T. brucei*, CC2D was identified as a FAZ2 partner (Q. Zhou *et al.*, 2015). The knockdown of either protein affected the other - RNAi of FAZ2 de-stabilised CC2D and RNAi of CC2D de-stabilised FAZ2 demonstrating the FAZ2/CC2D interdependency (Q. Zhou *et al.*, 2015). To assess if this applies for *L. mexicana*, the localisation of mCherry tagged CC2D was tested in the FAZ2 null mutant for comparison against FAZ2 localisation in CC2D null mutant.

In the parental cells, CC2D and FAZ2 displayed a linear signal on the cell body side in 1F1N1K cells and duplicated to form two visible signals from 2F1N1K throughout the cell cycle to 2F2N2K (**Fig 6.8 B&C**). As previously shown, for the CC2D null mutant, FAZ2 was localised as a stub at distal end of the flagellar pocket neck and remained in this localisation throughout the cell cycle. Additionally, a cytoplasmic signal was seen, suggesting that not all of the FAZ2 protein was integrated into the short FAZ (**Fig 6.8D**). This suggests that CC2D is important for the correct localisation of FAZ2. However, in the FAZ2 null mutant, CC2D signal was not seen within the FAZ region of cells throughout the cell cycle (1F1N1K-2F2N2K) (**Fig 6.8A**). CC2D signal instead was seen within the lysosome (**Fig 6.8A**). This suggests that FAZ2 is necessary for CC2D assembly into the FAZ. The data demonstrates a hierarchy of FAZ assembly with FAZ2 required for CC2D integration.

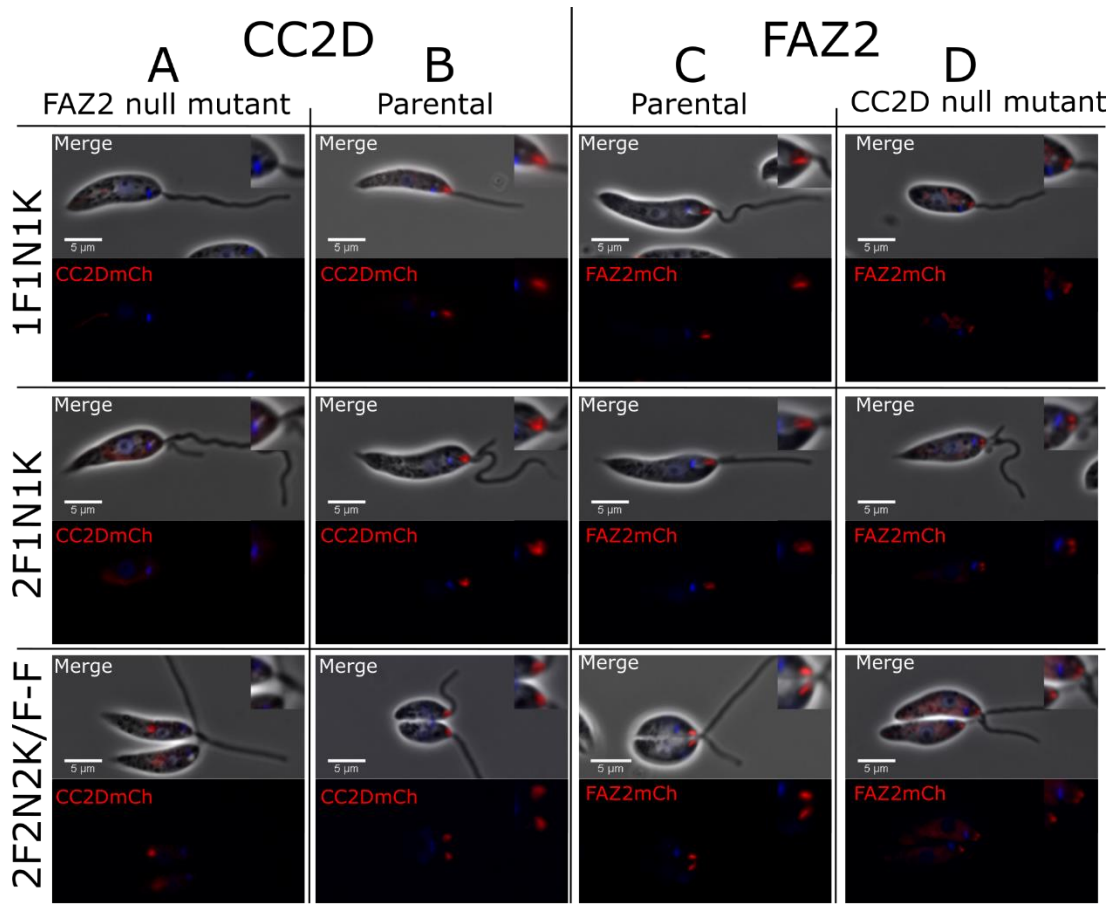


Figure 6.8 FAZ2 is required for CC2D assembly. Images of CC2D::mCh in A) FAZ2 null mutant, B) parental, and images of mCh::FAZ2 in C) parental and D) CC2D null mutant. CC2D and FAZ2 were tagged with mCherry and transfected into parental and FAZ2 or CC2D null mutant, respectively. Images shown are from 1F1N1K, 2F1N1K and 2F2N2K/F-F cells. Top-merge containing phase (grey), mCherry (red) and Hoechst 33342 (blue) and bottom-merge mCherry (red) and Hoechst 33342 (blue) only. Inserts included shows an enlarged image of FAZ region.

6.7 CC2D deletion reduced flagellar pocket size

The changes to the flagellum, intracellular, and cell body FAZ domains in the CC2D null mutant could cause a reduction in the size of the attachment interface between the flagellum and the flagellar pocket neck, leading to flagellum loss. Previous studies in FAZ5 and FAZ2 deletion cell lines showed that the flagellar pocket size was reduced and a similar effect was seen for FAZ27 and FAZ34 deletion described in chapter 5 (Sunter *et al.*, 2019; Halliday *et al.*, 2020). To assess if CC2D loss caused the same effect, the distance between the kinetoplast and the anterior cell tip was measured at 4 weeks post-storage. Light microscopy appeared to show that the kinetoplast was positioned closer to the anterior cell tip in the CC2D null mutant compared to the parental and add-back (**Fig 6.9A**).

To confirm this, the kinetoplast-anterior cell tip distances were measured in 1F1N1K cells from each cell line and the mean was calculated. The mean distance for the parental cells was 3 μm (**Fig 6.9B**). However, the distance in the CC2D null mutant was $\sim 1 \mu\text{m}$ shorter, while in the CC2D add-back cells the distance was similar to the parental cells (**Fig 6.9B**). The reduction in kinetoplast to anterior cell tip distance as result of CC2D loss suggests that the length of the flagellar pocket was reduced in the null mutant.

To look at the flagellar pocket in more detail, the flagellar pocket markers, LmxM.23.0630 and LmxM.06.0030 were used (Halliday *et al.*, 2018). These markers were expressed with a mCherry tag at their C-terminus in the parental and CC2D null mutant. LmxM.23.0630 was localised to the bulbous domain and LmxM.06.0030 was localised to the neck domain in the parental cells as expected (**Fig 6.9C**). In the CC2D null mutant, it was consistently observed that the LmxM.23.0630 signal was still present, and localised distal of the kinetoplast (**Fig 6.9C**). For LmxM.06.0030, the signal was localised within the flagellar pocket neck region, similar to the parental (**Fig 6.9C**), indicating that CC2D loss had a little effect on the localisation of these flagellar pocket markers unlike FAZ27 and FAZ34. This suggests that the organisation of the flagellar pocket was not grossly disrupted in the CC2D null mutant.

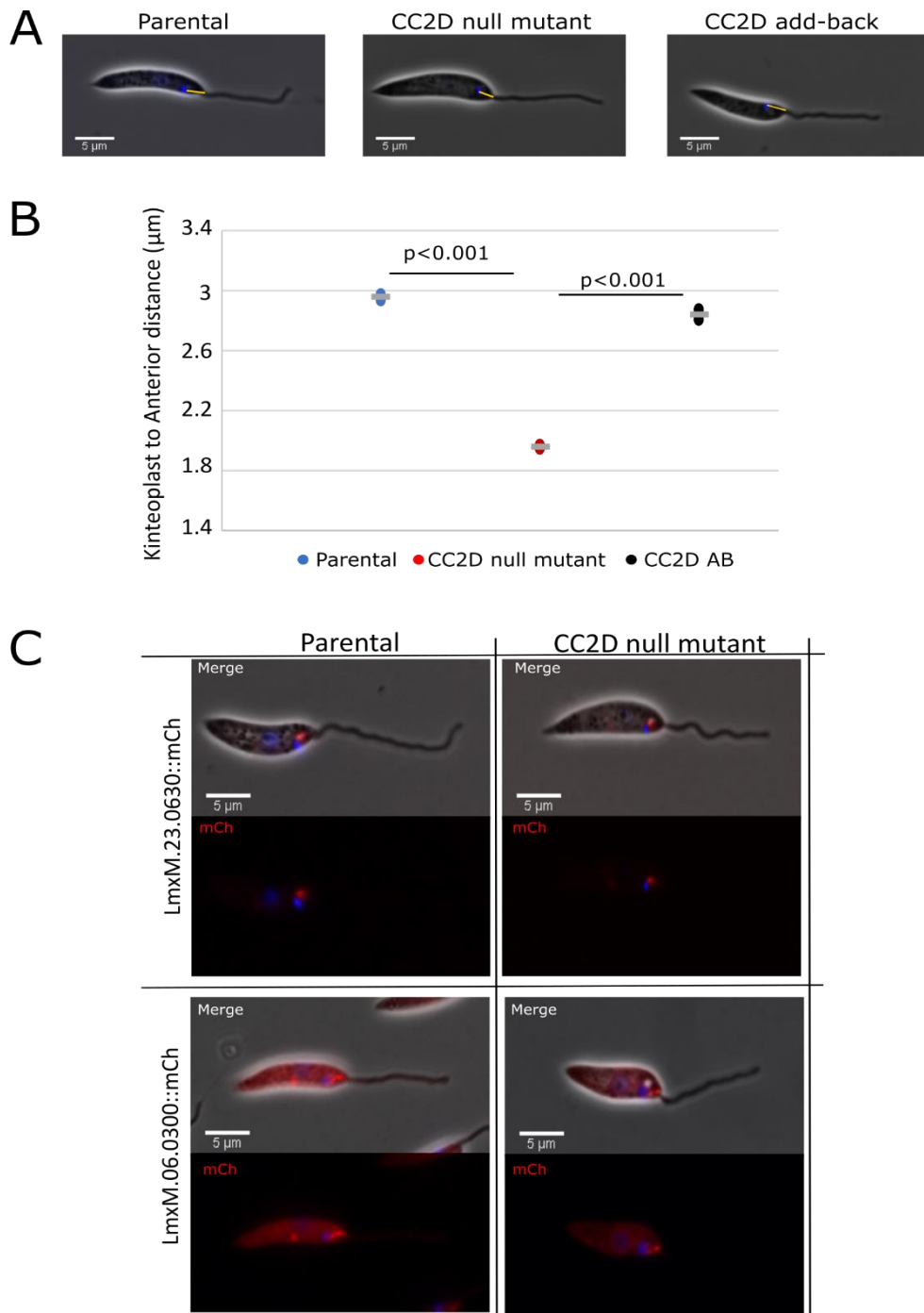


Figure 6.9 CC2D loss disrupted flagellar pocket shape. A) Example images of kinetoplast to anterior cell tip distances in the CC2D null mutant compared to the parental and add-back. Distances were measured in ImageJ. B) Mean kinetoplast to anterior cell tip distances calculated for CC2D null mutant, parental and CC2D add-back cell lines. 1F1N1K cells in duplicates were used to measure the means and p-values were calculated from two sets of lengths together. C) Widefield images showing FP markers tagged with mCherry in parental and null mutants. Top- overlay of phase (grey), Hoechst (Blue) and mCherry (red) combined and bottom- overlay of Hoechst 33342 (blue) and mCherry (red) only.

6.8 Change in FAZ organisation and attachment affected cell motility

The loss of CC2D caused flagellum attachment, flagellar pocket and cell tip morphogenesis defects, which might also impact cell motility as previously observed for FAZ5 and FAZ2 null mutants (Sunter *et al.*, 2019; Halliday *et al.*, 2020). To assess the effect of CC2D deletion on cell motility, movies of swimming tracks were taken from cell lines 4 weeks post storage. The parental, null mutant and add-back cells were tested directly from culture of equal density (1×10^7 cells/ml) and repeated three times.

The tracks and speed/persistence data combined showed that the CC2D null mutant were not as directionally progressive as the parental cells. In the CC2D null mutant, there appeared to be two populations of cells those that had a slower swimming speed and another with a swimming speed similar to the parental cells (**Fig 6.10A-C**). While the motility of the CC2D add-back was similar to the parental cells (**Fig 6.10A-C**). The reduction in directional persistence seen in CC2D null mutant suggests that the mutants had lost their ability to engage effectively in progressive movement as a direct result of CC2D loss.

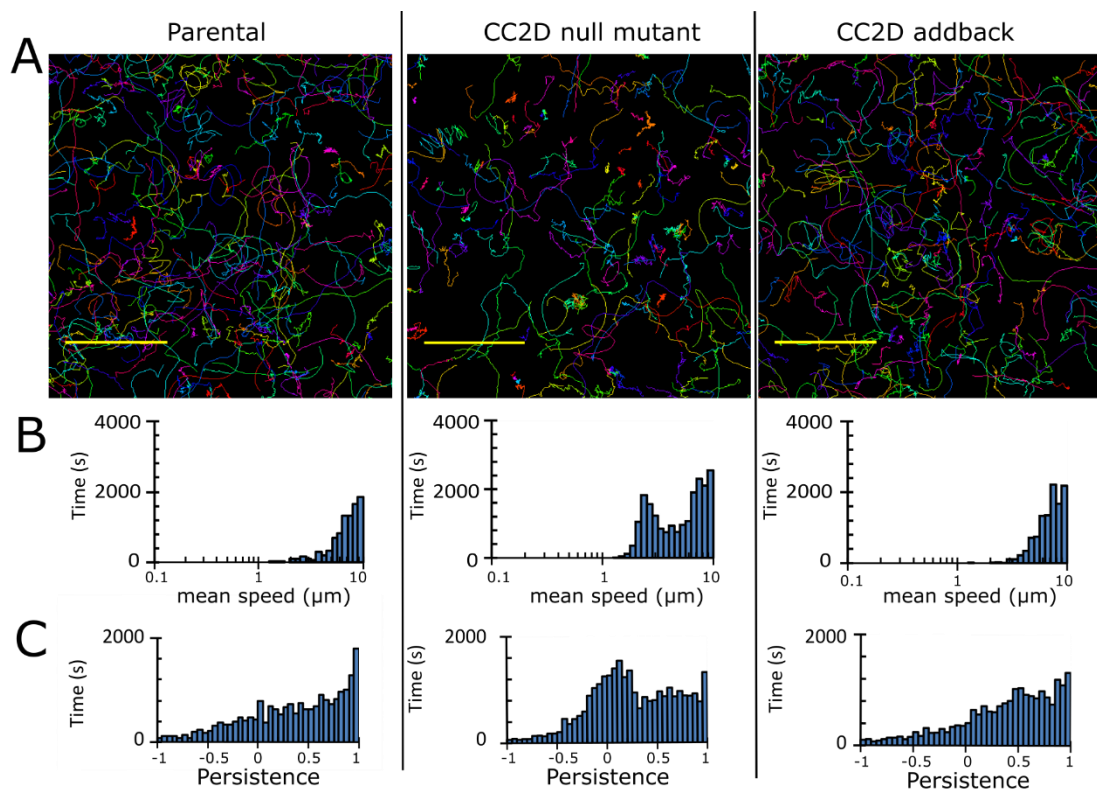


Figure 6.10 CC2D loss reduced swimming speed and progressive movement. A) Plots of the swimming tracks for the parental, CC2D null mutant and CC2D add-back cells (Scale bar- 100 μm). B) Histograms of the mean speed and C) directional persistence. The swimming tracks of the parental, null mutant and add back cells were tracked for 360 seconds, which permitted the mean speed and persistence to be calculated. This was repeated three times and data shown are representative of one experiment.

6.9 Discussion

6.9.1 CC2D has a key role in anterior cell tip morphogenesis

Loose flagella, short flagellum cells and F-F connections were observed in the CC2D null mutant. Like the FAZ27 and FAZ34 null mutants, presence of loose flagella and short flagellum cells numbers decreased overtime (Chapter 5). However, for the CC2D null mutant, this decrease was accompanied by an increase in F-F connections. This suggests that the retention of the flagellum in cells provides more opportunity for F-F connections to occur.

The results show that CC2D loss caused disruption to the FAZ structure, with similar effects as seen in the FAZ2 null mutant (Halliday *et al.*, 2020). In the CC2D null mutant, tagged FLAM3, FLABP and FAZ5 proteins, representing the flagellum and intracellular FAZ domains were localised on the flagellum beyond the anterior cell tip and they appear to mediate F-F connections, as observed with the FAZ2 null mutant (Halliday *et al.*, 2020). The cell body domain FAZ protein, FAZ2 appears as a short structure and remains within the neck, while FAZ10 and FAZ3 representing exit and collar regions were unaffected.

In the parental cells, the flagellum, intracellular and cell body domains are located together along the length of the flagellar pocket neck and as the new flagellum elongates, the new FAZ is also formed (**Fig 6.11A**). However, deletion of FAZ2 led to the disconnection of the flagellum and intracellular FAZ domains from the cell body

FAZ domain, causing the former domains to extend the anterior cell tip out along the flagellum during flagellum elongation (**Fig 6.11B**). This ultimately results in an extension of the anterior cell tip that connects both flagella (Halliday *et al.*, 2020). It was suggested that this anterior tip structure would eventually break away from the cell body and appear as membranous bridge, connecting two flagella as observed by SEM (**Fig 6.11B**) (Halliday *et al.*, 2020). Given that the deletion of CC2D disrupted the FAZ domain organisation in a similar manner to the FAZ2 null mutant, it is logical to predict that the F-F connections in the CC2D null mutant are the result of erroneous anterior cell tip extension leading to the formation of a membranous bridge (**Fig 6.11C**). CC2D like FAZ2 is therefore important for forming the connection between cell body and intracellular FAZ domains and by extension for anterior cell tip morphogenesis.

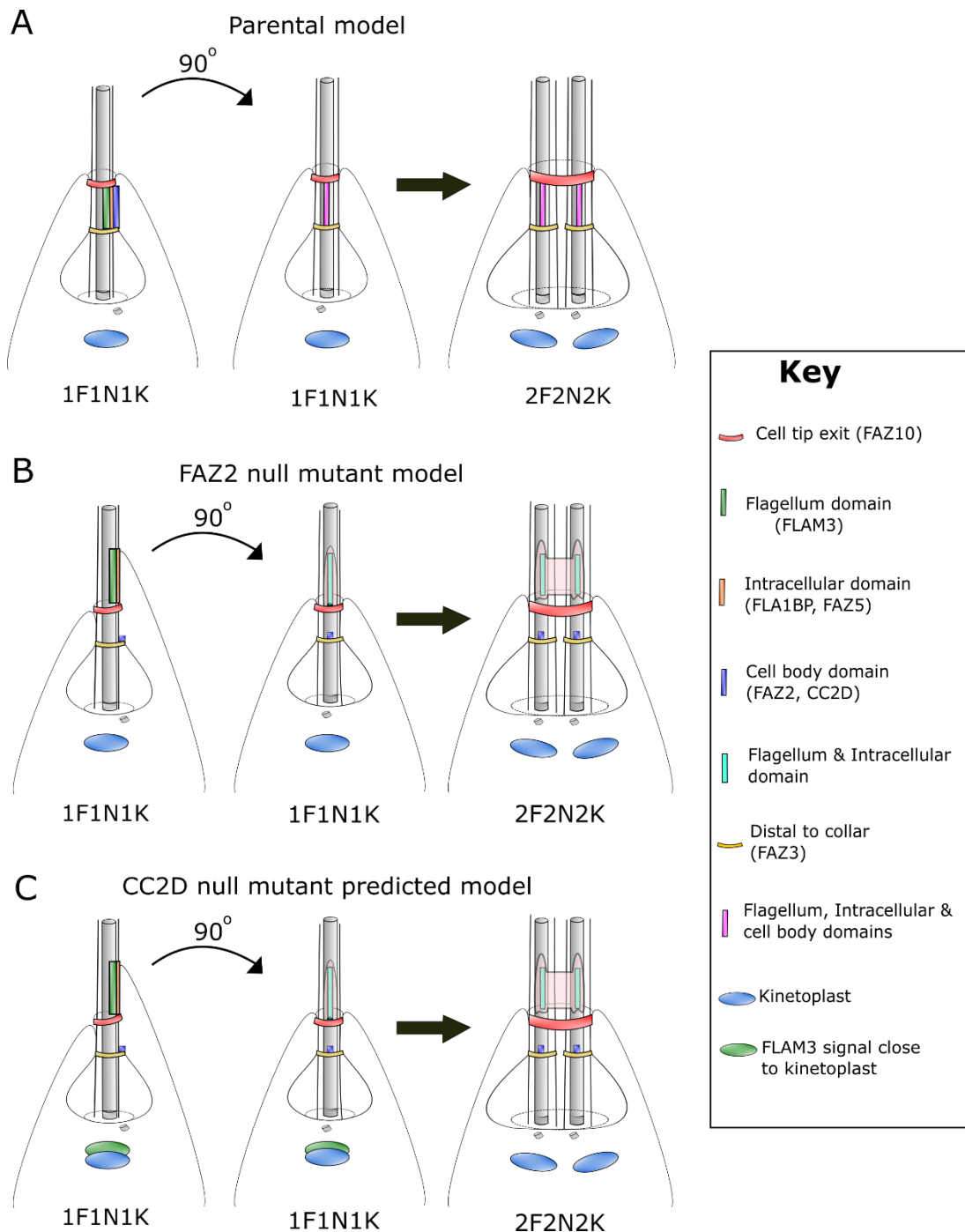


Figure 6.11 F-F connections in CC2D null mutant is predicted to be similar to FAZ2 null mutant. Organisation of FAZ domains in 1F1N1K and 2F2N2K cells of A) the parental, B) FAZ2 null mutant and C) CC2D null mutant. The following proteins FLAM3 (flagellum domain), FLA1BP and FAZ5 (intracellular proteins), FAZ2 (cell body domain), FAZ3 (distal to collar) and FAZ10 (exit) were used for the all cell lines, except ClpGM6 was used to represent flagellum domain and FAZ1 was used to represent cell body domain and distal to collar region in the FAZ2 null mutant. FAZ2 model was adapted from (Halliday *et al.*, 2020).

6.9.2 FAZ2 is the start of FAZ assembly hierarchy

The previous study on FAZ2 in *L. mexicana* showed that the absence of FAZ2 caused a big disruption to the FAZ structure. It was demonstrated that the intracellular domain proteins FAZ5 and FLA1BP and flagellum domain protein ClpGM6 were mislocalised (Halliday *et al.*, 2020). Additionally, the work described in this chapter demonstrated that CC2D, a cell body domain protein was also affected by FAZ2 deletion and was absent from the FAZ region. CC2D deletion was similar, it caused the mislocalisation of both intracellular proteins (FAZ5 and FLA1BP) and flagellum domain protein FLAM3, while FAZ2 remained, albeit with a shorter signal. Interestingly, deletion of FAZ5, a intracellular protein on the cell body membrane resulted in the mislocalisation of the flagellum domain protein (ClpGM6) and FLA1BP (intracellular domain on the flagellum side), while FAZ1 (cell body) was unaffected (Sunter *et al.*, 2019). This demonstrates that CC2D, FAZ2 and FAZ5 deletion has a similar impact on the flagellum domain, while CC2D and FAZ2 also have an additional impact on both membranes of the intracellular domain localisation (Sunter *et al.*, 2019; Halliday *et al.*, 2020). This suggests a hierarchy of FAZ assembly, with the cell body domain proteins, FAZ2 and CC2D, being required for the correct localisation of both flagellum and intracellular FAZ domain proteins and confirms their importance in forming connections between cell body and intracellular FAZ domains. Moreover, the cell body side of the intracellular domain is required for the assembly of the flagellum domain (Sunter *et al.*, 2019), suggesting that FAZ assembly proceeds from cell body to flagellum side (**Fig 6.12**).

Here, it was showed that FAZ2 is assembled into the FAZ before CC2D and that the subsequent assembly of CC2D is dependent on the presence of FAZ2. The relationship of CC2D and FAZ2 seen in *L. mexicana* differs to that seen in *T. brucei*. In *T. brucei*, FAZ2 and CC2D form a complex (with KMP11) that are interdependent (Q. Zhou *et al.*, 2015). RNAi studies demonstrated that CC2D knockdown led to depletion of FAZ2, and vice versa (Q. Zhou *et al.*, 2015). The phenotype and therefore function of CC2D diverges slightly from FAZ2 in *L. mexicana*, which suggests these proteins may not share the exact same location within the cell body domain. This may explain

the dependency relationship differences between these two proteins in *L. mexicana* and *T. brucei*.

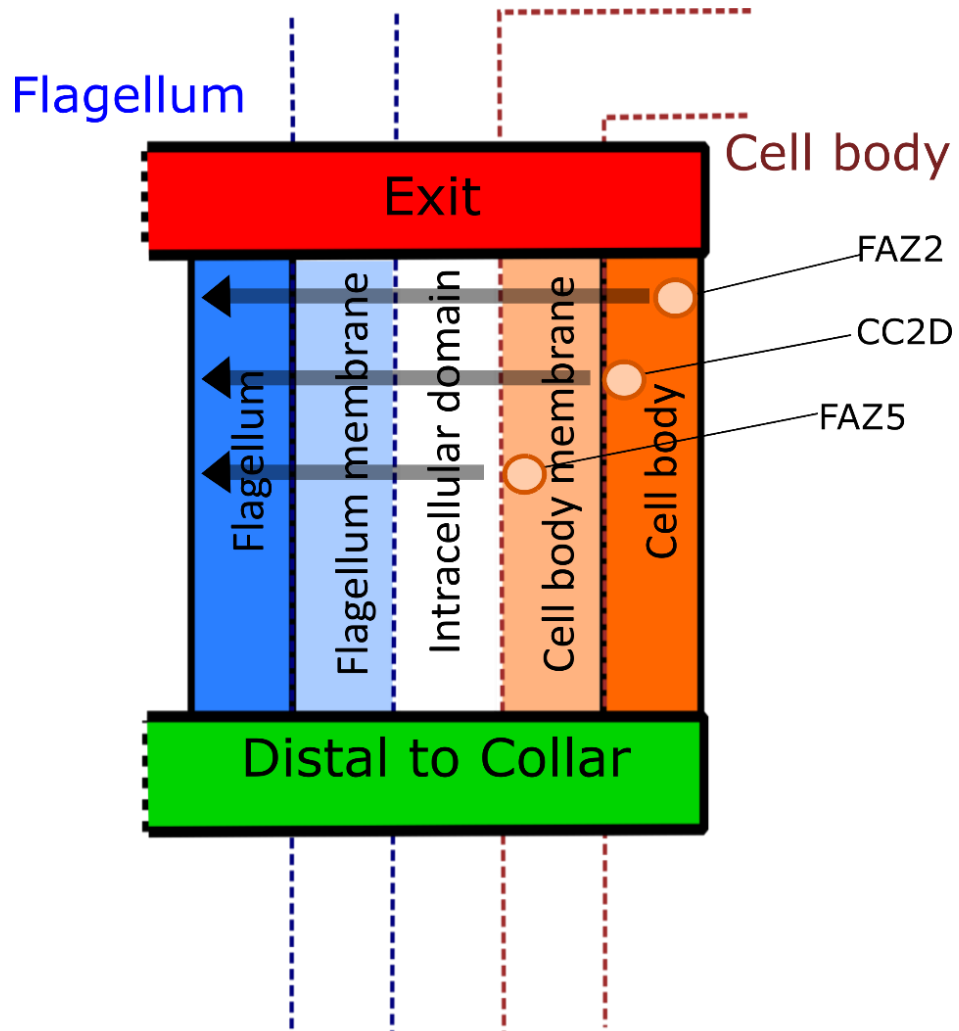


Figure 6.12 FAZ2 is head of FAZ assembly hierarchy. Cell body proteins FAZ2 and CC2D are required for assembly of flagellum and intracellular domain proteins, while FAZ2 is required for assembly of CC2D. FAZ5, an intracellular protein in cell body membrane, is required for flagellum domain assembly. This demonstrates an order of assembly starting at the cell body domain and ending at the flagellum domain.

6.9.3 CC2D has a role in flagellum attachment

Deletion of FAZ27 and FAZ34 led to short flagellum cells and loose flagella, with the detachment of the flagellum from the cell body the likely explanation for this phenotype. Given the similar phenotype seen after deletion of CC2D, flagellum detachment is also the logical explanation; however, intriguingly the flagellum of CC2D null mutants was not as easily detachable, as those in the FAZ27 and FAZ34 null mutants (**Chapter 5**). This demonstrates that while CC2D is required for flagellum attachment, its role on attachment is not as critical as the flagellum domain proteins FAZ27 and FAZ34. Moreover, this suggests that the residual FAZ structure in the CC2D null mutant is more robust than after the deletion of FAZ27 and FAZ34.

Additionally, CC2D deletion caused a disruption to the localisation of the flagellum domain protein FLAM3, which was also disrupted in the FAZ27 and lost in FAZ34 null mutants (**Chapter 5**) and FAZ5 (Sunter *et al.*, 2019). In all these mutants the flagellum FAZ domain protein signal was observed on the flagellum beyond the anterior cell tip. This demonstrates that CC2D, FAZ5, FAZ27 and FAZ34 share a similar role of being required for FLAM3 assembly. In the CC2D null mutant, an additional FLAM3 signal was also observed at a close proximity to the kinetoplast during 1F1N1K configuration, similar to what was seen for FAZ27 null mutant (**Chapter 5**).

With FAZ5 also suspected to be important for flagellum attachment (**Chapter 4**), this suggests that CC2D is likely positioned in close proximity to FAZ5 and the junctional complexes connecting the flagellum to the cell body. While FAZ2 which is not required for flagellum attachment could be positioned further away (Sunter *et al.*, 2019; Halliday *et al.*, 2020). This also suggests a hierarchy of importance for flagellum attachment for the different FAZ domains, with the flagellum and intracellular domains being more important than the cell body domain. This lower level of attachment impact seen in the CC2D null mutant could be explained by the FAZ filament not being closely associated with the primary attachment area in *L. mexicana* (Wheeler, Sunter and Gull, 2016).

6.9.4 CC2D and cell body domain proteins play a smaller role in cell morphogenesis

CC2D null mutant showed reduction in cell body length, similar to what was seen for FAZ2 null mutant (Halliday *et al.*, 2020). However, its impact on cell body length is not as dramatic as seen for the flagellum domain FAZ27 and FAZ34 null mutants (**Chapter 5**) and the intracellular domain FAZ5 null mutant (Sunter *et al.*, 2019). This suggests that cell body FAZ domain proteins play a smaller role in cell morphogenesis. This trend is similar to that seen in *T. brucei*. The flagellum domain proteins ClpGM6, FLAM3 and FAZ27 knockdown caused trypomastigote to epimastigote-like morphology changes, while CC2D and FAZ2 knockdown caused flagellum detachment and cell death in addition to cell morphogenesis defects (Rotureau, Subota and Bastin, 2011; Zhou *et al.*, 2011; Hayes *et al.*, 2014; Sunter *et al.*, 2015; An *et al.*, 2020).

6.9.5 CC2D is important for motility

Deletion of CC2D led to motility defects. The CC2D null mutant had lost its ability to engage in progressive movement. Interestingly, the CC2D null mutant also showed a bimodal speed distribution, with one similar to the parental and the add-back while the other was slower moving. A study on FAZ2 deletion showed that motility was impaired, which was due to both cell body to flagellum and flagellum to flagellum connection abnormalities, affecting progressive movement (Halliday *et al.*, 2020). FAZ5 deletion also showed motility was affected with little processive movement, which was caused by the lack of coordination in flagellar beat patterns (Sunter *et al.*, 2019). The CC2D null mutant shared a similar flagellum attachment disruption as seen for FAZ5, likely affecting the flagellar beat coordination and additionally a disconnection between flagellum and cell body domains and flagellum to flagellum connections seen for FAZ2, which explains the severity of motility affecting both directional persistence and speed.

Chapter 7

Conclusions and Outlook

7.1 Towards a greater understanding of FAZ function in *Leishmania*

This thesis sought to address two interlinked questions - 1) How is the molecular structure of the FAZ organised in *L. mexicana*? and 2) What are the specific roles of the FAZ proteins in relation to FAZ assembly and cell morphogenesis? Below, are the summarised key findings from this thesis, which has contributed to a much-improved insight into the molecular organisation and function of the FAZ in *Leishmania*.

7.1.1 Identification of FAZ proteins in *L. mexicana*

The endogenous tagging of FAZ orthologs identified through TrypTag led to the discovery of 20 additional FAZ proteins to the eight already discovered (FLA1BP, ClpGM6, FAZ1, FAZ8, FAZ2, FAZ5, FAZ10 and FAZ7) in *L. mexicana* (Wheeler, Sunter and Gull, 2016; Sunter *et al.*, 2019; Halliday *et al.*, 2020; Corrales *et al.*, 2021). The localisation classes of these 28 proteins within three structural domains (flagellum, intracellular and cell body) of the FAZ complex were determined; 1) Linear on the flagellum side, 2) Linear on the cell body side, 3) Ring/horseshoe distal to the collar region, 4) Ring/horseshoe at the exit point and 5) Linear on the flagellum side combined with ring/horseshoe distal to the collar region. These FAZ classes identified in *L. mexicana* was found to correlate with specific groups in *T. brucei*. Examples of this include Class I and II linear localisations on the flagellum side and cell body side in *L. mexicana* correlating with localisations in the flagellum and cell body domains in *T. brucei*, respectively. Meanwhile, Class IV, exit point localisations in *L. mexicana* are linked to distal enriched/only in *T. brucei*. The localisation screening and conservation analysis of FAZ orthologs also revealed FAZ proteins specific to the trypomastigote and epimastigote morphology, and included proteins involved in cytokinesis regulation and connections with the ER.

7.1.2 Identification of FAZ functional groups in *L. mexicana*

The deletion of 23 FAZ proteins described in Chapter 4 revealed a correlation of functions associated with different localisation classes and structural domains. Within each FAZ domain, different levels of phenotype were detected, suggesting that specific functions and the importance of the proteins analysed are connected to their exact location. FAZ27, FAZ34 and FLA1BP of Class I, linear on the flagellum side were associated with flagellum attachment and cell morphogenesis. While on the other hand, FAZ5, CC2D and FAZ2 of Class II, linear on the cell body side had roles in flagellum attachment, cell morphology and anterior cell tip morphogenesis. Class III, distal to the collar protein FAZ3, is potentially responsible for ensuring the correct assembly of the FAZ, while FAZ10 from Class IV, at the exit point demonstrated importance for cleavage furrow ingression. Class V proteins, linear on the flagellum side combined with ring/horseshoe distal to the collar region, which did not have a phenotype, were not required for core FAZ functions and could be associated with roles outside the attachment region.

7.1.3 Specific functions of FAZ27, FAZ34 and CC2D

Further analyses of FAZ27 and FAZ34 from the linear structure within the flagellum domain described in Chapter 5 revealed they are important for flagellum attachment. Moreover, work in Chapter 6 revealed that CC2D with the same linear structure from the cell body domain was found to be important for flagellum attachment and anterior cell tip morphogenesis and is dependent on FAZ2 for assembly. The function of CC2D in both flagellum attachment and cell tip morphogenesis suggested that CC2D is likely to be located between FAZ5 (suspected to be important for flagellum attachment) in the cell body membrane and FAZ2 (important for anterior cell tip morphogenesis) in the cell body region. The combined analysis of these three FAZ proteins also defined the assembly hierarchy of three structural domains, the cell body, intracellular and flagellum domains with FAZ2 of the cell body domain being a key foundational protein. In conclusion, the work described in this thesis made important discoveries on the FAZ structure of *L. mexicana* and the revealed the specific functions of flagellum and cell body domains.

7.2 Limitations and future perspectives

The discovery of FAZ proteins in *L. mexicana* was driven by analysing a cohort of FAZ orthologs conserved in *T. brucei*. The OrthoMCL output used to do this changes over time with data entries being added or removed, which creates the potential for missing a small number of FAZ orthologs. It is also important to consider that *Leishmania* promastigote/amastigote morphology differs from trypomastigote/epimastigote morphology seen for *T. brucei* (Hoare and Wallace, 1966; Wheeler, Gluenz and Gull, 2013; Sunter and Gull, 2017). In fact, the conservation analysis of FAZ proteins in *T. brucei* demonstrated that while 91% FAZ proteins are conserved in the more closely related organism *T. cruzi*, 36% are lost in *L. mexicana* suggesting that the difference and divergence of FAZ proteins are associated with their morphological differences. Additionally, the promastigote form is likely the ancestral form of trypanosomatids with the trypomastigote form evolving later (Flegontov *et al.*, 2013). It is therefore likely that *L. mexicana* would maintain promastigote specific FAZ proteins that are lost in *T. brucei* which would not be found by the experimental approach taken here. Interestingly, none of the proteins identified so far localised to both the exit point and linear structure along the neck. This could indicate that they are separate elements of the attachment structure or the proteins that localise to both these regions could be promastigote specific, yet to be discovered. The discovery of FAZ proteins and their localisations offers an opportunity to identify further FAZ partners using a range of experimental methods such as immunoprecipitation. This will give further insight into the complexity of FAZ molecular structure and potentially uncovering additional functions in relation to the specific cellular morphology of *L. mexicana*.

Flagellar pocket organisation in amastigotes is similar to promastigotes, except that the pocket is wider with narrower flagellum neck region. The FAZ organisation was also seen to surround the entire flagellum, which differs from the promastigotes (Wheeler, Sunter and Gull, 2016). These changes in response to flagellum restructuring is an adaptation to minimise the total area for survival in mammalian host (Eva Gluenz *et al.*, 2010; Wheeler, Sunter and Gull, 2016). The work described in this thesis focussed solely on promastigotes, so a little understanding of the FAZ

make up in amastigotes remains. In previous studies, it was demonstrated that FAZ5 and FAZ7B deletion affected flagellar pocket morphogenesis in amastigotes, and in addition to FAZ2 deletion, they reduced pathogenicity in mice (Sunter *et al.*, 2019; Halliday *et al.*, 2020; Corrales *et al.*, 2021). Meanwhile FAZ5 deletion was also found to reduce the rate of endocytosis (Sunter *et al.*, 2019). This suggests that FAZ is important for flagellar pocket function. This extent of flagellar pocket function (nutrient uptake and maintaining pathogenicity) was not tested for FAZ27, FAZ34 and CC2D null mutants. It is highly possible that especially for the flagellum domain proteins FAZ27 and FAZ34, which were found to be hugely critical for flagellum attachment in promastigotes, are important for maintaining narrow constriction of the flagellar pocket neck in amastigotes. This could be essential for survival in mammalian host. Examining the FAZ biology in amastigotes will give a further insight into FAZ role in flagellar pocket function in immune evasion and growth.

7.4 Concluding remarks

The FAZ is an important feature for the determination of the promastigote morphology in *L. mexicana*. Building on previous studies, the dissection of different components in a complex FAZ structure revealed functional groups important for a variety of functions including FAZ assembly and order, flagellum attachment and flagellar pocket architecture. This work supported the evidence for the importance of an ordered FAZ structure for maintaining flagellar pocket architecture and determining cell morphogenesis and motility.

Chapter 8

References

- Alcantara, C. L. *et al.* (2014) 'The three-dimensional structure of the cytostome-cytopharynx complex of *Trypanosoma cruzi* epimastigotes', *Journal of Cell Science*, 127(10), pp. 2227–2237. doi: 10.1242/jcs.135491.
- Alcantara, C. L. *et al.* (2017) 'The cytostome-cytopharynx complex of *Trypanosoma cruzi* epimastigotes disassembles during cell division', *Journal of Cell Science*, 130(1), pp. 164–176. doi: 10.1242/jcs.187419.
- Allen, C. L., Goulding, D. and Field, M. C. (2003) 'Clathrin-mediated endocytosis is essential in *Trypanosoma brucei*', *EMBO Journal*, 22(19), pp. 4991–5002. doi: 10.1093/emboj/cdg481.
- Alvar, J. *et al.* (2012) 'Leishmaniasis worldwide and global estimates of its incidence', *PLoS ONE*, 7(5). doi: 10.1371/journal.pone.0035671.
- Ambit, A. *et al.* (2011) 'Morphological events during the cell cycle of *leishmania major*', *Eukaryotic Cell*, 10(11), pp. 1429–1438. doi: 10.1128/EC.05118-11.
- An, T. *et al.* (2020) 'FAZ27 cooperates with FLAM3 and ClpGM6 to maintain cell morphology in *Trypanosoma brucei*', *Journal of Cell Science*, 133(11). doi: 10.1242/jcs.245258.
- An, T. and Li, Z. (2018) 'An orphan kinesin controls trypanosome morphology transitions by targeting FLAM3 to the flagellum', *PLoS Pathogens*, 14(5). doi: 10.1371/journal.ppat.1007101.
- Anantharaman, V., Iyer, L. M. and Aravind, L. (2012) 'Ter-dependent stress response systems: Novel pathways related to metal sensing, production of a nucleoside-like metabolite, and DNA-processing', *Molecular BioSystems*, 8(12), pp. 3142–3165. doi: 10.1039/c2mb25239b.
- Angelopoulos, E. (1970) 'Pellicular microtubules in the family Trypanosomatidae', *The Journal of Protozoology*, 17(1), pp. 39–51. doi: 10.1111/j.1550-7408.1970.tb05157.x.
- Antoine, J. C. *et al.* (1990) 'Parasitophorous vacuoles of *Leishmania amazonensis*-infected macrophages maintain an acidic pH', *Infection and Immunity*, 58(3), pp. 779–787. doi: 10.1128/iai.58.3.779-787.1990.
- Antoine, J. C. *et al.* (1998) 'The biogenesis and properties of the parasitophorous vacuoles that harbour *Leishmania* in murine macrophages', *Trends in Microbiology*, 6(10), pp. 392–401. doi: 10.1016/S0966-842X(98)01324-9.
- Aslett, M. *et al.* (2009) 'TriTrypDB: A functional genomic resource for the Trypanosomatidae', *Nucleic Acids Research*, (38), pp. 457–462. doi: 10.1093/nar/gkp851.
- Barnwell, E. M. *et al.* (2010) 'Developmental regulation and extracellular release of a VSG expression-site-associated gene product from *Trypanosoma brucei* bloodstream forms', *Journal of Cell Science*, 123(19), pp. 3401–3411. doi: 10.1242/jcs.068684.
- Batchelor, G. K. (1970) 'Slender-body theory for particles of arbitrary cross-section in Stokes flow', *Journal of Fluid Mechanics*, 44(3), pp. 419–440. doi: 10.1017/S002211207000191X.
- Bates, P. A. (2007) 'Transmission of *Leishmania* metacyclic promastigotes by phlebotomine sand flies', *International Journal for Parasitology*. International Journal for Parasitology, pp. 1097–1106. doi: 10.1016/j.ijpara.2007.04.003.

- Beneke, T. *et al.* (2017) 'A CRISPR Cas9 high-throughput genome editing toolkit for kinetoplastids', *Royal Society Open Science*, 4(5), pp. 1–16. doi: 10.1098/rsos.170095.
- Blum, M. *et al.* (2021) 'The InterPro protein families and domains database: 20 years on', *Nucleic Acids Research*, 49(1), pp. 344–354. doi: 10.1093/nar/gkaa977.
- Boehm, C. M. *et al.* (2017) 'The Trypanosome Exocyst: A Conserved Structure Revealing a New Role in Endocytosis', *PLoS Pathogens*, 13(1). doi: 10.1371/journal.ppat.1006063.
- Bonhivers, M. *et al.* (2008) 'Biogenesis of the trypanosome endo-exocytotic organelle is cytoskeleton mediated', *PLoS Biology*, 6(5). doi: 10.1371/journal.pbio.0060105.
- Brennand, A. *et al.* (2015) 'ATG24 represses autophagy and differentiation and is essential for homeostasis of the flagellar pocket in trypanosoma brucei', *PLoS ONE*, 10(6), pp. 1–23. doi: 10.1371/journal.pone.0130365.
- Calderwood, S. K., Mambula, S. S. and Gray, P. J. (2007) 'Extracellular heat shock proteins in cell signaling and immunity.', *Federation of European Biochemical Societies*, 581, pp. 3689–3694. doi: 10.1196/annals.1391.019.
- Collins, B. M. *et al.* (2002) 'Molecular architecture and functional model of the endocytic AP2 complex', *Cell*, 109(4), pp. 523–535. doi: 10.1016/S0092-8674(02)00735-3.
- Cooper, R., De Jesus, A. R. and Cross, G. A. M. (1993) 'Deletion of an immunodominant Trypanosoma cruzi surface glycoprotein disrupts flagellum-cell adhesion', *Journal of Cell Biology*, 122(1), pp. 149–156. doi: 10.1083/jcb.122.1.149.
- Corrales, R. M. *et al.* (2021) 'The kinesin of the flagellum attachment zone in Leishmania is required for cell morphogenesis, cell division and virulence in the mammalian host', *PLoS Pathogens*, 17(6). doi: 10.1371/journal.ppat.1009666.
- Davletov, B. A. and Sudhof, T. C. (1993) 'A single C2 domain from synaptotagmin I is sufficient for high affinity Ca²⁺/phospholipid binding', *Journal of Biological Chemistry*, 268(35), pp. 26386–26390. doi: 10.1016/s0021-9258(19)74326-9.
- Dean, S., Sunter, J. D. and Wheeler, R. J. (2017) 'TrypTag.org: A Trypanosome Genome-wide Protein Localisation Resource', *Trends in Parasitology*. Elsevier Ltd, 33(2), pp. 80–82. doi: 10.1016/j.pt.2016.10.009.
- Demmel, L. *et al.* (2016) 'The endocytic activity of the flagellar pocket in Trypanosoma brucei is regulated by an adjacent phosphatidylinositol phosphate kinase', *Journal of Cell Science*, 129(11), pp. 2285–2285. doi: 10.1242/jcs.191569.
- Elias, M. C. *et al.* (2007) 'Morphological Events during the Trypanosoma cruzi Cell Cycle', *Protist*, 158(2), pp. 147–157. doi: 10.1016/j.protis.2006.10.002.
- Esson, H. J. *et al.* (2012) 'Morphology of the trypanosome bilobe, a novel cytoskeletal structure', *Eukaryotic Cell*, 11(6), pp. 761–772. doi: 10.1128/EC.05287-11.
- Field, M. C. and Carrington, M. (2009) 'The trypanosome flagellar pocket', *Nature Reviews Microbiology*. Nature Publishing Group, 7(11), pp. 775–786. doi: 10.1038/nrmicro2221.
- Fischer, S. *et al.* (2011) 'Using OrthoMCL to assign proteins to OrthoMCL-DB groups or to cluster proteomes into new ortholog groups', *Current Protocols in Bioinformatics*. doi: 10.1002/0471250953.bi0612s35.

- Flegontov, P. *et al.* (2013) 'Paratrypanosoma is a novel early-branching trypanosomatid', *Current Biology*, 23(18), pp. 1787–1793. doi: 10.1016/j.cub.2013.07.045.
- Florimond, C. *et al.* (2015) 'BILBO1 Is a Scaffold Protein of the Flagellar Pocket Collar in the Pathogen Trypanosoma brucei', *PLoS Pathogens*, 11(3), pp. 1–28. doi: 10.1371/journal.ppat.1004654.
- Gabernet-Castello, C., Dacks, J. B. and Field, M. C. (2009) 'The single ENTH-domain protein of trypanosomes; endocytic functions and evolutionary relationship with epsin', *Traffic*, 10(7), pp. 894–911. doi: 10.1111/j.1600-0854.2009.00910.x.
- Gadelha, C. *et al.* (2009) 'Membrane domains and flagellar pocket boundaries are influenced by the cytoskeleton in African trypanosomes', *Proceedings of the National Academy of Sciences*, 106(41), pp. 17425–17430. doi: 10.1073/pnas.0909289106.
- Gaidarov, I. and Keen, J. H. (1999) 'Phosphoinositide-AP-2 interactions required for targeting to plasma membrane clathrin-coated pits', *Journal of Cell Biology*, 146(4), pp. 755–764. doi: 10.1083/jcb.146.4.755.
- Geiger, A. *et al.* (2010) 'Exocytosis and protein secretion in Trypanosoma', *BMC Microbiology*, 10. doi: 10.1186/1471-2180-10-20.
- Gluezn, E. *et al.* (2010) 'Beyond 9+0: noncanonical axoneme structures characterize sensory cilia from protists to humans', *The FASEB Journal*, 24(9), pp. 3117–3121. doi: 10.1096/fj.09-151381.
- Gluezn, Eva *et al.* (2010) 'Beyond 9+0: noncanonical axoneme structures characterize sensory cilia from protists to humans', *The FASEB Journal*, 24(9), pp. 3117–3121. doi: 10.1096/fj.09-151381.
- Halliday, C. *et al.* (2018) 'Cellular landmarks of Trypanosoma brucei and Leishmania mexicana', *Molecular and Biochemical Parasitology*, 230, pp. 24–36. doi: 10.1016/j.molbiopara.2018.12.003.
- Halliday, C. *et al.* (2020) 'Role for the flagellum attachment zone in Leishmania anterior cell tip morphogenesis', *PLoS Pathogens*, 16(10). doi: 10.1371/journal.ppat.1008494.
- Halliday, C. *et al.* (2021) 'Trypanosomatid Flagellar Pocket from Structure to Function', *Trends in Parasitology*, 37(4), pp. 317–329. doi: 10.1016/j.pt.2020.11.005.
- Hayes, P. *et al.* (2014) 'Modulation of a cytoskeletal calpain-like protein induces major transitions in trypanosome morphology', *Journal of Cell Biology*, 206(3), pp. 377–384. doi: 10.1083/jcb.201312067.
- Herwaldt, B. L. (1999) 'Leishmaniasis.', *Lancet (London, England)*. Elsevier, 354(9185), pp. 1191–9. doi: 10.1016/S0140-6736(98)10178-2.
- Hilton, N. A. *et al.* (2018) 'Identification of TOEFAZ1-interacting proteins reveals key regulators of Trypanosoma brucei cytokinesis', *Molecular Microbiology*, 109(3), pp. 306–326. doi: 10.1111/mmi.13986.
- Hoare, C. and Wallace, F. (1966) 'Developmental Stages of Trypanosomatid Flagellates: a New Terminology', *Nature*, 212, pp. 1385–1386. Available at: <https://www.nature.com/articles/2121385a0>.

- Höög, J. L. *et al.* (2012) 'Cryo-electron tomography and 3-D analysis of the intact flagellum in *Trypanosoma brucei*', *Journal of Structural Biology*. Elsevier Inc., 178(2), pp. 189–198. doi: 10.1016/j.jsb.2012.01.009.
- Horáková, E. *et al.* (2017) 'The *Trypanosoma brucei* TbHrg protein is a heme transporter involved in the regulation of stage-specific morphological transitions', *Journal of Biological Chemistry*, 292(17), pp. 6998–7010. doi: 10.1074/jbc.M116.762997.
- Hu, H. *et al.* (2019) 'The trypanosome-specific proteins FPRC and CIF4 regulate cytokinesis initiation by recruiting CIF1 to the cytokinesis initiation site', *Journal of Biological Chemistry*, 294(45), pp. 16672–16683. doi: 10.1074/jbc.RA119.010538.
- Hu, H., Zhou, Q. and Li, Z. (2015a) 'A novel basal body protein that is a polo-like kinase substrate is required for basal body segregation and flagellum adhesion in *trypanosoma brucei*', *Journal of Biological Chemistry*, 290(41), pp. 25012–25022. doi: 10.1074/jbc.M115.674796.
- Hu, H., Zhou, Q. and Li, Z. (2015b) 'SAS-4 protein in *Trypanosoma brucei* controls life cycle transitions by modulating the length of the flagellum attachment zone filament', *Journal of Biological Chemistry*, 290(51), pp. 30453–30463. doi: 10.1074/jbc.M115.694109.
- Hung, C. H. *et al.* (2004) 'Clathrin-dependent targeting of receptors to the flagellar pocket of procyclic-Form *Trypanosoma brucei*', *Eukaryotic Cell*, 3(4), pp. 1004–1014. doi: 10.1128/EC.3.4.1004-1014.2004.
- Kelly, B. T. *et al.* (2008) 'A structural explanation for the binding of endocytic dileucine motifs by the AP2 complex', *Nature*, 456(7224), pp. 976–979. doi: 10.1038/nature07422.
- Kořený, L., Oborník, M. and Lukeš, J. (2013) 'Make It, Take It, or Leave It: Heme Metabolism of Parasites', *PLoS Pathogens*, 9(1). doi: 10.1371/journal.ppat.1003088.
- Krishnamurthy, G. *et al.* (2005) 'Hemoglobin receptor in *Leishmania* is a hexokinase located in the flagellar pocket', *Journal of Biological Chemistry*, 280(7), pp. 5884–5891. doi: 10.1074/jbc.M411845200.
- Krüger, T. and Engstler, M. (2015) 'Flagellar motility in eukaryotic human parasites', *Seminars in Cell and Developmental Biology*. Elsevier Ltd, 46, pp. 113–127. doi: 10.1016/j.semcdb.2015.10.034.
- Kurasawa, Y. *et al.* (2018) 'The trypanosome-specific protein CIF3 cooperates with the CIF1 protein to promote cytokinesis in *Trypanosoma brucei*', *Journal of Biological Chemistry*, 293(26), pp. 10275–10286. doi: 10.1074/jbc.RA118.003113.
- Lacomble, S. *et al.* (2009) 'Three-dimensional cellular architecture of the flagellar pocket and associated cytoskeleton in trypanosomes revealed by electron microscope tomography', *Journal of Cell Science*, 122(8), pp. 1081–1090. doi: 10.1242/jcs.045740.
- Lacomble, S. *et al.* (2010) 'Basal body movements orchestrate membrane organelle division and cell morphogenesis in *Trypanosoma brucei*', *Journal of Cell Science*, 123(17), pp. 2884–2891. doi: 10.1242/jcs.074161.
- Lacomble, Sylvain *et al.* (2010) 'Basal body movements orchestrate membrane organelle division and cell morphogenesis in *Trypanosoma brucei*', *Journal of Cell Science*, 123(17), pp. 2884–2891. doi: 10.1242/jcs.074161.

- Lacomble, S. *et al.* (2012) 'A Trypanosoma brucei Protein Required for Maintenance of the Flagellum Attachment Zone and Flagellar Pocket ER Domains', *Protist*, 163(4), pp. 602–615. doi: 10.1016/j.protis.2011.10.010.
- Lacount, D. J., Barrett, B. and Donelson, J. E. (2002) 'Trypanosoma brucei FLA1 is required for flagellum attachment and cytokinesis', *Journal of Biological Chemistry*, 277(20), pp. 17580–17588. doi: 10.1074/jbc.M200873200.
- Landfear, S. M. and Ignatushchenko, M. (2001) 'The flagellum and flagellar pocket of trypanosomatids', *Molecular and Biochemical Parasitology*, 115(1), pp. 1–17. doi: 10.1016/S0166-6851(01)00262-6.
- Langousis, G. *et al.* (2016) 'Loss of the BBSome perturbs endocytic trafficking and disrupts virulence of Trypanosoma brucei', *Proceedings of the National Academy of Sciences of the United States of America*, 113(3), pp. 632–637. doi: 10.1073/pnas.1518079113.
- Lemos, M. *et al.* (2019) 'Timing and original features of flagellum assembly in trypanosomes during development in the tsetse fly', *bioRxiv*. doi: 10.1101/728964.
- Li, Z. *et al.* (2008) 'Identification of a novel chromosomal passenger complex and its unique localization during cytokinesis in Trypanosoma brucei', *PLoS ONE*, 3(6). doi: 10.1371/journal.pone.0002354.
- Li, Z. and Wang, C. C. (2008) 'KMP-11, a basal body and flagellar protein, is required for cell division in Trypanosoma brucei', *Eukaryotic Cell*, 7(11), pp. 1941–1950. doi: 10.1128/EC.00249-08.
- Manna, P. T. *et al.* (2017) 'Lineage-specific proteins essential for endocytosis in trypanosomes', *Journal of Cell Science*, 130(8), pp. 1379–1392. doi: 10.1242/jcs.191478.
- Manna, P. T. and Field, M. C. (2015) 'Phosphoinositides, kinases and adaptors coordinating endocytosis in Trypanosoma brucei', *Communicative and Integrative Biology*, 8(6), pp. 1–4. doi: 10.1080/19420889.2015.1082691.
- Manna, P. T., Kelly, S. and Field, M. C. (2013) 'Adaptin evolution in kinetoplastids and emergence of the variant surface glycoprotein coat in African trypanosomatids', *Molecular Phylogenetics and Evolution*, 67(1), pp. 123–128. doi: 10.1016/j.ympev.2013.01.002.
- McAllaster, M. R. *et al.* (2015) 'Proteomic identification of novel cytoskeletal proteins associated with TbPLK, an essential regulator of cell morphogenesis in Trypanosoma brucei', *Molecular Biology of the Cell*, 26(17), pp. 3013–3029. doi: 10.1091/mbc.E15-04-0219.
- McMahon, H. T. and Boucrot, E. (2011) 'Molecular mechanism and physiological functions of clathrin-mediated endocytosis', *Nature Reviews Molecular Cell Biology*, 12, pp. 517–533. doi: 10.1038/nrm3151.
- Mitchell, A. L. *et al.* (2019) 'InterPro in 2019: Improving coverage, classification and access to protein sequence annotations', *Nucleic Acids Research*, 47(1), pp. 351–360. doi: 10.1093/nar/gky1100.
- Moreira, B. P. *et al.* (2017) 'Giant FAZ10 is required for flagellum attachment zone stabilization and furrow positioning in Trypanosoma brucei', *Journal of Cell Science*, 130(6), pp. 1179–1193. doi: 10.1242/jcs.194308.

- Morriswood, B. *et al.* (2009) 'The bilobe structure of *Trypanosoma brucei* contains a MORN-repeat protein', *Molecular and Biochemical Parasitology*, 167(2), pp. 95–103. doi: 10.1016/j.molbiopara.2009.05.001.
- Morriswood, B. *et al.* (2013) 'Novel bilobe components in *Trypanosoma brucei* identified using proximity-dependent biotinylation', *Eukaryotic Cell*, 12(2), pp. 356–367. doi: 10.1128/EC.00326-12.
- Morriswood, B. (2015) 'Form, Fabric, and Function of a Flagellum-Associated Cytoskeletal Structure', *Cells*, 4(4), pp. 726–747. doi: 10.3390/cells4040726.
- Morriswood, B. and Schmidt, K. (2015) 'A morn repeat protein facilitates protein entry into the flagellar pocket of *Trypanosoma brucei*', *Eukaryotic Cell*, 14(11), pp. 1081–1093. doi: 10.1128/EC.00094-15.
- Mukhopadhyay, A. G. and Dey, C. S. (2016) 'Reactivation of flagellar motility in demembrated *Leishmania* reveals role of cAMP in flagellar wave reversal to ciliary waveform', *Scientific Reports*, 6. doi: 10.1038/srep37308.
- Nozaki, T., Haynes, P. A. and Cross, G. A. M. (1996) 'Characterization of the *Trypanosoma brucei* homologue of a *Trypanosoma cruzi* flagellum-adhesion glycoprotein', *Molecular and Biochemical Parasitology*, 82(2), pp. 245–255. doi: 10.1016/0166-6851(96)02741-7.
- Oberholzer, M. *et al.* (2011) 'Independent analysis of the flagellum surface and matrix proteomes provides insight into flagellum signaling in mammalian-infectious *Trypanosoma brucei*', *Molecular and Cellular Proteomics*, 10(10). doi: 10.1074/mcp.M111.010538.
- Oberholzer, M., Saada, E. A. and Hill, K. L. (2015) 'Cyclic AMP regulates social behavior in african trypanosomes', *mBio*, 6(3), pp. 1–11. doi: 10.1128/mBio.01954-14.
- Patel, N. *et al.* (2008) '*Leishmania* requires Rab7-mediated degradation of endocytosed hemoglobin for their growth', *Proceedings of the National Academy of Sciences of the United States of America*, 105(10), pp. 3980–3985. doi: 10.1073/pnas.0800404105.
- Pellé, R., Schramm, V. L. and Parkin, D. W. (1998) 'Molecular cloning and expression of a purine-specific N-ribohydrolase from *Trypanosoma brucei* brucei sequence: Expression and molecular analysis', *Journal of Biological Chemistry*, 273(4), pp. 2118–2126. doi: 10.1074/jbc.273.4.2118.
- Perdomo, D., Bonhivers, M. and Robinson, D. R. (2016) 'The trypanosome flagellar pocket collar and its ring forming protein—TbBILBO1', *Cells*, 5(1), p. 9. doi: 10.3390/cells5010009.
- Perry, J. A. *et al.* (2018) 'TbSmee1 regulates hook complex morphology and the rate of flagellar pocket uptake in *Trypanosoma brucei*', *Molecular Microbiology*, 107(3), pp. 344–362. doi: 10.1111/mmi.13885.
- Price, H. P. *et al.* (2013) 'The *Leishmania major* BBSome subunit BBS1 is essential for parasite virulence in the mammalian host', *Molecular Microbiology*, 90(3), pp. 597–611. doi: 10.1111/mmi.12383.
- Robinson, D. R. *et al.* (1995) 'Microtubule polarity and dynamics in the control of organelle positioning, segregation, and cytokinesis in the trypanosome cell cycle', *Journal of Cell Biology*, 128(6), pp. 1163–1172. doi: 10.1083/jcb.128.6.1163.
- Rocha, G. M. *et al.* (2006) 'The flagellar attachment zone of *Trypanosoma cruzi*

- epimastigote forms', *Journal of Structural Biology*, 154(1), pp. 89–99. doi: 10.1016/j.jsb.2005.11.008.
- Rotureau, B. *et al.* (2014) 'Flagellar adhesion in *Trypanosoma brucei* relies on interactions between different skeletal structures in the flagellum and cell body', *Journal of Cell Science*, 127(1), pp. 204–215. doi: 10.1242/jcs.136424.
- Rotureau, Brice *et al.* (2014) 'Flagellar adhesion in *Trypanosoma brucei* relies on interactions between different skeletal structures in the flagellum and cell body', *Journal of Cell Science*, 127(1), pp. 204–215. doi: 10.1242/jcs.136424.
- Rotureau, B., Subota, I. and Bastin, P. (2011) 'Molecular bases of cytoskeleton plasticity during the *Trypanosoma brucei* parasite cycle', *Cellular Microbiology*, 13(5), pp. 705–716. doi: 10.1111/j.1462-5822.2010.01566.x.
- Salmon, D. (2018) 'Adenylate cyclases of *Trypanosoma brucei*, environmental sensors and controllers of host innate immune response', *Pathogens*, 7(2). doi: 10.3390/pathogens7020048.
- Schell, D., Borowy, N. K. and Overath, P. (1991) 'Transferrin is a growth factor for the bloodstream form of *Trypanosoma brucei*', *Parasitology Research*, 77(7), pp. 558–560. doi: 10.1007/BF00931012.
- Schneider, C. A., Rasband, W. S. and Eliceiri, K. W. (2012) 'NIH Image to ImageJ: 25 years of image analysis', *Nature Methods*, 9(7), pp. 671–675. doi: 10.1038/nmeth.2089.
- Sherwin, T. and Gull, K. (1989) 'The cell division cycle of *Trypanosoma brucei brucei*: timing of event markers and cytoskeletal modulations.', *Philosophical transactions of the Royal Society of London. Series B, Biological sciences*, 323(1218), pp. 573–588. doi: 10.1098/rstb.1989.0037.
- Silverman, J. S. *et al.* (2011) 'Late endosomal Rab7 regulates lysosomal trafficking of endocytic but not biosynthetic cargo in *Trypanosoma brucei*', *Molecular Microbiology*, 82(3), pp. 664–678. doi: 10.1111/j.1365-2958.2011.07842.x.
- Sinclair-Davis, A. N., McAllaster, M. R. and De Graffenried, C. L. (2017) 'A functional analysis of TOEFAZ1 uncovers protein domains essential for cytokinesis in *Trypanosoma brucei*', *Journal of Cell Science*, 130(22), pp. 3918–3932. doi: 10.1242/jcs.207209.
- De Souza, W. (2009) 'Structural organization of *Trypanosoma cruzi*', *Memorias do Instituto Oswaldo Cruz*, 104, pp. 89–100. doi: 10.1590/s0074-02762009000900014.
- Steverding, D. *et al.* (1995) 'Transferrin-binding protein complex is the receptor for transferrin uptake in *Trypanosoma brucei*', *Journal of Cell Biology*, 131(5), pp. 1173–1182. doi: 10.1083/jcb.131.5.1173.
- Steverding, D. (2000) 'The transferrin receptor of *Trypanosoma brucei*', *Parasitology International*, 48(3), pp. 191–198. doi: 10.1016/S1383-5769(99)00018-5.
- Subota, I. *et al.* (2014) 'Proteomic analysis of intact flagella of procyclic *Trypanosoma brucei* cells identifies novel flagellar proteins with unique sub-localization and dynamics', *Molecular and Cellular Proteomics*, 13(7), pp. 1769–1786. doi: 10.1074/mcp.M113.033357.
- Sun, S. Y. *et al.* (2012) 'An intracellular membrane junction consisting of flagellum adhesion glycoproteins links flagellum biogenesis to cell morphogenesis in *Trypanosoma brucei*',

Journal of Cell Science, 126(2), pp. 520–531. doi: 10.1242/jcs.113621.

Sun, S. Y. *et al.* (2013) 'An intracellular membrane junction consisting of flagellum adhesion glycoproteins links flagellum biogenesis to cell morphogenesis in *Trypanosoma brucei*', *Journal of Cell Science*, 126(2), pp. 520–531. doi: 10.1242/jcs.113621.

Sun, S. Y. *et al.* (2018) 'Flagellum couples cell shape to motility in *Trypanosoma brucei*', *Proceedings of the National Academy of Sciences of the United States of America*, 115(26), pp. 5916–5925. doi: 10.1073/pnas.1722618115.

Sunter *et al.* (2015) 'A dynamic coordination of flagellum and cytoplasmic cytoskeleton assembly specifies cell morphogenesis in trypanosomes', 128(8), pp. 1580–1594. doi: 10.1242/jcs.166447.

Sunter, Jack D. *et al.* (2015) 'Modulation of flagellum attachment zone protein FLAM3 and regulation of the cell shape in *Trypanosoma brucei* life cycle transitions', *Journal of Cell Science*. doi: 10.1242/jcs.171645.

Sunter, J. D. *et al.* (2015) 'Modulation of flagellum attachment zone protein FLAM3 and regulation of the cell shape in *Trypanosoma brucei* life cycle transitions', *Journal of Cell Science*, 128(16), pp. 3117–3130. doi: 10.1242/jcs.171645.

Sunter, J. D. *et al.* (2019) 'Leishmania flagellum attachment zone is critical for flagellar pocket shape, development in the sand fly, and pathogenicity in the host', *Proceedings of the National Academy of Sciences*, 116(13), pp. 6351–6360. doi: 10.1073/pnas.1812462116.

Sunter, J. D. and Gull, K. (2016) 'The Flagellum Attachment Zone: "The Cellular Ruler" of Trypanosome Morphology', *Trends in Parasitology*. Elsevier Ltd, 32(4), pp. 309–324. doi: 10.1016/j.pt.2015.12.010.

Sunter, J. and Gull, K. (2017) 'Shape, form, function and Leishmania pathogenicity: from textbook descriptions to biological understanding: Sunter J, Gull K', *Open Biology*, 7(170165). doi: 10.1098/rsob.170165.

Tripodi, K. E. J., Menendez Bravo, S. M. and Cricco, J. A. (2011) 'Role of heme and heme-proteins in trypanosomatid essential metabolic pathways', *Enzyme Research*, 2011(1). doi: 10.4061/2011/873230.

Vanhollebeke, B. *et al.* (2008) 'A haptoglobin-hemoglobin receptor conveys innate immunity to *Trypanosoma brucei* in humans', *Science*, 320(5876), pp. 677–681. doi: 10.1126/science.1156296.

Vaughan, S. *et al.* (2008) 'A Repetitive Protein Essential for the Flagellum Attachment Zone Filament Structure and Function in *Trypanosoma brucei*', *Protist*, 159(1), pp. 127–136. doi: 10.1016/j.protis.2007.08.005.

Vaughan, S. and Gull, K. (2016) 'Basal body structure and cell cycle-dependent biogenesis in *Trypanosoma brucei*', *Cilia*. BioMed Central, 5(1), pp. 1–7. doi: 10.1186/s13630-016-0023-7.

Vickerman, K. (1969) 'On the surface coat and flagellar adhesion in trypanosomes.', *Journal of cell science*, 5(1), pp. 163–193.

Vidilaseris, K. *et al.* (2015) 'Assembly mechanism of *Trypanosoma brucei* BILBO1 at the flagellar pocket collar', *Communicative and Integrative Biology*, 8(1), pp. 1–3. doi:

10.4161/19420889.2014.992739.

Wheeler, R. J. *et al.* (2013) 'Cytokinesis in trypanosoma brucei differs between bloodstream and tsetse trypomastigote forms: Implications for microtubule-based morphogenesis and mutant analysis', *Molecular Microbiology*, 90(6), pp. 1339–1355. doi: 10.1111/mmi.12436.

Wheeler, R. J. (2017) 'Use of chiral cell shape to ensure highly directional swimming in trypanosomes', *PLoS Computational Biology*, 13(1). doi: 10.1371/journal.pcbi.1005353.

Wheeler, R. J., Gluenz, E. and Gull, K. (2011) 'The cell cycle of Leishmania: Morphogenetic events and their implications for parasite biology', *Molecular Microbiology*, 79(3), pp. 647–662. doi: 10.1111/j.1365-2958.2010.07479.x.

Wheeler, R. J., Gluenz, E. and Gull, K. (2013) 'The limits on trypanosomatid morphological diversity', *PLoS ONE*, 8(11). doi: 10.1371/journal.pone.0079581.

Wheeler, R. J., Gull, K. and Sunter, J. D. (2019) 'Coordination of the Cell Cycle in Trypanosomes', *Annual Review of Microbiology*, 73, pp. 133–154. doi: 10.1146/annurev-micro-020518-115617.

Wheeler, R. J., Sunter, J. D. and Gull, K. (2016) 'Flagellar pocket restructuring through the Leishmania life cycle involves a discrete flagellum attachment zone', *Journal of Cell Science*, 129(4), pp. 854–867. doi: 10.1242/jcs.183152.

Wingfield, J. L., Lechtreck, K. F. and Lorentzen, E. (2018) 'Trafficking of ciliary membrane proteins by the intraflagellar transport/BBSome machinery', *Essays in Biochemistry*, 62(6), pp. 753–763. doi: 10.1042/EBC20180030.

Woods, K. *et al.* (2013) 'Identification and Characterization of a Stage Specific Membrane Protein Involved in Flagellar Attachment in Trypanosoma brucei', *PLoS ONE*, 8(1). doi: 10.1371/journal.pone.0052846.

Zhang, X. *et al.* (2019) 'Functional Analyses of Cytokinesis Regulators in Bloodstream Stage Trypanosoma brucei Parasites Identify Functions and Regulations Specific to the Life Cycle Stage', *mSphere*, 4(3). doi: 10.1128/msphere.00199-19.

Zhou, Q. *et al.* (2010) 'A comparative proteomic analysis reveals a new bi-lobe protein required for bi-lobe duplication and cell division in Trypanosoma brucei', *PLoS ONE*, 5(3). doi: 10.1371/journal.pone.0009660.

Zhou, Q. *et al.* (2011) 'A coiled-coil- and C2-domain-containing protein is required for FAZ assembly and cell morphology in Trypanosoma brucei', *Journal of Cell Science*. doi: 10.1242/jcs.087676.

Zhou, Q. *et al.* (2015) 'Assembly and maintenance of the flagellum attachment zone filament in Trypanosoma brucei', *Journal of Cell Science*, 128(13), pp. 2361–2372. doi: 10.1242/jcs.168377.

Zhou, Qing *et al.* (2015) 'Assembly and maintenance of the flagellum attachment zone filament in Trypanosoma brucei', *Journal of Cell Science*. doi: 10.1242/jcs.168377.

Zhou, Q. *et al.* (2016) 'Two distinct cytokinesis pathways drive trypanosome cell division initiation from opposite cell ends', *Proceedings of the National Academy of Sciences of the United States of America*, 113(12), pp. 3287–3292. doi: 10.1073/pnas.1601596113.

Zhou, Q., Lee, K. J., *et al.* (2018) 'Faithful chromosome segregation in *Trypanosoma brucei* requires a cohort of divergent spindle-associated proteins with distinct functions', *Nucleic Acids Research*, 46(16), pp. 8216–8231. doi: 10.1093/nar/gky557.

Zhou, Q., An, T., *et al.* (2018) 'The CIF1 protein is a master orchestrator of trypanosome cytokinesis that recruits several cytokinesis regulators to the cytokinesis initiation site', *Journal of Biological Chemistry*, 293(42), pp. 16177–16192. doi: 10.1074/jbc.RA118.004888.

Zhou, Q., Hu, H. and Li, Z. (2016) 'An EF-hand-containing protein in *Trypanosoma brucei* regulates cytokinesis initiation by maintaining the stability of the cytokinesis initiation factor CIF1', *Journal of Biological Chemistry*, 291(28), pp. 14395–14409. doi: 10.1074/jbc.M116.726133.

Chapter 9

Appendix

Appendix A

Primers for tagging FAZ orthologs in *L.mexicana*

N-terminal

GeneID	Upstream forward	Upstream reverse	5' sgRNA
LmxM.02.0140	GAGCCATCCAGCCCTCCTCTGTCTCCTgtataatgcagacctgctgc	TTTGCTTCTGCCGCCAGCGAACTCCATactaccgatcctgatccag	gaaattaatcgactcactataggCTGGACGTGAGTAAGCGTGGgttttagagctagaaatagc
LmxM.04.0890	CATACCCCGTGCCTCCCCCTCCCCGgtataatgcagacctgctgc	CCGGCTGGGCTCGACGCGGTTCCCATactaccgatcctgatccag	gaaattaatcgactcactataggATGGCGGCTTCGCAGAGgttttagagctagaaatagc
LmxM.04.1100	AACCTCGTGTGACGCTCCTGTGTCTgtataatgcagacctgctgc	CGCCGCTGCTGTGGCTTACTCGGACATactaccgatcctgatccag	gaaattaatcgactcactataggGGGAGAGAGGGAGGGGTGCGgttttagagctagaaatagc
LmxM.09.0520	ACACGAACGTATCCTCCACGGACTTCGCCTgtataatgcagacctgctgc	CGTGGCCAACGTCTGAACGGCTGCGCTCATactaccgatcctgatccag	gaaattaatcgactcactataggAGAGAGTTTACGACGAGAGgttttagagctagaaatagc
LmxM.09.1050	CGTGTCCCTTGGTGCAGCGACGGGAACCCgtataatgcagacctgctgc	CACGATGATGTTGGGGCTTAGCATCCATactaccgatcctgatccag	gaaattaatcgactcactataggTTTCCGTCTTCTCTCGgttttagagctagaaatagc
LmxM.10.0620	TCGCGCACTCTCTCTTAGAGCAGACCCgtataatgcagacctgctgc	CGCAGACTCGACGGATGACGCTCCATactaccgatcctgatccag	gaaattaatcgactcactataggGTGCGTCAACGTCTTTATgttttagagctagaaatagc
LmxM.11.1320	AGGATACAGTTGCTCATCTTCTCTCTgtataatgcagacctgctgc	TGGACCAACTACCAGCTTTGGGTGCCATactaccgatcctgatccag	gaaattaatcgactcactataggACTTGGACAAAAACAGGCGgttttagagctagaaatagc
LmxM.12.0360	TCTCCGCAACCCCTCCCCGCGCTCCGgtataatgcagacctgctgc	GTCCAGCGCCCAATGAGTGAGACAACCATactaccgatcctgatccag	gaaattaatcgactcactataggACAGCAGCGTAGGTGGCCTGgttttagagctagaaatagc
LmxM.12.1120	GCACGACGGGAAAGTTTATTTTCTCCAgataatgcagacctgctgc	CGCCATCGTAAGGGCGGGATGACGTCACTactaccgatcctgatccag	gaaattaatcgactcactataggGAAGGTAAGGGGCAGAAACgttttagagctagaaatagc
LmxM.12.1190	CCCGCGCTCTGACGCGGTCCACCCgtataatgcagacctgctgc	GTCACCGCGTGGAGCCATGAAAGTGCATactaccgatcctgatccag	gaaattaatcgactcactataggTTCACGAGCGCGCGAGTTgttttagagctagaaatagc
LmxM.13.1590	TTTTCTTGTCTGATTGTGCTCTCTgtataatgcagacctgctgc	CTGCCCTGCAACACGAGACGCGACATactaccgatcctgatccag	gaaattaatcgactcactataggCGGCACAAAAATAATTAGCAgttttagagctagaaatagc
LmxM.13.1610	CTACCGGTGAGCTTCATTTCTTTCTCTgtataatgcagacctgctgc	AACAAGCAGCTGCTTACGCTGCGACTCCATactaccgatcctgatccag	gaaattaatcgactcactataggGCCCTTGGTTCAAGTTCAAgttttagagctagaaatagc
LmxM.14.1200	TCTCTTTTCCACTCACTCACATATAGCgtataatgcagacctgctgc	CGCCACTCGTATCTGACCCGATGCATactaccgatcctgatccag	gaaattaatcgactcactataggGCATCACACAGGACTGCCATgttttagagctagaaatagc
LmxM.16.0490	CAACGGACCGAAACACCAGAAGCTACCCGgtataatgcagacctgctgc	CATGAAGACGAATACGCGGACGACTTCACTactaccgatcctgatccag	gaaattaatcgactcactataggGCTGCACGGTGACACAGATCgttttagagctagaaatagc
LmxM.16.1660	CTCTGCGCTGGAGGTTGCGGTTTGGCGgtataatgcagacctgctgc	GGCTGGTGTGGCGCTCGTGGCCCTCATactaccgatcctgatccag	gaaattaatcgactcactataggTGTGGCGTTGTTCTGTGTgttttagagctagaaatagc
LmxM.18.1080	CCTCTTTCGCGCTTAAGATTTTGTCTgtataatgcagacctgctgc	CCATTTGGAAGCTTCGGCTTGGTGTATCACTactaccgatcctgatccag	gaaattaatcgactcactataggTAAGGATACGACCGAGCAAgttttagagctagaaatagc
LmxM.18.1440	CATCTCTCGTTTATCTGCCACGCTCTgtataatgcagacctgctgc	CATCTGCTCGCGGAGATCCGGCCCATactaccgatcctgatccag	gaaattaatcgactcactataggGATGGTCTCTGGTACGCAGgttttagagctagaaatagc

LmxM.18.1560	AGACGTCGTGCCAGCTTTGCTCCATCCGgtataatgcagacctgctgc	CGATTATGTGCAGGGTGCACCGGGAACATactaccgatcctgatccag	gaaattaacgactcactataggCTTGTTGTTGTCGGTATgttttagagctagaatagc
LmxM.19.0140	TCGCAGTGCCCTTTTTGTTTTCTATCTGtataatgcagacctgctgc	GCTCGCCCCGTTGTCGCTACTCGGTCATactaccgatcctgatccag	gaaattaacgactcactataggCGCGGCACCTCGATAAAAAgttttagagctagaatagc
LmxM.19.0680	TCTCGACCCGCTCGTCCAGGACAGCCGgtataatgcagacctgctgc	GAGGGAGCGGGCAGACATGGATCCGTTTactaccgatcctgatccag	gaaattaacgactcactataggAGGATGTAGCAAGATGGCAAgtttagagctagaatagc
LmxM.21.0700	TGTCACGTAAAAGCGAGCGGTAGTTTCATgtataatgcagacctgctgc	CTTGATGCGCACCACTAAATCTCCATactaccgatcctgatccag	gaaattaacgactcactataggACATTCGGGAGGTCTGATTGgttttagagctagaatagc
LmxM.21.0940	CTCGGCTCTCTCACTCTCACTGTACAgataatgcagacctgctgc	GCGCAGCGGCGACTCGAGAGAGGACGGCATactaccgatcctgatccag	gaaattaacgactcactataggCTGCTGTTGGTTCGCGACgttttagagctagaatagc
LmxM.21.1220	CTCCCCACAACACTCGCACTACGCCAgataatgcagacctgctgc	ATCATAGCGTTCAGTTGCGGTTTTCCATactaccgatcctgatccag	gaaattaacgactcactataggCACGAGTAAGCCGCGTGCgttttagagctagaatagc
LmxM.21.1240	AGACGAAGAAGGAAACCCTCAGCACAgataatgcagacctgctgc	CTCCGCCGGGAGTGGGGCGGTACATCAactaccgatcctgatccag	gaaattaacgactcactataggAATACTGTCAGCTGCGTGCgttttagagctagaatagc
LmxM.21.1350	GCTCTACCTCCACCACCCCTTCCCTCCgtataatgcagacctgctgc	GCCGCTGCCTTATCTCCACGTAGCTCAactaccgatcctgatccag	gaaattaacgactcactataggAGACGAACGTGTGCGACGGCgttttagagctagaatagc
LmxM.22.1010	GTCACGCCGGGGAGGGGGGGCGCACCGgtataatgcagacctgctgc	GCTATCTGCGAACCCGCGTCAACGACATactaccgatcctgatccag	gaaattaacgactcactataggAGAAAAGACAAAACGACAGgttttagagctagaatagc
LmxM.22.1320	TTACGTCGTATATCTTATTCTCACACTgtataatgcagacctgctgc	CGCCGCTGTGGTAGATGCCGCTAGAGCAactaccgatcctgatccag	gaaattaacgactcactataggGGGAGACGATGTTGGAAGAGgttttagagctagaatagc
LmxM.23.0080	ACACACACACACACACAGCACAGACAgataatgcagacctgctgc	CTCGGTGGGACTATCGTCCGTGACATactaccgatcctgatccag	gaaattaacgactcactataggCAACAATAACACGTCACAAgttttagagctagaatagc
LmxM.24.0700	GGTGGTGTGCGCCAGCCCAAGAAAAAgtataatgcagacctgctgc	GGCCGCCGCTGCCGCTGTTTTGCGCACATactaccgatcctgatccag	gaaattaacgactcactataggACTTTCGATTTGTGAGCCAgttttagagctagaatagc
LmxM.24.1430	GCGAGTGCAGCTCGTACAGGAGACAGGAGCgtataatgcagacctgctgc	GGGTTGACGACGGTGGTGGACCGTTCATactaccgatcctgatccag	gaaattaacgactcactataggGCGCTCCGCTTTTGTGATTgttttagagctagaatagc
LmxM.27.0490	GCATCGTACAACCGTTTTTCTTTTTCGCTgtataatgcagacctgctgc	TGTTTCGTGGTGAGAAGATGCCCATCAactaccgatcctgatccag	gaaattaacgactcactataggGACGTCACGAAATAAGATGgttttagagctagaatagc
LmxM.27.1040	CCTTTTTCCCTTTTCATATCTTTTCCAgataatgcagacctgctgc	TGGGAAGTCCCGTGCCGTTGCGTGCATactaccgatcctgatccag	gaaattaacgactcactataggACGTGTGTTACGTGGAATGgttttagagctagaatagc
LmxM.27.1400	TTCTTGATTGGTTAGACTGTGTTACCTgtataatgcagacctgctgc	CGTGAGCAACCCGTAAGCACTCGGACATactaccgatcctgatccag	gaaattaacgactcactataggTCACAGCGCTCTGCAAGgttttagagctagaatagc
LmxM.28.1650	ACGCACTCGCACATGTGCGTCATATCTgtataatgcagacctgctgc	GCCGATGCTAAGTACCTTCTGCGAATCAactaccgatcctgatccag	gaaattaacgactcactataggCGTCGTCGCTGCTTTTTCTgttttagagctagaatagc
LmxM.29.2580	CATATATACACACACTACTCCCCCTCCgtataatgcagacctgctgc	CCCCGTAACCTCTCGGATGGCCGACATactaccgatcctgatccag	gaaattaacgactcactataggAGCTCGTGTGGGTTAAGgttttagagctagaatagc
LmxM.29.2670	TGTATATCGACATCAAAGTGCACAACCAAgataatgcagacctgctgc	ACGACGGTTTTCAAAGGCCAGTCAACCAactaccgatcctgatccag	gaaattaacgactcactataggGGTTTTTTTTCTTCTTTgttttagagctagaatagc
LmxM.30.2590	TCCGTCGTCTTCATTTTGTGCGGACGCCgtataatgcagacctgctgc	CACCTTGTGGCAGCTCCGCGGACGACATactaccgatcctgatccag	gaaattaacgactcactataggGCCTACGTGAGAGCGGTTTgttttagagctagaatagc
LmxM.30.3110	GCCTGCGTGGCAGAGACACCTGCTCGTgtataatgcagacctgctgc	CACGCTGATTTCTCAGGAGCAGTGACATactaccgatcctgatccag	gaaattaacgactcactataggTTCTAGCCTCGCACTACAGgttttagagctagaatagc
LmxM.31.0220	TGTGAGGAGAAAGCGACCAAGAGACTCCAgataatgcagacctgctgc	ACTCTGGCACTGGCAGAGAGGTGAACATactaccgatcctgatccag	gaaattaacgactcactataggGCGCGCCTGCGCTCACgttttagagctagaatagc
LmxM.31.0140	CGAGGGGGAGGGTTAGGGTACAGAGACCGgtataatgcagacctgctgc	CGAGGCTATTTACACCCACCGTGTCAactaccgatcctgatccag	gaaattaacgactcactataggTGACAGTTGAGGCTCCGGgttttagagctagaatagc
LmxM.31.2610	TTGCTGCACAACGAGCGACGTCCTCTCTgtataatgcagacctgctgc	CTCACTGCTGTAAGTGTAGTGGCTCAactaccgatcctgatccag	gaaattaacgactcactataggTCTGATGCAAGAACTGTGgttttagagctagaatagc

LmxM.31.2680	ACACACACACAATATCTTCAACAGTCCgtataatgcagacctgctgc	GCCGCTCATCGGTACGAGCGGTTCTGGCATactaccgatcctgatccag	gaaattaatcgactcactataggCTGATAGGCAGGGCCGAAAGgttttagagctagaatagc
LmxM.32.1035	CAAGGTGATTGTCATTCAGTCGAGCAGCCAgtataatgcagacctgctgc	CTCCTTGTTCTTGGAAAGTGCTGCACCCCActaccgatcctgatccag	gaaattaatcgactcactataggATTAATACTTGTGACGTGAGgttttagagctagaatagc
LmxM.32.2460	TCACTCCACAGCACCCCTCATCTCTGCAgtataatgcagacctgctgc	CAGCTCTTGGGTGTCGGGACAAGCGACATactaccgatcctgatccag	gaaattaatcgactcactataggAGCACAAAGTTCGTTGAAGCgttttagagctagaatagc
LmxM.33.0060	CGTATTACCTGTTGTGCGTGCAGCGCCCCgtataatgcagacctgctgc	TACCCACATAGCCGAATTCGACATGCATactaccgatcctgatccag	gaaattaatcgactcactataggTTTCAAAGCCGAGCCGATGgttttagagctagaatagc
LmxM.33.0190	AATCATCTAAAGCCCTCCCGCTCTCTCCgtataatgcagacctgctgc	CACAGCAGGGGCGACAATCTCTCCGTCATactaccgatcctgatccag	gaaattaatcgactcactataggGATATATAAAGCGTATGTGAgtttagagctagaatagc
LmxM.33.0690	AACCCCGAAAGTTTTAGTGTGACTCCgtataatgcagacctgctgc	GGGGGATTGATGTTGCTCGAAAAGACATactaccgatcctgatccag	gaaattaatcgactcactataggTATGTTGTTGATTTTTCTgttttagagctagaatagc
LmxM.33.2540	CTCTTATCTCCCGTTTTCAAGTGTTCGgtataatgcagacctgctgc	CACAGAGTCGACGGGTGCTATACGGGACATactaccgatcctgatccag	gaaattaatcgactcactataggAGCTGGACAGCAGACAACAgtttagagctagaatagc
LmxM.33.2570	TGAAAACGACGTTAGTCCCTCACTCTCCgtataatgcagacctgctgc	GCTACCCAGGAGCTCAAGCGGCTCATactaccgatcctgatccag	gaaattaatcgactcactataggAAGGGAGTTGTGGGATGTGgttttagagctagaatagc
LmxM.34.2221	CCTATCCATTTAACCCACACCAACACCAgtataatgcagacctgctgc	CGCCGAAAACCTCTGTACGTGGTGGCCATactaccgatcctgatccag	gaaattaatcgactcactataggGAGCGCGTAAAGGAGAGGGgttttagagctagaatagc
LmxM.34.3720	ACTCTGCGTGTTCCTCACTCCCGTCCgtataatgcagacctgctgc	CGCAACAGGGTCCATTGTGGCGAGTCCATactaccgatcctgatccag	gaaattaatcgactcactataggTGCTTCTCGTGTGCGGAGgttttagagctagaatagc
LmxM.34.5010	CTTCCGTTTTCTCCCGCTCGTGTTCGgtataatgcagacctgctgc	CTTCTTGCCTAAGATTTGGTACTTCTGCATactaccgatcctgatccag	gaaattaatcgactcactataggGCACACCACTGATGAGAAGTgttttagagctagaatagc
LmxM.36.0830	CACCGGGACGCGTTTTCTTTTCTCTCTgtataatgcagacctgctgc	CGAAGCAGAAGCCTGCGAAGAGTTGGCATactaccgatcctgatccag	gaaattaatcgactcactataggGCGTTTTGAAAACACCCAAAgtttagagctagaatagc
LmxM.36.1920	GAAGAGGAGAAATACTTTCAAGGAGATAGgtataatgcagacctgctgc	GGCGCCGTAGCCGACACTTGTGGGCTGCATactaccgatcctgatccag	gaaattaatcgactcactataggGCGAGCGAGCGAGTGCACACTgttttagagctagaatagc
LmxM.36.4330	AACACTTCTTCTCTCTGTCTTAGATCCTgtataatgcagacctgctgc	TGACGATGTGCTGCGGCGAGTGCCTGGCATactaccgatcctgatccag	gaaattaatcgactcactataggTCATCAAAGAAGACGTTGgttttagagctagaatagc
LmxM.36.5970	TCCCGCTGTGTTGTGCTGTGACTGCCTgtataatgcagacctgctgc	GCGCTTGCAGCGGGTGGCCGTTGCACATactaccgatcctgatccag	gaaattaatcgactcactataggCCAAAAAAACGTCGAAGgttttagagctagaatagc
LmxM.36.6960	GTTGACCATCGTTAGAGTTTGTCTTTGgtataatgcagacctgctgc	CTCGATAGACTGTTGCTGCTCCATCGTCATactaccgatcctgatccag	gaaattaatcgactcactataggCTTCCACTTTGTGCTGTGgttttagagctagaatagc

C-terminal

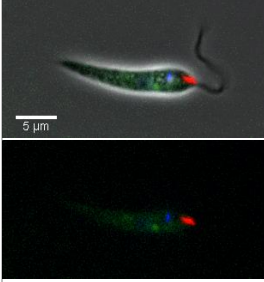
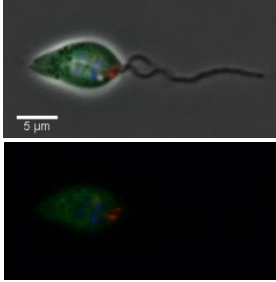
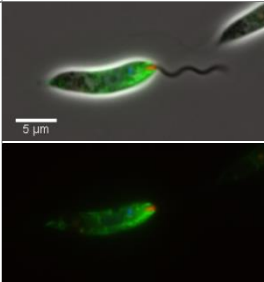
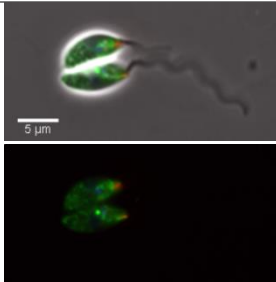
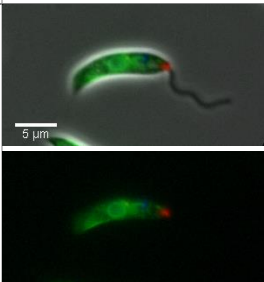
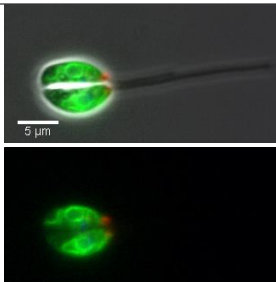
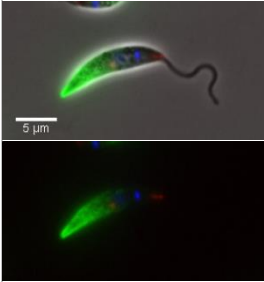
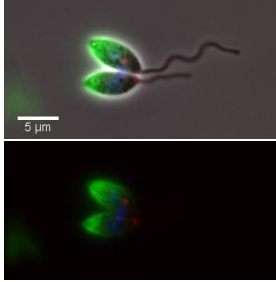
GeneID	Downstream forward	Downstream reverse	3' sgRNA
LmxM.02.0140	GCCGTGCAGAAATGTGCTGGAGGTCTTTCTAggttctgtagtggttccgg	GATACAGCTCGTGACGAGGGGGAGGGCCCAcaatttgagagacctgtgc	gaaattaatacactactataggAGGGATCGTCGCGTGTGATGgttttagagctagaaatagc
LmxM.04.0890	ACGCGTCGCTCAGCACCTCCACCAACTGggttctgtagtggttccgg	CCCAGCCACCCGACATCCCTCACCTCCCCcaatttgagagacctgtgc	gaaattaatacactactataggGGTGACAGTGTGTGCCTGTgttttagagctagaaatagc
LmxM.04.1100	CATTATCATCCGCTTGGCTCTCGCGCGCAggttctgtagtggttccgg	TTCTTTGGCCACCCGCCCTGCCCTCCGcaatttgagagacctgtgc	gaaattaatacactactataggAGTCCGTCTCAGACAGAGAGgttttagagctagaaatagc
LmxM.09.0520	TCGAGCTACACCGCAAGCGTTGCCTGTACTggttctgtagtggttccgg	CCTTGACCCCGCCCGCCTCTCTCCcaatttgagagacctgtgc	gaaattaatacactactataggAGGGAACGACGGCAAGCCAgttttagagctagaaatagc
LmxM.09.1050	GCGCATCTCGATGTGGAGGAGATGGCGGAGggttctgtagtggttccgg	GGTCATGTGCGATGGTGTCTGCTCCcaatttgagagacctgtgc	gaaattaatacactactataggATGTCGTGTGCGGTATCGgttttagagctagaaatagc
LmxM.10.0620	GAGGAGGGAAGTCGTAACCCACTGAACGGGggttctgtagtggttccgg	GAATGGTATTGTGCACTACGAGCTCTTcaatttgagagacctgtgc	gaaattaatacactactataggTACGGGGCCCTCTCTAGgttttagagctagaaatagc
LmxM.11.1320	TCCACTGTCTCCTTTGACGGTGAACCTGggttctgtagtggttccgg	GCACTGTGCGGACAATCAACGACAACCTTcaatttgagagacctgtgc	gaaattaatacactactataggTTCGTTGTGACTTTCCAGCGgttttagagctagaaatagc
LmxM.12.0360	AAAGCGATTGCGCTCAACATCATCAAGGAGggttctgtagtggttccgg	TCGGCTCTGTGTCAGTGCAGCCGTAACCCcaatttgagagacctgtgc	gaaattaatacactactataggAGGAAAGGCATCTGGCTGAGgttttagagctagaaatagc
LmxM.12.1120	TGTGAGATCTACCAGATCATTGTTGCTCCggttctgtagtggttccgg	AAGGGAGGAGGGGGACAGCAGGCTCGCTTcaatttgagagacctgtgc	gaaattaatacactactataggGGGCTGGTGAGGGCGTGTGcgttttagagctagaaatagc
LmxM.12.1190	GCGGTGGCAGATCAGGTCGTGCTGCTGCCggttctgtagtggttccgg	CCCACTCCCTCCCTCTCTGTTGCCAcaatttgagagacctgtgc	gaaattaatacactactataggGAATCGCTTGCATATTGTGgttttagagctagaaatagc
LmxM.13.1590	TTCTACCCTGATGAAAGCTGATGGAGGAGggttctgtagtggttccgg	AGGCTAGAGCAGAGATGTCGACGCGAAAAcaatttgagagacctgtgc	gaaattaatacactactataggGTGAATAAGACAACAAGgttttagagctagaaatagc
LmxM.13.1610	ACCCGCATGCTGGTGGCTGCGCCGCGggttctgtagtggttccgg	TCCGCGATCTGCTTAACGCTGTTCAgcaatttgagagacctgtgc	gaaattaatacactactataggTTCCTCCACTCACAACGCAGgttttagagctagaaatagc
LmxM.14.0120	TACCGCTACTACGGCTGCTCCATCGAAGggttctgtagtggttccgg	GTGTGTGTTGTGCTCTGGTGGCCTCCcaatttgagagacctgtgc	gaaattaatacactactataggTTTTTTTCTTACGCAGCGgttttagagctagaaatagc
LmxM.14.1200	CCGTACGAGCGGTACATCTTCTTTGGCGggttctgtagtggttccgg	CCTGCATGTGAGTGCCTCTCTCTTCTTcaatttgagagacctgtgc	gaaattaatacactactataggGGAGAGGGCGACAGGCAAAcgttttagagctagaaatagc
LmxM.16.0490	GACGACGACGACGACGACGACGACGAGggttctgtagtggttccgg	CCAACGGAATAGATGTATGGTTCGAGTGCcaatttgagagacctgtgc	gaaattaatacactactataggGTGCACGCTACCGGGGAAGgttttagagctagaaatagc
LmxM.16.1660	TACGAGGGCAAACGGCTCATGAACTCTGggttctgtagtggttccgg	GTGCAGACGACGCCAAGTTGTTTACCcgaatttgagagacctgtgc	gaaattaatacactactataggGGCTACGTGAACGGAACAAGgttttagagctagaaatagc
LmxM.18.1080	AACTTCTGCAACGGCCAGTATACGACGAGggttctgtagtggttccgg	CCGTGCTCCCCCTCCCTTTCCGCACTTcaatttgagagacctgtgc	gaaattaatacactactataggCAACACCTTGAAGCAGGAAGgttttagagctagaaatagc
LmxM.18.1440	CAAGTGTGGAGAAGATGAAGAATTTGATGggttctgtagtggttccgg	GACGCTCCACGACGACTACTCTCTCGcaatttgagagacctgtgc	gaaattaatacactactataggGCTACATCGTCTCTCTCTGgttttagagctagaaatagc
LmxM.18.1560	TCCGATGACGGCAACGGTCTAGACGCACCggttctgtagtggttccgg	TCCCGCAGCATATCATGCTGCCCTCTcaatttgagagacctgtgc	gaaattaatacactactataggAAAGAGGTGCGCTAGGCTGGgttttagagctagaaatagc
LmxM.19.0140	GTGCGCCCTCCAGGTGAAGAAGCTGGGcgttctgtagtggttccgg	GAACTGTGATTGTAAGGACCGCATCCCAcaatttgagagacctgtgc	gaaattaatacactactataggGTGAGCGAGTGTGAATATGgttttagagctagaaatagc

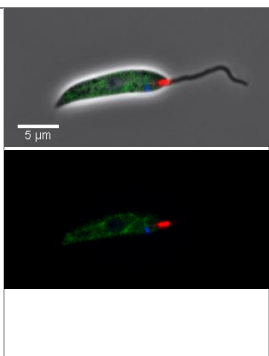
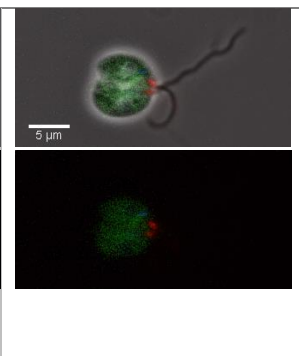
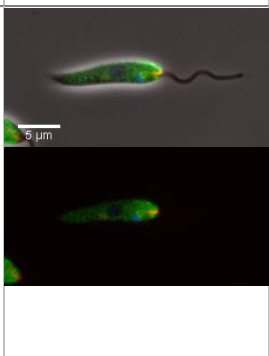
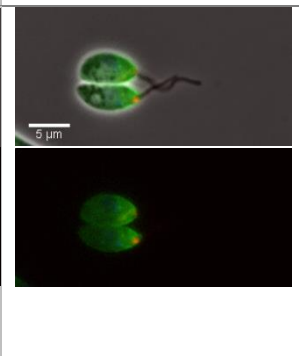
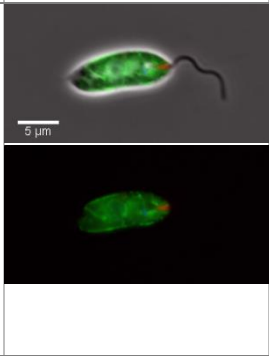
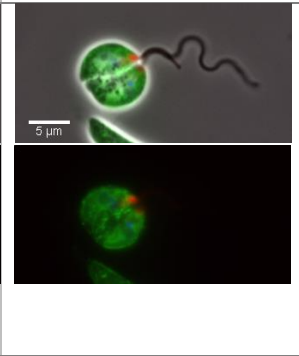
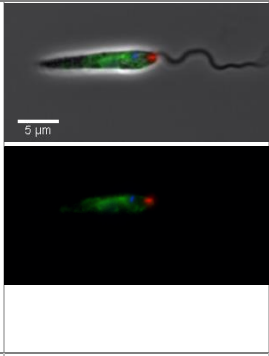
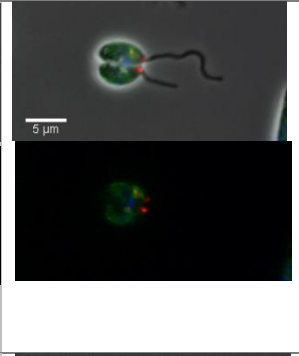
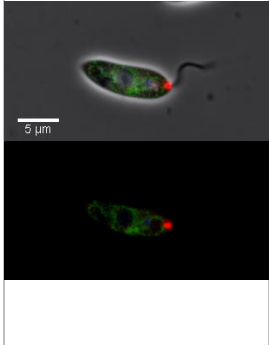
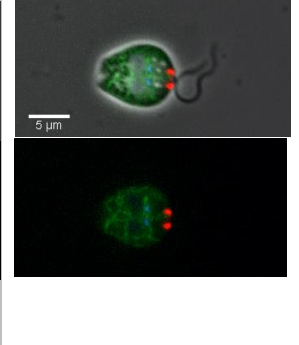
LmxM.19.0680	ACCCCTGCTCGAAACGGCAATACGGCGGCGggttctgtagtggttccgg	AGCGTCACGAGTGTGACCCGCACTCGCTccaattgagagacctgtgc	gaaattaacgactcactataggGAGAGGCGTCTGACTGATGgttttagagctagaaatagc
LmxM.21.0700	CCGTCGCTGATTTTCATCGAGGAGGACGCTggttctgtagtggttccgg	AAGAGATAGGCACGTGTGGGACCTCGGCCTccaattgagagacctgtgc	gaaattaacgactcactataggCTACCTGTACTCTTCCATCGgttttagagctagaaatagc
LmxM.21.0940	GTCGTGAACGGCTCTCTTCGCTACTCCGggttctgtagtggttccgg	CCCCTCTCTCTCTGTTTTTCGCGCTccaattgagagacctgtgc	gaaattaacgactcactataggTCGGCTGCTCTCGCGCTTACgttttagagctagaaatagc
LmxM.21.1220	CTGACAAGACGAACCCGTCACGACACGggttctgtagtggttccgg	CTAACCATACCGTTTCGTTCTTTTCCaattgagagacctgtgc	gaaattaacgactcactataggGCTGTGTGTTCAAGTACGTTgttttagagctagaaatagc
LmxM.21.1240	CCCTCAAATCGCCGTCGAGAACCAGGggttctgtagtggttccgg	TGTACATGGGCGCCAGATAAGGGATTCCccaattgagagacctgtgc	gaaattaacgactcactataggAGTTTGTGTGGAGTGTGCGgttttagagctagaaatagc
LmxM.21.1350	GCCATGGCGCAGCAGCAAGTCATCATGGCAGggttctgtagtggttccgg	GTGGTCTGGCATAGCAGCTCGAGCGCGccaattgagagacctgtgc	gaaattaacgactcactataggCGGTGTGTGAGGACTGTCGgttttagagctagaaatagc
LmxM.22.1010	TCGTACCACGAAAAGCAAGAAGACGAGggttctgtagtggttccgg	CCGTTGAACTCGCGGACCGCCCTTCTccaattgagagacctgtgc	gaaattaacgactcactataggAAAGGTACCGAGACGACGgttttagagctagaaatagc
LmxM.22.1320	CGTAGCAGCGCACATCCGACCTCTCGCggttctgtagtggttccgg	CACACATGCGTATTGCTTACATCAACcaattgagagacctgtgc	gaaattaacgactcactataggATCGACGTTCTATTTTCTgttttagagctagaaatagc
LmxM.23.0080	ACGGTGTGCGGAATCGACTTGAGTTGTTGggttctgtagtggttccgg	CACCACCAGAAAGACAAAACATTACATAGccaattgagagacctgtgc	gaaattaacgactcactataggTAAAGAACTCAGAGAGCAAgtttagagctagaaatagc
LmxM.24.0700	GAGGAGGAGGCCTCGATGGTGGTATCACAggttctgtagtggttccgg	TGCGCGCTGAGCAGCGCGCGCTCGACCCcaattgagagacctgtgc	gaaattaacgactcactataggCATGAGTCCCTCCAGAGCGgttttagagctagaaatagc
LmxM.24.1430	TACTTGAGAAGTGCCTCTCGGGTCTGggttctgtagtggttccgg	GAACTGCAGACTCTCTCTCTGTCGCCCCcaattgagagacctgtgc	gaaattaacgactcactataggCGGCGGGGGGAGACGTGTgttttagagctagaaatagc
LmxM.27.1040	GTGCTGCTCTCGGGTCTCGGATGGGCGggttctgtagtggttccgg	GACGCGCATATCCCCGTGTTGCGCCCCcaattgagagacctgtgc	gaaattaacgactcactataggGCTCACGGGCTGTGGTGTgttttagagctagaaatagc
LmxM.27.1400	GCGAGGCGGACAGCAGACAGCCGTCAGggttctgtagtggttccgg	TTCCCCCTCTCTGACTTCTCTCTccaattgagagacctgtgc	gaaattaacgactcactataggTGTGTGTGTACGAATGACGAgtttagagctagaaatagc
LmxM.28.1650	TCCAGCGCCGCCCTTCTCGGACAGGATAggttctgtagtggttccgg	TGCGCCGTGGATGTGGGCGCATGACCTccaattgagagacctgtgc	gaaattaacgactcactataggAGGACAGAGAGGGGTAGGTgttttagagctagaaatagc
LmxM.29.2580	CAGCTTGAGGACATGGAGCGCAAGCCAGggttctgtagtggttccgg	GTCTTGTCTAGCCGTCCTACCTTGCCcaattgagagacctgtgc	gaaattaacgactcactataggGAAATGCGGATTGGTGTACGgttttagagctagaaatagc
LmxM.29.2670	TCTTTACAGAATCCGGACGATCCCTACGCGggttctgtagtggttccgg	CTATCTCTCTCTCTCGGCTGACCCAGccaattgagagacctgtgc	gaaattaacgactcactataggTCCCTACACATACGCTTCCgttttagagctagaaatagc
LmxM.30.2590	AACAAGCAGTACAAGCCTTGACCGTCATGggttctgtagtggttccgg	GAGTCTCTGTCTGCTTGCCTGCTAGGACcaattgagagacctgtgc	gaaattaacgactcactataggCGTGACGCTTAGGTGTGTGgttttagagctagaaatagc
LmxM.30.3110	AGGACCCGGAAGGCGAAGGGCGGTGCTGCGggttctgtagtggttccgg	TCCCCCTTGTCTCTGCGCTCAGCACcaattgagagacctgtgc	gaaattaacgactcactataggGCTTCTCTCGGCTTTCGCTgttttagagctagaaatagc
LmxM.31.0220	GGAGTGTGACCGCTCTACGTGATGATGggttctgtagtggttccgg	TCAGCAGGCAAAGCAGCATGAAGTACAAGccaattgagagacctgtgc	gaaattaacgactcactataggGATAGCATGCACGACACGgttttagagctagaaatagc
LmxM.31.0140	CTGCAAGTCTCTCGAAGCCGCGAAGAGggttctgtagtggttccgg	CCGCGATGCAGTCCCTCCCCCTCCGCCcaattgagagacctgtgc	gaaattaacgactcactataggCCTGTGTGTGTGTGACTCgttttagagctagaaatagc
LmxM.31.2610	CTGGAGCGCATCGAACACGGCTCGCAAGAGggttctgtagtggttccgg	GAGGAAGATGTGCATCTGTTTTCTCCcaattgagagacctgtgc	gaaattaacgactcactataggGCGAAAAGTCAAAAAAAGAgtttagagctagaaatagc
LmxM.31.2680	AAGGCCATTAGACTTAAACCGGAGGTGggttctgtagtggttccgg	CTCGCCCCACCCCTCCACCGCACCCcaattgagagacctgtgc	gaaattaacgactcactataggTCACGAGAGGAGGCAAGAgtttagagctagaaatagc
LmxM.32.1035	CGCGACGAAGGCTCGGATGTGAGGCGCTggttctgtagtggttccgg	CAGTCTACTAGTTCGTTTTCTCTCGGTGccaattgagagacctgtgc	gaaattaacgactcactataggACCTTGTCAAACGAAAGAAAgtttagagctagaaatagc
LmxM.32.2460	TCTCCCTCGGCGTGCGCCAACCGCGCGggttctgtagtggttccgg	ACAAGCCGACTTCCAACAGCAAGCAACCcaattgagagacctgtgc	gaaattaacgactcactataggGTACGTCTCTCGCTCTGTTgttttagagctagaaatagc

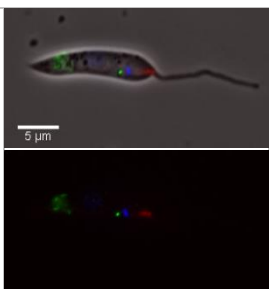
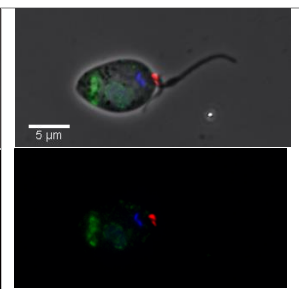

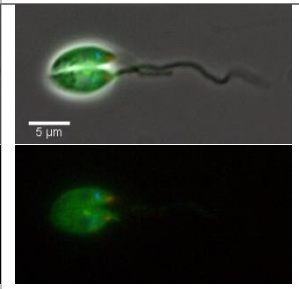
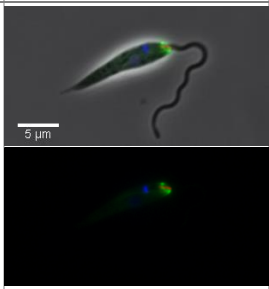
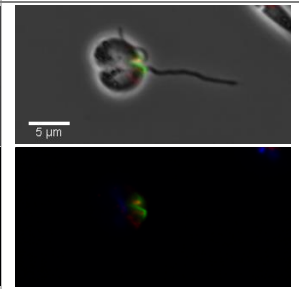
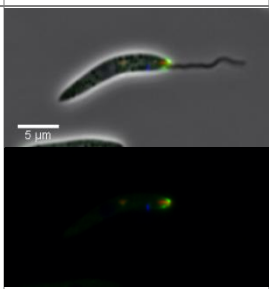
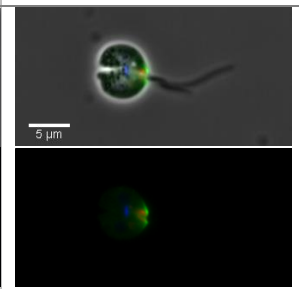
LmxM.33.0060	AACTCGGAGAAGTTGTCGAGGTCCAAGAGGggttctgtagtggttccgg	CACGACAGGCAATTCCTAGCGCGGAGCCccaattgagagacctgtgc	gaaattaatacactactataggGACTTTAGGTAGCTTCAGTgttttagagctagaatagc
LmxM.33.0190	AAGCGTAGGACGTCCGTGCCGACACTGCGggttctgtagtggttccgg	GCGTATTGGAGGTGGAGAGTGCACAGGGTTccaattgagagacctgtgc	gaaattaatacactactataggGTGGTTTACACAAGTCCCTgttttagagctagaatagc
LmxM.33.0690	AACATCAAACAAGTGAGCTTTGATCACGACggttctgtagtggttccgg	ACTCAGAACTGCGCCACACATCACCCGCTccaattgagagacctgtgc	gaaattaatacactactataggAGTCGTGATTCCTGCTCGGGgttttagagctagaatagc
LmxM.33.2540	GATGTTTACATGCGTCCAACGAGCTACAGggttctgtagtggttccgg	CAAAAAGAAATCACCGCAAGACTCCGCTccaattgagagacctgtgc	gaaattaatacactactataggATCAACGGCACAGGCGCAAgttttagagctagaatagc
LmxM.33.2570	GCACTGATGGACGAGAAGGTGACCAAAGCGggttctgtagtggttccgg	ATAGAAAGAGAAAGGGGGCGGGGAGTAGGccaattgagagacctgtgc	gaaattaatacactactataggTGGAGTGAGACAGCAGAAAAgttttagagctagaatagc
LmxM.34.2221	CAGCAGAAGGCTGCGCAGTACCCGTCCAAGggttctgtagtggttccgg	GCCTACACGCTTCTCTCGACTATCTCTccaattgagagacctgtgc	gaaattaatacactactataggCTACTTGATTCATAGAAACgttttagagctagaatagc
LmxM.34.3720	GCTCACAAGGCGGTATCGGGTCACAGGAAAggttctgtagtggttccgg	TGCTCGCTTACGCGATTTTTTCCCTCTccaattgagagacctgtgc	gaaattaatacactactataggTAAGGCAACAAGGGGAGGTgttttagagctagaatagc
LmxM.34.5010	CTAGTCGCCGAAGCCTGCCAAAGCTGATAggttctgtagtggttccgg	CCCAAAAAAAAAAGTGTACCAGACACGGCCAccaattgagagacctgtgc	gaaattaatacactactataggAGTCACTGTCATGTGTGCGCgttttagagctagaatagc
LmxM.36.0830	GTCTCGTTCTGTATCTTTGGCAACCGCTCggttctgtagtggttccgg	GGGTATCCCTCTCCGCTCTCTGCCGCCccaattgagagacctgtgc	gaaattaatacactactataggTAGGCAAGCTTGGCACAGTgttttagagctagaatagc
LmxM.36.1920	GAGCGCGCATGGTGTGCGGCAAAGCCGggttctgtagtggttccgg	CACAGACAGGCATGATCACGCATGTATGCCccaattgagagacctgtgc	gaaattaatacactactataggTCTCGGTGCCGTCTGCCGTgttttagagctagaatagc
LmxM.36.4330	GCGGCGTCAGCGGAAGCGGTGGACCGCTTcggttctgtagtggttccgg	GGCAAAGGGGGTGTGAGAGAGACAACATccaattgagagacctgtgc	gaaattaatacactactataggTGGCATAAAAGAAAGCACTgttttagagctagaatagc
LmxM.36.5970	TCTGCAACCAGAGCGCGGAGAGGAAGAGGggttctgtagtggttccgg	AATGACGTACCAAGCAAGAGAGAGAGCCCTccaattgagagacctgtgc	gaaattaatacactactataggATACTTGTGTGGGGTTATTCgttttagagctagaatagc
LmxM.36.6960	TGCATACTCTGCTGGGTCGCTCGATGACggttctgtagtggttccgg	TGCAGCCGAAAGAAGGATACTCGAGCAGAGccaattgagagacctgtgc	gaaattaatacactactataggCGTGTACAGCTGGCAGTGTgttttagagctagaatagc

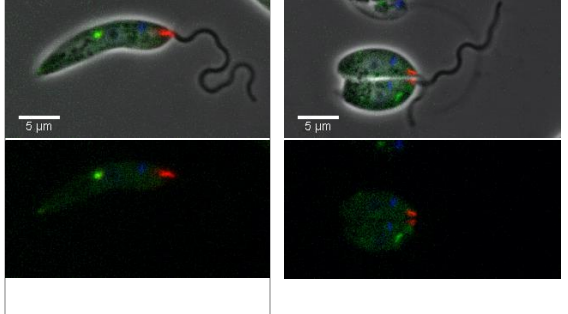
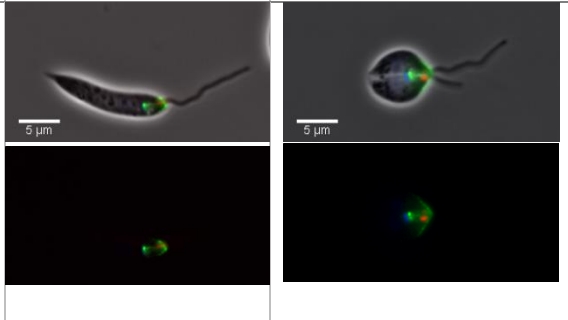
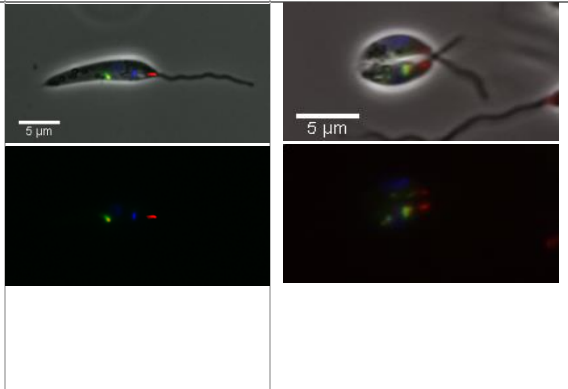
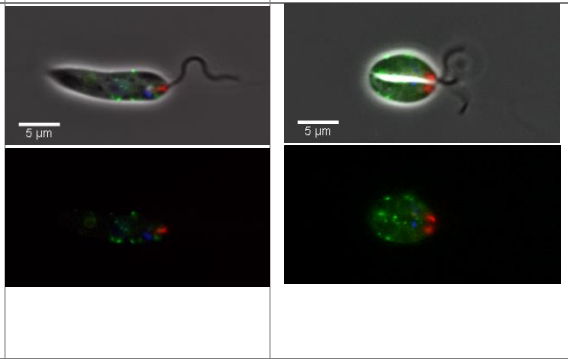
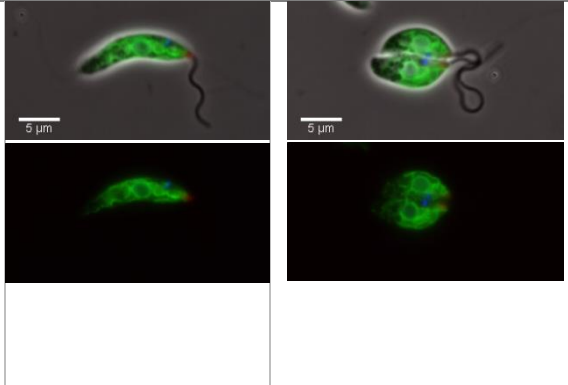
Appendix B

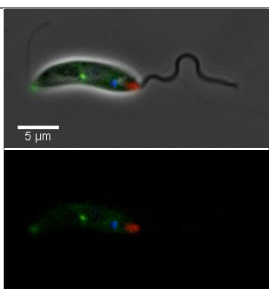
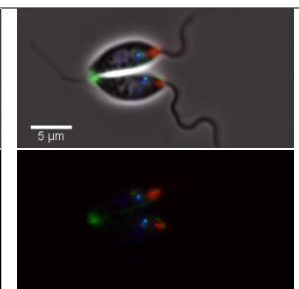
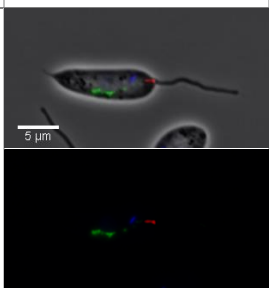
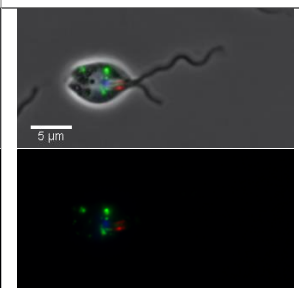
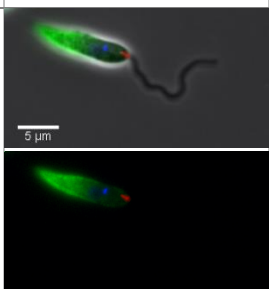

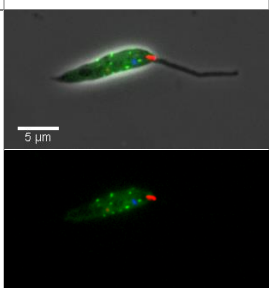
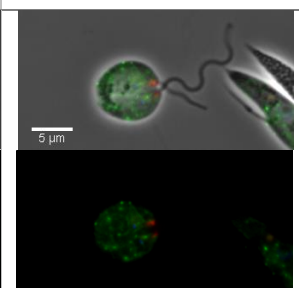
Non-FAZ localisations in *L. mexicana*

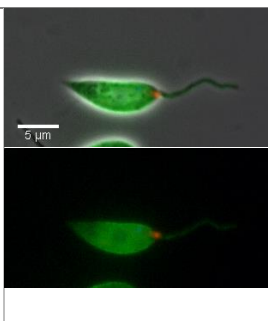
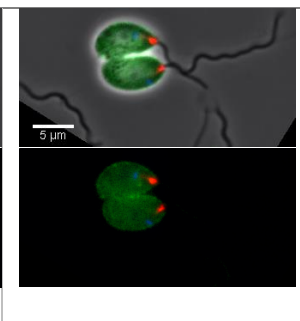

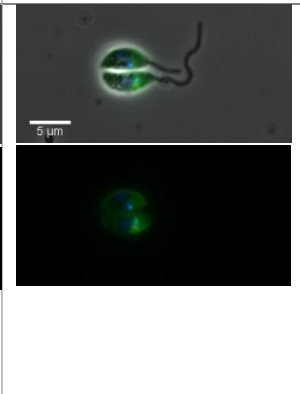
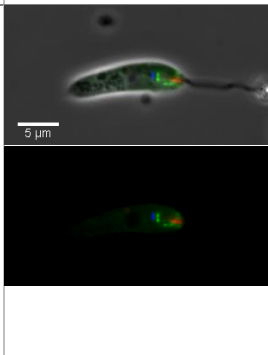
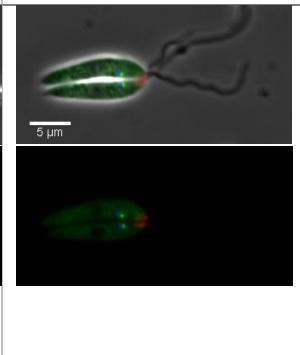
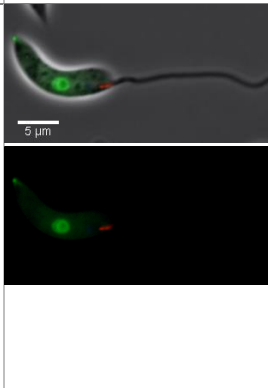
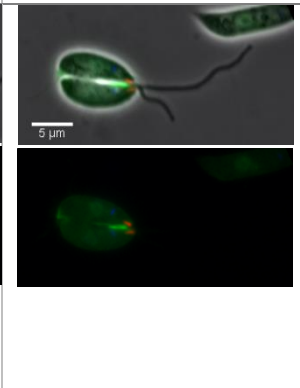
<i>L.mexicana</i> ortholog	1F1N1K image	2F2N2K image	Localisations
LmxM.12.1190			Cytoplasm (weak)
LmxM.29.2580			cytoskeleton anterior, cytoplasm points
LmxM.22.1010			ER
LmxM.23.0080			cytoskeleton posterior

<p>LmxM.34.5010</p>			<p>Cytoplasm reticulated (weak)</p>
<p>LmxM.21.0700</p>			<p>Cytoplasm, cytoskeleton anterior</p>
<p>LmxM.09.1050</p>			<p>ER</p>
<p>LmxM.14.1200</p>			<p>Cytoplasm, lysosome</p>
<p>LmxM.31.2680</p>			<p>ER</p>

<p>LmxM.24.0700</p>			<p>Cytoplasm posterior points</p>
<p>LmxM.02.0140</p>			<p>cytoplasm</p>
<p>LmxM.36.1920</p>			<p>Cytoskeleton anterior, cleavage furrow</p>
<p>LmxM.36.6960</p>			<p>Cytoskeleton anterior, cleavage furrow</p>

<p>LmxM.27.1040</p>		<p>Cytoplasm points</p>
<p>LmxM.13.1590</p>		<p>Cell tip anterior, BB, kinetoplast, Cytoskeleton anterior</p>
<p>LmxM.29.2670</p>		<p>endocytic, lysosome</p>
<p>LmxM.31.0220</p>		<p>Cytoplasm points</p>
<p>LmxM.11.1320</p>		<p>ER</p>

<p>LmxM.21.1220</p>			<p>Cell tip posterior, cytoplasm point</p>
<p>LmxM.16.0490</p>			<p>Cytoplasm points, lysosome</p>
<p>LmxM.34.3720</p>			<p>Cytoskeleton posterior</p>
<p>LmxM.33.0060</p>			<p>Cytoplasm points</p>

<p>LmxM.18.1080</p>			<p>Cytoskeleton , cytoplasm</p>
<p>LmxM.19.0140</p>			<p>Cytoplasm, lysosome, kinetoplast</p>
<p>LmxM.19.0680</p>			<p>Cytoskeleton anterior, BB, ρBB</p>
<p>LmxM.31.2610</p>			<p>Cell tip posterior, nucleus, cleavage furrow</p>

Appendix C

Primers for FAZ deletion in *L. mexicana*

Forward/Reverse

Gene ID	Upstream forward	Downstream reverse
LmxM.04.0890	CATCACCCCGTGCCCTCCCCCTCCCCGgtataatgcagacctgtgc	CCCAGCCACCCCGACATCCCTCACCTCCCccaatttgagagacctgtgc
LmxM.04.1100	AACCTCGTCGTGCAGCGCTCCTTGTCCTgtataatgcagacctgtgc	TTCTTTGGCCACGCCCCCTGCCCTCCccaatttgagagacctgtgc
LmxM.09.0520	ACACGAACGTATCCTCCACGGACTTCGCCTgtataatgcagacctgtgc	CCTTGACCCCGCCCCGCCTCCTCTCCccaatttgagagacctgtgc
LmxM.10.0620	TCGCGCACTCTCTCTTAGAGCAGACCCGgtataatgcagacctgtgc	GAATGGTATTGTGCACACTACGAGCTCCTTccaatttgagagacctgtgc
LmxM.12.0360	TCTCCGCAACCCCTCCCCGCCGTCCGgtataatgcagacctgtgc	TCGGTCTCTGTGTCAGTGCAGCCGTACCCccaatttgagagacctgtgc
LmxM.12.1120	GCACGCAGGGGAAAGTTTATTTTCTCCAgataatgcagacctgtgc	AAGGGAGGAGGGGGACAGCAGGCTCGCTccaatttgagagacctgtgc
LmxM.16.1660	CTCCTGCGCTGGAGGTTGCGGTTTGGCGGgtataatgcagacctgtgc	GTGCAGACGCACCCAAGTTTGTTCACCGccaatttgagagacctgtgc
LmxM.18.1440	CATCTCTCGTTTATCTGCCACGCTCCTgtataatgcagacctgtgc	GACGCTCCACGAGCAGCACTACTCCTCGCccaatttgagagacctgtgc
LmxM.18.1560	AGACGTCGTGCGCCAGCTTTGCTCCATCCGgtataatgcagacctgtgc	TCCCGCAGCATATCATCGTGCCTCCTccaatttgagagacctgtgc
LmxM.21.1240	AGACGAAGAAGGAAACCACCTCAGACCAgtataatgcagacctgtgc	TGTACATGGGCGCCAGGATAAAGGATTCCCccaatttgagagacctgtgc
LmxM.22.1320	TTACGTCGGTATATCTTATTTCTCACACCTgtataatgcagacctgtgc	CACACATGCGTATTGCTTACATCAATCCAccaatttgagagacctgtgc
LmxM.24.1430	GCGAGTGCAGCTCGTACAGGAGACAGGAGCgtataatgcagacctgtgc	GAAGTGCAGACCTCTCTCTCTCGTCCCCccaatttgagagacctgtgc
LmxM.27.0490	GCATCGTACAACCGTTTTTCTTTTTCGCTgtataatgcagacctgtgc	ACAACGGCACAGACACAAGTTCACGCAGACAGAGGCACCGCTACACGTTCCAatttgagagacctgtgc
LmxM.30.2590	TCCGTCGTCTTCATTTTGTGCCGACGCCgtataatgcagacctgtgc	GAGTCTCTGTCTGCTTGCCTGCTAGGACccaatttgagagacctgtgc
LmxM.30.3110	GCCTGCGCTGGCAGAGACACCTGCTCGTgtataatgcagacctgtgc	TCCCCCTTGTCTCTGCGCTCAGACCAccaatttgagagacctgtgc
LmxM.32.2460	TCACTCCACAGCACCCCTCATCTGCAgtataatgcagacctgtgc	ACAAGCCGACTTCCAACACGAAGCAACCccaatttgagagacctgtgc
LmxM.33.0690	AACCCCGGAAAGTTTGTAGTGTGACTCCGgtataatgcagacctgtgc	ACTCAGAAGTGCAGCACATACCCGCTccaatttgagagacctgtgc
LmxM.33.2540	CTCTTATCTCCCGTTTTCAAGTGTTCGGgtataatgcagacctgtgc	CAAAAAGAAATCACCGCAAGACTCCGCTccaatttgagagacctgtgc
LmxM.33.2570	TGAAAACGACGTTAGTCCCTCACTCTCCGgtataatgcagacctgtgc	ATAGAAAAGAGAAAGGGGGCGGGAGTAGGccaatttgagagacctgtgc
LmxM.36.0830	CACCGGGACGGCGTTTTCTTTTCTCCTgtataatgcagacctgtgc	GGGTATCCCTCTCCGCTCTCTGCGCCAccaatttgagagacctgtgc
LmxM.36.5970	TCCCGCTGTGTGTGTCGCTGTGACTGCCTgtataatgcagacctgtgc	AATGACGTACCAAGCAAGAGAGAGCCCTccaatttgagagacctgtgc

Guide

Gene ID	5' sgRNA	3' sgRNA
LmxM.04.0890	gaaattaatacgactcactataggATGGCGCGCTTCGAGAGAgttttagagctagaatagc	gaaattaatacgactcactataggGGTGACAGTGTGGTGCCTGTgttttagagctagaatagc
LmxM.04.1100	gaaattaatacgactcactataggGGCGAGAGAGGGAGGGTGCgttttagagctagaatagc	gaaattaatacgactcactataggAGTCCGTCTCAGACAGAGAgtttttagagctagaatagc
LmxM.09.0520	gaaattaatacgactcactataggAGAGAGGTTGAGAGGAGAgtttttagagctagaatagc	gaaattaatacgactcactataggAGGGAACGGACGGCAAGCCAgtttttagagctagaatagc
LmxM.10.0620	gaaattaatacgactcactataggGTGCGTGCAACGTCGTTATgttttagagctagaatagc	gaaattaatacgactcactataggCTACGGGGCCCTCTCTAgtttttagagctagaatagc
LmxM.12.0360	gaaattaatacgactcactataggACAGCAGCGTAGGTGGCCTGgttttagagctagaatagc	gaaattaatacgactcactataggAGGGAAGGCATCTGGCTGAgtttttagagctagaatagc
LmxM.12.1120	gaaattaatacgactcactataggGAAGTAAGGGGAGAAACGgttttagagctagaatagc	gaaattaatacgactcactataggGGGCTGGTGAGGGCGTGTGcgttttagagctagaatagc
LmxM.16.1660	gaaattaatacgactcactataggTGTGGCGGTTGGTCTGTGgttttagagctagaatagc	gaaattaatacgactcactataggGGCTACGTGAACGGAACAAGgttttagagctagaatagc
LmxM.18.1440	gaaattaatacgactcactataggGATGTTCTCTGGGTACGAGgttttagagctagaatagc	gaaattaatacgactcactataggGCTACATCGTCTCTCTCgttttagagctagaatagc
LmxM.18.1560	gaaattaatacgactcactataggCTTGTGTGTCGTCGGTATgttttagagctagaatagc	gaaattaatacgactcactataggAAAGAGGTGCGCTAGGCTGGgttttagagctagaatagc
LmxM.21.1240	gaaattaatacgactcactataggAATACTGTGAGCTGCGTGCgttttagagctagaatagc	gaaattaatacgactcactataggAGTTTGTGTGAGTGTGCGgttttagagctagaatagc
LmxM.22.1320	gaaattaatacgactcactataggGGGAGACGATGTTGGAAGAGgttttagagctagaatagc	gaaattaatacgactcactataggATCGACGTTCTATTTTCTTgttttagagctagaatagc
LmxM.24.1430	gaaattaatacgactcactataggGCGCTCCGCGTTTTGTGATTgttttagagctagaatagc	gaaattaatacgactcactataggCGGCGGGGGGAGACGTGTgttttagagctagaatagc
LmxM.27.0490	gaaattaatacgactcactataggGACGTCACGAAATAAGATGgttttagagctagaatagc	gaaattaatacgactcactataggCCCTGAGGGTAGTATAACAGgttttagagctagaatagc
LmxM.30.2590	gaaattaatacgactcactataggGCCTACGTGAGAGCGTTTTgttttagagctagaatagc	gaaattaatacgactcactataggCGTGACGCTTAGTGTGTGcgttttagagctagaatagc
LmxM.30.3110	gaaattaatacgactcactataggTTCTAGCCTCGCCACTACAGgttttagagctagaatagc	gaaattaatacgactcactataggGCTTTCTCTCGCTTTCGCTgttttagagctagaatagc
LmxM.32.2460	gaaattaatacgactcactataggAGCACAACGTTGTTGAAGCgttttagagctagaatagc	gaaattaatacgactcactataggGTACGTCTCTGCTCTTGTgttttagagctagaatagc
LmxM.33.0690	gaaattaatacgactcactataggTATGTTGTTGAGTTTTCTTgttttagagctagaatagc	gaaattaatacgactcactataggAGTCGTGATTCTTGCTCGGgttttagagctagaatagc
LmxM.33.2540	gaaattaatacgactcactataggAGCTGGACAGCAGACAACAGgttttagagctagaatagc	gaaattaatacgactcactataggATCAACGGCACAGGCGCAAgttttagagctagaatagc
LmxM.33.2570	gaaattaatacgactcactataggAAGGGAGTTGTTGGGGATGTGgttttagagctagaatagc	gaaattaatacgactcactataggTGGAGTGAGACAGCAGAAAAgttttagagctagaatagc
LmxM.36.0830	gaaattaatacgactcactataggGCGTTTGAACACCCCAAgttttagagctagaatagc	gaaattaatacgactcactataggTAGGCAAGCTTGGCACAGTgttttagagctagaatagc
LmxM.36.5970	gaaattaatacgactcactataggCCAAAAAACGTCGAAGAgtttttagagctagaatagc	gaaattaatacgactcactataggATACTTGTGGGGTTATTCgttttagagctagaatagc

Appendix D

Deletion confirmation primers

Gene ID	Forward	Reverse
LmxM.04.0890	ACGCCACCCACCCTACACAC	CTGCGGGCCTGGACACCGAG
LmxM.04.1100	TCCCGAGTAAAGCCACAGCAG	CATGCCGCGCGAGAGCCAAG
LmxM.09.0520	AGATTGTGGACGCGGCCTAC	CCTGTGCGTTCAGGAAGGCG
LmxM.10.0620	CTGCGCCAACCTCGACACCG	GGTCGCGGCCACGACGATGC
LmxM.12.0360	GAGCGCCGGGGCGAATAATG	GGCTTGACTGTTGAGGGTGC
LmxM.12.1120	GGCGTTTGTGCCACCGTTCC	GCGGGCGGGGCACCTCCACC
LmxM.16.1660	GGCAATGGAGGGCGAGTTGCGTG	CTCAAAGCGCACTCAGAACGCC
LmxM.18.1440	GACCCCGCTTCTCTTTAAAC	GAGTCGCATGTCCTCCATCTG
LmxM.18.1560	CTGCTCACCGCTGTGGAGCC	CCTCGCAGCCCAGGTACGAG
LmxM.21.1240	ATCCGTTCTCTGCCAAGGG	CCACAGCTGGCTCGCGTGTG
LmxM.22.1320	AGACCTCCACTAAGGCCGATG	GTTGGCAAGTTGGATTTCTAG
LmxM.24.1430	TTACCACAACCGCCATGGGC	GAAGCCCAACTGTGCGCTTC
LmxM.27.0490	CGGCATCTTCTCACCACGAAAC	GGCCCAACGGACAGTCTAGCAC
LmxM.30.2590	CGGCAGCGAATGTGTTCAACCG	CAGCCGTTTGCTCATCGGTTTGC
LmxM.30.3110	CGAGGATACGTTGCGGCGCC	CAGACTGGTGAGCTCCTTCTC
LmxM.32.2460	GGTACAACCTCTCAGATCAG	GATGACTGCGTAGCGCAGGC
LmxM.33.0690	CCTTTACCCAACCTGCAACCTGG	CTTGCAGACAGAACCGCTAGAG

LmxM.33.2540	GAGCACTAGACATCTGTGCG	CTCCACTACACCGCTCTTTAC
LmxM.33.2570	CACGAACGGCAGCGCTCTC	CGGGTTTTCTTGCTATCCTC
LmxM.36.0830	TGCGCGTAATCCTACGTTT	GGTGGTCGGCGACGCCTGCG
LmxM.36.5970	CTATCAGGCCTATCTTGTTT	CAGAATGTCACCCACGATGG

Appendix E

Publications that were derived from work in this thesis

Chapter 1

Halliday, C. *et al.* (2021) 'Trypanosomatid Flagellar Pocket from Structure to Function', *Trends in Parasitology*, 37(4), pp. 317–329. doi: 10.1016/j.pt.2020.11.005.

Chapter 4

Halliday, C. *et al.* (2020) 'Role for the flagellum attachment zone in *Leishmania* anterior cell tip morphogenesis', *PLoS Pathogens*, 16(10). doi: 10.1371/journal.ppat.1008494.